

Formation Control of Multi-agent Systems via Impulsive Strategy

by

Zhanlue Liang

A thesis
presented to the University of Waterloo
in fulfillment of the
thesis requirement for the degree of
Doctor of Philosophy
in
Applied Mathematics

Waterloo, Ontario, Canada, 2023

© Zhanlue Liang 2023

Examining Committee Membership

The following served on the Examining Committee for this thesis. The decision of the Examining Committee is by majority vote.

External Examiner: Zhong-Ping Jiang
 Professor,
 Dept. of Electrical and Computer Engineering,
 New York University

Supervisor: Xinzhi Liu
 Professor,
 Dept. of Applied Mathematics, University of Waterloo

Internal Member: Hans De Sterck
 Professor,
 Dept. of Applied Mathematics, University of Waterloo

Internal Member: Jun Liu
 Associate Professor,
 Dept. of Applied Mathematics, University of Waterloo

Internal-External Member: Xuemin (Sherman) Shen
 Professor,
 Dept. of Electrical and Computer Engineering,
 University of Waterloo

Author's Declaration

I hereby declare that I am the sole author of this thesis. This is a true copy of the thesis, including any required final revisions, as accepted by my examiners.

I understand that my thesis may be made electronically available to the public.

Abstract

Multi-agent systems (MASs) involving cooperative control problems such as consensus tracking of distributed networks, flocking control with obstacle avoidance, and attitude alignment have received a considerable amount of interest over the past few decades because of their broad real-time applications in various fields. As one of the most significant aspects of cooperative control, the formation stabilization process has been studied extensively in relation to cooperative surveillance, unmanned aerial vehicles, spacecraft coordination, autonomous underwater vehicles, etc. In formation tracking control, the fundamental goal is to reach a desired configuration and align with the formation leader from any arbitrary starting position. This can be achieved using various types of distributed control protocols in practice, which facilitate efficient communication and information exchange among agents.

To begin with, we discuss the design of hybrid impulsive control protocols for the formation stabilization of multi-agent systems. By taking various sizes of time delay into account, some sufficient formation stabilization criteria are established via the Razumikhin technique and Lyapunov functional method. It is important to emphasize that the guarantee of stabilization is largely determined by the impulsive strength, the size of the time delays, and the length of the impulsive intervals. In the meantime, the general structure of collision avoidance mechanisms using artificial potential fields (APFs) or braking/gyroscopic forces is also discussed since they are critical for ensuring safety and reducing accident risk in a variety of applications. In comparison, the approach of braking and gyroscopic forces provides better performance by preventing undesired local minima. Moreover, one should realize that the inclusion of such mechanisms will raise the complexity of asymptotic formation stabilization under delay-dependent impulses. Thus, we further consider treating the collision avoidance mechanism as an external input and investigate input-to-state formation stabilization with respect to different impulse classes. In this way, stabilization can still be achieved once environmental obstacles are out of sensing range. Some sufficient conditions benefiting from stabilizing control impulses are derived by employing the Lyapunov Krasovskii functional and impulsive comparison principle. The hybrid impulsive control framework will be kept using throughout the rest of this thesis.

Then, on top of the hybrid impulsive control framework, we extend our formation stabilization results into the following aspects:

1. Multi-group formation stabilization for heterogeneous MASs with different dynamics order is investigated. In this setup, each subgroup can pursue its own control objectives, while group-wise coordination can be established via directed inter-group

communication links. The stabilization is then dependent on the overall topological structure of the network.

2. The hybrid event-triggered impulsive formation stabilization associated with non-linearity strength of intrinsic dynamics is considered. By incorporating pinning mechanisms and delayed control inputs, the corresponding event-triggered strategies are developed. Based on the Lyapunov-Razumikhin technique regarding delayed impulsive systems, some novel results for maintaining local formation stabilization are obtained.
3. We also investigate the finite-time formation tracking control of multi-agents via aperiodic intermittent communication under the hybrid impulsive control framework. In addition, the concepts of average impulsive interval and state-dependent intermittent control width are also implemented. The finite-time stabilization results illustrate the effectiveness of the proposed control protocol on the basis of the weak Lyapunov inequality condition.
4. Furthermore, we investigate the formation stabilization of vehicle platoons using switching control, which is a trending application of multi-agent systems. Based on time-dependent switching between stable and unstable control inputs, or state-dependent switching utilizing convex switching regions and chatter-free switching rules, exponential stabilization results are obtained.

Finally, numerical simulations are provided to demonstrate the effectiveness and performance of our analytical results.

Acknowledgements

First and foremost, Prof. Xinzhi Liu, please accept my heartfelt thanks for the guidance and support I received during my PhD at Waterloo from you. My sincere appreciation extends out to my examining committee, Professor Hans De Sterck, Professor Jun Liu, Professor Zhong-Ping Jiang and Professor Sherman Shen for their valuable advice to further enhance the quality of this thesis.

Many thanks to former, current and visiting members of my research group for the help and insights that enlightened me. My deepest gratitude and love go to my family for their consistent support over the years, especially my grandpa that had accompanied me since my childhood. I continue to be thankful to my beloved fiancée, Siman, for her emotional understanding and love.

Dedication

This is dedicated to my dearest parents, and beloved fiancée.

Table of Contents

Examining Committee	ii
Author's Declaration	iii
Abstract	iv
Acknowledgements	vi
Dedication	vii
List of Figures	xi
List of Tables	xiv
List of Algorithms	xv
1 Introduction	1
1.1 Motivations	1
1.2 Thesis Outline	5
1.3 Thesis Scopes	6
1.4 Notations	7

2	Background	9
2.1	Multi-agent System Model	9
2.2	Formation Control	10
2.3	Impulsive Control Method	14
3	Hybrid Impulsive Formation Control of MASs	17
3.1	Problem Formulations	18
3.2	Formation Stabilization	22
3.2.1	Case I: $\tau < \inf\{t_k - t_{k-1}\}, k \in \mathbb{N}^+$	22
3.2.2	Case II: $\tau > \inf\{t_k - t_{k-1}\}, k \in \mathbb{N}^+$	25
3.2.3	Distributed Impulse Delay	28
3.3	Collision Avoidance Mechanism	29
3.4	Formation Stabilization with Collision Avoidance	34
3.5	Input-to-state Formation Stabilization	38
3.5.1	Preliminaries	39
3.5.2	ISS/iISS Formation Stabilization	42
3.5.3	Numerical Simulations	50
4	Multi-group Hybrid Impulsive Control of Heterogeneous MASs	54
4.1	Problem Formulation	55
4.2	Multi-group Formation Stabilization	57
4.2.1	Delay-free Formation Stabilization	61
4.2.2	Formation Stabilization with Time-varying Delay	62
4.3	Numerical Simulations	64
5	Hybrid Event-triggered Impulsive Control of MASs via Pinning Mechanism	76
5.1	Event-triggered Mechanism	76
5.2	Pinning Mechanism	77

5.3	Problem Formulation	77
5.4	Formation Stabilization	78
5.4.1	Delay-free Hybrid Event-triggered Pinning Impulsive control (HET-PIC)	78
5.4.2	HETPIC with Transmittal Delays	86
5.5	Numerical simulations	92
6	Finite-time Hybrid Impulsive Control of MASs via Intermittent Communication	103
6.1	Finite-time Stability	103
6.2	Intermittent Communication	104
6.3	Problem Formulation	104
6.4	Formation Stabilization	106
6.4.1	FTHIIC with Stabilizing Impulses	106
6.4.2	FTHIIC with Impulsive Disturbances	116
6.4.3	FTS via Average Impulsive Interval	119
6.4.4	FTS with State-dependent Control Width	121
6.5	Numerical Simulations	122
7	Application to Self-driving Vehicle Platoons	126
7.1	Switched System	128
7.2	Problem Formulation	129
7.3	Vehicle Platoon Control via Time-dependent Switching	132
7.4	Vehicle Platoon Control via State-dependent Switching	142
7.5	Numerical Simulations	146
8	Conclusions and Future Research	153
	References	157

List of Figures

1.1	Illustration of MAS in real life (a) school of fish herd (b) self-propelled particles (c) flight squadron (d) computer network	3
1.2	Example of the topological structure of MAS	4
2.1	Sensing capability vs. interaction topology	11
2.2	(a) i-th vehicle and corresponding virtual vehicle (b) position of VSs	12
3.1	Example of topology structure under protocol (3.3) during (a) continuous (b) impulsive transmission	19
3.2	Trapped α -agents upon encountering (a) a convex obstacle and (b) a non-convex obstacle	31
3.3	(a) Total mismatch without external inputs (b) Total mismatch with periodic external inputs (c) Total mismatch with exponentially decaying external inputs over $\mathcal{F}(h_2)$	51
3.4	(a) Total mismatch without external inputs (b) Total mismatch with periodic external inputs (c) Total mismatch with exponentially decaying external inputs over $\mathcal{F}[T_\alpha, \varrho]$	52
4.1	Connectivity of the overall topology with 3 subgroups	56
4.2	Connectivity of the overall topology for simulation	65
4.3	Convergence of (a) velocity mismatch of inter-group communication (b) position mismatch of inter-group communication (c) acceleration	66
4.4	Formation evolution for N=20 agents without time delay (2nd-order dynamics in red scatter points, 3rd-order dynamics in blue scatter points, and virtual leaders in red pentagrams)	67

4.5	Convergence of (a) velocity mismatch of group 1 (b) velocity mismatch of group 2 (c) velocity mismatch of group 3 (d) position mismatch of group 1 (e) position mismatch of group 2 and (f) position mismatch of group 3 . . .	68
4.6	Convergence of (a) velocity mismatch of inter-group communication (b) position mismatch of inter-group communication (c) acceleration	70
4.7	Formation evolution for N=20 agents with time delay (2nd-order dynamics in red scatter points, 3rd-order dynamics in blue scatter points, and virtual leaders in red pentagrams)	71
4.8	Convergence of (a) velocity mismatch of group 1 (b) velocity mismatch of group 2 (c) velocity mismatch of group 3 (d) position mismatch of group 1 (e) position mismatch of group 2 and (f) position mismatch of group 3 . . .	72
4.9	Convergence of (a) velocity mismatch (b) position mismatch (c) acceleration of agent 1 with $r(t)=0s$, $r(t)=0.42s$ and $r(t)=0.5s$ (d) velocity mismatch of agent 1 with $r(t)=1s$	73
4.10	Distortion index of agent 1 via (a) braking/gyroscopic forces in this paper (b) artificial potential functions; Distortion index of agent 4 via (c) braking/gyroscopic forces in this paper (d) artificial potential functions.	75
5.1	(a) Connectivity of the communication topology (a) before and (b) after switching	79
5.2	Two-loop feedback control scheme for the multi-quadrotor system	92
5.3	Hardware structure of the quadrotor platform	93
5.4	(a) Displacement mismatch (b) Velocity mismatch (c) Triggered instants of strategy (5.6) with $\theta_l=0.022, 0.2, 0.55$	95
5.5	2D formation evolution for n=6 agents with real-time inputs	96
5.6	2D formation evolution for n=6 agents with delayed inputs	97
5.7	(a) Displacement mismatch (b) Velocity mismatch (c) Triggered instants of strategy (5.21) with $\theta_l=0.022, 0.035, 0.05$	98
5.8	3D formation tracking trajectories	101
5.9	Convergence of (a) velocity mismatch (b) displacement mismatch of agent 1 with $r(t)=0s$, $r(t)=4s$ and $r(t)=10s$	102

6.1	(a) Communication topology structure with respect to $u_{pi}(t)$ (b) Communication topology structure with respect to $u_{vi}(t)$	112
6.2	(a)&(b) Trajectory evolution of MASs (6.3) over stabilizing impulses (c) Velocity mismatch of error dynamics (d) Displacement mismatch of error dynamics	123
6.3	(a)&(b) Trajectory evolution of MASs (6.3) over stabilizing impulses and impulsive disturbances (c) Velocity mismatch of error dynamics (d) Displacement mismatch of error dynamics	124
7.1	Structure of a vehicle platoon	127
7.2	Switching via (a) time-dependent and (b) state-dependent signals	128
7.3	(a) Topology structure of leader-following vehicle platoon at $t \neq t_{s,l}$ (b) Topology structure of leader-following vehicle platoon at $t = t_{s,l}$	133
7.4	(a) Two-predecessor following (b) Full control deactivation	134
7.5	Convergence of (a) position (b) velocity (c) acceleration mismatch of vehicle platoon with time-dependent switching (d) Time-dependent switching signals	148
7.6	Evolution of vehicle platoon with time-dependent switching	149
7.7	Evolution of vehicle platoon with state-dependent switching	150
7.8	Convergence of (a) position (b) velocity (c) acceleration mismatch of vehicle platoon with state-dependent switching (d)-(e) State-dependent switching signals	151

List of Tables

4.1	Comparison of distortion index of agent 1	74
5.1	Comparison among different types of control protocols.	99
5.2	Comparison among different parameter settings of strategy (5.21).	100
5.3	Comparison of distortion index of agent 1	100
5.4	Comparison of distortion index of agent 4	101

List of Algorithms

5.4.1 Formation Stabilization Algorithm via Control Law (5.3) and Strategy (5.6)	85
5.4.2 Formation Stabilization Algorithm via Control Law (5.19) and Strategy (5.21)	91

Chapter 1

Introduction

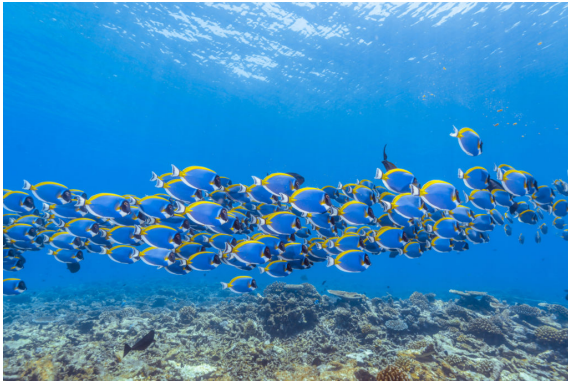
1.1 Motivations

The main idea of multi-agent systems (MAS) was originally inspired by the biological behaviors of animals in nature; such as the movement and migration patterns of fish, birds, etc [1, 2]. Figure 1.1(a) describes the flocking habit of a fish herd, which is an example of animal collective behaviour and can be modeled by MAS. In recent years, MAS often refers to a field of physics [3, 4, 5, 6], engineering [7, 8, 9], computer science and artificial intelligence (AI) [10, 11] that deals with the study of multiple agents interacting with each other in a shared environment. For instance, Figure 1.1(b) shows that self-propelled particles can condense by turning and moving toward crowded areas, Figure 1.1(c) shows the operation and coordination of a flight squadron, while Figure 1.1(d) shows a typical computer network consisting of a firewall and central server that is connected via optical fibre links. The research of MAS involves developing models, algorithms, and architectures for designing, analyzing, and controlling multi-agent systems. Common topics in MAS research include coordination control, learning algorithms, game theory, and decision-making processes. In particular, an agent can be a computational entity or physical body that is capable of perceiving its environment, making decisions, and taking actions to achieve its goals. Meanwhile, in a multi-agent system, agents are autonomous and can have their own objectives, knowledge, beliefs, and capabilities. They can interact with each other through various communication channels and coordinate their actions to achieve collective goals or solve complex problems that are difficult or impossible for a single agent to solve. Mathematically, the dynamic behaviour of MAS and its corresponding interconnections among agents can be established using graph and matrix theories [12, 13, 14]. Then, the

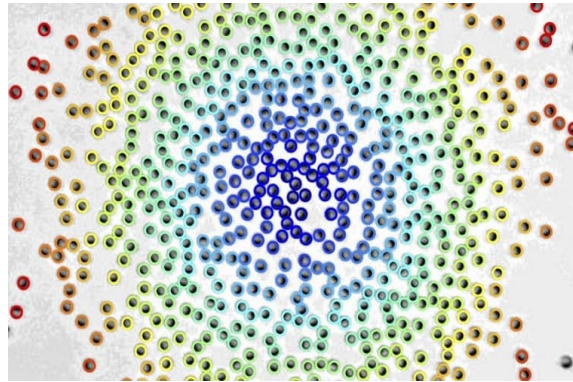
topological structure $\mathcal{G} = (\mathcal{V}, \mathcal{E})$ of MAS can be devised accordingly (see example in Figure 1.2), where V represents the set of vertices/nodes and E represents the set of edges/links connecting any two distinct vertices.

Relying on the basic concept and features of MAS, the design of proper control schemes for a MAS in terms of node capability, connection diversity, dynamic complexity and overall performance has received considerable research interest over the years. In 2006, Olfati-Saber [15] provided detailed illustration of the decentralized (reactive) control architecture for MAS, in which each agent only requires to gather local information from its surrounding environment to cooperate with other agents. Under such a framework, the use of MAS demonstrates significant advantages in reducing control costs, parallel processing, improving fault tolerance and maintaining stable performance when agents are partially disabled. In the meantime, the idea of distributed control has been widely implemented into the consensus problem of multi-agent systems, which aims to reach an agreement on a common value or state via the interaction or communication network among agents. For example, Olfati et al.[16] investigated the decentralized consensus problem in networks of agents with switching topology and time-delays; Hou et al.[17] investigated the distributed robust adaptive control for the multi-agent system consensus problem using neural networks; Gong [18] discussed the distributed consensus of non-linear fractional-order multi-agent systems with directed topologies; and the distributed finite-time consensus tracking of multi-agent systems were discussed in [19].

Similar to the consensus problem of MAS, formation control is another actively studied topic within the realm of multi-agent systems, which generally aims to drive multiple physical agents to achieve prescribed constraints on their states. Formation control schemes are characterized in terms of the sensing capability and the interaction topology of agents. The corresponding real-life applications include but are not limited to cooperative surveillance [20], unmanned aerial vehicles [21], and spacecraft coordination [22]. Moreover, in the presence of a virtual or physical formation leader, formation tracking control is fundamentally designed to ensure follower agents reach a desired configuration upon aligning with the leader from any arbitrary initial position. This can be achieved using a variety of conventional and novel control techniques, which facilitate necessary information exchange. For instance, protocols involve event-triggered control with time-delay [23], finite-time sliding control [24], robust control with stochastic link failure [25], robust adaptive control [26], leader-following pinning control [27], etc. In addition, one also needs to consider collision avoidance mechanisms (separation feature [2, 3]) among agents and environmental obstacles, which is crucial in practice such as air-traffic control [28]. Most recent formation control results with collision avoidance rely on the construction of decentralized artificial potential functions introduced in [15, 29], which then act as repulsive forces. Nevertheless,



(a)



(b)



(c)



(d)

Figure 1.1: Illustration of MAS in real life (a) school of fish herd (b) self-propelled particles (c) flight squadron (d) computer network

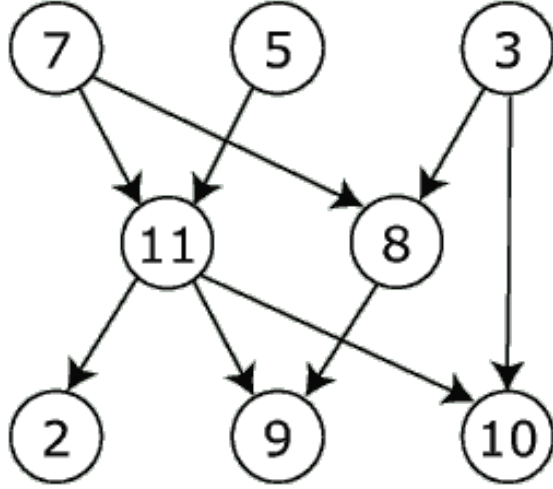


Figure 1.2: Example of the topological structure of MAS

an alternative approach utilizing braking and gyroscopic forces has been investigated in [30, 31, 32], yet they have been adapted in very few studies of formation control. We will therefore use braking and gyroscopic forces to carry out our analysis and validate their potential superiority in the obstacle avoidance process.

Furthermore, even though different types of control protocols can be used to accomplish formation control objectives, each agent’s device will have capacity and source limitations. This further reduces communication efficiency and increases network vulnerability due to external interference. This indicates that information transmission constraints need to be considered, and a fully continuous control scheme is no longer feasible. Therefore, impulsive control can be considered as an effective method to generate more reliable transmission on sampling instants while maintaining stability; particularly, the tolerance of instability in continuous system dynamics will be improved depending on the impulse strength. However, the stabilization process via Lyapunov-based stability theory cannot be directly applied and needs to be revised; instead, there have been several pioneering results [33, 34] that provide the fundamentals regarding stabilization of impulsive systems rigorously, including modified Lyapunov-based stability theory and impulsive control theory. Therefore, this thesis aims to derive analytical results for MAS formation stabilization based on these theoretical frameworks.

Inspired by the above discussion, the extensive applications of multi-agent systems and the effectiveness of impulsive control techniques suggest the need and importance to study formation control of multi-agent systems within an impulsive framework. In order to

further improve information transmission efficiency, data security and compensate limited signal processing speed, the main goal of this thesis is to develop impulsive control protocols that combine with several other practical control techniques such as hybrid control, event-triggered control, periodic intermittent control, pinning control; and then derive sufficient conditions for maintaining formation stabilization and collision-free motion of MAS subject to node heterogeneity and time delay effects.

1.2 Thesis Outline

The organization of this thesis is summarized as follows:

- **Chapter 1.** The introduction of this thesis is given, including thesis contributions and necessary notations.
- **Chapter 2.** General setup of multi-agent systems will be introduced, an overview of formation control/stabilization of multi-agent systems will be given, and the mathematical background information on impulsive control of multi-agent systems involving time delays will be provided.
- **Chapter 3.** The formation tracking control of multi-agent systems with time delays under a hybrid impulsive framework will be investigated. Additionally, the effectiveness of collision avoidance mechanisms using braking and gyroscopic forces will be compared with artificial potential functions (APFs). By utilizing the method of Lyapunov function/functional, Razumikhin technique, graph theory and linear matrix inequality (LMI), sufficient conditions for achieving global asymptotic stability and input-to-state stability of error dynamics will be derived.
- **Chapter 4.** Under the hybrid impulsive framework and directed inter-group communication, the multi-group formation tracking control of heterogeneous multi-agent system with a mixture of second-order and third order dynamics will be discussed.
- **Chapter 5.** This chapter will present the formation tracking control of unmanned aerial vehicle (UAV) systems by incorporating hybrid impulsive control schemes. Meanwhile, event-triggered and pinning mechanisms are also employed to further reduce control resource usage and transmission redundancy.
- **Chapter 6.** This chapter will address the finite-time hybrid impulsive formation tracking control of multi-agent systems via aperiodic intermittent communication.

Moreover, the concept of average impulsive interval and state-dependent control width can be used to handle an indefinite number of impulsive instants and automatic control width selection.

- **Chapter 7.** This chapter features an application of vehicle platoon to hybrid impulsive formation stabilization with time-dependent and state-dependent switching. To maintain designated string structure, the control objective is to ensure exponential stabilization of platoon tracking error.
- **Chapter 8.** In this chapter, we will conclude the thesis. A few potential research aspects for future research on the basis of this thesis will be addressed.

1.3 Thesis Scopes

The main scopes of this thesis are summarized as follows:

1. This thesis studies formation control problems of multi-agent systems under the hybrid impulsive framework, while incorporating a variety of control techniques and dynamic features. By exploiting the Lyapunov function/functional method, Razumikhin technique, graph theory and LMI approach, some novel criteria for maintaining asymptotic stabilization are established.
2. Delayed inputs including time-varying delays and delayed impulses are considered to compensate for transmission latency. The corresponding stability analysis is conducted with respect to the size of time delays and the length of the impulsive interval.
3. In contrast to [35, 36], heterogeneous networks with a mixture of second- and third-order dynamics are now considered, allowing the models to become more diverse and extend to higher orders. Meanwhile, the multi-group structure is established based on directed inter-group information exchange, as opposed to the undirected exchange discussed in [37]. In this manner, group-wise position and velocity alignment can be achieved with a relaxed interaction topology.
4. The development of hybrid impulsive control protocols with a pinning mechanism reduces transmission redundancy and eliminates the need to manually set impulsive instants.

5. Contrary to [38], we further improve the finite-time stability results into formation stabilization by using hybrid impulsive protocol with aperiodic intermittent communication and delayed impulses.
6. To facilitate real-life application, switching process between stable and unstable control of vehicle platoons is analyzed so that an exponential stabilization can still be realized.
7. Additionally, we use the concept of nonlinearity strength to adapt more generalized nonlinear multi-agent systems. Hence, local formation stabilization results can be obtained in the absence of conventional Lipschitz conditions, which differ from most existing results. Furthermore, braking and gyroscopic forces are deployed as collision avoidance mechanisms to prevent unexpected local minima using APFs [15].

1.4 Notations

In this section, we will introduce some necessary notations that are commonly used in this thesis. Some are modified from their standard notation to avoid confusion in future contexts.

Denote $\mathcal{G} = (\mathcal{V}, \mathcal{E})$ as a directed graph (or digraph) of order n , which consists of a vertex set $\mathcal{V} = \{\nu_1, \nu_2, \nu_3, \dots, \nu_n\}$, and an edge set $\mathcal{E} = \{(\nu_i, \nu_j)\} \subset \mathcal{V} \times \mathcal{V}$. As long as node ν_j can receive information from node ν_i , an edge $e_{ij} = (\nu_i, \nu_j)$ is added. $N_i = \{j \in \mathcal{V} | e_{ij} \in \mathcal{E}\}$ denotes the i -th neighbour set associated with \mathcal{G} . Furthermore, the weighted adjacency matrix $\mathcal{A} = [a_{ij}] \in \mathbb{R}^{n \times n}$ satisfies $a_{ij} > 0$ for $e_{ij} \in \mathcal{E}$ and $a_{ij} = 0$ otherwise. The Laplacian matrix of the graph $L = [l_{ij}] \in \mathbb{R}^{n \times n}$ is defined as $L = \mathcal{D} - \mathcal{A}$, where \mathcal{D} is a diagonal matrix with $l_{ii} = \sum_{i \neq j} a_{ij}$ and $l_{ij} = -a_{ij}$, $\forall i \neq j$. A sequence of edges e_{12}, e_{23}, \dots represents a directed path in \mathcal{G} . Moreover, if there is a directed path connecting any two arbitrary vertices of \mathcal{G} , then \mathcal{G} is said to be strongly connected; while \mathcal{G} is balanced if $\sum_{j=1, j \neq i}^n a_{ij} = \sum_{j=1, j \neq i}^n a_{ji}$.

Meanwhile, let $\mathbb{R}, \mathbb{N}, \mathbb{R}^+, \mathbb{N}^+$ to be the set of real numbers, natural numbers, positive real numbers and positive natural numbers respectively, \mathbb{R}^n as the set of n -dimensional real vector space, $\mathbb{R}^{n \times n}$ as the set of $n \times n$ real-valued matrices, $\|\cdot\|$ as the Euclidean norm, \otimes as the Kronecker product, while the smallest and largest eigenvalue of matrix L are $\lambda_{min}(L)$, $\lambda_{max}(L)$ respectively and $\|L\| = \sqrt{\lambda_{max}(L^T L)}$. In addition, $\mathbf{0}_{n \times n}$, $\mathbf{0}_n$ and $\mathbf{1}_n$ are set to be the $n \times n$ zero matrix, $n \times 1$ column vector of zeros and ones. For $a, b \in \mathbb{R}$ with $a < b$ and $S \subseteq \mathbb{R}^n$, we define $\mathcal{PC}([a, b], S) = \{\psi : [a, b] \rightarrow S | \psi(t) = \psi(t^+), \text{ for any } t \in$

$[a, b]$; $\psi(t^-)$ exists in S , for any $t \in (a, b]$; $\psi(t^-) = \psi(t)$ for all but at most a finite number of points $t \in (a, b]$, $\mathcal{PC}([a, \infty), S) = \{\psi : [a, \infty) \rightarrow S \mid \text{for any } c > a, \psi|_{[a, c]} \in \mathcal{PC}([a, c], S)\}$. $\delta(\cdot)$ represents the Dirac delta function satisfying $\int_{-\infty}^{\infty} \delta(x) dx = 1$ and

$$\delta(x) = \begin{cases} 0, & x \neq 0 \\ \infty, & x = 0 \end{cases}$$

Moreover, we denote the following:

- Given $h > 0$, a norm defined by $\|\varphi\|_h := \sup_{s \in [-h, 0]} \|\varphi(s)\|$ for $\varphi \in \mathcal{PC}([-h, 0], \mathbb{R}^n)$ is equipped by the linear space $\mathcal{PC}([-h, 0], \mathbb{R}^n)$; for simplicity, we consider $\|\varphi\|_h = \varphi(0)$ and $\mathcal{PC} = \mathcal{PC}([-h, 0], \mathbb{R}^n)$.
- If function $\alpha : \mathbb{R}^+ \rightarrow \mathbb{R}^+$ is continuous, strictly increasing with $\alpha(0) = 0$, then α is said to be class \mathcal{K} . Then $\mathcal{K}_\infty = \{\alpha \in C(\mathbb{R}^+, \mathbb{R}^+) \mid \alpha(0) = 0, \alpha(k) \text{ is strictly increasing in } k, \text{ and } \alpha(k) \rightarrow \infty \text{ as } k \rightarrow \infty\}$.
- A function $\beta : \mathbb{R}^+ \times \mathbb{R}^+ \rightarrow \mathbb{R}^+$ is said to be of class \mathcal{KL} if $\beta(\cdot, t) \in \mathcal{K}$ for each $t \in \mathbb{R}^+$ and $\beta(s, t)$ decreases to 0 as $t \rightarrow \infty$ for each $s \in \mathbb{R}^+$.
- A function $\bar{\delta} : \mathbb{R}^+ \times \mathbb{R}^n \rightarrow \mathbb{R}^+$ is said to be of class ν_0 if for each $x \in \mathcal{PC}(\mathbb{R}^+, \mathbb{R}^n)$, the composite function $t \mapsto \bar{\delta}(t, x(t))$ is also in $\mathcal{PC}(\mathbb{R}^+, \mathbb{R}^n)$ and can be discontinuous at some $t' \in \mathbb{R}^+$ only when t' is a discontinuity point of x .
- A functional $\bar{\delta} : \mathbb{R}^+ \times \mathcal{PC}([-r, 0], \mathbb{R}^n) \rightarrow \mathbb{R}^n$ is said to be of class ν_0^* if for each function $x \in \mathcal{PC}([-r, \infty), \mathbb{R}^n)$, the composite function $t \mapsto \bar{\delta}(t, x_t)$ is continuous in t for all $t \geq 0$ with $x_t(s) = x(t + s)$ if $s \in [-r, 0]$.

Chapter 2

Background

2.1 Multi-agent System Model

According to the introduction on multi-agent systems in Chapter 1, the generalized leader-following dynamics of multi-agent systems with $n+1$ nodes can be described as follows:

$$\begin{cases} \dot{x}_i = f_i(t, x_i, x_{it}) + u_i(t, \mathbf{x}), & i = 1, \dots, n \\ \dot{x}_0 = f_0(t, x_0, x_{0t}) \end{cases} \quad (2.1)$$

where $x_i \in \mathbb{R}^m$ for $i = 1, \dots, n$ denotes the state of the i -th follower node and $x_0 \in \mathbb{R}^m$ represents the leader state. We define $x_{0t} = x_0(t+s)$, $x_{it} = x_i(t+s)$ for $s \in [-\tau, 0]$ and $\tau > 0$ represents the time delay, denote $\mathbf{x} = [(x_1 - x_0)^T, \dots, (x_n - x_0)^T]^T$. The function $f_i : \mathbb{R}^+ \times \mathcal{PC}(\mathbb{R}^+, \mathbb{R}^m) \times \mathcal{PC}([-\tau, 0], \mathbb{R}^m) \rightarrow \mathbb{R}^m$ describes the intrinsic dynamics of node i ; $u_i : \mathbb{R}^+ \times \mathcal{PC}(\mathbb{R}^+, \mathbb{R}^{mn}) \rightarrow \mathbb{R}^m$ is the control input of node i to be designed.

Remark 2.1.1. *Different from the structure of neural networks (i.e., BAM [39], Cohen-Grossberg [40], Hopfield [41] and cellular [42]), the interactions of node i with other nodes in terms of delay-free/delayed coupling and tracking navigation now need to be established in the controller rather than intrinsically. Such manner can also be regarded as the conceptual distinction between formation consensus problem and synchronization [43].*

In practice, the double-integrator dynamic model is commonly used to monitor position (p) and velocity (v) evolution, while ensuring their convergence to desired configuration [44, 45, 46]:

$$\begin{cases} \dot{p}_i = v_i \\ \dot{v}_i = u_i, & i = 1, \dots, n \end{cases} \quad (2.2)$$

Besides double-integrator dynamic model, various other types of MAS dynamic model can also be adapted from (2.1), such as single-integrator dynamic model [47], high-order dynamic model [48] and general linear dynamic model [49]. Therefore, formation control results obtained from this thesis can be applied to these MAS dynamic models.

2.2 Formation Control

Formation control is a concept in control theory and robotics that refers to the coordination of multiple autonomous agents, such as robots or drones, to move together in a predetermined formation. The agents are equipped with sensors and communication devices that allow them to share information about their positions and velocities, and to adjust their movements in real-time to maintain the desired formation.

Due to the features of multi-agent systems, formation control has advantages over single-agent systems in terms of efficiency, robustness, and scalability. By working together in a formation, the agents can cover more operation area, reduce redundancy, and perform tasks that would be difficult or impossible for a single agent to accomplish alone. So far, formation control still remains as an active research area, with ongoing efforts to improve the design and implementation of formation control algorithms, to address issues such as communication delays, sensor noise, and environmental uncertainties, etc.

Based on the survey of multi-agent formation control conducted in [50], existing results of formation control can be classified in terms of different system and control aspects. Firstly, according to the sensing capabilities as show in Figure 2.1, it can be categorized into:

1. **Position-based control** [44]: Agents sense their own positions with respect to a global coordinate system (i.e., an entity that gathers information from all agents, makes decision, and then distributes coordination command to the agents). It is particularly beneficial in terms of interaction topology, yet it requires more advanced sensors equipped.
2. **Displacement-based control** [51, 52]: Agents actively control displacements of their neighboring agents to achieve the desired formation, which is specified by the desired displacement with respect to a global coordinate system (i.e., the orientation of global coordinate system). It has moderate requirement of both sensing capability and the interaction topology of agents.

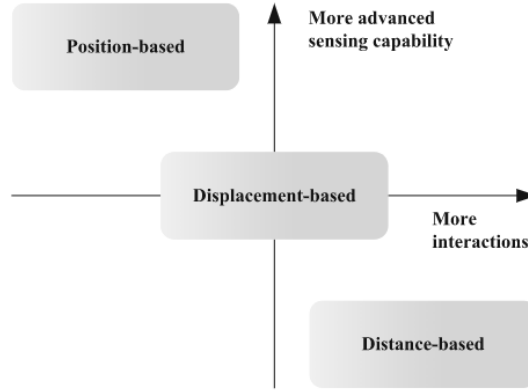


Figure 2.1: Sensing capability vs. interaction topology

3. **Distance-based control** [15]: Inter-agent distances are actively controlled to achieve the desired formation, which is given by the desired inter-agent distances. It is advantageous in terms of sensing capability, but it requires more interaction among agents. If the interaction graph of the multi-agent system is not complete, the agents are required to achieve desired distance by controlling partial inter-agent distances. This imposes the requirement on the interaction graph, which can be characterized by rigidity or persistence.

Secondly, according to whether or not desired formations are time-varying [53], the formation control problems can be classified as:

1. **Formation producing:** The objective is to achieve a prescribed desire formation shape.
2. **Formation tracking:** Reference trajectories for agents are prescribed and the agents are controlled to track the trajectories.

Thirdly, according to fundamental ideas in control schemes, [10, 22] have classified formation control into:

1. **Leader-follower approach:** The follower agents track the state of the leader with some prescribed offsets while the leader tracks its desired trajectory [15, 27].

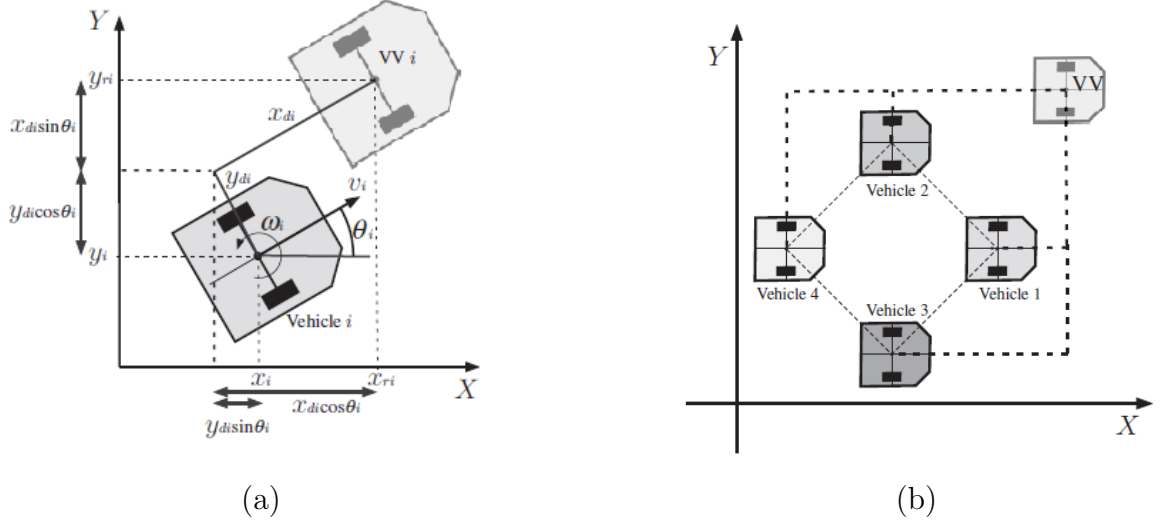


Figure 2.2: (a) i -th vehicle and corresponding virtual vehicle (b) position of VSs

2. **Behavioral approach:** Such desired behaviours include inter-agent collision/environmental obstacle avoidance via artificial potential fields [15], braking and gyroscopic forces [30, 31]. This approach is related to amorphous formation control described below.
3. **Virtual structure approach:** In this approach, the formation of agents is considered as a single object, so-called a virtual structure (VS). The desired motion for the virtual structure is given, while the desired motions for the agents are determined from that of the virtual structure. To maintain any formations [54], the corresponding VS of each agent has to converge to a common desired configuration as shown in Figure 2.2.

Lastly, according to whether or not desired formation shapes are explicitly prescribed, the formation control problem can be classified as:

1. **Morphous formation control:** Desired formations are explicitly specified.
2. **Amorphous formation control:** Without explicitly specified desired formations, and it is related to behavioral approach.

There are some other approaches that do not fit neatly into the categorization above, yet they are highly relevant to formation control.

1. **Flocking** [2, 15, 27]

Flocking is the collective behaviour discovered in various fields, in which the coordinated motion of a large number of agents is generated using only limited environmental information and Reynolds rules: cohesion, separation and alignment. Majority of the flocking control laws can be viewed as the implementation of Reynolds rules via distance-based approach.

2. **Containment control** [55, 56]

In containment control problems, follower agents are driven into the convex hull spanned by leader agents based on consensus protocol while leaders behave autonomously. In this manner, leader agents can drive the follower agents to specified target destination. This approach is practically advantageous since followers do not require expensive sensors.

3. **Angle-based control** [57]

Although position, displacement, and distance measurements have been dominantly used, angular measurements can be used for multi-agent formation control as well, such as bearing-based or attitude stabilization control of spacecraft and autonomous underwater vehicle (AUV).

4. **Cyclic pursuit** [58]

The cyclic pursuit strategy is based on the idea that each agent tracks and pursues its nearest neighbor in a cyclic order. The agents are organized in a circular or elliptical formation, where the order of pursuit is predefined.

Throughout this thesis, we primarily focus on the design of displacement-based formation tracking control of double-integrator multi-agent systems, along with collision avoidance. Meanwhile, the intuitive definition of formation tracking objectives is given as:

Definition 2.2.1. *The leader-following multi-agent systems described by (2.2) are said to*

achieve formation stabilization under proper control inputs u_i if

$$\begin{cases} \lim_{t \rightarrow \infty} \|p_i(t) - p_0(t) - p_{id}\| = 0 \\ \lim_{t \rightarrow \infty} \|v_i(t) - v_0(t)\| = 0, \quad i = 1, \dots, n \end{cases} \quad (2.3)$$

where $p_{id} \in \mathbb{R}^m$ represents the predetermined desired displacement between node i and the leader.

2.3 Impulsive Control Method

Consider the nonlinear multi-agent systems with time-delay

$$\begin{cases} \dot{x} = f(t, x_t) \\ x_{t_0} = \phi \end{cases} \quad (2.4)$$

where $x \in \mathbb{R}^m$ is the state vector, x_t is defined as $x_t(s) = x(t+s)$ for $s \in [-\tau, 0]$ and τ is the time-delay in system (2.4); $f : \mathbb{R}^+ \times \mathcal{PC}([-\tau, 0], \mathbb{R}^m) \rightarrow \mathbb{R}^m$ is the nonlinear intrinsic function and $\phi \in \mathcal{PC}([-\tau, 0], \mathbb{R}^m)$ is the initial function.

For the nonlinear system (2.4), an impulsive control law can be constructed as the sequence $\{t_k, U_k(t_k, x(t_k))\}$, where $0 \leq t_0 < t_1 < \dots < t_k < \dots, \lim_{t \rightarrow \infty} t_k = \infty$ and $U_k : \mathbb{R}^+ \times \mathbb{R}^m \rightarrow \mathbb{R}^m$ indicates the control input at each impulsive instant t_k . Then it leads to the following impulsive system:

$$\begin{cases} \dot{x} = f(t, x_t), \quad t \neq t_k \\ \Delta x(t_k) = U_k(t_k, x(t_k)), \quad k = 1, 2, \dots \\ x_{t_0} = \phi \end{cases} \quad (2.5)$$

with $\Delta x(t_k) = x(t_k^+) - x(t_k^-)$, $x(t_k^-)$ indicates the state before the jump, while $x(t_k^+)$ indicates the state after the jump (i.e., $x(t_k^+) = x(t_k^-) + U_k(t_k^-, x(t_k^-))$). Therefore, according to system (2.5), there will be an abruptly state change (i.e., $\Delta x(t_k)$) at each impulsive instant t_k when adapting an impulsive control law to system (2.4). Such process will maintain as long as the solution of system (2.4) exists with initial condition $x_{t_k} = x(t_k + s)$ for $s \in [-\tau, 0]$, and the impulsive controller can be designed as:

$$u(t, x) = \sum_{k=1}^{\infty} U_k(t, x(t)) \delta(t - t_k) \quad (2.6)$$

Then its corresponding impulsive system can be written as:

$$\begin{cases} \dot{x} = f(t, x_t) + u(t, x) \\ x_{t_0} = \phi \end{cases} \quad (2.7)$$

In fact, system (2.7) under impulsive controller (2.6) is equivalent to system (2.5).

The existence and uniqueness results for impulsive delay differential equations (2.5) has been address in [59]:

Theorem 2.3.1. *(Existence and Uniqueness) Assume that for each compact set $F \subset D$, there exists a locally Lebesgue integrable function $m \in L_1^{loc}(J, \mathbb{R}^+)$ such that $\|f(t, x_t)\| \leq m(t)$ and $f(t, x_t)$ is a measurable function of t for all $t \in J$ and for all $x \in \mathcal{PC}([l_J - \tau, r_J], F)$ (recall $J = [l_J, r_J]$). Assume also that for each fixed $t \in J$, $f(t, \psi)$ is a continuous function of ψ . Then for each $t_0 \in J$, $\omega \in D$ and $\psi \in \mathcal{PC}([-\tau, 0], D)$ there exists a solution of (2.5) on $t \in [t_0 - \tau, t_0 + \beta)$ for some $\beta > 0$ where $[t_0, t_0 + \beta) \in J$. Meanwhile, if there exists a Lebesgue integrable function $\Gamma \in L_1([t_0, t_0 + \beta], \mathbb{R}^+)$ such that $\|f(t, \psi_1) - f(t, \psi_2)\| \leq \Gamma(t)\|\psi_1 - \psi_2\|_\tau$ for all $t \in [t_0, t_0 + \beta]$ and for all $\psi_1, \psi_2 \in \mathcal{PC}([-\tau, 0], F)$. Then there exists at most one solution of (2.5) on $t \in [t_0 - \tau, t_0 + \beta]$*

Further existence and uniqueness results for impulses at variable times and impulsive hybrid stochastic delay system can be found in [33, 60], respectively.

Moreover, we need to ensure the stability of system (2.7) can be achieved by applying impulsive controller (2.6) (i.e., impulsive stabilization). Previously, numerous Lyapunov stability criteria subject to nonlinear impulsive systems have been developed by incorporating Lyapunov functional method [61, 62], Razumikhin technique [34, 43] and impulsive comparison principle [63, 64]. All of them require the allocation of the relationship associated with the rate of change of Lyapunov candidate ($D^+V(t)$) and state jump magnitude of Lyaunov function ($\Delta V(t_k)$). Specifically,

Definition 2.3.1. *Given a function $V \in \nu_0$, the upper right-hand derivative $D^+V(t, \psi(0))$ is defined as*

$$D^+V(t, \psi(0)) = \limsup_{h \rightarrow 0^+} \frac{1}{h} [V(t+h, \psi(0) + hf(t, \psi)) - V(t, \psi(0))] \quad (2.8)$$

where $(t, \psi) \in [t_0, \infty) \times \mathcal{PC}([-\tau, 0], \mathbb{R}^m)$.

Definition 2.3.2. *Given a functional $V \in \nu_0^*$, the upper right-hand derivative $D^+V(t, \psi)$ is defined as*

$$D^+V(t, \psi) = \limsup_{h \rightarrow 0^+} \frac{1}{h} [V(t+h, x_{t+h}(t, \psi)) - V(t, \psi)] \quad (2.9)$$

where $(t, \psi) \in \mathbb{R}^+ \times \mathcal{PC}([-\tau, 0], \mathbb{R}^m)$.

We use \dot{V} to represent the upper right-hand derivative D^+V in later chapters for simplicity.

As soon as the impulsive dynamical relationship with respect to $D^+V(t)$ and $\Delta V(t_k)$ has been established, the impulsive comparison system can be determined using the upper bound of the relationship. In practice, on the one hand, the rate of change of Lyapunov function can be fully utilized via Razumikhin technique when dealing with stability of delay systems. On the other hand, Lyapunov-Razumikhin technique has the advantage of bringing down the value of a Lyapunov function at each impulsive instant, whereas the instantaneous impulse fails to reduce the value of a functional. Therefore, although Lyapunov functional method remains more general as the Razumikhin technique can be treated as a special case of it, it is still more complicated and challenging upon the selection of appropriate Lyapunov functional with more control techniques involved.

Chapter 3

Hybrid Impulsive Formation Control of MASs

In this chapter, we present the formation stabilization of nonlinear multi-agent systems with time-varying delay and delayed impulses under a hybrid impulsive control scheme. On top of impulsive control method, we employ hybrid control mechanism so that partially continuous interactions among agents are generated, in order to mitigate the effect of abrupt information transmission via full scale control impulses. Typical types of hybrid consensus protocols with the coexistence of discontinuous-time and continuous-time subsystems have been studied in [65, 66]. Stability results are derived using the Lyapunov-Razumikhin technique with respect to different sizes of delayed impulses. In addition, we examine the effectiveness of formation stabilization when collision avoidance mechanisms via braking and gyroscopic forces are included. The hybrid impulsive control framework investigated here will be inherited throughout the remainder of the thesis.

It is worth mentioning that in control systems, time delay can arise due to a variety of factors such as communication delays in networked control systems, transport delays in physical systems, or processing delays in digital control systems. It often has a significant impact on the performance and stability of control systems, since it can lead to oscillations, instability, and poor tracking accuracy, among other issues. For instance, in a temperature control system, a delay in the temperature sensor can cause the control system to overshoot or undershoot the desired temperature. Recently, many studies such as [34] has investigated consensus or synchronization problem of impulsive systems involving time delays. Therefore, it is inevitable to consider delayed transmission in the hybrid impulsive control process of MASs.

3.1 Problem Formulations

Consider the leader-following double-integrator multi-agent systems consisting of $n+1$ agents. The dynamics of each follower agent is described as:

$$\begin{cases} \dot{p}_i(t) = v_i(t) \\ \dot{v}_i(t) = \alpha_p p_i(t) + \alpha_v v_i(t) + f(v_i(t)) + u_i, \quad i = 1, \dots, n \end{cases} \quad (3.1)$$

and the dynamics of the leader is described as:

$$\begin{cases} \dot{p}_0(t) = v_0(t) \\ \dot{v}_0(t) = \alpha_p p_0(t) + \alpha_v v_0(t) + f(v_0(t)) \end{cases} \quad (3.2)$$

where $p_i, v_i \in \mathbb{R}^2$ for $i = 0, \dots, n$ are the position and velocity states of agent i respectively; $\alpha_p, \alpha_v \in \mathbb{R}$ are constants; $f(v_i(t)) : \mathbb{R}^2 \rightarrow \mathbb{R}^2$ represents the nonlinear intrinsic dynamics of agent i ; u_i is the hybrid impulsive control inputs to be designed hereafter. In addition, for $i = 1, \dots, n$ we denote $\hat{p}_i = p_i - p_0 - p_{id}$ where p_{id} is the predetermined desired displacement between nod i and the leader, $\hat{v}_i = v_i - v_0$, $\hat{f}_i = f(v_i) - f(v_0)$; $\bar{p} = [\hat{p}_1^T, \dots, \hat{p}_n^T]^T$, $\bar{v} = [\hat{v}_1^T, \dots, \hat{v}_n^T]^T$ and $\bar{f} = [\hat{f}_1^T, \dots, \hat{f}_n^T]^T$ for later use.

Remark 3.1.1. *In this thesis, we consider $p_i, v_i \in \mathbb{R}^2$ as indicated (3.1) for the rest of chapters except Chapter 5 where a specific unmanned aerial vehicle (UAV) dynamics is considered with $p_i, v_i \in \mathbb{R}^3$. In general, any arbitrary dimension of state variables can be applied under our proposed formation stabilization results (i.e., $p_i, v_i \in \mathbb{R}^n$) for consistency. Therefore, in practice, it enables to adapt any specific model dynamics such as UAV in Chapter 5 and vehicle platoon in Chapter 7.*

In order to ensure formation stabilization of leader-following dynamics (3.1) and (3.2), we design the hybrid impulsive control protocol as follows:

$$u_i = -\alpha_p p_{id} + P_C(\hat{p}_i(t-r(t)), \hat{v}_i(t-r(t))) + \mu_i P_D(\hat{p}_i(t), \hat{v}_i(t)) + \mu_i P_L(\hat{p}_i(t-\tau), \hat{v}_i(t-\tau)) \quad (3.3)$$

with

$$\begin{cases} P_C(\hat{p}_i(t), \hat{v}_i(t)) = -\sum_{j \in N_i^1} b_{ij}(\hat{p}_i(t) - \hat{p}_j(t)) - \sum_{j \in N_i^1} b_{ij}(\hat{v}_i(t) - \hat{v}_j(t)) \\ P_D(\hat{p}_i(t), \hat{v}_i(t)) = -\sum_{k=1}^{\infty} \sum_{j \in N_i} b_{ij}(\hat{p}_i(t) - \hat{p}_j(t))\delta(t - t_k) \\ \quad - \sum_{k=1}^{\infty} \sum_{j \in N_i} b_{ij}(\hat{v}_i(t) - \hat{v}_j(t))\delta(t - t_k) \\ P_L(\hat{p}_i(t), \hat{v}_i(t)) = -\sum_{k=1}^{\infty} c\hat{p}_i(t)\delta(t - t_k) - \sum_{k=1}^{\infty} c\hat{v}_i(t)\delta(t - t_k) \end{cases} \quad (3.4)$$

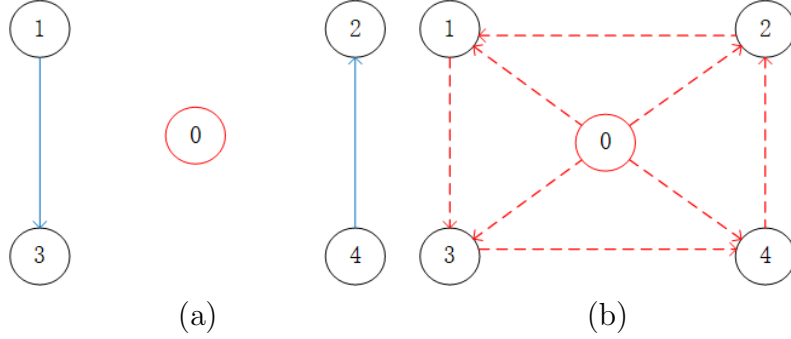


Figure 3.1: Example of topology structure under protocol (3.3) during (a) continuous (b) impulsive transmission

where $0 < \mu_i < 1$ is an adjustment parameter, $r(t) \leq \bar{r}$ and τ are bounded time-varying delay and impulse delay respectively. $\{t_k\}_{k \in \mathbb{N}^+}$ is the sequence of impulse times and satisfies $0 \leq t_0 < t_1 < \dots < t_k < t_{k+1} < \dots$, $\lim_{k \rightarrow \infty} t_k = \infty$. Meanwhile, $\delta(\cdot)$ is the dirac function, $N_i^1 \subset N_i$ is the neighbor set of the hybrid topology (see Figure 3.1) for $t \neq t_k$, b_{ij} stands for coupling strength among follower agents. $c > 0$ is the position navigation feedback gain.

Remark 3.1.2. *Figure 3.1 illustrates the interaction topology among agents via the hybrid impulsive control protocol (3.3). Specifically, follower agents experience partial continuous transmission (i.e., blue solid lines), resulting in hybrid behaviour. In the meantime, at each impulsive instant, the strongly connected and balanced transmission topology (i.e., red dashed lines) will be created, while the leader node acts as root node of a spanning tree.*

Then based on (3.3), the corresponding error dynamics of (3.1) and (3.2) can be written as:

$$\begin{cases} \dot{\hat{p}}_i(t) = \hat{v}_i(t) \\ \dot{\hat{v}}_i(t) = \alpha_p \hat{p}_i(t) + \alpha_v \hat{v}_i(t) + \hat{f}_i(t) + P_C(\hat{p}_i(t - r(t)), \hat{v}_i(t - r(t))), & t \neq t_k \\ \Delta \hat{v}_i(t_k) = \mu_i P_D(\hat{p}_i(t_k), \hat{v}_i(t_k)) + \mu_i P_L(\hat{p}_i(t_k - \tau), \hat{v}_i(t_k - \tau)), & t = t_k \quad i = 1, \dots, n \end{cases} \quad (3.5)$$

where $\Delta \hat{v}_i(t_k) = \hat{v}_i(t_k^+) - \hat{v}_i(t_k^-)$, and for simplicity we take $\hat{v}_i(t_k) = \hat{v}_i(t_k^+)$. The initial condition of system (3.5) is denoted as $\hat{\xi}_i(t_0 + \theta) = \phi_i(\theta) - \xi_0(t_0)$ for $i = 1, \dots, n$ where $\phi_i \in \mathcal{PC}([- \max\{r(t), \tau\}, 0], \mathbb{R}^4)$ and $\hat{\xi}_i = [\hat{p}_i^T, \hat{v}_i^T]^T$. Moreover, denote $\bar{\xi} = [\bar{p}^T, \bar{v}^T]^T$, we

can write system (3.5) in compact form as:

$$\begin{cases} \dot{\bar{\xi}}(t) = \begin{pmatrix} \mathbf{0}_{2n \times 2n} & I_{2n} \\ \alpha_p I_{2n} & \alpha_v I_{2n} \end{pmatrix} \bar{\xi}(t) + \begin{pmatrix} \mathbf{0}_{2n \times 2n} & \mathbf{0}_{2n \times 2n} \\ -L' & -L' \end{pmatrix} \bar{\xi}(t - r(t)) + \begin{pmatrix} \mathbf{0}_{2n} \\ \bar{f}(t) \end{pmatrix} \\ = E_0 \bar{\xi}(t) + E_1 \bar{\xi}(t - r(t)) + E_2(t), \quad t \neq t_k \\ \Delta \bar{v}(t_k) = -\mu_i L \bar{p}(t_k) - \mu_i L \bar{v}(t_k) - \mu_i c \bar{p}(t_k - \tau) - \mu_i c \bar{v}(t_k - \tau), \quad t = t_k \end{cases} \quad (3.6)$$

where $L' \in \mathbb{R}^{2n \times 2n}$ represents the Laplacian matrix corresponding to the neighbor set N_i^1 during continuous transmission, and the initial condition of system (3.6) becomes $\bar{\xi}(t_0 + \theta) = [\phi_i(\theta) - \xi_0(t_0)] \otimes \mathbf{1}_n$. For further discussion, we may need the following assumptions and lemmas for formation stabilization results.

Assumption 3.1.1. *The overall interaction topology \mathcal{G} remains strongly connected and balanced, where the leader acts as the root node.*

Assumption 3.1.2. *Suppose the nonlinear intrinsic function f satisfies the Lipschitz condition such that*

$$\|f(u) - f(v)\| \leq \alpha \|u - v\| \quad (3.7)$$

where $\alpha > 0$ for all $u, v \in \mathbb{R}^2$.

Remark 3.1.3. *In practice, both state values and control signals being transmitted are bounded, hence Assumption 3.1.2 is obtained as long as f is continuously differentiable.*

Lemma 3.1.1. *For any vectors $x, y \in \mathbb{R}^n$ and any symmetric positive definite matrix M , we have $2x^T y \leq x^T M x + y^T M^{-1} y$.*

Consider the impulsive system

$$\begin{aligned} \dot{x} &= f(t, x_t), \quad t \neq t_k \\ \Delta x(t) &= I_k(t, x_{t-}), \quad t = t_k, \quad k \in \mathbb{N}^+ \\ x_{t_0} &= \phi \end{aligned} \quad (3.8)$$

where $f, I_k : \mathbb{R}^+ \times \mathcal{PC}([-\tau, 0], \mathbb{R}^n) \rightarrow \mathbb{R}^n$, $\phi \in \mathcal{PC}([-\tau, 0], \mathbb{R}^n)$.

Lemma 3.1.2. [34] *For constant ω and non-negative constants β , ρ_1 , and ρ_2 , the function $V \in \mathcal{PC}([t_0 - \tau, \infty), \mathbb{R}^+)$ satisfies*

$$\begin{aligned} V'(t) &\leq \omega V(t) + \beta \sup_{s \in [-\tau, 0]} V(t + s), \quad t \neq t_k \\ V(t_k) &\leq \rho_1 V(t_k^-) + \rho_2 \sup_{s \in [-\tau, 0]} V(t_k^- + s), \quad k \in \mathbb{N}^+ \\ V_{t_0} &= \Upsilon \end{aligned} \quad (3.9)$$

where $\Upsilon \in \mathcal{PC}([-\tau, 0], \mathbb{R}^+)$. If $\omega + \beta \geq 0$ and

$$\frac{1}{\rho_1 + \rho_2} > e^{(\omega + \frac{\beta}{\rho_1 + \rho_2})\sigma} > 1 \quad (3.10)$$

where $\sigma = \sup_{k \in \mathbb{N}^+} \{t_k - t_{k-1}\}$, then $\lim_{t \rightarrow \infty} V(t) = 0$.

Lemma 3.1.3. [62] Assume that there exists $V_1 \in \nu_0$, $V_2 \in \nu_0^*$, and constants $p, c, w_1, w_2, w_3, \rho_1 > 0$ and $\rho_2 \geq 0$, such that

(i) $w_1 \|x\|^p \leq V_1(t, x) \leq w_2 \|x\|^p$, $0 \leq V_2(t, \psi) \leq w_3 \|\psi\|_\tau^p$, for $t \in \mathbb{R}^+$, $x \in \mathbb{R}^+$ and $\psi \in \mathcal{PC}([-\tau, 0], \mathbb{R}^n)$;

(ii) for $V(t, \psi) = V_1(t, \psi(0)) + V_2(t, \psi)$,

$$V'(t, \psi) \leq cV(t, \psi)$$

for $t \in [t_{k-1}, t_k)$, $\psi \in \mathcal{PC}([-\tau, 0], \mathbb{R}^n)$, and $k \in \mathbb{N}^+$;

(iii) for $k \in \mathbb{N}^+$ and $\psi \in \mathcal{PC}([-\tau, 0], \mathbb{R}^n)$,

$$V_1(t_k, \psi(0) + I_k(t_k, \psi)) \leq \rho_1 V_1(t_k^-, \psi(0)) + \rho_2 \sup_{s \in [-\tau, 0]} \{V_1(t_k^- + s, \psi(s))\}$$

(iv) $\ln(\rho + \frac{w_3}{w_1}) < -c\delta$, where $\rho = \rho_1 + \rho_2$ and $\delta = \sup_{k \in \mathbb{N}^+} \{t_k - t_{k-1}\}$.

Then the trivial solution of system (3.8) is globally exponentially stable.

Remark 3.1.4. By utilizing Razumikhin technique and the method of Lyapunov functional respectively, Lemma 3.1.2 and Lemma 3.1.3 provide sufficient criteria to stabilize nonlinear delay systems via proper design of impulsive control inputs, while the detail proof of both lemmas can be found in [34, 62, 67] and we may use them in later chapters. Based on their conditions, we see that both impulsive strength coefficients ρ_1 and ρ_2 are independent of impulsive instant t_k with $k \in \mathbb{N}^+$, while the uniform upper bound of the length of each impulsive interval is required to be restricted. However, the uniform condition on the upper bound of each impulsive interval can be removed, according to [62], by replacing condition (iv) with $\ln(\rho_{1k} + \rho_{2k}e^{\alpha\tau} + \frac{w_3}{w_1}e^{\alpha\tau}) < -c(t_{k+1} - t_k)$ for all $k \in \mathbb{N}$. Furthermore, the tolerance of instability on continuous dynamics (i.e., value of ω, β and c) exhibits negative correlation with respect to the upper bound of the impulsive interval and impulsive strengths.

3.2 Formation Stabilization

In this section, we derive delay-dependent formation stabilization criteria for MASs (3.1) and (3.2) under hybrid impulsive control (3.3) via Lyapunov-Razumikhin technique.

3.2.1 Case I: $\tau < \inf\{t_k - t_{k-1}\}$, $k \in \mathbb{N}^+$

In order to compensate impulsive delay τ , we need to utilize the Halanay-type inequality as the following.

Lemma 3.2.1. [34] *For $x, y, z \in \mathbb{R}$ and any $\varepsilon, \zeta > 0$, the following inequality holds*

$$(x + y + z)^2 \leq (1 + \varepsilon)x^2 + (1 + \varepsilon^{-1})(1 + \zeta)y^2 + (1 + \varepsilon^{-1})(1 + \zeta^{-1})z^2 \quad (3.11)$$

Theorem 3.2.1. *Consider the leader-following multi-agent systems with dynamics (3.1) and (3.2) followed by control protocol (3.3). Suppose Assumption 3.1.1 and Assumption 3.1.2 hold, $P \in \mathbb{R}^{4n \times 4n}$ is a positive definite matrix, $\varepsilon_0, \varepsilon_1, \varepsilon_2, \zeta_1 > 0$ and $\tau_{max} = \bar{r} + \tau$. If the following conditions are satisfied:*

$$\rho_1 + \rho_2 < 1 \quad (3.12)$$

$$e^{(\omega + \frac{\beta}{\rho_1 + \rho_2})\sigma} > 1 \quad (3.13)$$

where $\bar{\alpha} = \sqrt{n\alpha^2}$, $\sigma = \sup_{k \in \mathbb{N}^+} \{t_k - t_{k-1}\}$, $\omega = M + \varepsilon_0 P^{-1}$, $\beta = \frac{Q\lambda_{max}(P^{-1})}{\varepsilon_0}$, $\rho_1 = \frac{\pi_1(1+\varepsilon_2)}{2}$, $\rho_2 = \frac{1}{2}(1+\varepsilon_2^{-1})\pi_2$, $\pi_1 = 2\lambda_{max}((J+K)^T P (J+K) P^{-1})$ and $\pi_2 = 2\lambda_{max}(P)\tau^2 \|K\|^2 \kappa \lambda_{max}(P^{-1})$ with $\kappa = (1 + \varepsilon_1)\|E_0\|^2 + (1 + \varepsilon_1^{-1})(1 + \zeta_1)\|E_1\|^2 + \bar{\alpha}^2(1 + \varepsilon_1^{-1})(1 + \zeta_1^{-1})$, $M = [PE_0 + E_0^T P + 2\bar{\alpha}P]P^{-1}$, $Q = \|PE_1\|^2$, $E_3 = J - I_{4n}$, $J = \begin{pmatrix} I_{2n} & \mathbf{0}_{2n \times 2n} \\ -\mu_i L & I_{2n} - \mu_i L \end{pmatrix}$, and $K = \begin{pmatrix} \mathbf{0}_{2n \times 2n} & \mathbf{0}_{2n \times 2n} \\ -\mu_i c I_{2n} & -\mu_i c I_{2n} \end{pmatrix}$. Then the compact error dynamics (3.6) will be driven to zero asymptotically, and all the objectives of formation stabilization will be achieved.

Proof. Construct the following Lyapunov function for $t \in [t_k, t_{k+1})$ as:

$$V(t) = \frac{1}{2} \bar{\xi}^T(t) P \bar{\xi}(t) \quad (3.14)$$

Then, based on Assumption 3.1.1, Assumption 3.1.2 and Lemma 3.1.1 and system (3.6), we take the time derivative of V which gives:

$$\begin{aligned}
\dot{V}(t) &\leq \frac{1}{2}\bar{\xi}^T(t)[PE_0 + E_0^T P]\bar{\xi}(t) + \frac{1}{2}\bar{\xi}^T(t)PE_1\bar{\xi}(t-r(t)) + \frac{1}{2}\bar{\xi}^T(t-r(t))E_1^T P\bar{\xi}(t) + \bar{\alpha}\bar{\xi}^T(t)P\bar{\xi}(t) \\
&\leq \frac{1}{2}\bar{\xi}^T(t)[PE_0 + E_0^T P]\bar{\xi}(t) + \frac{\varepsilon_0}{2}\bar{\xi}^T(t)\bar{\xi}(t) + \frac{Q}{2\varepsilon_0}\bar{\xi}^T(t-r(t))\bar{\xi}(t-r(t)) + \bar{\alpha}\bar{\xi}^T(t)P\bar{\xi}(t) \\
&= \frac{1}{2}\bar{\xi}^T(t)[PE_0 + E_0^T P + 2\alpha P]\bar{\xi}(t) + \frac{\varepsilon_0}{2}\bar{\xi}^T(t)P^{-1}P\bar{\xi}(t) + \frac{Q}{2\varepsilon_0}\bar{\xi}^T(t-r(t))P^{-1}P\bar{\xi}(t-r(t)) \\
&\leq \frac{1}{2}\bar{\xi}^T(t)[PE_0 + E_0^T P + 2\bar{\alpha}P]P^{-1}P\bar{\xi}(t) + \frac{\varepsilon_0\lambda_{\max}(P^{-1})}{2}\bar{\xi}^T(t)P\bar{\xi}(t) \\
&\quad + \frac{Q\lambda_{\max}(P^{-1})}{2\varepsilon_0}\bar{\xi}^T(t-r(t))P\bar{\xi}(t-r(t)) \\
&\leq \frac{1}{2}\lambda_{\max}(M + \varepsilon_0P^{-1})\bar{\xi}^T(t)P\bar{\xi}(t) + \frac{Q\lambda_{\max}(P^{-1})}{2\varepsilon_0}\bar{\xi}^T(t-r(t))P\bar{\xi}(t-r(t)) \\
&= \omega V(t) + \beta V(t-r(t)) \leq \omega V(t) + \beta \sup_{s \in [-\tau_{\max}, 0]} V(t+s)
\end{aligned} \tag{3.15}$$

Meanwhile, at each impulsive instant t_k , we integrate both sides of system (3.6) from $t_k - \tau$ to t_k^- yields:

$$\bar{\xi}(t_k^-) - \bar{\xi}(t_k - \tau) = \int_{t_k - \tau}^{t_k} (E_0\bar{\xi}(s) + E_1\bar{\xi}(s-r(s)) + E_2(s))ds \tag{3.16}$$

Followed from (3.6) and (3.16), we have

$$\begin{aligned}
\bar{\xi}(t_k) &= \bar{\xi}(t_k^-) + E_3\bar{\xi}(t_k^-) + K\bar{\xi}(t_k^- - \tau) \\
&= (I_{4n} + E_3 + K)\bar{\xi}(t_k^-) - K \int_{t_k - \tau}^{t_k} (E_0\bar{\xi}(s) + E_1\bar{\xi}(s-r(s)) + E_2(s))ds \\
&= \Gamma_1 + \Gamma_2
\end{aligned} \tag{3.17}$$

where $\Gamma_1 = (I_{4n} + E_3 + K)\bar{\xi}(t_k^-)$ and $\Gamma_2 = -K \int_{t_k - \tau}^{t_k} (E_0\bar{\xi}(s) + E_1\bar{\xi}(s-r(s)) + E_2(s))ds$. Then, by applying Schwartz's inequality and Lemma 3.2.1 we have:

$$\begin{aligned}
\Gamma_1^T P \Gamma_1 &= \bar{\xi}(t_k^-)^T (I_{4n} + E_3 + K)^T P (I_{4n} + E_3 + K) \bar{\xi}(t_k^-) \\
&= \bar{\xi}(t_k^-)^T (J + K)^T P (J + K) \bar{\xi}(t_k^-) \\
&\leq \pi_1 V(t_k^-)
\end{aligned} \tag{3.18}$$

$$\begin{aligned}
\Gamma_2^T P \Gamma_2 &\leq \lambda_{max}(P) \|K\|^2 \left[\int_{t_k-\tau}^{t_k} (E_0 \bar{\xi}(s) + E_1 \bar{\xi}(s-r(s)) + E_2(s)) ds \right]^T \\
&\quad \left[\int_{t_k-\tau}^{t_k} (E_0 \bar{\xi}(s) + E_1 \bar{\xi}(s-r(s)) + E_2(s)) ds \right] \\
&\leq \lambda_{max}(P) \tau \|K\|^2 \int_{t_k-\tau}^{t_k} (E_0 \bar{\xi}(s) + E_1 \bar{\xi}(s-r(s)) + E_2(s))^T \\
&\quad (E_0 \bar{\xi}(s) + E_1 \bar{\xi}(s-r(s)) + E_2(s)) ds \\
&\leq \lambda_{max}(P) \tau \|K\|^2 \int_{t_k-\tau}^{t_k} [(1+\varepsilon_1) \|E_0\|^2 \bar{\xi}^T(s) \bar{\xi}(s) + (1+\varepsilon_1^{-1})(1+\zeta_1^{-1}) E_2^T(s) E_2(s) \\
&\quad + (1+\varepsilon_1^{-1})(1+\zeta_1) \|E_1\|^2 \bar{\xi}^T(s-r(s)) \bar{\xi}(s-r(s))] ds \\
&\leq \lambda_{max}(P) \tau \|K\|^2 \int_{t_k-\tau}^{t_k} \kappa \sup_{r(s) \in [0, \bar{r}]} \bar{\xi}^T(s-r(s)) \bar{\xi}(s-r(s)) ds \\
&\leq 2\lambda_{max}(P) \tau^2 \|K\|^2 \kappa \lambda_{max}(P^{-1}) \sup_{s \in [-\bar{r}-\tau, 0]} V(t_k^- + s) \\
&\leq \pi_2 \sup_{s \in [-\tau_{max}, 0]} V(t_k^- + s)
\end{aligned} \tag{3.19}$$

Based on (3.18) and (3.19), it gives:

$$\begin{aligned}
2V(t_k) &= (\Gamma_1 + \Gamma_2)^T P (\Gamma_1 + \Gamma_2) \\
&\leq (1+\varepsilon_2) \Gamma_1^T P \Gamma_1 + (1+\varepsilon_2^{-1}) \Gamma_2^T P \Gamma_2 \\
&\leq \pi_1 (1+\varepsilon_2) V(t_k^-) + (1+\varepsilon_2^{-1}) \pi_2 \sup_{s \in [-\tau_{max}, 0]} V(t_k^- + s)
\end{aligned} \tag{3.20}$$

Thus,

$$\begin{aligned}
V(t_k) &\leq \frac{\pi_1(1+\varepsilon_2)}{2} V(t_k^-) + \frac{(1+\varepsilon_2^{-1})\pi_2}{2} \sup_{s \in [-\tau_{max}, 0]} V(t_k^- + s) \\
&= \rho_1 V(t_k^-) + \rho_2 \sup_{s \in [-\tau_{max}, 0]} V(t_k^- + s)
\end{aligned} \tag{3.21}$$

Therefore, according to Lemma 3.1.2, we conclude that $\lim_{t \rightarrow \infty} V(t) = 0$ so that $\lim_{t \rightarrow \infty} \bar{\xi}(t) = 0$, which implies all the objectives of formation stabilization for MASs (3.1) and (3.2) are achieved via proposed hybrid impulsive control protocol (3.3).

□

3.2.2 Case II: $\tau > \inf\{t_k - t_{k-1}\}$, $k \in \mathbb{N}^+$

In this case, as the size of impulse delay exceeds the length of impulsive interval, there will be multiple impulsive instants allocated on the interval $(t - \tau, t)$. Hence, similar to Theorem 3.2.1 we obtain the following.

Theorem 3.2.2. *Consider the leader-following multi-agent systems with dynamics (3.1) and (3.2) followed by control protocol (3.3). Suppose Assumption 3.1.1 and Assumption 3.1.2 hold, $\inf\{t_k - t_{k-1}\} = h_1$ for $k \in \mathbb{N}^+$, $P \in \mathbb{R}^{4n \times 4n}$ is a positive definite matrix, $\varepsilon_0, \varepsilon_1, \varepsilon_2, \varepsilon_3, \zeta_1, \zeta_2 > 0$ and $\tau_{max} = \max\{\bar{r} + \tau, 2\tau\}$. If the following conditions are satisfied:*

$$\rho_1 + \rho_2 < 1 \quad (3.22)$$

$$e^{(\omega + \frac{\beta}{\rho_1 + \rho_2})\sigma} > 1 \quad (3.23)$$

where $\sigma = \sup_{k \in \mathbb{N}^+} \{t_k - t_{k-1}\}$, $\omega = \lambda_{max}(M + \varepsilon_0 P^{-1})$, $\beta = \frac{Q \lambda_{max}(P^{-1})}{\varepsilon_0}$, $\rho_1 = \frac{\pi_1(1 + \varepsilon_3)}{2}$, $\rho_2 = \frac{1}{2}(1 + \varepsilon_3^{-1})((1 + \zeta_2)\pi_2 + (1 + \zeta_2^{-1})\pi_3)$, $\pi_1 = 2\lambda_{max}((J + K)^T P (J + K) P^{-1})$, $\pi_2 = 2\lambda_{max}(P)\tau^2 \|K\|^2 \kappa \lambda_{max}(P^{-1})$ and $\pi_3 = 2\lambda_{max}(P)\lambda_{max}(P^{-1})\bar{\theta}^2 \|K\|^2 ((1 + \varepsilon_2)\|E_3\|^2 + (1 + \varepsilon_2^{-1})\|K\|^2)$ with $\bar{\theta} = \lfloor \frac{\tau}{h_1} \rfloor$, $\kappa = (1 + \varepsilon_1)\|E_0\|^2 + (1 + \varepsilon_1^{-1})(1 + \zeta_1)\|E_1\|^2 + \bar{\alpha}^2(1 + \varepsilon_1^{-1})(1 + \zeta_1^{-1})$, $M = [PE_0 + E_0^T P + 2\bar{\alpha}P]P^{-1}$, $Q = \|PE_1\|^2$, $J = \begin{pmatrix} I_{2n} & \mathbf{0}_{2n \times 2n} \\ -\mu_i L & I_{2n} - \mu_i L \end{pmatrix}$, $K = \begin{pmatrix} \mathbf{0}_{2n \times 2n} & \mathbf{0}_{2n \times 2n} \\ -\mu_i c I_{2n} & -\mu_i c I_{2n} \end{pmatrix}$ and $E_3 = J - I_{4n}$. Then the compact error dynamics (3.6) will be driven to zero asymptotically, and all the objectives of formation stabilization will be achieved.

Proof. Again, we construct the following Lyapunov function for $t \in [t_k, t_{k+1})$ as:

$$V(t) = \frac{1}{2} \bar{\xi}^T(t) P \bar{\xi}(t) \quad (3.24)$$

The continuous part of dynamics remains the same as derived in (3.15). Then, by integrating both sides of system (3.6) from $t_k - \tau$ to t_k^- yields:

$$\begin{aligned} \bar{\xi}(t_k^-) - \bar{\xi}(t_k - \tau) &= \int_{t_k - \tau}^{t_k} (E_0 \bar{\xi}(s) + E_1 \bar{\xi}(s - r(s)) + E_2(s)) ds + \sum_{m=1}^{\theta_k} E_3 \bar{\xi}(t_{k-m}) \\ &\quad + \sum_{m=1}^{\theta_k} K \bar{\xi}(t_{k-m} - \tau) \end{aligned} \quad (3.25)$$

where θ_k denotes the number of impulses occurred during $(t_k - \tau, t_k)$. Followed from (3.6) and (3.25), we have

$$\begin{aligned}
\bar{\xi}(t_k) &= \bar{\xi}(t_k^-) + E_3 \bar{\xi}(t_k^-) + K \bar{\xi}(t_k^- - \tau) \\
&= (I_{4n} + E_3 + K) \bar{\xi}(t_k^-) - K \int_{t_k - \tau}^{t_k} (E_0 \bar{\xi}(s) + E_1 \bar{\xi}(s - r(s)) + E_2(s)) ds \\
&\quad - K E_3 \sum_{m=1}^{\theta_k} \bar{\xi}(t_{k-m}) - K K \sum_{m=1}^{\theta_k} \bar{\xi}(t_{k-m} - \tau) \\
&= \Gamma_1 + \Gamma_2 + \Gamma_3
\end{aligned} \tag{3.26}$$

where $\Gamma_1 = (I_{4n} + E_3 + K) \bar{\xi}(t_k^-)$, $\Gamma_2 = -K \int_{t_k - \tau}^{t_k} (E_0 \bar{\xi}(s) + E_1 \bar{\xi}(s - r(s)) + E_2(s)) ds$, and $\Gamma_3 = -K E_3 \sum_{m=1}^{\theta_k} \bar{\xi}(t_{k-m}) - K K \sum_{m=1}^{\theta_k} \bar{\xi}(t_{k-m} - \tau)$. Therefore, by applying Schwartz's inequality and Lemma 3.2.1, we have:

$$\begin{aligned}
\Gamma_1^T P \Gamma_1 &= \bar{\xi}(t_k^-)^T (I_{4n} + E_3 + K)^T P (I_{4n} + E_3 + K) \bar{\xi}(t_k^-) \\
&= \bar{\xi}(t_k^-)^T (J + K)^T P (J + K) \bar{\xi}(t_k^-) \\
&\leq \pi_1 V(t_k^-)
\end{aligned} \tag{3.27}$$

$$\begin{aligned}
\Gamma_2^T P \Gamma_2 &\leq \lambda_{max}(P) \|K\|^2 \left[\int_{t_k - \tau}^{t_k} (E_0 \bar{\xi}(s) + E_1 \bar{\xi}(s - r(s)) + E_2(s)) ds \right]^T \\
&\quad \left[\int_{t_k - \tau}^{t_k} (E_0 \bar{\xi}(s) + E_1 \bar{\xi}(s - r(s)) + E_2(s)) ds \right] \\
&\leq \lambda_{max}(P) \tau \|K\|^2 \int_{t_k - \tau}^{t_k} (E_0 \bar{\xi}(s) + E_1 \bar{\xi}(s - r(s)) + E_2(s))^T \\
&\quad (E_0 \bar{\xi}(s) + E_1 \bar{\xi}(s - r(s)) + E_2(s)) ds \\
&\leq \lambda_{max}(P) \tau \|K\|^2 \int_{t_k - \tau}^{t_k} [(1 + \varepsilon_1) \|E_0\|^2 \bar{\xi}^T(s) \bar{\xi}(s) + (1 + \varepsilon_1^{-1})(1 + \zeta_1^{-1}) E_2^T(s) E_2(s) \\
&\quad + (1 + \varepsilon_1^{-1})(1 + \zeta_1) \|E_1\|^2 \bar{\xi}^T(s - r(s)) \bar{\xi}(s - r(s))] ds \\
&\leq \lambda_{max}(P) \tau \|K\|^2 \int_{t_k - \tau}^{t_k} \kappa \sup_{r(s) \in [0, \bar{r}]} \bar{\xi}^T(s - r(s)) \bar{\xi}(s - r(s)) ds \\
&\leq 2 \lambda_{max}(P) \tau^2 \|K\|^2 \kappa \lambda_{max}(P^{-1}) \sup_{s \in [-\bar{r} - \tau, 0]} V(t_k^- + s) \\
&\leq \pi_2 \sup_{s \in [-\tau_{max}, 0]} V(t_k^- + s)
\end{aligned} \tag{3.28}$$

$$\begin{aligned}
\Gamma_3^T P \Gamma_3 &= [-K E_3 \sum_{m=1}^{\theta_k} \bar{\xi}(t_{k-m}) - K K \sum_{m=1}^{\theta_k} \bar{\xi}(t_{k-m} - \tau)]^T P \\
& \quad [-K E_3 \sum_{m=1}^{\theta_k} \bar{\xi}(t_{k-m}) - K K \sum_{m=1}^{\theta_k} \bar{\xi}(t_{k-m} - \tau)] \\
& \leq \lambda_{\max}(P) [(1 + \varepsilon_2) \|K\|^2 \|E_3\|^2 \sum_{m=1}^{\theta_k} \bar{\xi}^T(t_{k-m}) \sum_{m=1}^{\theta_k} \bar{\xi}(t_{k-m}) \\
& \quad + (1 + \varepsilon_2^{-1}) \|K\|^4 \sum_{m=1}^{\theta_k} \bar{\xi}^T(t_{k-m} - \tau) \sum_{m=1}^{\theta_k} \bar{\xi}(t_{k-m} - \tau)] \\
& \leq \lambda_{\max}(P) \theta_k (1 + \varepsilon_2) \|K\|^2 \|E_3\|^2 \sum_{m=1}^{\theta_k} \bar{\xi}^T(t_{k-m}) \bar{\xi}(t_{k-m}) \\
& \quad + \lambda_{\max}(P) \theta_k (1 + \varepsilon_2^{-1}) \|K\|^4 \sum_{m=1}^{\theta_k} \bar{\xi}^T(t_{k-m} - \tau) \bar{\xi}(t_{k-m} - \tau) \\
& \leq \lambda_{\max}(P) \lambda_{\max}(P^{-1}) \theta_k (1 + \varepsilon_2) \|K\|^2 \|E_3\|^2 \sum_{m=1}^{\theta_k} \bar{\xi}^T(t_{k-m}) P \bar{\xi}(t_{k-m}) \\
& \quad + \lambda_{\max}(P) \lambda_{\max}(P^{-1}) \theta_k (1 + \varepsilon_2^{-1}) \|K\|^4 \sum_{m=1}^{\theta_k} \bar{\xi}^T(t_{k-m} - \tau) P \bar{\xi}(t_{k-m} - \tau) \\
& \leq 2\lambda_{\max}(P) \lambda_{\max}(P^{-1}) \theta_k^2 (1 + \varepsilon_2) \|K\|^2 \|E_3\|^2 \sup_{s \in [-2\tau, 0]} V(t_k^- + s) \\
& \quad + 2\lambda_{\max}(P) \lambda_{\max}(P^{-1}) \theta_k^2 (1 + \varepsilon_2^{-1}) \|K\|^4 \sup_{s \in [-2\tau, 0]} V(t_k^- + s) \\
& \leq 2\lambda_{\max}(P) \lambda_{\max}(P^{-1}) \bar{\theta}^2 \|K\|^2 ((1 + \varepsilon_2) \|E_3\|^2 + (1 + \varepsilon_2^{-1}) \|K\|^2) \sup_{s \in [-2\tau, 0]} V(t_k^- + s) \\
& \leq \pi_3 \sup_{s \in [-\tau_{\max}, 0]} V(t_k^- + s)
\end{aligned} \tag{3.29}$$

Based on (3.27), (3.28) and (3.29), it gives:

$$\begin{aligned}
2V(t_k) &= (\Gamma_1 + \Gamma_2 + \Gamma_3)^T P(\Gamma_1 + \Gamma_2 + \Gamma_3) \\
&\leq (1 + \varepsilon_3)\Gamma_1^T P\Gamma_1 + (1 + \varepsilon_3^{-1})(1 + \zeta_2)\Gamma_2^T P\Gamma_2 + (1 + \varepsilon_3^{-1})(1 + \zeta_2^{-1})\Gamma_3^T P\Gamma_3 \\
&\leq \pi_1(1 + \varepsilon_3)V(t_k^-) + (1 + \varepsilon_3^{-1})(1 + \zeta_2)\pi_2 \sup_{s \in [-\tau_{max}, 0]} V(t_k^- + s) \\
&\quad + (1 + \varepsilon_3^{-1})(1 + \zeta_2^{-1})\pi_3 \sup_{s \in [-\tau_{max}, 0]} V(t_k^- + s)
\end{aligned} \tag{3.30}$$

Thus,

$$\begin{aligned}
V(t_k) &\leq \frac{\pi_1(1 + \varepsilon_3)}{2}V(t_k^-) + \frac{(1 + \varepsilon_3^{-1})((1 + \zeta_2)\pi_2 + (1 + \zeta_2^{-1})\pi_3)}{2} \sup_{s \in [-\tau_{max}, 0]} V(t_k^- + s) \\
&= \rho_1 V(t_k^-) + \rho_2 \sup_{s \in [-\tau_{max}, 0]} V(t_k^- + s)
\end{aligned} \tag{3.31}$$

Consequently, according to Lemma 3.1.2, we conclude that $\lim_{t \rightarrow \infty} V(t) = 0$ so that $\lim_{t \rightarrow \infty} \bar{\xi}(t) = 0$, which implies all the objectives of formation stabilization for MASs (3.1) and (3.2) are achieved via proposed hybrid impulsive control protocol (3.3). \square

3.2.3 Distributed Impulse Delay

We discussed discrete impulse delay in the previous subsections. However, different parts of the system may experience different amounts of delay in practice. This can occur, for instance, in a communication network where packets of data travel through different nodes and links. Thus, distributed impulse delay can be employed to deal with situation where the delay is spread out over the system. Here, we modify the tracking term $P_L(\hat{p}_i(t - \tau), \hat{v}_i(t - \tau))$ in protocol (3.3) by

$$P_L(\hat{p}_i(t - \tau), \hat{v}_i(t - \tau)) = - \sum_{k=1}^{\infty} c \int_{t-\tau}^t \hat{p}_i(s) ds \delta(t - t_k) - \sum_{k=1}^{\infty} c \int_{t-\tau}^t \hat{v}_i(s) ds \delta(t - t_k) \tag{3.32}$$

When performing formation stabilization analysis, similar to (3.25), we have:

$$\begin{aligned}
\bar{\xi}(t_k^-) - \bar{\xi}(t) &= \int_t^{t_k} (E_0 \bar{\xi}(s) + E_1 \bar{\xi}(s - r(s)) + E_2(s)) ds \\
&\quad + E_3 \sum_{m=1}^{\theta_k} \bar{\xi}(t_{k-m}) + K \sum_{m=1}^{\theta_k(t)} \int_{-\tau}^0 \bar{\xi}(t_{k-m} + s) ds
\end{aligned} \tag{3.33}$$

where $\theta_k(t)$ denotes the number of impulses occurred on the interval (t, t_k) . Then by integrating both sides of (3.33) from $t_k - \tau$ to t_k^- further yields:

$$\begin{aligned} \tau \bar{\xi}(t_k^-) - \int_{t_k - \tau}^{t_k} \bar{\xi}(t) dt &= \int_{t_k - \tau}^{t_k} \int_t^{t_k} (E_0 \bar{\xi}(s) + E_1 \bar{\xi}(s - r(s)) + E_2(s)) ds dt \\ &+ E_3 \int_{t_k - \tau}^{t_k} \sum_{m=1}^{\theta_k} \bar{\xi}(t_{k-m}) dt + K \int_{t_k - \tau}^{t_k} \sum_{m=1}^{\theta_k(t)} \int_{-\tau}^0 \bar{\xi}(t_{k-m} + s) ds dt \end{aligned} \quad (3.34)$$

Followed from (3.6) and (3.34), we have

$$\begin{aligned} \bar{\xi}(t_k) &= \bar{\xi}(t_k^-) + E_3 \bar{\xi}(t_k^-) + K \int_{t_k - \tau}^{t_k} \bar{\xi}(s) ds \\ &= (I_{4n} + E_3 + \tau K) \bar{\xi}(t_k^-) - K \int_{t_k - \tau}^{t_k} \int_t^{t_k} (E_0 \bar{\xi}(s) + E_1 \bar{\xi}(s - r(s)) + E_2(s)) ds dt \\ &\quad - K E_3 \int_{t_k - \tau}^{t_k} \sum_{m=1}^{\theta_k} \bar{\xi}(t_{k-m}) dt - K K \int_{t_k - \tau}^{t_k} \sum_{m=1}^{\theta_k(t)} \int_{-\tau}^0 \bar{\xi}(t_{k-m} + s) ds dt \\ &= \Gamma_4 + \Gamma_5 + \Gamma_6 \end{aligned} \quad (3.35)$$

where $\Gamma_4 = (I_{4n} + E_3 + \tau K) \bar{\xi}(t_k^-)$, $\Gamma_5 = -K \int_{t_k - \tau}^{t_k} \int_t^{t_k} (E_0 \bar{\xi}(s) + E_1 \bar{\xi}(s - r(s)) + E_2(s)) ds dt$ and $\Gamma_6 = -K E_3 \int_{t_k - \tau}^{t_k} \sum_{m=1}^{\theta_k} \bar{\xi}(t_{k-m}) dt - K K \int_{t_k - \tau}^{t_k} \sum_{m=1}^{\theta_k(t)} \int_{-\tau}^0 \bar{\xi}(t_{k-m} + s) ds dt$. The rest part of proof is related to that of Theorem 3.2.2 by utilizing Schwartz's inequality and Lemma 3.2.1, while similar results can also be found in [34], thus omitted.

Remark 3.2.1. *This section has established sufficient criteria for MAS formation stabilization under hybrid impulsive control schemes along with delayed impulses and time-varying delays. Specifically, we have shown that the Lyapunov-Razumikhin technique is valid for both discrete and distributed impulse delays of arbitrary sizes. In the next section, different collision avoidance mechanisms will be discussed. Based on their properties, we will also examine the corresponding results of formation stabilization by employing such mechanisms.*

3.3 Collision Avoidance Mechanism

In general, collision avoidance mechanisms are techniques used in MASs to prevent or reduce collisions between entities, such as vehicles, robots, or particles. The purpose of

these mechanisms is to ensure the safe and efficient operation of the system. There are several types of collision avoidance mechanisms that can be used, including:

1. **Control-based:** This mechanism uses control algorithms to adjust the trajectory or speed of the system to avoid a collision. For instance, if a collision is detected, the system may slow down or change direction to avoid the obstacle.
2. **Sensor-based:** This mechanism uses sensors such as cameras, LIDAR, or RADAR to detect obstacles or other entities in the environment. The system can then use this information to adjust its behavior to avoid a collision.
3. **Communication-based:** This mechanism uses communication between entities to coordinate their movements and avoid collisions. For example, vehicles equipped with vehicle-to-vehicle (V2V) communication systems can exchange information about their positions and velocities to avoid collisions.
4. **Planning-based:** This mechanism uses planning algorithms to generate collision-free trajectories for the system. For example, a robot can use path planning algorithms to plan a collision-free path to its destination.

The choice of collision avoidance mechanism depends on the specific application and system requirements. Some systems may use a combination of these mechanisms to achieve the desired level of safety and efficiency.

Collision and obstacle avoidance mechanisms are indeed an essential part of Formation control, most of recent collision avoidance results rely on the construction of decentralized artificial potential function approach introduced in [15], which have the form

$$V(x) = \sum_{i=1}^n \sum_{j \in N_i} \psi_{\beta}(\|p_i - p_j\|_{\sigma}), \quad (3.36)$$

with repulsive potential

$$\psi_{\beta}(z) = \int_{d_{\alpha}}^z \phi_{\beta}(s) ds \geq 0 \quad (3.37)$$

and repulsive action function (force) that vanishes when reaching out of sensing range d_{β} (i.e., $z \geq d_{\beta}$):

$$\phi_{\beta}(z) = \rho_h\left(\frac{z}{d_{\beta}}\right) \left(\frac{z - d_{\beta}}{\sqrt{1 + (z - d_{\beta})^2}} - 1 \right) \quad (3.38)$$

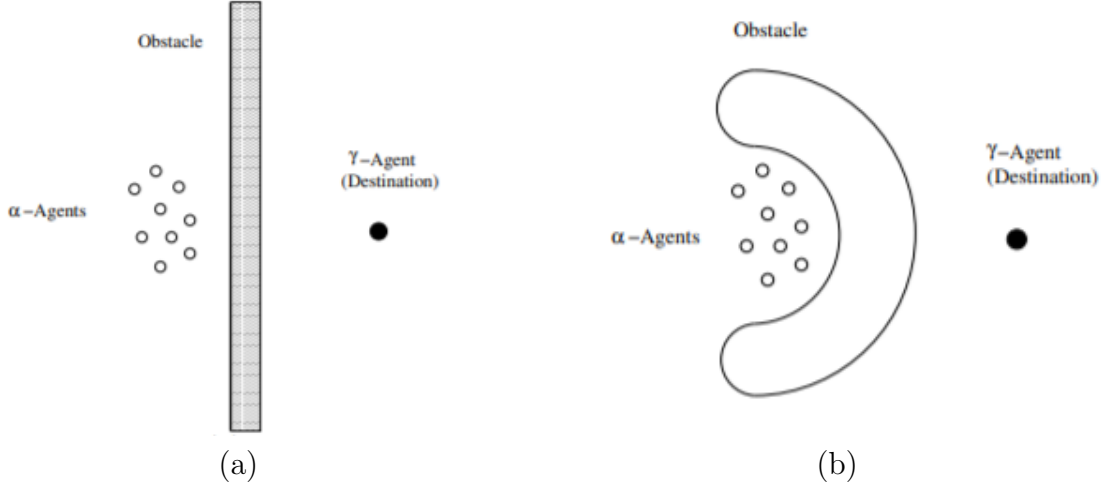


Figure 3.2: Trapped α -agents upon encountering (a) a convex obstacle and (b) a non-convex obstacle

where $\|z\|_\sigma = \frac{1}{\epsilon}(\sqrt{1 + \epsilon\|z\|^2} - 1)$ is the σ -norm of a vector that is differentiable everywhere including $z = 0$, ρ_h is a bump function with one possible choice as

$$\rho_z = \begin{cases} 1, & z \in [0, h] \\ \frac{1}{2}[1 + \cos(\frac{\pi(z-h)}{1-h})], & z \in [h, 1] \\ 0, & \text{otherwise} \end{cases} \quad (3.39)$$

so that $\rho'_h(z) = 0$ over the interval $[1, \infty)$, $|\rho'_h(z)|$ is uniformly bounded in z , and the element of the adjacency matrix $\rho_h(\frac{\|p_i - p_j\|_\sigma}{d_\beta}) \in [0, 1]$ for $i \neq j$. Based on this setup, then the control protocol needs to employ the gradient-based term of (3.36) (i.e., $-\nabla V(x)$). Although this potential-based approach overcomes the drawbacks of global information sensing [68] and non-smooth potential function [69], the main disadvantage of creating undesired local minima still remains. Particularly, as shown in Figure 3.2, α -agents represent the follower agents and γ -agent represents the leader agent or desired destination, then the repulsive potential function may prevent the agents from reaching the target configuration. Meanwhile, with the extra term (3.36) involved in Lyapunov function/functional, the nonlinear nature of artificial potential functions makes it more difficult and challenging to achieve formation stabilization of MASs via impulsive control.

Therefore, in order to avoid the aforementioned main drawbacks of artificial potential

functions, we consider the collision avoidance mechanism by using braking and gyroscopic forces, which was firstly introduced in [30, 31]. In general, the braking force (F_b) serves the purpose of slowing down the agents and allowing them to have enough reaction time to avoid obstacles and collisions, which can be viewed as a damping term to the velocity. On the other hand, the gyroscopic force (F_g) denotes the force which does not do any work, but in turn rotate the velocity vector. They can be viewed as steering forces to make the agents move around the obstacles. Mathematically, a gyroscopic force F_g is defined to satisfy $F_g v = 0$, thus it is always acting perpendicular to the direction of motion.

In [30, 31], an example of the braking force is expressed as

$$F_b = -D_b(n)v = -(c_1 e^{-\|n\|} - c_2)v \quad (3.40)$$

where $c_1 e^{-\|n\|} \geq c_2$, $D_b(n) \geq 0$ is an imposed braking term depending on the vector n from the agent to its nearest obstacle. Adding the braking force will improve the damping performance and it also has the property of $v^T F_b \leq 0$. A general class of gyroscopic force was given as

$$F_g = S(x, v)v \quad (3.41)$$

where $S(x, v)$ is a skew symmetric matrix such that $v^T F_b = 0$.

According to [32], another distributed braking force on agent i , which performs as energy dissipation, can be expressed as follows.

$$\begin{cases} \Theta_i^{obs}(v_i) = \sum_{i^\beta \in N_i^\beta} -\sigma_{ii^\beta}(v_i) \zeta_{ii^\beta} (s_{ii^\beta} + e^{-s_{ii^\beta}}) \frac{n_{ii^\beta}}{\|n_{ii^\beta}\|} \\ \Theta_i(v_i) = \sum_{j \in N_i} -\sigma_{ij}(v_i) \zeta_{ij} (s_{ij} + e^{-s_{ij}}) \frac{n_{ij}}{\|n_{ij}\|} \end{cases} \quad (3.42)$$

where $\zeta_{ij} > 0$, $\zeta_{ii^\beta} > 0$, $s_{ij} = v_i^T \frac{n_{ij}}{\|n_{ij}\|}$, $s_{ii^\beta} = v_i^T \frac{n_{ii^\beta}}{\|n_{ii^\beta}\|}$. $\Theta_i^{obs}(v_i)$, $\Theta_i(v_i)$ are the braking forces subject to obstacle and other agents respectively. $i^\beta \in N_i^\beta$ is the β -agent induced by agent i allocated on the boundary of convex obstacle as introduced in [20], and its coordinates information can be computed directly by Lemma 3.3.1. n_{ii^β} is the vector connecting i -th agent to the corresponding β -agent on the boundary of the obstacle, and n_{ij} is the vector connecting i -th agent to the j -th agent. Moreover, the activation indicator is defined

$$\sigma_{ij}(v_i) = \begin{cases} 1, & \|n_{ij}\| \leq r_s \text{ and } v_i^T n_{ij} > 0 \\ 0, & \text{otherwise} \end{cases} \quad (3.43)$$

and similar for σ_{ii^β} . The braking forces (3.42) are more elaborate since their activation only occurs when the agent is moving toward other agents or environmental obstacles (i.e., $v_i^T n_{ij} > 0$), and they are bounded by some constant since $e^{-q} \geq 1 - q$ for all $q \geq$

0. Meanwhile, an improved version of gyroscopic force is formulated via the orthogonal projection of desired formation control term u_{di} given by

$$\begin{cases} w_i = \begin{cases} u_{di} - (u_{di}^T \frac{\pi_i}{\|\pi_i\|}) \frac{\pi_i}{\|\pi_i\|}, & \|u_{di} - (u_{di}^T \frac{\pi_i}{\|\pi_i\|}) \frac{\pi_i}{\|\pi_i\|}\| \neq 0 \\ \tilde{u}_{di} - (\tilde{u}_{di}^T \frac{\pi_i}{\|\pi_i\|}) \frac{\pi_i}{\|\pi_i\|}, & \text{otherwise} \end{cases} \\ G_i(v_i) = K_g \frac{w_i}{\|w_i\|} \end{cases} \quad (3.44)$$

and similarly for $G_i^{obs}(v_i)$. Here, K_g is a tunable matrix gain with appropriate dimension, \tilde{u}_{di} is obtained by adding a small perturbation to u_{di} , and π_i is defined as

$$\pi_i = \begin{cases} v_i, & \|v_i\| \neq 0 \\ \sum_{j \in N_i} \zeta_{ij} \frac{n_{ij}}{\|n_{ij}\|}, & \text{otherwise.} \end{cases} \quad (3.45)$$

From the above construction, w_i is eventually the orthogonal projection of u_{di} on the plane which is perpendicular to v_i , thus gyroscopic force $G_i(v_i)$ is perpendicular to v_i as well. Moreover, $G_i(v_i)$ is well defined when $\|v_i\| = 0$ thanks to (3.45) or $\|w_i\| = 0$ by adding noise, so that zero-velocity collision [30] can be prevented with a non-zero minimum velocity and undesired local minima can be avoided. In practice, based on the definition of braking and gyroscopic forces, many other feasible and efficient reaction schemes can be devised.

Lemma 3.3.1. [15] *Let $x_{i\beta}$ and $v_{i\beta}$ denote the position and velocity of a β -agent generated by an α -agent with state (x_i, v_i) on an convex and compact obstacle with smooth boundaries. Then*

1. *For a spherical obstacle with radius r_k center at y_k , the position and velocity of the β -agent are given by:*

$$\begin{aligned} x_{i\beta} &= \mu x_i + (1 - \mu) y_k \\ v_{i\beta} &= \mu P v_i \end{aligned}$$

where $\mu = \frac{r_k}{\|x_i - y_k\|}$, $P = I - a_k a_k^T$ and unit normal $a_k = \frac{(x_i - y_k)}{\|x_i - y_k\|}$.

2. *For an obstacle with a hyperplane boundary that has a unit normal a_k and passes through the point y_k , the position and velocity of the β -agent are given by:*

$$\begin{aligned} x_{i\beta} &= P x_i + (I - P) y_k \\ v_{i\beta} &= P v_i \end{aligned}$$

where P is a projection matrix.

Remark 3.3.1. *In reality, undesired local minima often occurs in optimization problems where a solution that is not the global minimum is found instead of the desired global minimum. This can happen when the function is highly nonlinear or has many input variables. The setup of (3.44) can be viewed as the so-called adding noise technique, which is designed to keep agents from getting stuck at undesired local minima.*

3.4 Formation Stabilization with Collision Avoidance

In this section, we study the formation stabilization criteria of MASs with collision avoidance by utilizing the braking force (3.42) and gyroscopic force (3.44). Thus, we set

$$P_G(\hat{v}_i(t)) = \Theta_i(\hat{v}_i(t)) + \Theta_i^{obs}(\hat{v}_i(t)) + G_i(\hat{v}_i(t)) + G_i^{obs}(\hat{v}_i(t)) \quad (3.46)$$

as our collision avoidance mechanism throughout the rest of thesis content where indicator (3.43) is modified to

$$\sigma_{ij}(\hat{v}_i) = \begin{cases} 1, & \|n_{ij}\| \leq r_s \quad \text{and} \quad v_i^T n_{ij} > 0 \quad \text{and} \quad \hat{v}_i^T n_{ij} > 0 \\ -1, & \|n_{ij}\| \leq r_s \quad \text{and} \quad v_i^T n_{ij} > 0 \quad \text{and} \quad \hat{v}_i^T n_{ij} < 0 \\ 0, & \text{otherwise} \end{cases} \quad (3.47)$$

and $G_i(\hat{v}_i(t)) = K_g \frac{w_i}{\|w_i\|}$ with $\hat{v}_i^T K_g = v_i^T$, thus the hybrid impulsive control scheme (3.3) becomes

$$u_i = P_C(\hat{p}_i(t - r(t)), \hat{v}_i(t - r(t))) + P_D(\hat{p}_i(t), \hat{v}_i(t)) + P_L(\hat{p}_i(t - \tau), \hat{v}_i(t - \tau)) + \hat{P}_{22}^{-1} P_G(\hat{v}_i(t)) \quad (3.48)$$

where $\hat{P}_{22} \in \mathbb{R}^{2 \times 2}$ is a positive definite gain matrix.

Theorem 3.4.1. *Consider the leader-following multi-agent systems with dynamics (3.1) and (3.2) followed by control protocol (3.48). Suppose Assumption 3.1.1 and Assumption 3.1.2 hold, $P = \begin{pmatrix} \hat{P}_{11} \otimes I_n & \mathbf{0}_{2n \times 2n} \\ \mathbf{0}_{2n \times 2n} & \hat{P}_{22} \otimes I_n \end{pmatrix} \in \mathbb{R}^{4n \times 4n}$ is a positive definite matrix, the maximal structure energy is bounded by $E \geq V(t) > 0$, $\zeta_{ij} = \zeta_{ii^\beta} > \frac{2E}{r_s}$, $\varepsilon_1, \varepsilon_2 > 0$ and $\tau_{max} = \bar{r} + \tau$. If all the conditions with same parameter settings in Theorem 3.2.1 are satisfied, then the compact error dynamics (3.6) will be driven to zero asymptotically with collision-free motion, and all the objectives of formation stabilization will be achieved.*

Proof. Similar to Theorem 3.2.1, we consider the following Lyapunov function for $t \in [t_k, t_{k+1})$ as:

$$V(t) = \frac{1}{2} \bar{\xi}^T(t) P \bar{\xi}(t) \quad (3.49)$$

By the definition of $\sigma_{ij}(\hat{v}_i)$ in (3.47) and $\zeta_{ij} > 0$, it gives:

$$\sum_{i=1}^n \hat{v}_i^T(t) \Theta_i(\hat{v}_i(t)) = \sum_{i=1}^n \sum_{j \in N_i} -\sigma_{ij} \hat{v}_i^T(t) \zeta_{ij} (s_{ij} + e^{-s_{ij}}) \frac{n_{ij}}{\|n_{ij}\|} \leq 0$$

and also $\sum_{i=1}^n \hat{v}_i^T(t) \Theta_i^{obs}(\hat{v}_i(t)) \leq 0$; while $\sum_{i=1}^n \hat{v}_i^T(t) G_i(\hat{v}_i(t)) = \sum_{i=1}^n \hat{v}_i^T(t) G_i^{obs}(\hat{v}_i(t)) = 0$ by the feature of the gyroscopic force. Hence, we obtain $\bar{v}^T(t) P_{22} P_{22}^{-1} [P_G(\hat{v}_i(t)) \otimes \mathbf{1}_n] \leq 0$ and denote $P_G(\bar{v}(t)) = P_G(\hat{v}_i(t)) \otimes \mathbf{1}_n$. Then, based on Assumption 3.1.1, Assumption 3.1.2 and Lemma 3.1.1, system (3.6), we take the time derivative of V which gives:

$$\begin{aligned} \dot{V}(t) &= \frac{1}{2} [\bar{\xi}^T(t) P \dot{\bar{\xi}}(t) + \dot{\bar{\xi}}^T(t) P \bar{\xi}(t)] \\ &\leq \frac{1}{2} \bar{\xi}^T(t) [P E_0 + E_0^T P] \bar{\xi}(t) + \frac{1}{2} \bar{\xi}^T(t) P E_1 \bar{\xi}(t - r(t)) + \frac{1}{2} \bar{\xi}^T(t - r(t)) E_1^T P \bar{\xi}(t) \\ &\quad + \bar{\alpha} \bar{\xi}^T(t) P \bar{\xi}(t) + \bar{v}^T(t) P_{22} P_{22}^{-1} P_G(\bar{v}(t)) \\ &\leq \frac{1}{2} \bar{\xi}^T(t) [P E_0 + E_0^T P] \bar{\xi}(t) + \frac{\varepsilon_0}{2} \bar{\xi}^T(t) \bar{\xi}(t) + \frac{Q}{2\varepsilon_0} \bar{\xi}^T(t - r(t)) \bar{\xi}(t - r(t)) + \bar{\alpha} \bar{\xi}^T(t) P \bar{\xi}(t) \\ &= \frac{1}{2} \bar{\xi}^T(t) [P E_0 + E_0^T P + 2\bar{\alpha} P] \bar{\xi}(t) + \frac{\varepsilon_0}{2} \bar{\xi}^T(t) P^{-1} P \bar{\xi}(t) + \frac{Q}{2\varepsilon_0} \bar{\xi}^T(t - r(t)) P^{-1} P \bar{\xi}(t - r(t)) \\ &\leq \frac{1}{2} \bar{\xi}^T(t) [P E_0 + E_0^T P + 2\bar{\alpha} P] P^{-1} P \bar{\xi}(t) + \frac{\varepsilon_0 \lambda_{\max}(P^{-1})}{2} \bar{\xi}^T(t) P \bar{\xi}(t) \\ &\quad + \frac{Q \lambda_{\max}(P^{-1})}{2\varepsilon_0} \bar{\xi}^T(t - r(t)) P \bar{\xi}(t - r(t)) \\ &\leq \frac{1}{2} \lambda_{\max}(M + \varepsilon_0 P^{-1}) \bar{\xi}^T(t) P \bar{\xi}(t) + \frac{Q \lambda_{\max}(P^{-1})}{2\varepsilon_0} \bar{\xi}^T(t - r(t)) P \bar{\xi}(t - r(t)) \\ &= \omega V(t) + \beta V(t - r(t)) \leq \omega V(t) + \beta \sup_{s \in [-\tau_{\max}, 0]} V(t + s) \end{aligned} \quad (3.50)$$

Denote $W(t) = [\mathbf{0}_{2n}^T, (P_{22}^{-1} P_G(\bar{v}(t)))^T]^T$ and suppose that $W^T(t) W(t) \leq \bar{\omega}$ for $\bar{\omega} > 0$, then

(3.25) in Theorem 3.2.2 becomes

$$\begin{aligned} \bar{\xi}(t_k^-) - \bar{\xi}(t_k - \tau) &= \int_{t_k - \tau}^{t_k} (E_0 \bar{\xi}(s) + E_1 \bar{\xi}(s - r(s)) + E_2(s) + W(s)) ds \\ &\quad + \sum_{m=1}^{\theta_k} E_3 \bar{\xi}(t_{k-m}) + \sum_{m=1}^{\theta_k} K \bar{\xi}(t_{k-m} - \tau) \end{aligned} \quad (3.51)$$

with $\Gamma_2 = -K \int_{t_k - \tau}^{t_k} (E_0 \bar{\xi}(s) + E_1 \bar{\xi}(s - r(s)) + E_2(s) + W(s)) ds$, while Γ_1 and Γ_3 remain the same. Moreover, it yields:

$$\begin{aligned} \Gamma_2^T P \Gamma_2 &\leq \lambda_{max}(P) \|K\|^2 \left[\int_{t_k - \tau}^{t_k} (E_0 \bar{\xi}(s) + E_1 \bar{\xi}(s - r(s)) + E_2(s) + W(s)) ds \right]^T \\ &\quad \left[\int_{t_k - \tau}^{t_k} (E_0 \bar{\xi}(s) + E_1 \bar{\xi}(s - r(s)) + E_2(s) + W(s)) ds \right] \\ &\leq \lambda_{max}(P) \tau \|K\|^2 \int_{t_k - \tau}^{t_k} (E_0 \bar{\xi}(s) + E_1 \bar{\xi}(s - r(s)) + E_2(s) + W(s))^T \\ &\quad (E_0 \bar{\xi}(s) + E_1 \bar{\xi}(s - r(s)) + E_2(s) + W(s)) ds \\ &\leq \lambda_{max}(P) \tau \|K\|^2 \int_{t_k - \tau}^{t_k} [(1 + \varepsilon_1) \|E_0 + \bar{\alpha} I_{4n}\|^2 \bar{\xi}^T(s) \bar{\xi}(s) \\ &\quad + (1 + \varepsilon_1^{-1})(1 + \zeta_1) \|E_1\|^2 \bar{\xi}^T(s - r(s)) \bar{\xi}(s - r(s)) + (1 + \varepsilon_1^{-1})(1 + \zeta_1^{-1}) W^T(s) W(s)] ds \\ &\leq \lambda_{max}(P) \tau \|K\|^2 \int_{t_k - \tau}^{t_k} \kappa_1 \sup_{r(s) \in [0, \bar{r}]} \bar{\xi}^T(s - r(s)) \bar{\xi}(s - r(s)) ds \\ &\quad + \lambda_{max}(P) \tau^2 \|K\|^2 (1 + \varepsilon_1^{-1})(1 + \zeta_1^{-1}) \bar{\omega} \\ &\leq 2\lambda_{max}(P) \tau^2 \|K\|^2 \kappa_1 \lambda_{max}(P^{-1}) \sup_{s \in [-\bar{r} - \tau, 0]} V(t_k^- + s) \\ &\quad + \lambda_{max}(P) \tau^2 \|K\|^2 (1 + \varepsilon_1^{-1})(1 + \zeta_1^{-1}) \bar{\omega} \\ &\leq \pi_2 \sup_{s \in [-\tau_{max}, 0]} V(t_k^- + s) + \kappa_2 \end{aligned} \quad (3.52)$$

where $\kappa_1 = (1 + \varepsilon_1) \|E_0 + \bar{\alpha} I_{4n}\|^2 + (1 + \varepsilon_1^{-1})(1 + \zeta_1) \|E_1\|^2$, and $\kappa_2 = \lambda_{max}(P) \tau^2 \|K\|^2 (1 + \varepsilon_1^{-1})(1 + \zeta_1^{-1}) \bar{\omega}$. Due to the extra constant term κ_2 , the asymptotic convergence of the compact error system can be realized based on Lemma 3.1.2 when collision avoidance mechanism is off. Lastly, denote $v_{ij}^d = v_i^T \frac{n_{ij}}{\|n_{ij}\|}$ and $v_{ii\beta}^{obs} = v_i^T \frac{n_{ii\beta}}{\|n_{ii\beta}\|}$. then the part of energy

dissipated by $\Theta_i^{obs}(\hat{v}_i)$ for agent i when $E \geq V(t) > 0$ can be expressed as:

$$\begin{aligned}
V_i^{obs} &= \sum_{i^\beta \in N_i^\beta} \left\| \int \zeta_{ii^\beta} v_{ii^\beta}^{obs}(s) (v_{ii^\beta}^{obs}(s) + e^{-v_{ii^\beta}^{obs}(s)}) ds \right\| \\
&\geq \sum_{i^\beta \in N_i^\beta} \left\| \int \zeta_{ii^\beta} v_{ii^\beta}^{obs}(s) (v_{ii^\beta}^{obs}(s) + 1 - v_{ii^\beta}^{obs}(s)) ds \right\| \\
&= \sum_{i^\beta \in N_i^\beta} \left\| \int \zeta_{ii^\beta} v_{ii^\beta}^{obs}(s) ds \right\| = \sum_{i^\beta \in N_i^\beta} \zeta_{ii^\beta} \|q_{ii^\beta}\|
\end{aligned} \tag{3.53}$$

where q_{ii^β} is the displacement of i -th agent towards the corresponding β -agent on the boundary of the obstacle, since $v_{ii^\beta}^{obs}$ can be viewed as the scalar projection of v_i onto n_{ii^β} . Also it is chosen to be zero at the moment of detection. Then we can derive further that:

$$\|q_{ii^\beta}\| \leq \frac{V_i^{obs}}{\zeta_{ii^\beta}} < \frac{V_i(t)r_s}{2E} \leq \frac{r_s}{2} < r_s$$

which implies the maximum displacement will not exceed the sensing range, thus no collision with obstacles. Similarly, we have

$$\|q_{ij}\| \leq \frac{V_i^d}{\zeta_{ij}} < \frac{V_i(t)r_s}{2E} \leq \frac{r_s}{2}$$

where V_i^d is the part of energy dissipated by $\Theta_i(\hat{v}_i)$. Therefore, according to Lemma 3.1.2, we conclude that $\lim_{t \rightarrow \infty} V(t) = 0$ so that $\lim_{t \rightarrow \infty} \bar{\xi}(t) = 0$, which implies all the objectives of formation stabilization for MASs (3.1) and (3.2) are achieved with collision-free motion via proposed hybrid impulsive control protocol (3.48).

□

Remark 3.4.1. *According to above analysis, the properties of braking and gyroscopic forces ensure no further increase of the upper bound of $\dot{V}(t)$ as shown in (3.50). Meanwhile, due to the non-linearity of braking and gyroscopic forces in general design, the asymptotic stabilization of MASs cannot be guaranteed during the process of collision avoidance as expected. However, the collision avoidance mechanism on each agent only needs to be activated upon detecting any environment obstacles or other agents. Therefore, in the following section, we may treat them as external inputs to investigate the input-to-state (ISS) stability of MASs.*

3.5 Input-to-state Formation Stabilization

Input-to-state stability (ISS) characterizes the behavior of dynamical systems under external inputs and perturbations. A system is said to be ISS if, for any bounded input signal and any bounded initial state, the output of the system remains bounded for all future times. In other words, ISS guarantees that the system's response to external disturbances is bounded and decays over time. The ISS property can be viewed as a natural generalization of the concept of asymptotic stability.

Over the past decades, the properties of both input-to-state stability (ISS) and integral input-to-state stability (iISS) have been investigated in terms of dynamical systems with impulse effects, where iISS can be viewed as a relaxed form of ISS [70]. The appropriate concepts of ISS/iISS for impulsive systems were introduced based on Lyapunov-based conditions in [71]. [72] examined the ISS of nonlinear impulsive systems over a larger sequence satisfying the generalized average dwell-time condition. The ISS of impulse-triggered switched systems was investigated in [73], while recently [74] discussed the ISS/iISS of impulsive systems via event-triggered impulsive control.

Moreover, under impulsive frameworks, delayed impulses are inevitable for information transmission and parameter selection in multi-agent systems, which results in control performance reduction and network instability. Specifically, the ISS/iISS/stochastic-ISS were investigated for impulsive stochastic delayed systems with time-varying continuous delays by means of Lyapunov-Krasovskii functional, average impulse interval and comparison system in [75, 76]; while effect of delayed impulses on ISS/iISS of nonlinear systems was discussed in [77], where the continuous dynamics are stabilizing. A theoretical analysis of ISS of impulsive systems with both time-varying continuous delays and delay-dependent impulses, where continuous dynamics can be either stabilizing or destabilizing, was recently presented by Liu et al. [78].

3.5.1 Preliminaries

We shall use the following definitions and lemmas to support the ISS formation stabilization results. Consider the compact error system

$$\begin{cases} \dot{\bar{\xi}}(t) = \begin{pmatrix} \mathbf{0}_{2n \times 2n} & I_{2n} \\ \alpha_p I_{2n} & \alpha_v I_{2n} \end{pmatrix} \bar{\xi}(t) + \begin{pmatrix} \mathbf{0}_{2n \times 2n} & \mathbf{0}_{2n \times 2n} \\ -L' & -L' \end{pmatrix} \bar{\xi}(t - r(t)) + \begin{pmatrix} \mathbf{0}_{2n} \\ \bar{f} + P_{22}^{-1} P_G(\bar{v}(t)) \end{pmatrix} \\ = E_0 \bar{\xi}(t) + E_1 \bar{\xi}(t - r(t)) + E_2(t) + W(t), \quad t \neq t_k \\ \Delta \bar{v}(t_k) = -\mu_i L \bar{p}(t_k) - \mu_i L \bar{v}(t_k) - \mu_i c \bar{p}(t_k - \tau) - \mu_i c \bar{v}(t_k - \tau), \quad t = t_k \end{cases} \quad (3.54)$$

Definition 3.5.1. [77] For the prescribed impulse sequence $\{t_l, l \in \mathbb{N}^+\}$, the compact system (3.54) is said to reach input-to-state stability (ISS) if there exist functions $\beta \in \mathcal{KL}$ and $\gamma \in \mathcal{K}_\infty$ such that for any initial condition (t_0, ϕ) and any control input $\bar{u}(t)$, the corresponding solution of (3.54) satisfies

$$\|\bar{\xi}(t)\| \leq \beta(\|\phi\|_{\bar{\tau}}, t - t_0) + \gamma(\|\bar{u}\|_{[t_0, t]}), \quad t \geq t_0 \quad (3.55)$$

where $\bar{\tau} > 0$, $\|\bar{u}\|_{[t_0, t]} = \max\{\text{ess sup}_{s \in [t_0, t]} \|\bar{u}(s)\|, \sup_{t_l \in [t_0, t]} \|\bar{u}(t_l)\|\}$, $\|\phi\|_{\bar{\tau}} = \sup_{s \in [-\bar{\tau}, 0]} \|\phi(s)\|$, $\phi \in \mathbb{C}([-\bar{\tau}, 0], \mathbb{R}^n)$. It is said to be uniformly ISS over a given class \mathcal{F} of admissible sequences of impulse times if the ISS property (3.66) holds for every sequence in \mathcal{F} , with functions β and γ that are independent of the choice of the sequence.

Definition 3.5.2. [77] For the prescribed impulse sequence $\{t_l, l \in \mathbb{N}^+\}$, the compact system (3.54) is said to reach integral input-to-state stability (iISS) if there exist functions $\beta \in \mathcal{KL}$ and $\alpha, \gamma \in \mathcal{K}_\infty$ such that for any initial condition (t_0, ϕ) and any control input $\bar{u}(t)$, the corresponding solution of (3.54) satisfies

$$\alpha(\|\bar{\xi}(t)\|) \leq \beta(\|\phi\|_{\bar{\tau}}, t - t_0) + \int_{t_0}^t \gamma(|\bar{u}(s)|) ds + \sum_{l \in N(t_0, t)} \gamma(|\bar{u}(t_l^-) - \bar{\tau}|), \quad t \geq t_0 \quad (3.56)$$

It is said to be uniformly iISS over a given class \mathcal{F} of admissible sequences of impulse times if the ISS property (3.56) holds for every sequence in \mathcal{F} , with functions β and γ that are independent of the choice of the sequence.

Definition 3.5.3. [79] The average impulsive interval of the impulsive sequence $\mathcal{F}[T_\alpha, \varrho] = \{t_l\}_{l \in \mathbb{N}^+}$ is equal to $T_\alpha > 0$ if there exists a positive integer ϱ so that

$$\frac{T-t}{T_\alpha} - \varrho \leq N(t, T) \leq \frac{T-t}{T_\alpha} + \varrho, \quad \forall 0 \leq t \leq T \quad (3.57)$$

where $N(t, T)$ denotes the number of impulse times of the impulsive sequence $\mathcal{F}[T_\alpha, \varrho]$ in the time interval (t, T) .

Lemma 3.5.1. [78] Assume that there exist $V_1 \in \nu_0$, $V_2 \in \nu_0^*$, functions $\alpha_1, \alpha_2, \alpha_3, \psi \in \mathcal{K}_\infty$ and constants $\mu > 0$, $\kappa > 0$, $0 \leq \rho_1 < 1$ and $\rho_2 \geq 0$ such that for all $t \in \mathbb{R}^+$, $x \in \mathbb{R}^n$, and $\nu \in \mathcal{PC}([-r, 0], \mathbb{R}^n)$, the following conditions hold:

1. $\alpha_1(\|x\|) \leq V_1(t, x) \leq \alpha_2(\|x\|)$ and $0 \leq V_2(t, \nu) \leq \alpha_3(\|\nu\|_r)$;
2. $D^+V(t, \nu) \leq \mu V(t, \nu) + \psi(\|w(t)\|)$ where $V(t, \nu) = V_1(t, \nu(0)) + V_2(t, \nu)$;
3. $V_1(t, \nu(0) + g_k(t, \nu, w(t^-)))$
 $\leq \rho_1 V_1(t^-, \nu(0)) + \rho_2 \sup_{s \in [-r, 0]} \{V_1(t^- + s, \nu(s))\} + \psi(\sup_{s \in [-r, 0]} \|w(t^- + s)\|)$;
4. $V_2(t, \nu) \leq \kappa \sup_{s \in [-r, 0]} \{V_1(t + s, \nu(s))\}$;
5. $\ln[\rho_1 + \rho_2 + (1 - \rho_1)\kappa] < -\mu h_2$

Then, the following system is uniformly ISS over $\mathcal{F}(h_2)$ (i.e., the class of impulse time sequences satisfying $\sup\{t_k - t_{k-1}\} = h_2$)

$$\begin{cases} \dot{x}(t) = f(t, x_t, w(t)), & t \neq t_k, & k \in \mathbb{N}^+ \\ \Delta x(t) = g_k(t, x_{t^-}, w(t^-)), & t = t_k, & k \in \mathbb{N}^+ \\ x_{t_0} = \vartheta \end{cases} \quad (3.58)$$

where $x_{t^-}(s) = x(t^- + s)$ if $s \in [-r, 0)$, $w \in \mathcal{PC}([0, \infty), \mathbb{R}^m)$ is the input function; $\vartheta \in \mathcal{PC}([-r, 0], \mathbb{R}^n)$ is the initial function; $f, g_k : \mathbb{R}^+ \times \mathcal{PC}([-r, 0], \mathbb{R}^n) \times \mathbb{R}^m \rightarrow \mathbb{R}^n$ satisfy $f(t, 0, 0) = g_k(t, 0, 0) = 0$ for all $k \in \mathbb{N}^+$.

Remark 3.5.1. Here, Lemma 3.5.1 aims to develop an ISS criteria for nonlinear delayed systems with delay-dependent impulses by using the method of Lyapunov functional. The setup of ISS criteria serves the same purposes as those of Lemma 3.1.3. In particular, condition 1 ensures the decrescent properties of V_1, V_2 being positive definite, condition 2 indicates that continuous dynamics can be unstable, condition 3 and 4 describe the impulse effects at each state jump moments, and condition 5 acts as the bridge between continuous and impulsive dynamics so that ISS of V can be achieved. Moreover, in the absence of external inputs (i.e., $w(t) = 0$), Lemma 3.5.1 can be transformed into Lemma 3.1.3 with $\kappa = \frac{\omega_3}{\omega_1}$ and $\mu = c$.

Lemma 3.5.2. *Suppose $u, v \in \mathcal{PC}([t_0 - \tau_{max}, +\infty), \mathbb{R}^+)$ are continuous in each interval $[t_{k-1}, t_k), k \in \mathbb{N}^+, \psi(t) \in \mathcal{PC}([t_0, +\infty), \mathbb{R}^+)$ and constants $\lambda_1, \lambda_2, \gamma_1, \gamma_2 > 0$ such that*

$$\begin{cases} D^+u(t) \leq \lambda_1 u(t) + \lambda_2 u(t - r(t)) + \psi(t), & t \geq 0, \quad t \neq t_k \\ u(t_k) \leq \gamma_1 u(t_k^-) + \gamma_2 \sup_{s \in [-\bar{\tau}, 0]} u(t_k^- + s) + \psi(t_k^-), & k \in \mathbb{N} \end{cases} \quad (3.59)$$

$$\begin{cases} D^+v(t) \geq \lambda_1 v(t) + \lambda_2 v(t - r(t)) + \psi(t), & t \geq 0, \quad t \neq t_l \\ v(t_k) \geq \gamma_1 v(t_k^-) + \gamma_2 \sup_{s \in [-\bar{\tau}, 0]} v(t_k^- + s) + \psi(t_k^-), & k \in \mathbb{N} \end{cases} \quad (3.60)$$

where $0 < r(t) \leq h < \infty, 0 < \bar{\tau} < \infty$ and $\tau_{max} = \max\{h, \bar{\tau}\}$. Then $u(t) \leq v(t)$ for $-\tau_{max} \leq t \leq 0$ implies $u(t) \leq v(t)$ for $t \geq 0$.

Proof. Without loss of generality, consider $u(t) \leq v(t)$ fails to hold for $t \in (t_0, t_1)$, then there must exist some $t \in (t_0, t_1)$ such that $u(t) > v(t)$. Choose $\hat{t} = \inf\{t \in (t_0, t_1) | v(t) > u(t)\}$, then $u(t) \leq v(t)$ for $t \in (t_0, \hat{t}); u(\hat{t}) = v(\hat{t});$ and $u(t) > v(t)$ for $t \in (\hat{t}, \hat{t} + \epsilon)$, where $\epsilon > 0$ is sufficiently small so that $\hat{t} + \epsilon < t_1$. Thus, one can obtain $D^+u(\hat{t}) \geq D^+v(\hat{t})$ from

$$\lim_{\epsilon \rightarrow 0} \frac{u(t) - u(\hat{t})}{t - \hat{t}} > \frac{v(t) - v(\hat{t})}{t - \hat{t}}, \quad t \in (\hat{t}, \hat{t} + \epsilon) \quad (3.61)$$

Nevertheless, since $\lambda_1, \lambda_2 > 0$ and $u(t) \leq v(t)$ for $-\tau_{max} \leq t \leq 0$, it gives:

$$D^+u(\hat{t}) \leq \lambda_1 u(\hat{t}) + \lambda_2 u(\hat{t} - r(\hat{t})) + \psi(\hat{t}) \leq \lambda_1 v(\hat{t}) + \lambda_2 v(\hat{t} - r(\hat{t})) + \psi(\hat{t}) \leq D^+v(\hat{t}) \quad (3.62)$$

Thus $u(t) \leq v(t)$ holds for $t \in (t_0, t_1)$ by contradiction. Suppose $u(t) \leq v(t)$ holds for $t \in [t_q, t_{q+1}), q = 1, 2, \dots, k-1, k \in \mathbb{N}^+;$ which follows that $u(t) \leq v(t)$ for $t \in [t_k - \tau_{max}, t_k)$ with $u(t_k^-) \leq v(t_k^-)$ and $u(t_k^- - \bar{\tau}) \leq v(t_k^- - \bar{\tau})$. Then based on (3.59) and (3.60), it implies

$$u(t_k) \leq \gamma_1 u(t_k^-) + \gamma_2 \sup_{s \in [-\bar{\tau}, 0]} u(t_k^- + s) + \psi(t_k^-) \leq \gamma_1 v(t_k^-) + \gamma_2 \sup_{s \in [-\bar{\tau}, 0]} v(t_k^- + s) + \psi(t_k^-) \leq v(t_k) \quad (3.63)$$

Therefore, $u(t) \leq v(t)$ for $t \in (t_k - \tau_{max}, t_k];$ and one can also obtain $u(t) \leq v(t)$ for $t \in [t_k, t_{k+1})$ using the similar proof of (t_0, t_1) . By mathematical induction, $u(t) \leq v(t)$ holds for all $t \geq t_0$. \square

3.5.2 ISS/iISS Formation Stabilization

Theorem 3.5.1. Consider the leader-following multi-agent systems with dynamics (3.1) and (3.2) followed by control protocol (3.48). Suppose Assumption 3.1.1 and Assumption 3.1.2 hold, $\dot{r}(t) < 0$, $\inf_{k \in \mathbb{N}^+} \{t_k - t_{k-1}\} = h_1$, $\sup_{k \in \mathbb{N}^+} \{t_k - t_{k-1}\} = h_2$, $P = \begin{pmatrix} \hat{P}_{11} \otimes I_n & \hat{P}_{12} \otimes I_n \\ \hat{P}_{21} \otimes I_n & \hat{P}_{22} \otimes I_n \end{pmatrix} \in \mathbb{R}^{4n \times 4n}$ is a positive definite matrix, $\varepsilon_0, \varepsilon_1, \varepsilon_2, \varepsilon_3, \zeta_1, \zeta_2 > 0$ and $\tau_{max} = \max\{\bar{r} + \tau, 2\tau\}$. If the following conditions are satisfied with $\eta_1 > 0$, $0 \leq \rho_1 < 1$ and $\rho_2 \geq 0$:

$$\ln(\rho_1 + \rho_2 + \frac{\tau_{max}(1 - \rho_1)Q\lambda_{max}(P^{-1})\lambda_{max}(P)}{\varepsilon_0\lambda_{min}(P)}) < -\eta_1 h_2 \quad (3.64)$$

where

$$\begin{aligned} \eta_1 &= \lambda_{max}(M + \varepsilon_0 P^{-1}), \quad \beta = \frac{Q\lambda_{max}(P^{-1})}{\varepsilon_0} \\ \rho_1 &= \frac{\pi_1(1 + \varepsilon_3)}{2}, \quad \rho_2 = \frac{1}{2}(1 + \varepsilon_3^{-1})((1 + \zeta_2)\pi_2 + (1 + \zeta_2^{-1})\pi_3) \\ \pi_1 &= 2\lambda_{max}((J + K)^T P (J + K) P^{-1}) \\ \pi_2 &= 2\lambda_{max}(P)\tau^2 \|K\|^2 \kappa \lambda_{max}(P^{-1}) \\ \pi_3 &= 2\lambda_{max}(P)\lambda_{max}(P^{-1})\bar{\theta}^2 \|K\|^2 ((1 + \varepsilon_2)\|E_3\|^2 + (1 + \varepsilon_2^{-1})\|K\|^2) \end{aligned}$$

with $\bar{\theta} = \lfloor \frac{\tau}{h_1} \rfloor$, $\kappa_1 = (1 + \varepsilon_1)\|E_0 + \bar{\alpha}I_{4n}\|^2 + (1 + \varepsilon_1^{-1})(1 + \zeta_1)\|E_1\|^2$, $M = [PE_0 + E_0^T P + 2\bar{\alpha}P]P^{-1}$, $Q = \|PE_1\|^2$, $J = \begin{pmatrix} I_{2n} & \mathbf{0}_{2n \times 2n} \\ -\mu_i L & I_{2n} - \mu_i L \end{pmatrix}$, $K = \begin{pmatrix} \mathbf{0}_{2n \times 2n} & \mathbf{0}_{2n \times 2n} \\ -\mu_i c I_{2n} & -\mu_i c I_{2n} \end{pmatrix}$ and $E_3 = J - I_{4n}$. Then the error dynamics of formation control (3.54) achieves uniformly ISS/iISS over the class $\mathcal{F}(h_2)$.

Proof. Consider the Lyapunov functional for $t \in [t_k, t_{k+1})$ as:

$$H_1(t) = V_1(t) + V_2(t) = \frac{1}{2}\bar{\xi}^T(t)P\bar{\xi}(t) + \frac{Q\lambda_{max}(P^{-1})}{2\varepsilon_0} \int_{t-r(t)}^t \bar{\xi}^T(s)P\bar{\xi}(s)ds \quad (3.65)$$

Then, based on Assumption 3.1.1, Assumption 3.1.2 and Lemma 3.1.1 and system (3.54),

we take the time derivative of V_1 which gives:

$$\begin{aligned}
\dot{V}_1(t) &\leq \frac{1}{2}\bar{\xi}^T(t)[PE_0 + E_0^T P]\bar{\xi}(t) + \frac{1}{2}\bar{\xi}^T(t)PE_1\bar{\xi}(t-r(t)) + \frac{1}{2}\bar{\xi}^T(t-r(t))E_1^T P\bar{\xi}(t) \\
&\quad + \bar{\alpha}\bar{\xi}^T(t)P\bar{\xi}(t) + \bar{\xi}^T(t)PW(t) \\
&\leq \frac{1}{2}\bar{\xi}^T(t)[PE_0 + E_0^T P]\bar{\xi}(t) + \frac{\varepsilon_0}{2}\bar{\xi}^T(t)\bar{\xi}(t) + \frac{Q}{2\varepsilon_0}\bar{\xi}^T(t-r(t))\bar{\xi}(t-r(t)) + \bar{\alpha}\bar{\xi}^T(t)P\bar{\xi}(t) \\
&= \frac{1}{2}\bar{\xi}^T(t)[PE_0 + E_0^T P + 2\bar{\alpha}P]\bar{\xi}(t) + \frac{\varepsilon_0}{2}\bar{\xi}^T(t)P^{-1}P\bar{\xi}(t) + \frac{Q}{2\varepsilon_0}\bar{\xi}^T(t-r(t))P^{-1}P\bar{\xi}(t-r(t)) \\
&\leq \frac{1}{2}\bar{\xi}^T(t)[PE_0 + E_0^T P + 2\bar{\alpha}P]P^{-1}P\bar{\xi}(t) + \frac{\varepsilon_0\lambda_{\max}(P^{-1})}{2}\bar{\xi}^T(t)P\bar{\xi}(t) \\
&\quad + \frac{Q\lambda_{\max}(P^{-1})}{2\varepsilon_0}\bar{\xi}^T(t-r(t))P\bar{\xi}(t-r(t)) \\
&\leq \frac{1}{2}\lambda_{\max}(M + \varepsilon_0P^{-1})\bar{\xi}^T(t)P\bar{\xi}(t) + \frac{Q\lambda_{\max}(P^{-1})}{2\varepsilon_0}\bar{\xi}^T(t-r(t))P\bar{\xi}(t-r(t))
\end{aligned} \tag{3.66}$$

Since $\dot{r}(t) < 0$, we also have:

$$\begin{aligned}
\dot{V}_2(t) &= \frac{Q\lambda_{\max}(P^{-1})}{2\varepsilon_0}\bar{\xi}^T(t)P\bar{\xi}(t) - \frac{Q\lambda_{\max}(P^{-1})}{2\varepsilon_0}(1 - \dot{r}(t))\bar{\xi}^T(t-r(t))P\bar{\xi}(t-r(t)) \\
&\leq \frac{Q\lambda_{\max}(P^{-1})}{2\varepsilon_0}\bar{\xi}^T(t)P\bar{\xi}(t) - \frac{Q\lambda_{\max}(P^{-1})}{2\varepsilon_0}\bar{\xi}^T(t-r(t))P\bar{\xi}(t-r(t))
\end{aligned} \tag{3.67}$$

Thus,

$$\begin{aligned}
\dot{H}_1(t) &\leq \frac{1}{2}[\lambda_{\max}(M + \varepsilon_0P^{-1}) + \frac{Q\lambda_{\max}(P^{-1})}{\varepsilon_0}]\bar{\xi}^T(t)P\bar{\xi}(t) \\
&\leq \eta_1 H_1(t) + \psi(\|W(t)\|)
\end{aligned} \tag{3.68}$$

Furthermore, by integrating both sides of (3.6) from $t_k - \tau$ to t_k^- yields:

$$\begin{aligned}
\bar{\xi}(t_k^-) - \bar{\xi}(t_k - \tau) &= \int_{t_k - \tau}^{t_k} (E_0\bar{\xi}(s) + E_1\bar{\xi}(s-r(s)) + E_2(s) + W(s))ds \\
&\quad + \sum_{m=1}^{\theta_k} E_3\bar{\xi}(t_{k-m}) + \sum_{m=1}^{\theta_k} K\bar{\xi}(t_{k-m} - \tau)
\end{aligned} \tag{3.69}$$

with $\Gamma_2 = -K \int_{t_k-\tau}^{t_k} (E_0 \bar{\xi}(s) + E_1 \bar{\xi}(s-r(s)) + E_2(s) + W(s)) ds$ followed from (3.26). Moreover, it yields:

$$\begin{aligned}
\Gamma_2^T P \Gamma_2 &\leq \lambda_{max}(P) \|K\|^2 \left[\int_{t_k-\tau}^{t_k} (E_0 \bar{\xi}(s) + E_1 \bar{\xi}(s-r(s)) + E_2(s) + W(s)) ds \right]^T \\
&\quad \left[\int_{t_k-\tau}^{t_k} (E_0 \bar{\xi}(s) + E_1 \bar{\xi}(s-r(s)) + E_2(s) + W(s)) ds \right] \\
&\leq \lambda_{max}(P) \tau \|K\|^2 \int_{t_k-\tau}^{t_k} (E_0 \bar{\xi}(s) + E_1 \bar{\xi}(s-r(s)) + E_2(s) + W(s))^T \\
&\quad (E_0 \bar{\xi}(s) + E_1 \bar{\xi}(s-r(s)) + E_2(s) + W(s)) ds \\
&\leq \lambda_{max}(P) \tau \|K\|^2 \int_{t_k-\tau}^{t_k} [(1 + \varepsilon_1) \|E_0 + \bar{\alpha} I_{4n}\|^2 \bar{\xi}^T(s) \bar{\xi}(s) \\
&\quad + (1 + \varepsilon_1^{-1})(1 + \zeta_1) \|E_1\|^2 \bar{\xi}^T(s-r(s)) \bar{\xi}(s-r(s)) + (1 + \varepsilon_1^{-1})(1 + \zeta_1^{-1}) W^T(s) W(s)] ds \\
&\leq \lambda_{max}(P) \tau \|K\|^2 \int_{t_k-\tau}^{t_k} \kappa_1 \sup_{r(s) \in [0, \bar{r}]} \bar{\xi}^T(s-r(s)) \bar{\xi}(s-r(s)) ds \\
&\quad + \lambda_{max}(P) \tau^2 \|K\|^2 (1 + \varepsilon_1^{-1})(1 + \zeta_1^{-1}) \sup_{s \in [-\bar{r}-\tau, 0]} \|W(t_k^- + s)\|^2 \\
&\leq 2\lambda_{max}(P) \tau^2 \|K\|^2 \kappa_1 \lambda_{max}(P^{-1}) \sup_{s \in [-\bar{r}-\tau, 0]} V_1(t_k^- + s) \\
&\quad + \lambda_{max}(P) \tau^2 \|K\|^2 (1 + \varepsilon_1^{-1})(1 + \zeta_1^{-1}) \sup_{s \in [-\bar{r}-\tau, 0]} \|W(t_k^- + s)\|^2 \\
&\leq \pi_2 \sup_{s \in [-\tau_{max}, 0]} V_1(t_k^- + s) + \kappa_3 \sup_{s \in [-\tau_{max}, 0]} \|W(t_k^- + s)\|^2
\end{aligned} \tag{3.70}$$

where $\kappa_3 = \lambda_{max}(P) \tau^2 \|K\|^2 (1 + \varepsilon_1^{-1})(1 + \zeta_1^{-1})$. By combining (3.27), (3.70) and (3.29), we get:

$$\begin{aligned}
2V_1(t_k) &\leq \pi_1(1 + \varepsilon_3) V_1(t_k^-) + (1 + \varepsilon_3^{-1})(1 + \zeta_2) \pi_2 \sup_{s \in [-\tau_{max}, 0]} V_1(t_k^- + s) \\
&\quad + (1 + \varepsilon_3^{-1})(1 + \zeta_2) \kappa_3 \sup_{s \in [-\tau_{max}, 0]} \|W(t_k^- + s)\|^2 + (1 + \varepsilon_3^{-1})(1 + \zeta_2^{-1}) \pi_3 \sup_{s \in [-\tau_{max}, 0]} V_1(t_k^- + s)
\end{aligned} \tag{3.71}$$

so that

$$\begin{aligned}
V_1(t_k) &\leq \frac{\pi_1(1 + \varepsilon_3)}{2} V_1(t_k^-) + \frac{(1 + \varepsilon_3^{-1})((1 + \zeta_2)\pi_2 + (1 + \zeta_2^{-1})\pi_3)}{2} \sup_{s \in [-\tau_{max}, 0]} V_1(t_k^- + s) \\
&\quad + (1 + \varepsilon_3^{-1})(1 + \zeta_2)\kappa_3 \|W(t)\|^2 \\
&= \rho_1 V_1(t_k^-) + \rho_2 \sup_{s \in [-\tau_{max}, 0]} V_1(t_k^- + s) + (1 + \varepsilon_3^{-1})(1 + \zeta_2)\kappa_3 \sup_{s \in [-\tau_{max}, 0]} \|W(t_k^- + s)\|^2
\end{aligned} \tag{3.72}$$

with $\psi(\|W(t)\|) = (1 + \varepsilon_3^{-1})(1 + \zeta_2)\kappa_3 \|W(t)\|^2$. Hence, based on (3.64) and $V_2(t) \leq \frac{\tau_{max} Q \lambda_{max}(P^{-1}) \lambda_{max}(P)}{\varepsilon_0 \lambda_{min}(P)} \sup_{s \in [-\tau_{max}, 0]} V_1(t + s)$, then all the conditions in Lemma 3.5.1 are satisfied so that uniformly ISS of MASs over $\mathcal{F}(h_2)$ is achieved. Meanwhile, we can derive that

$$\left\{ \begin{aligned}
\dot{H}_1(t) &\leq \eta_1 H_1(t) + \psi(\|W(t)\|), \quad t \neq t_k \\
H_1(t_k) &\leq \rho_1 V_1(t_k^-) + \rho_2 \sup_{s \in [-\tau_{max}, 0]} V_1(t_k^- + s) + V_2(t_k^-) + \psi(\|W(t_k^-)\|) \\
&\leq \rho_1 V_1(t_k^-) + (\rho_2 + \frac{\tau_{max} Q \lambda_{max}(P^{-1}) \lambda_{max}(P)}{\varepsilon_0 \lambda_{min}(P)}) \sup_{s \in [-\tau_{max}, 0]} V_1(t_k^- + s) + \psi(\|W(t_k^-)\|) \\
&\leq \rho_1 H_1(t_k^-) + (\rho_2 + \frac{\tau_{max} Q \lambda_{max}(P^{-1}) \lambda_{max}(P)}{\varepsilon_0 \lambda_{min}(P)}) \sup_{s \in [-\tau_{max}, 0]} H_1(t_k^- + s) \\
&\quad + \psi(\sup_{s \in [-\tau_{max}, 0]} \|W(t_k^- + s)\|), \quad t = t_k
\end{aligned} \right. \tag{3.73}$$

and it is upper bounded by the non-negative solution $\tilde{H}_1(t)$ of the following system

$$\left\{ \begin{aligned}
\dot{\tilde{H}}_1(t) &= \eta_1 \tilde{H}_1(t) + \psi(\|W(t)\|), \quad t \neq t_k \\
\tilde{H}_1(t_k) &= \rho_1 \tilde{H}_1(t_k^-) + (\rho_2 + \frac{\tau_{max} Q \lambda_{max}(P^{-1}) \lambda_{max}(P)}{\varepsilon_0 \lambda_{min}(P)}) \sup_{s \in [-\tau_{max}, 0]} \tilde{H}_1(t_k^- + s) \\
&\quad + \psi(\sup_{s \in [-\tau_{max}, 0]} \|W(t_k^- + s)\|), \quad t = t_k \\
\tilde{H}_1(t_0) &= \vartheta
\end{aligned} \right. \tag{3.74}$$

where $\vartheta \in \mathcal{PC}(\in [-\tau_{max}, 0], \mathbb{R})$. Then, let $\hat{H}_1(t)$ be the non-negative solution of the system

$$\left\{ \begin{aligned}
\dot{\hat{H}}_1(t) &= \psi(\|W(t)\|), \quad t \neq t_k \\
\hat{H}_1(t_k) &= \hat{H}_1(t_k^-) + \psi(\sup_{s \in [-\tau_{max}, 0]} \|W(t_k^- + s)\|), \quad t = t_k \\
\hat{H}_1(t_0) &= 0
\end{aligned} \right. \tag{3.75}$$

which gives that for $t \geq 0$

$$\hat{H}_1(t) \leq \int_{t_0}^t \psi(\|W(s)\|) ds + \sum_{k \in N(t_0, t)} \psi(\sup_{s \in [-\tau_{max}, 0]} \|W(t_k^- + s)\|) \tag{3.76}$$

where $N(t_0, t)$ denotes the total number of impulsive instants on the interval (t_0, t) . Accordingly, we can obtain the following system by defining $\bar{H}_1(t) = \tilde{H}_1(t) - \hat{H}_1(t)$,

$$\left\{ \begin{array}{l} \dot{\hat{H}}_1(t) \leq \eta_1 \bar{H}_1(t) + \eta_1 \hat{H}_1(t), \quad t \neq t_l \\ \bar{H}_1(t_k) \leq \rho_1 \bar{H}_1(t_k^-) + (\rho_1 - 1) \hat{H}_1(t_k^-) + (\rho_2 + \frac{\tau_{max} Q \lambda_{max}(P^{-1}) \lambda_{max}(P)}{\varepsilon_0 \lambda_{min}(P)}) \sup_{s \in [-\tau_{max}, 0]} \bar{H}_1(t_k^- + s) \\ \quad + (\rho_2 + \frac{\tau_{max} Q \lambda_{max}(P^{-1}) \lambda_{max}(P)}{\varepsilon_0 \lambda_{min}(P)}) \sup_{s \in [-\tau_{max}, 0]} \hat{H}_1(t_k^- + s) \\ \leq \rho_1 \bar{H}_1(t_k^-) + (\rho_2 + \frac{\tau_{max} Q \lambda_{max}(P^{-1}) \lambda_{max}(P)}{\varepsilon_0 \lambda_{min}(P)}) \sup_{s \in [-\tau_{max}, 0]} \bar{H}_1(t_k^- + s) \\ \quad + (\rho_1 - 1 + \rho_2 + \frac{\tau_{max} Q \lambda_{max}(P^{-1}) \lambda_{max}(P)}{\varepsilon_0 \lambda_{min}(P)}) \sup_{s \in [-\tau_{max}, 0]} \hat{H}_1(t_k^- + s), \quad t = t_k \\ \bar{H}_{1t_0} = \vartheta \end{array} \right. \quad (3.77)$$

By treating $\bar{H}_1(t)$, $\hat{H}_1(t)$ as the role of $H_1(t)$ and $\psi(\|W(t)\|)$ respectively, the system (3.77) is uniformly ISS with linear gain $\bar{H}_1(t) \leq \beta(\|\vartheta\|_{\tau_{max}}, t - t_0) + \phi \hat{H}_1(t)$, $t \geq t_0$ for some function $\beta \in \mathcal{KL}$ as (3.64) holds and constant $\phi = \max\{\eta_1, \rho_1 - 1 + \rho_2 + \frac{\tau_{max} Q \lambda_{max}(P^{-1}) \lambda_{max}(P)}{\varepsilon_0 \lambda_{min}(P)}\} > 0$. Hence, it follows from Definition 3.5.1 and (3.76) that:

$$\begin{aligned} H_1(t) &\leq \tilde{H}_1(t) \leq \beta(\|\vartheta\|_{\tau_{max}}, t - t_0) + (\phi + 1) \hat{H}_1(t) \\ &\leq \beta(\|\vartheta\|_{\tau_{max}}, t - t_0) + \int_0^t (\phi + 1) \psi(\|W(s)\|) ds \\ &\quad + (\phi + 1) \sum_{k \in N(t_0, t)} \psi(\sup_{s \in [-\tau_{max}, 0]} \|W(t_k^- + s)\|) \end{aligned} \quad (3.78)$$

Therefore, the uniformly iISS of MASs over $\mathcal{F}(h_2)$ is also realized. As a result, the input-to-state/integral input-to-state formation stabilization are achieved for the leader-following MASs. \square

Remark 3.5.2. *Theorem 3.5.1 provides sufficient conditions for uniformly input-to-state and integral input-to-state formation stabilization of MASs over impulsive sequence class $\mathcal{F}(h_2)$, which depends on the relation among impulsive gains, continuous feedback gains and upper bound of impulse interval. In particular, the discrete delay-dependent impulses under destabilizing continuous dynamics is considered. Nevertheless, the class of $\mathcal{F}(h_2)$ is considered conservative owing to the restriction on the uniform upper bound of the length of impulse interval. Therefore, we present the following results with $\tau_{max} < \inf\{t_k - t_{k-1}\}$ for $k \in \mathbb{N}^+$ by using the method of average impulsive interval.*

Theorem 3.5.2. Consider the leader-following multi-agent systems (3.1) and (3.2) followed by the hybrid impulsive control protocol (3.48). Suppose the Assumptions 3.1.1-3.1.2 hold, $P = \begin{pmatrix} \hat{P}_{11} \otimes I_n & \hat{P}_{12} \otimes I_n \\ \hat{P}_{21} \otimes I_n & \hat{P}_{22} \otimes I_n \end{pmatrix} \in \mathbb{R}^{4n \times 4n}$ is a positive definite matrix, and $\tau_{max} < h_1$. If there exists a $q_1 > 0$ such that the following condition is satisfied:

$$\eta_1 + \frac{\ln(\rho_1 + \rho_3)}{T_\alpha} < -q_1 < 0 \quad (3.79)$$

where $\rho_2 = \frac{(1+\varepsilon_3^{-1})\pi_2}{2}$, $\rho_3 = \rho_2 + \frac{\tau_{max}Q\lambda_{max}(P^{-1})\lambda_{max}(P)}{\varepsilon_0\lambda_{min}(P)}$, and the rest of parameters remains the same as defined in Theorem 3.5.1. Then the error dynamics of formation control (3.54) achieves uniformly ISS/iISS over the average impulsive interval class $\mathcal{F}[T_\alpha, \varrho]$.

Proof. From the proof of Theorem 3.5.1, similar argument of (3.66)-(3.72) can be maintained with $\theta_k = \bar{\theta} = 0$ such that $\Gamma_3 P \Gamma_3 = 0$. Then we have:

$$\begin{aligned} 2V_1(t_k) &\leq \pi_1(1 + \varepsilon_3)V_1(t_k^-) + (1 + \varepsilon_3^{-1})\pi_2 \sup_{s \in [-\tau_{max}, 0]} V_1(t_k^- + s) \\ &\quad + (1 + \varepsilon_3^{-1})\kappa_3 \sup_{s \in [-\tau_{max}, 0]} \|W(t_k^- + s)\|^2 \end{aligned} \quad (3.80)$$

and

$$\begin{aligned} V_1(t_k) &\leq \frac{\pi_1(1 + \varepsilon_3)}{2}V_1(t_k^-) + \frac{(1 + \varepsilon_3^{-1})\pi_2}{2} \sup_{s \in [-\tau_{max}, 0]} V_1(t_k^- + s) \\ &\quad + (1 + \varepsilon_3^{-1})\kappa_3 \|W(t_k)\|^2 \\ &= \rho_1 V_1(t_k^-) + \rho_2 \sup_{s \in [-\tau_{max}, 0]} V_1(t_k^- + s) + (1 + \varepsilon_3^{-1})\kappa_3 \sup_{s \in [-\tau_{max}, 0]} \|W(t_k^- + s)\|^2 \end{aligned} \quad (3.81)$$

with $\psi(\|W(t)\|) = (1 + \varepsilon_3^{-1})\kappa_3 \|W(t)\|^2$ and $\rho_2 = \frac{(1+\varepsilon_3^{-1})\pi_2}{2}$. It follows from (3.73) and Lemma 3.5.2 that for any positive constant $\varepsilon_e > 0$, one has the following impulsive comparison system:

$$\begin{cases} \dot{H}_{max}(t) &= \eta_1 H_{max}(t) + \psi(\|W(t)\|) + \varepsilon_e, & t \neq t_k \\ H_{max}(t_k) &= \rho_1 H_{max}(t_k^-) + \rho_3 \sup_{s \in [-\tau_{max}, 0]} H_{max}(t_k^- + s) + \psi(\|W(t_k^-)\|), & t = t_k \\ H_{max}(t_0 + s) &= \vartheta, & s \in [-\tau_{max}, 0] \end{cases} \quad (3.82)$$

where $H_1(t) \leq H_{max}(t)$ for $t > t_0$. Then one has

$$H_{max}(t) = \vartheta e^{\eta_1(t-t_0)} + \int_{t_0}^t e^{\eta_1(t-z)} (\psi(\|W(z)\|) + \varepsilon_e) dz, \quad t \in [t_0, t_1) \quad (3.83)$$

and

$$\begin{aligned} H_{max}(t_1) &= \rho_1 H_{max}(t_1^-) + \rho_3 \sup_{s \in [-\tau_{max}, 0]} H_{max}(t_1^- + s) + \psi(\|W(t_1^-)\|) \\ &= \rho_1 \vartheta e^{\eta_1(t_1-t_0)} + \rho_1 \int_{t_0}^{t_1} e^{\eta_1(t_1-z)} (\psi(\|W(z)\|) + \varepsilon_e) dz \\ &\quad + \rho_3 \sup_{s \in [-\tau_{max}, 0]} [\vartheta e^{\eta_1(t_1+s-t_0)} + \int_{t_0}^{t_1+s} e^{\eta_1(t_1+s-z)} (\psi(\|W(z)\|) + \varepsilon_e) dz] + \psi(\|W(t_1^-)\|) \\ &= (\rho_1 + \rho_3) \vartheta e^{\eta_1(t_1-t_0)} + (\rho_1 + \rho_3) \int_{t_0}^{t_1} e^{\eta_1(t_1-z)} (\psi(\|W(z)\|) + \varepsilon_e) dz + \psi(\|W(t_1^-)\|) \end{aligned} \quad (3.84)$$

Recursively for $t \in [t_1, t_2)$, we have

$$\begin{aligned} H_{max}(t) &= H_{max}(t_1) e^{\eta_1(t-t_1)} + \int_{t_1}^t e^{\eta_1(t-z)} (\psi(\|W(z)\|) + \varepsilon_e) dz \\ &= (\tilde{\rho}_1 + \tilde{\rho}_3) \vartheta e^{\eta_1(t-t_1+t_1-t_0)} + (\rho_1 + \rho_3) \int_{t_0}^{t_1} e^{\eta_1(t-t_1+t_1-z)} (\psi(\|W(z)\|) + \varepsilon_e) dz \\ &\quad + e^{\eta_1(t-t_1)} \psi(\|W(t_1^-)\|) \\ &\quad + \int_{t_1}^t e^{\eta_1(t-z)} (\psi(\|W(z)\|) + \varepsilon_e) dz \end{aligned} \quad (3.85)$$

and

$$\begin{aligned} H_{max}(t_2) &= \rho_1 H_{max}(t_2^-) + \rho_3 \sup_{s \in [-\tau_{max}, 0]} H_{max}(t_2^- + s) + \psi(\|W(t_2^-)\|) \\ &= (\rho_1 + \rho_3)^2 e^{\eta_1(t_2-t_0)} + (\rho_1 + \rho_3)^2 \int_{t_0}^{t_1} e^{\eta_1(t_2-z)} (\psi(\|W(z)\|) + \varepsilon_e) dz \\ &\quad + (\rho_1 + \rho_3) e^{\eta_1(t_2-t_1)} \psi(\|W(t_1^-)\|) \\ &\quad + (\rho_1 + \rho_3) \int_{t_1}^{t_2} e^{\eta_1(t_2-z)} (\psi(\|W(z)\|) + \varepsilon_e) dz + \psi(\|W(t_2^-)\|) \end{aligned} \quad (3.86)$$

Hence, one can obtain the following for $t \in [t_{k-1}, t_k)$ by mathematical induction:

$$\begin{aligned}
H_{max}(t) &= (\rho_1 + \rho_3)^{k-1} \vartheta e^{\eta_1(t-t_0)} + \sum_{m=1}^{k-1} \int_{t_{m-1}}^{t_m} (\rho_1 + \rho_3)^{k-m} e^{\eta_1(t-z)} (\psi(\|W(z)\|) + \varepsilon_e) dz \\
&+ \sum_{m=1}^{k-1} (\rho_1 + \rho_3)^{k-m-1} e^{\eta_1(t-t_m)} \psi(\|(t_m^-)\|) + \int_{t_{k-1}}^t e^{\eta_1(t-z)} (\psi(\|W(z)\|) + \varepsilon_e) dz
\end{aligned} \tag{3.87}$$

Meanwhile, based on Definition 3.5.3, (3.87) can be rewritten as for any $t \geq t_0$:

$$\begin{aligned}
H_{max}(t) &= (\rho_1 + \rho_3)^{N(t_0,t)} \vartheta e^{\eta_1(t-t_0)} + \int_{t_0}^t (\rho_1 + \rho_3)^{N(z,t)} e^{\eta_1(t-z)} (\psi(\|W(z)\|) + \varepsilon_e) dz \\
&+ \sum_{t_0 < t_k \leq t} (\rho_1 + \rho_3)^{N(t_k,t)} e^{\eta_1(t-t_k)} \psi(\|W(t_k^-)\|)
\end{aligned} \tag{3.88}$$

while letting $\varepsilon_e \rightarrow 0$, according to (3.79), it further implies:

$$\begin{aligned}
H_1(t) \leq H_{max}(t) &\leq (\rho_1 + \rho_3)^q \vartheta e^{(\eta_1 + \frac{\ln(\rho_1 + \rho_3)}{T_\alpha})(t-t_0)} + \int_{t_0}^t (\rho_1 + \rho_3)^q e^{(\eta_1 + \frac{\ln(\rho_1 + \rho_3)}{T_\alpha})(t-z)} \psi(\|W(z)\|) dz \\
&+ \sum_{t_0 < t_k \leq t} (\rho_1 + \rho_3)^q e^{(\eta_1 + \frac{\ln(\rho_1 + \rho_3)}{T_\alpha})(t-t_k)} \psi(\|W(t_k^-)\|) \\
&\leq (\rho_1 + \rho_3)^q \vartheta e^{-q_1(t-t_0)} + \int_{t_0}^t (\rho_1 + \rho_3)^q e^{-q_1(t-z)} \psi(\|W(z)\|) dz \\
&+ \sum_{t_0 < t_k \leq t} (\rho_1 + \rho_3)^q e^{-q_1(t-t_k)} \psi(\|W(t_k^-)\|)
\end{aligned} \tag{3.89}$$

Therefore, it follows from (3.89) that

$$\begin{aligned}
H_1(t) &\leq (\rho_1 + \rho_3)^q \vartheta e^{-q_1(t-t_0)} + \frac{1}{q_1} (\rho_1 + \rho_3)^q (\psi(\|W\|_{[t_0,t]})) + \frac{1}{1 - e^{-q_1 h_1}} (\rho_1 + \rho_3)^q \psi(\|W\|_{[t_0,t]}) \\
&\leq (\rho_1 + \rho_3)^q \vartheta e^{-q_1(t-t_0)} + \max\left\{ \frac{1}{q_1} (\rho_1 + \rho_3)^q, \frac{1}{1 - e^{-q_1 h_1}} (\rho_1 + \rho_3)^q \right\} \psi(\|W\|_{[t_0,t]})
\end{aligned} \tag{3.90}$$

and

$$H_1(t) \leq (\rho_1 + \rho_3)^q \vartheta e^{-q_1(t-t_0)} + (\rho_1 + \rho_3)^q \int_{t_0}^t (\psi(\|W(z)\|)) dz + (\rho_1 + \rho_3)^q \sum_{t_0 < t_k \leq t} \psi(\|W\|_{[t_k - \tau_{max}, t_k]}) \tag{3.91}$$

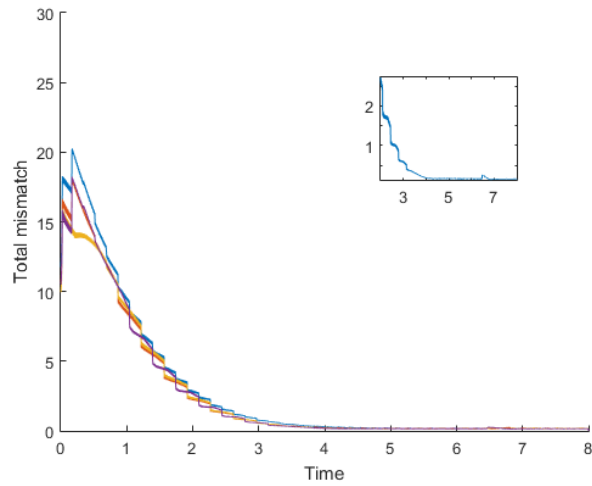
Consequently, the uniformly input-to-state/integral input-to-state formation stabilization of MAS over the average impulsive interval class $\mathcal{F}[T_\alpha, \varrho]$ are also achieved based on (3.90) and (3.91). □

Remark 3.5.3. *It is worth noting that the average impulsive interval T_α is still required to be upper bounded (i.e., $T_\alpha < \frac{|\ln(\rho_1 + \rho_3)|}{q_1 + \eta_1}$) when impulsive instants are unknown or indefinite; it indicates that our stabilizing delayed control impulses should not be activated too sparsely. However, the upper bound of T_α can be increased by either mitigating the destabilizing effects on continuous dynamics (i.e., reduce η_1) or strengthening the impulse effects (i.e., reduce $\rho_1 + \rho_3$) according to (3.79), which further reduces the frequency of control impulses.*

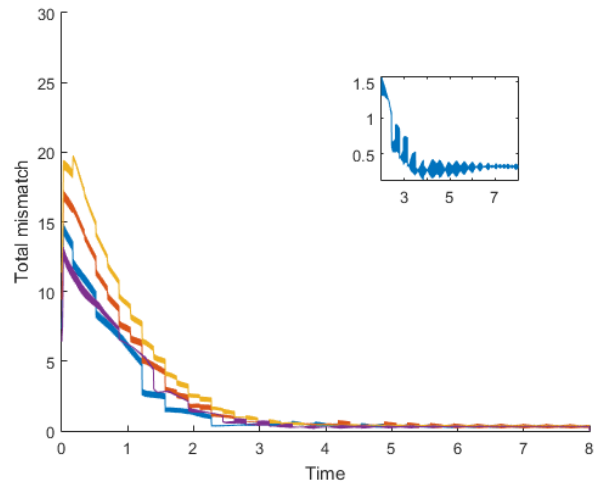
Remark 3.5.4. *In this section, we have investigated the input-to-state formation stabilization of MASs systems by treating the collision avoidance mechanisms as external control inputs. By using the method of Lyapunov functional, the average impulsive interval approach as well as impulsive comparison theory, sufficient conditions benefiting from delayed control impulses have been derived for maintaining input-to-state/integral input-to-state formation stabilization over the impulse sequence class $\mathcal{F}(h_2)$ and $\mathcal{F}[T_\alpha, \varrho]$ respectively, in terms of continuous/impulsive feedback gains, size of time delays, uniform upper bound of impulsive interval and length of average impulsive interval. Finally, the numerical examples are provided to validate the effectiveness of our theoretical results.*

3.5.3 Numerical Simulations

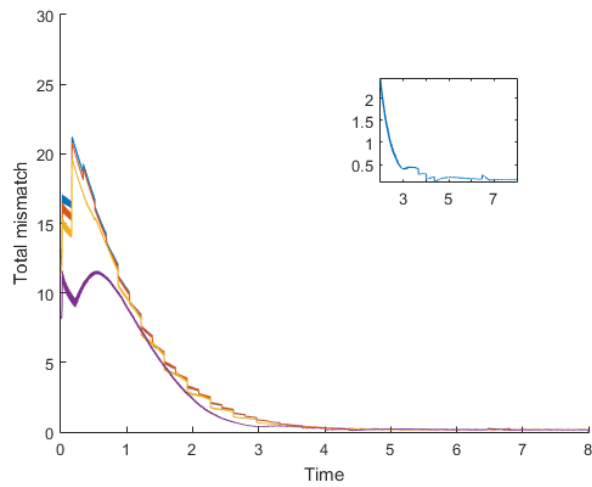
Two numerical simulation examples are presented based on the theoretical results in Theorem 3.5.1 and Theorem 3.5.2 respectively. The formation simulation period is 8s with respect to the leader-following MASs, and its corresponding topology connectivity is indicated in Figure 3.1. The initial position $p_i(0)$ is arbitrarily generated within the admissible range of $[0, 5] \times [0, 5]$, and the initial velocity $v_i(0)$ is set to be zero; while the initial conditions of the leader are set to be $p_0(0) = [0, -5]^T$ and $v_0(0) = [0.2, 0.2]^T$. We also set the nonlinear intrinsic dynamics $f(\hat{v}_i(t)) = 0.1\sqrt{\hat{v}_i^T(t)\hat{v}_i(t)} + 5$, $\alpha_p = \alpha_v = 0$, $b_{ij} = 1.5$ and $c = 5$. In addition, the exponentially decaying $W(t) = [5e^{-0.5t}, 5e^{-0.5t}]^T$ and periodic $W(t) = [\frac{1}{5}\cos(5\pi t), \frac{1}{5}\cos(5\pi t)]^T$ external inputs are considered respectively.



(a)



(b)



(c)

Figure 3.3: (a) Total mismatch without external inputs (b) Total mismatch with periodic external inputs (c) Total mismatch with exponentially decaying external inputs over $\mathcal{F}(h_2)$

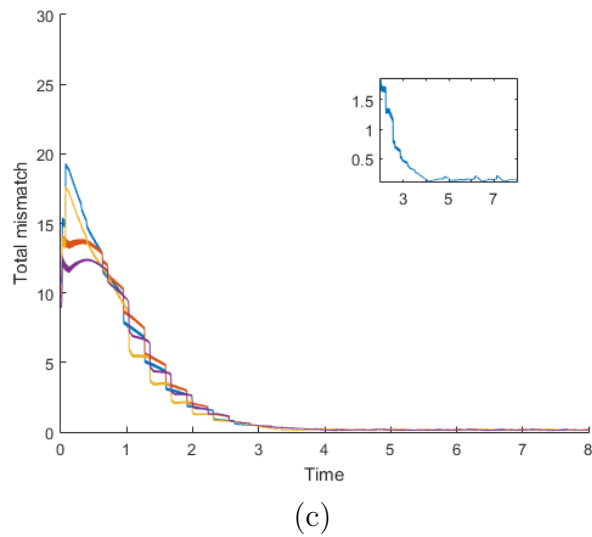
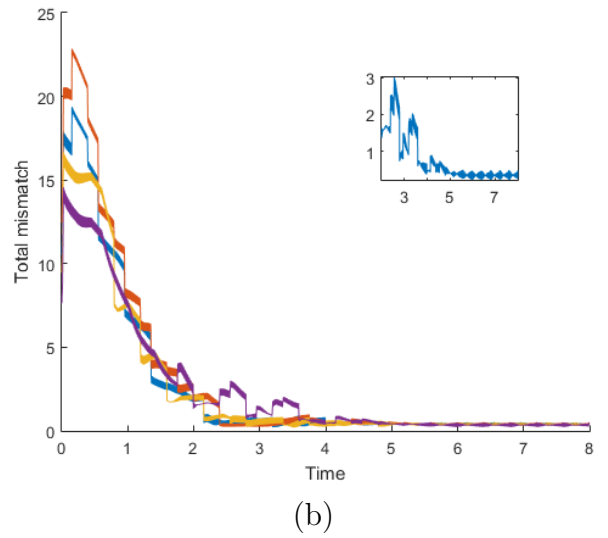
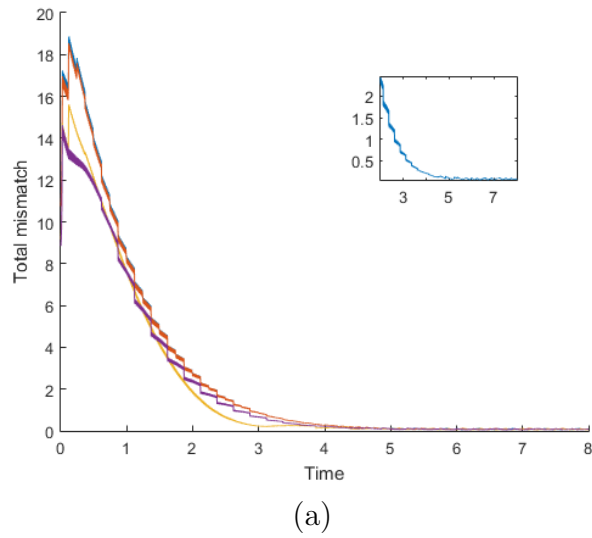


Figure 3.4: (a) Total mismatch without external inputs (b) Total mismatch with periodic external inputs (c) Total mismatch with exponentially decaying external inputs over $\mathcal{F}[T_\alpha, \varrho]$

Example 1. (Impulse sequence class $\mathcal{F}(h_2)$) Consider $h_1 = 0.01$, $\bar{r} = 0.02$, $\bar{\tau} = 0.0133$ and $\tau_{max} = 0.0333$; then by using LMI toolbox, we obtain $\rho_1 = 0.314$, $\rho_2 = 0.631$, and $\eta_1 = 3.24$. Consider the uniform impulsive sequence with $t_k - t_{k-1} = T_\alpha = 0.0117 < 0.0145$ and $\varrho = 1$ as (3.64) is satisfied. The sum of velocity and displacement mismatch (i.e., total mismatch) with respect to the leader are all converging to zero asymptotically in the absence of external inputs as shown in Figure 3.3(a). Meanwhile, in order to further characterize the effects of external inputs, the periodic and exponentially decaying inputs are implemented accordingly. Thus, in Figure 3.3(b)-(c), the total error trajectories for each type of inputs are demonstrated. As a result, it verifies that uniformly ISS/iISS properties under desired formation tracking are guaranteed; hence the theoretical results in Theorem 3.5.1 are valid over the impulse sequence class $\mathcal{F}(h_2)$.

Example 2. (Impulse sequence class $\mathcal{F}[T_\alpha, \varrho]$) By using LMI toolbox, we obtain $\rho_1 = 0.251$, $\rho_2 = 0.68$ and $\eta_1 = 3.47$. Consider the impulsive sequence $\{t_k\}_{k \in \mathbb{N}^+} = \{t_{2n-1} = 0.04n - 0.03, t_{2n} = 0.04n\}_{n \in \mathbb{N}^+}$ with $h_1 = 0.01$, $T_\alpha = 0.02$ and $\varrho = 5$ as (3.79) is satisfied. Let $\bar{r} = 0.0065$, $\bar{\tau} = 0.003$ and $\tau_{max} = 0.0097$. Figure 3.4 demonstrates the simulation results regarding asymptotic convergence of error dynamics without external inputs, and its corresponding characteristics under different types of external inputs; which are aligned with the results in Example 1. Therefore, the analytic results in Theorem 3.5.2, which the uniformly input-to-state/integral input-to-state formation stabilization over the average impulsive class of $\mathcal{F}[T_\alpha, \varrho]$ are validated.

Chapter 4

Multi-group Hybrid Impulsive Control of Heterogeneous MASs

Many previous studies have focused on homogeneous multi-agent systems. However, agents often exhibit different dynamics at different nodes in reality. The study of stability analysis and control of heterogeneous dynamics has progressed rapidly in recent years. For example, the consensus problem for heterogeneous multi-agent systems has been extensively investigated [80, 81]. The containment control of heterogeneous linear systems via distributed hybrid active control and output regulation has been considered in [82]; while impulsive containment control in heterogeneous multi-layer complex networks was studied in [83]. In [84, 85], they have focused on the flocking control of heterogeneous multi-agent systems. Nevertheless, in the above works, heterogeneous dynamics of the same order were employed among agents. Thus, the formation control problem of heterogeneous systems with distinct orders naturally arises as a study motivation. Furthermore, it is more practical to divide large groups of agents into subgroups and track their leaders separately. This will increase the capability of task diversion and allocation efficiency. A basic concept of multi-group consensus has been discussed in [86] by assuming that the total weight of communication exchange from other groups remains zero. In [87, 88], multi-group formation control via fully continuous control was investigated.

Therefore, this chapter aims to investigate multi-group formation control problem of heterogeneous multi-agent systems under the hybrid impulsive framework. Specifically, the heterogeneous networks with a mixture of second- and third-order dynamics are now considered in contrast to [84, 85], where extra control components must be adapted to compensate for order differences. As a result of such generalization, MAS networks become more diverse and can be extended to higher order dynamics. Meanwhile, a multi-group

formation tracking structure is established based on directed inter-group information exchange, as opposed to the undirected exchange discussed in [86]. In this manner, group-wise cohesion and velocity alignment can be achieved with a relaxed interaction topology.

4.1 Problem Formulation

Consider a group of n agents moving in the 2D Euclidean space, which consists m second-order agents and $n - m$ third-order agents. The dynamics of the heterogeneous multi-agent systems can be modelled as follows.

$$\begin{cases} \dot{x}_i(t) = v_i(t) \\ \dot{v}_i(t) = \alpha_x x_i(t) + \alpha_v v_i(t) + f(v_i(t)) + \phi(v_i(t)) + u_i(t), & i = 1, 2, \dots, m \end{cases} \quad (4.1)$$

$$\begin{cases} \dot{x}_i(t) = v_i(t) \\ \dot{v}_i(t) = \alpha_x x_i(t) + \alpha_v v_i(t) + f(v_i(t)) + \phi(v_i(t)) + u_{i1}(t) + a_i(t) \\ \dot{a}_i(t) = u_{i2}(t), & i = m + 1, \dots, n \end{cases}$$

where x_i, v_i, a_i and $u_i \in \mathbb{R}^2$ are the position, velocity, acceleration and control input of agent i respectively. $\alpha_x, \alpha_v \in \mathbb{R}$ are constants, $f(\cdot) : \mathbb{R}^2 \rightarrow \mathbb{R}^2$ represents the nonlinear intrinsic dynamics of agent i . Agents have second-order dynamics for $i = 1, \dots, m$, and third-order dynamics for $i = m + 1, \dots, n$. Meanwhile, the multi-agent systems are exposed to the external disturbances which cannot be neglected in reality; thus the term $\phi(\cdot) : \mathbb{R}^2 \rightarrow \mathbb{R}^2$ is added into the agent i 's dynamics to describe the external disturbance.

The dynamics of the s -th virtual leader is constructed as

$$\begin{cases} \dot{x}_s^0(t) = v_s^0(t) \\ \dot{v}_s^0(t) = \alpha_x x_s^0(t) + \alpha_v v_s^0(t) + f(v_s^0(t)) + \phi(v_s^0(t)), & s = 1, 2, \dots, l \end{cases} \quad (4.2)$$

where virtual leaders' signals $x_s^0(t), v_s^0(t)$ are bounded.

Without loss of generality, denote $m_s, n_s - m_s$ as the number of agents with second-order and third-order dynamics in (4.1) respectively, and $\sum_{s=1}^l n_s = n$ be the total number of follower agents in the s -th subgraph with $n_0 = 0$. Then topology $\mathcal{G}_s = (\mathcal{V}_s, \mathcal{E}_s)$ describes the topology of the s -th subgraph, and $N_{i,s}$ is the corresponding neighbour set of agent i which belongs to this subgraph. In addition, denote $\eta_s = \sum_{p=1}^s n_{s-p}$, then $\mathcal{V}_s = \{1 + \eta_s, 2 + \eta_s, \dots, n_s + \eta_s\}$ is the agent index of the s -th subgraph. Thus, we construct the inter-group communication links between subgroup g and subgroup h as follows:

$$\sum_{i \in N_{i,g}} \sum_{j \in N_{i,h}} -a_{ij}(x_i - x_j - x_g^0 + x_h^0 - x_i^d + x_j^d) - a_{ij}(v_i - v_j - v_g^0 + v_h^0) \quad (4.3)$$

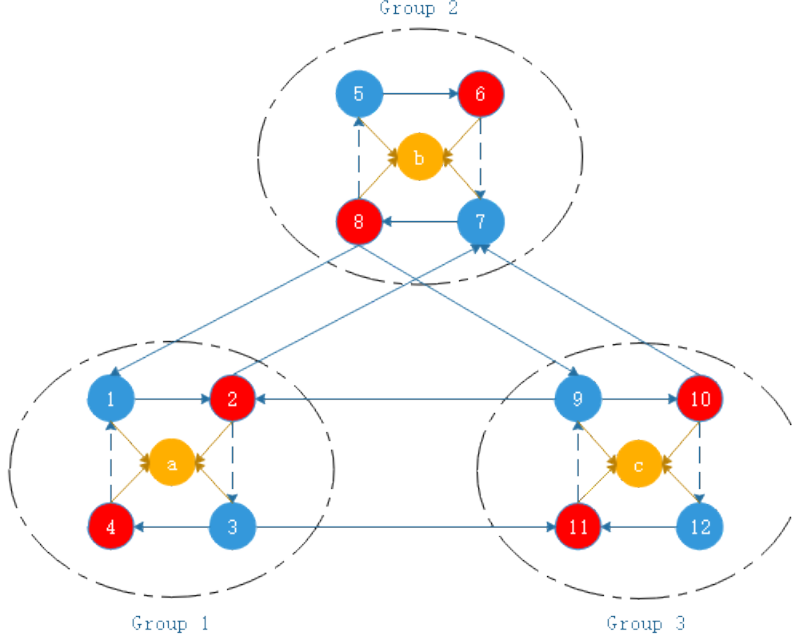


Figure 4.1: Connectivity of the overall topology with 3 subgroups

where $g, h = 1, \dots, l$, $x_i^d \in \mathbb{R}^2$ represents the desired displacement vector connecting agent i and its corresponding virtual leader. We shall make the following assumptions.

Assumption 4.1.1. *Suppose in dynamics (4.1) and (4.2) that the Lipschitz conditions are satisfied as follows:*

$$\begin{aligned} \|f(u) - f(v)\| &\leq \alpha \|u - v\| \\ \|\phi(u) - \phi(v)\| &\leq \gamma \|u - v\| \end{aligned} \tag{4.4}$$

where α and γ are positive constants, for all $u, v \in \mathbb{R}^2$.

Assumption 4.1.2. *Assume the overall topology \mathcal{G} is strongly connected and any of its subgraph's topology $\mathcal{G}_s \subset \mathcal{G}$ with $s = 1, 2, \dots, l$ is balanced and strongly connected; meanwhile, each group tracks exactly one virtual leader, which acts as root node of a spanning tree. Also, assume that $\mathcal{V}_s \cap \mathcal{V}_z = \emptyset$ for $s \neq z$, $\cup_{s=1}^l \mathcal{V}_s = \Xi$, and $\cup_{s=1}^l \mathcal{E}_s = E$.*

Remark 4.1.1. In Figure 4.1, the interaction topology within each group and communication connectivity among groups are illustrated, under Assumption 4.1.2. The blue and red circles represent the second-order and third-order dynamics of the heterogeneous systems (4.1) respectively, while the yellow circle represents the virtual leader to be tracked in each group. Meanwhile, all blue solid lines represent continuous transmission, whereas blue dashed lines represent connectivity recovery at each impulsive instant. Therefore, the topology of each group is balanced and strongly connected, and the overall topology is strongly connected. There are many real-life applications of such multi-group structures, including multi-target hunting, cooperative searching for multiple objectives, and so forth.

4.2 Multi-group Formation Stabilization

Let $\hat{x}_i(t) = x_i(t) - x_s^0(t) - x_i^d$ where x_i^d is the desired displacement between agent i and the leader in s -th subgroup, $\hat{v}_i(t) = v_i(t) - v_s^0(t)$. By applying braking and gyroscopic forces, the delay-free hybrid impulsive formation control protocol for each group is constructed as follows.

$$\left\{ \begin{array}{l} u_i(t) = -\alpha_x x_i^d + P_C(\hat{x}_i(t), \hat{v}_i(t)) + \mu_i P_D(\hat{x}_i(t), \hat{v}_i(t)) + \mu_i P_L(\hat{x}_i(t), \hat{v}_i(t)) \\ \quad + \hat{P}_{S22}^{-1} P_G(\hat{v}_i(t)), \quad i = 1, 2, \dots, m_s \\ \left\{ \begin{array}{l} u_{i1}(t) = -\alpha_x x_i^d + \hat{P}_{T22}^{-1} P_G(\hat{v}_i(t)), \quad i = m_s + 1, m_s + 2, \dots, n_s \\ u_{i2}(t) = P_C(\hat{x}_i(t), \hat{v}_i(t)) + \mu_i P_D(\hat{x}_i(t), \hat{v}_i(t)) + \mu_i P_L(\hat{x}_i(t), \hat{v}_i(t)) + P_A(a_i(t)) \end{array} \right. \end{array} \right. \quad (4.5)$$

with

$$\left\{ \begin{array}{l} P_C(\hat{x}_i(t), \hat{v}_i(t)) = -\sum_{j \in N_{i,s}^1} b_{ij}(\hat{x}_i(t) - \hat{x}_j(t)) - \sum_{j \in N_{i,s}^1} b_{ij}(\hat{v}_i(t) - \hat{v}_j(t)) \\ P_D(\hat{x}_i(t), \hat{v}_i(t)) = -\sum_{k=1}^{\infty} \sum_{j \in N_{i,s}} b_{ij}(\hat{x}_i(t) - \hat{x}_j(t))\delta(t - t_k) \\ \quad - \sum_{k=1}^{\infty} \sum_{j \in N_{i,s}} b_{ij}(\hat{v}_i(t) - \hat{v}_j(t))\delta(t - t_k) \\ P_L(\hat{x}_i(t), \hat{v}_i(t)) = -\sum_{k=1}^{\infty} c\hat{x}_i(t)\delta(t - t_k) - \sum_{k=1}^{\infty} d\hat{v}_i(t)\delta(t - t_k) \\ P_A(a_i(t)) = -\sum_{k=1}^{\infty} d_a a_i(t)\delta(t - t_k) \\ P_G(\hat{v}_i(t)) = \Theta_i(\hat{v}_i) + \Theta_i^{obs}(\hat{v}_i) + G_i(\hat{v}_i) + G_i^{obs}(\hat{v}_i) \end{array} \right. \quad (4.6)$$

where $\{t_k\}_{k \in \mathbb{N}^+}$ is the sequence of impulse times and satisfies $0 \leq t_0 < t_1 < \dots < t_k < t_{k+1} < \dots$, $\lim_{k \rightarrow \infty} t_k = \infty$. Meanwhile, $\delta(\cdot)$ is the dirac function, $N_{i,s}^1 \subset N_{i,s}$ is the neighbor set of the hybrid topology when $t \neq t_k$, \hat{P}_{22}^{-1} is a positive definite matrix with appropriate dimension, b_{ij} stands for coupling strength among follower agents. $c > 0$ is the position

navigation feedback gains, $d > 0$ is the velocity navigation feedback gain, and $d_a > 0$ is the acceleration navigation feedback gain.

Then from control protocol (4.5), the corresponding error dynamics of (4.1) can be written as

$$\begin{cases} \dot{\hat{x}}_i(t) &= \hat{v}_i(t) \\ \dot{\hat{v}}_i(t) &= \alpha_x \hat{x}_i(t) + \alpha_v \hat{v}_i(t) + f(\hat{v}_i(t)) + \phi(\hat{v}_i(t)) + P_C(\hat{x}_i(t), \hat{v}_i(t)) + P_G(\hat{v}_i(t)), \quad t \neq t_k \\ \Delta \hat{v}_i(t_k) &= \mu_i P_D(\hat{x}_i(t_k), \hat{v}_i(t_k)) + \mu_i P_L(\hat{x}_i(t_k), \hat{v}_i(t_k)), \quad t = t_k, \quad i = 1, 2, \dots, m_s \end{cases}$$

$$\begin{cases} \dot{\hat{x}}_i(t) &= \hat{v}_i(t) \\ \dot{\hat{v}}_i(t) &= \alpha_x \hat{x}_i(t) + \alpha_v \hat{v}_i(t) + f(\hat{v}_i(t)) + \phi(\hat{v}_i(t)) + P_G(\hat{v}_i(t)) + a_i(t) \\ \dot{a}_i(t) &= P_C(\hat{x}_i(t), \hat{v}_i(t)), \quad t \neq t_k \\ \Delta a_i(t_k) &= \mu_i P_D(\hat{x}_i(t_k), \hat{v}_i(t_k)) + \mu_i P_L(\hat{x}_i(t_k), \hat{v}_i(t_k)) + P_A(a_i(t_k)), \quad t = t_k, \\ & \quad i = m_s + 1, m_s + 2, \dots, n_s \end{cases} \quad (4.7)$$

where $\Delta \hat{v}_i(t_k) = \hat{v}_i(t_k^+) - \hat{v}_i(t_k^-)$, $\Delta a_i(t_k) = a_i(t_k^+) - a_i(t_k^-)$, and for simplicity we take $\hat{v}(t_k) = \hat{v}(t_k^+)$ and $a(t_k) = a(t_k^+)$.

Rearranging the state notations by order of dynamics gives

$$\begin{aligned} [\hat{x}_{S_s}^T(t), \hat{x}_{T_s}^T(t)]^T &= [\hat{x}_{1+\eta_s}^T(t), \dots, \hat{x}_{m_s+\eta_s}^T(t), \hat{x}_{m_s+1+\eta_s}^T(t), \dots, \hat{x}_{n_s+\eta_s}^T(t)]^T \\ [\hat{v}_{S_s}^T(t), \hat{v}_{T_s}^T(t)]^T &= [\hat{v}_{1+\eta_s}^T(t), \dots, \hat{v}_{m_s+\eta_s}^T(t), \hat{v}_{m_s+1+\eta_s}^T(t), \dots, \hat{v}_{n_s+\eta_s}^T(t)]^T \\ [\mathbf{0}_{2m_s}^T, a_{T_s}^T(t)]^T &= [\mathbf{0}_{1+\eta_s}^T, \dots, \mathbf{0}_{m_s+\eta_s}^T, a_{m_s+1+\eta_s}^T(t), \dots, a_{n_s+\eta_s}^T(t)]^T \\ [F_{S_s}^T(t), F_{T_s}^T(t)]^T &= [(f(\hat{v}_{1+\eta_s}(t)) + \phi(\hat{v}_{1+\eta_s}(t)))^T, \dots, (f(\hat{v}_{m_s+\eta_s}(t)) + \phi(\hat{v}_{m_s+\eta_s}(t)))^T, \dots, \\ & \quad (f(\hat{v}_{m_s+1+\eta_s}(t)) + \phi(\hat{v}_{m_s+1+\eta_s}(t)))^T, \dots, (f(\hat{v}_{n_s+\eta_s}(t)) + \phi(\hat{v}_{n_s+\eta_s}(t)))^T]^T \end{aligned} \quad (4.8)$$

where indices S, T describe the second-order dynamics and the third-order dynamics in (4.1) respectively. Thus the error dynamics of the s -th group, $s = 1, \dots, l$, can be expressed

as the following compact form

$$\begin{cases}
\dot{\hat{x}}_{S_s}(t) &= \hat{v}_{S_s}(t) \\
\dot{\hat{v}}_{S_s}(t) &= F_{S_s}(t) + B'_{ST}\hat{x}_{T_s}(t) + (\alpha_x I_{2m_s} + B'_{SS})\hat{x}_{S_s}(t) + B'_{ST}\hat{v}_{T_s}(t) \\
&\quad + (\alpha_v I_{2m_s} + B'_{SS})\hat{v}_{S_s}(t) - D'_S\hat{x}_{S_s}(t) - D'_S\hat{v}_{S_s}(t) + P_G(\hat{v}_{S_s}(t)), \quad t \neq t_k \\
\Delta\hat{v}_{S_s}(t_k) &= B_{ST}\hat{x}_{T_s}(t_k) + B_{SS}\hat{x}_{S_s}(t_k) + B_{ST}\hat{v}_{T_s}(t_k) + B_{SS}\hat{v}_{S_s}(t_k) \\
&\quad - \mu_i D_S\hat{x}_{S_s}(t_k) - \mu_i D_S\hat{v}_{S_s}(t_k) - \mu_i c\hat{x}_{S_s}(t_k) - \mu_i d\hat{v}_{S_s}(t_k), \quad t = t_k, \\
&\quad i = 1 + \eta_s, \dots, m_s + \eta_s \\
\dot{\hat{x}}_{T_s}(t) &= \hat{v}_{T_s}(t) \\
\dot{\hat{v}}_{T_s}(t) &= \alpha_x I_{2(n_s - m_s)}\hat{x}_{T_s}(t) + \alpha_v I_{2(n_s - m_s)}\hat{v}_{T_s}(t) + F_{T_s}(t) + a_{T_s}(t) + P_G(\hat{v}_{T_s}(t)) \\
\dot{a}_{T_s}(t) &= B'_{TS}\hat{x}_{S_s}(t) + B'_{TT}\hat{x}_{T_s}(t) + B'_{TS}\hat{v}_{S_s}(t) + B'_{TT}\hat{v}_{T_s}(t) - D'_T(\hat{x}_{T_s}(t) + \hat{v}_{T_s}(t)), \quad t \neq t_k \\
\Delta a_{T_s}(t_k) &= B_{TS}\hat{x}_{S_s}(t_k) + B_{TT}\hat{x}_{T_s}(t_k) + B_{TS}\hat{v}_{S_s}(t_k) + B_{TT}\hat{v}_{T_s}(t_k) - \mu_i D_T\hat{x}_{T_s}(t_k) \\
&\quad - \mu_i D_T\hat{v}_{T_s}(t_k) - \mu_i c\hat{x}_{T_s}(t_k) - \mu_i d\hat{v}_{T_s}(t_k) - d_a a_{T_s}(t_k), \quad t = t_k, \\
&\quad i = m_s + 1 + \eta_s, \dots, n_s - m_s + \eta_s
\end{cases} \tag{4.9}$$

where at each impulsive instant t_k , $B_{SS} \in \mathbb{R}^{2m_s \times 2m_s}$ and $B_{TT} \in \mathbb{R}^{2(n_s - m_s) \times 2(n_s - m_s)}$ represent the adjacency matrices among dynamics with identical order, while $B_{ST} \in \mathbb{R}^{2m_s \times 2(n_s - m_s)}$ and $B_{TS} \in \mathbb{R}^{2(n_s - m_s) \times 2m_s}$ represent the adjacency matrices among dynamics with distinct order. $D_S \in \mathbb{R}^{2m_s \times 2m_s}$ and $D_T \in \mathbb{R}^{2(n_s - m_s) \times 2(n_s - m_s)}$ are corresponding diagonal matrices resulting Laplacian matrices. In addition, B' , D' with indices are those matrices for $t \neq t_k$. Follows from Assumption 4.1.2, the compact form of error dynamics for overall topology \mathcal{G} can be described as

$$\begin{cases}
\dot{\bar{x}}_S(t) &= \bar{v}_S(t) \\
\dot{\bar{v}}_S(t) &= \bar{F}_S(t) + \bar{B}'_{ST}\bar{x}_T(t) + (\alpha_x I_{2m} + \bar{B}'_{SS})\bar{x}_S(t) + \bar{B}'_{ST}\bar{v}_T(t) + (\alpha_v I_{2m} + \bar{B}'_{SS})\bar{v}_S(t) \\
&\quad - \bar{D}'_S\bar{x}_S(t) - \bar{D}'_S\bar{v}_S(t) + P_G(\bar{v}_S(t)), \quad t \neq t_k \\
\Delta\bar{v}_S(t_k) &= \bar{B}_{ST}\bar{x}_T(t_k) + \bar{B}_{SS}\bar{x}_S(t_k) + \bar{B}_{ST}\bar{v}_T(t_k) + \bar{B}_{SS}\bar{v}_S(t_k) \\
&\quad - \mu_i \bar{D}_S\bar{x}_S(t_k) - \mu_i \bar{D}_S\bar{v}_S(t_k) - \mu_i c\bar{x}_S(t_k) - \mu_i d\bar{v}_S(t_k), \quad t = t_k, \quad i = 1, \dots, m \\
\dot{\bar{x}}_T(t) &= \bar{v}_T(t) \\
\dot{\bar{v}}_T(t) &= \alpha_x I_{2(n-m)}\bar{x}_T(t) + \alpha_v I_{2(n-m)}\bar{v}_T(t) + \bar{F}_T(t) + \bar{a}_T(t) + P_G(\bar{v}_T(t)) \\
\dot{\bar{a}}_T(t) &= \bar{B}'_{TS}\bar{x}_S(t) + \bar{B}'_{TT}\bar{x}_T(t) + \bar{B}'_{TS}\bar{v}_S(t) + \bar{B}'_{TT}\bar{v}_T(t) - \bar{D}'_T(\bar{x}_T(t) + \bar{v}_T(t)), \quad t \neq t_k \\
\Delta\bar{a}_T(t_k) &= \bar{B}_{TS}\bar{x}_S(t_k) + \bar{B}_{TT}\bar{x}_T(t_k) + \bar{B}_{TS}\bar{v}_S(t_k) + \bar{B}_{TT}\bar{v}_T(t_k) - \mu_i \bar{D}_T\bar{x}_T(t_k) \\
&\quad - \mu_i \bar{D}_T\bar{v}_T(t_k) - \mu_i c\bar{x}_T(t_k) - \mu_i d\bar{v}_T(t_k) - d_a \bar{a}_T(t_k), \quad t = t_k, \quad i = m + 1, \dots, n
\end{cases} \tag{4.10}$$

where

$$\begin{aligned}
[\bar{x}_S^T(t), \bar{x}_T^T(t)]^T &= [\hat{x}_{S1}^T(t), \dots, \hat{x}_{Sl}^T(t), \hat{x}_{T1}^T(t), \dots, \hat{x}_{Tl}^T(t)]^T \\
[\bar{v}_S^T(t), \bar{v}_T^T(t)]^T &= [\hat{v}_{S1}^T(t), \dots, \hat{v}_{Sl}^T(t), \hat{v}_{T1}^T(t), \dots, \hat{v}_{Tl}^T(t)]^T \\
[\mathbf{0}_{2m}^T, \bar{a}_T^T(t)]^T &= [\mathbf{0}_{S1}^T(t), \dots, \mathbf{0}_{Sl}^T(t), a_{T1}^T(t), \dots, a_{Tl}^T(t)]^T \\
[\bar{F}_S^T(t), \bar{F}_T^T(t)]^T &= [F_{S1}^T(t), \dots, F_{Sl}^T(t), F_{T1}^T(t), \dots, F_{Tl}^T(t)]^T
\end{aligned} \tag{4.11}$$

Similarly, let \bar{B} , \bar{D} with indices be the adjacency and corresponding diagonal matrices for $t = t_k$ after implementing inter-group links (4.3); while \bar{B}' , \bar{D}' with indices are those matrices within non-impulsive interval. Furthermore, for simplicity, denote $\chi(t) = [\bar{x}_S^T(t), \bar{v}_S^T(t), \bar{x}_T^T(t), \bar{v}_T^T(t), \bar{a}_T^T(t)]^T$, we can rewrite system (4.10) within the non-impulsive interval into the matrix form

$$\begin{aligned}
\dot{\chi}(t) &= \begin{pmatrix} \mathbf{0} & I_{2m} & \mathbf{0} & \mathbf{0} & \mathbf{0} \\ \alpha_x I_{2m} - L'_S & \alpha_v I_{2m} - L'_S & \bar{B}'_{ST} & \bar{B}'_{ST} & \mathbf{0} \\ \mathbf{0} & \mathbf{0} & \mathbf{0} & I_{2(n-m)} & \mathbf{0} \\ \mathbf{0} & \mathbf{0} & \alpha_x I_{2(n-m)} & \alpha_v I_{2(n-m)} & I_{2(n-m)} \\ \bar{B}'_{TS} & \bar{B}'_{TS} & -L'_T & -L'_T & \mathbf{0} \end{pmatrix} \chi(t) \\
&+ \begin{pmatrix} \mathbf{0} \\ \bar{F}_S(t) \\ \mathbf{0} \\ \bar{F}_T(t) \\ \mathbf{0} \end{pmatrix} + \begin{pmatrix} \mathbf{0} \\ \Phi_S(t) \\ \mathbf{0} \\ \Phi_T(t) \\ \mathbf{0} \end{pmatrix} \\
&= \Lambda \chi(t) + \Lambda_2(t) + \Lambda_3(t)
\end{aligned} \tag{4.12}$$

where notation $\mathbf{0}$ denotes the zero matrix and vector with appropriate dimension, $\Phi_S(t) = P_G(\bar{v}_S(t)) \in \mathbb{R}^{2m}$ with $\hat{P}_{22} = \hat{P}_{S22}$ and $\Phi_T(t) = P_G(\bar{v}_T(t)) \in \mathbb{R}^{2(n-m)}$ with $\hat{P}_{22} = \hat{P}_{T22}$. $L'_S = -\bar{B}'_{SS} + \bar{D}'_S$ and $L'_T = -\bar{B}'_{TT} + \bar{D}'_T$ are the positive semi-definite matrices for each type of dynamics within non-impulsive interval. Accordingly, the Laplacian matrix for the overall strongly connected topology \mathcal{G} can then be expressed as

$$L_G = \begin{pmatrix} L_S & -\bar{B}'_{ST} \\ -\bar{B}'_{TS} & L_T \end{pmatrix} \tag{4.13}$$

4.2.1 Delay-free Formation Stabilization

Theorem 4.2.1. Consider the multi-group MASs with dynamics (4.1),(4.2) and control protocol (4.5). Suppose that Assumption 4.1.1 and Assumption 4.1.2 hold,

$$P = \begin{pmatrix} \hat{P}_{S11} \otimes I_m & \mathbf{0} & \mathbf{0} & \mathbf{0} & \mathbf{0} \\ \mathbf{0} & \hat{P}_{S22} \otimes I_m & \mathbf{0} & \mathbf{0} & \mathbf{0} \\ \mathbf{0} & \mathbf{0} & \hat{P}_{T11} \otimes I_{n-m} & \mathbf{0} & \hat{P}_{T13} \otimes I_{n-m} \\ \mathbf{0} & \mathbf{0} & \mathbf{0} & \hat{P}_{T22} \otimes I_{n-m} & \mathbf{0} \\ \mathbf{0} & \mathbf{0} & \hat{P}_{T31} \otimes I_{n-m} & \mathbf{0} & \hat{P}_{T33} \otimes I_{n-m} \end{pmatrix} \in \mathbb{R}^{(6n-2m) \times (6n-2m)}$$

is positive definite and the following condition is satisfied,

$$\lambda_{\max}((I_{6n-2m} + \Omega)^T P (I_{6n-2m} + \Omega) P^{-1}) - \rho < 0 \quad (4.14)$$

with $\bar{\alpha} = \sqrt{n\alpha^2}$, $\bar{\gamma} = \sqrt{n\gamma^2}$, $\sigma < \frac{\ln(\rho^{-1})}{\omega}$, $\omega = \lambda_{\max}([P\Lambda + \Lambda^T P + 2(\bar{\alpha} + \bar{\gamma})P]P^{-1})$, $0 < \rho < 1$,

$$I_{6n-2m} + \Omega = \begin{pmatrix} I_{2m} & \mathbf{0} & \mathbf{0} & \mathbf{0} & \mathbf{0} \\ \mu_i J_1 & \mu_i J_2 & \bar{B}_{ST} & \bar{B}_{ST} & \mathbf{0} \\ \mathbf{0} & \mathbf{0} & I_{2(n-m)} & \mathbf{0} & \mathbf{0} \\ \mathbf{0} & \mathbf{0} & \mathbf{0} & I_{2(n-m)} & \mathbf{0} \\ \bar{B}_{TS} & \bar{B}_{TS} & \mu_i J_3 & \mu_i J_4 & (1 - d_a)I_{2(n-m)} \end{pmatrix},$$

$J_1 = -(L_S + cI_{2m})$, $J_2 = I_{2m} - (L_S + dI_{2m})$, $J_3 = -(L_T + cI_{2(n-m)})$ and $J_4 = -(L_T + dI_{2(n-m)})$. Then the asymptotic stabilization of distributed formation control is guaranteed, and the group-wise state mismatch among agents and virtual leaders converges to zero asymptotically. Moreover, suppose the maximal structure energy is bounded by $E \geq H(t) > 0$ and $\zeta_{ij} = \zeta_{ii\beta} > \frac{2E}{r_s}$, then collision-free motion can be achieved.

Proof. The energy-like Lyapunov function H for $t \neq t_k$ is defined as

$$H(t) = \frac{1}{2} \chi^T(t) P \chi(t). \quad (4.15)$$

Similar to Theorem 3.4.1, we obtain $\chi^T(t) P \Lambda_3(t) \leq 0$ by the properties of braking and gyroscopic forces. Taking the derivative of $H(t)$ based on Assumption 4.1.1 gives:

$$\begin{aligned} \dot{H}(t) &\leq \frac{1}{2} \chi^T(t) (P\Lambda + \Lambda^T P) \chi(t) + (\bar{\alpha} + \bar{\gamma}) \chi^T(t) P \chi(t) + \chi^T(t) P \Lambda_3(t) \\ &\leq \frac{1}{2} \chi^T(t) [P\Lambda + \Lambda^T P + 2(\bar{\alpha} + \bar{\gamma})P] P^{-1} P \chi(t) \\ &\leq \omega H(t) \end{aligned} \quad (4.16)$$

Then at each impulsive instant t_k , we obtain

$$\begin{aligned}
\Delta \bar{v}_S(t_k^-) &= -\mu_i L_S \bar{x}_S(t_k^-) - \mu_i L_S \bar{v}_S(t_k^-) + \bar{B}_{ST} \bar{x}_T(t_k^-) + \bar{B}_{ST} \bar{v}_T(t_k^-) \\
&\quad - \mu_i c \bar{x}_S(t_k^-) - \mu_i d \bar{v}_S(t_k^-) \\
\Delta \bar{a}_T(t_k^-) &= -\mu_i L_T \bar{x}_T(t_k^-) - \mu_i L_T \bar{v}_T(t_k^-) + \bar{B}_{TS} \bar{x}_S(t_k^-) + \bar{B}_{TS} \bar{v}_S(t_k^-) \\
&\quad - \mu_i c \bar{x}_T(t_k^-) - \mu_i d \bar{v}_T(t_k^-) - d_a \bar{a}_T(t_k^-)
\end{aligned} \tag{4.17}$$

where $L_S = \bar{D}_S - \bar{B}_{SS}$, $L_T = \bar{D}_T - \bar{B}_{TT}$ are the Laplacian matrices for each type of dynamics at each impulsive instant. Then according to condition (4.14), we can further obtain

$$H(t_k) = \frac{1}{2} \chi^T(t_k^-) (I_{6n-2m} + \Omega)^T P (I_{6n-2m} + \Omega) \chi(t_k^-) \leq \rho H(t_k^-) \tag{4.18}$$

Therefore, based on Lemma 3.1.2, we have $\beta = 0$, $\rho_1 = \rho$ and $\rho_2 = 0$; thus it gives $\sigma < \frac{\ln(\rho^{-1})}{\omega}$. Consequently, the asymptotic error convergence via distributed formation control is guaranteed, where $\lim_{t \rightarrow \infty} \bar{x}_S(t) = \lim_{t \rightarrow \infty} \bar{x}_T(t) = 0$, $\lim_{t \rightarrow \infty} \bar{v}_S(t) = \lim_{t \rightarrow \infty} \bar{v}_T(t) = 0$ and $\lim_{t \rightarrow \infty} \bar{a}_T(t) = 0$ (i.e., both desired formation and velocity alignment are achieved within each group). In addition, group-wise alignment also holds. The proof of collision-free motion with respect to $H(t)$ follows the same procedure as that of the Theorem 3.4.1, thus omitted. \square

Remark 4.2.1. *It can be seen from the proof that the hybrid impulsive part of the control protocol (4.5) plays a key role in maintaining asymptotic stability of multi-agent systems. Meanwhile, in accordance with $\bar{v}_S^T \Phi_S + \bar{v}_T^T \Phi_T \leq 0$, the state-dependent collision avoidance control term $P_G(\hat{v}_i(t))$ does not affect the overall stability analysis under the Lyapunov function (4.15), regardless of whether it is activated.*

4.2.2 Formation Stabilization with Time-varying Delay

Next, we discuss the multi-group formation control with time-varying delay (i.e., replacing $P_C(\hat{x}_i(t), \hat{v}_i(t))$ by $P_C(\hat{x}_i(t - r(t)), \hat{v}_i(t - r(t)))$ in protocol (4.5). where $r(t)$ denotes the bounded time-varying delay with $0 \leq r(t) \leq \bar{r}$. Similarly to (4.13), we can obtain the

overall compact error dynamics for $t \neq t_k$ as the following:

$$\begin{aligned}
\dot{\chi}(t) &= \begin{pmatrix} \mathbf{0} & I_{2m} & \mathbf{0} & \mathbf{0} & \mathbf{0} \\ \alpha_x I_{2m} & \alpha_v I_{2m} & \mathbf{0} & \mathbf{0} & \mathbf{0} \\ \mathbf{0} & \mathbf{0} & \mathbf{0} & I_{2(n-m)} & \mathbf{0} \\ \mathbf{0} & \mathbf{0} & \alpha_x I_{2(n-m)} & \alpha_v I_{2(n-m)} & I_{2(n-m)} \\ \mathbf{0} & \mathbf{0} & \mathbf{0} & \mathbf{0} & \mathbf{0} \end{pmatrix} \chi(t) \\
&+ \begin{pmatrix} \mathbf{0} & \mathbf{0} & \mathbf{0} & \mathbf{0} & \mathbf{0} \\ -L'_S & -L'_S & \bar{B}'_{ST} & \bar{B}'_{ST} & \mathbf{0} \\ \mathbf{0} & \mathbf{0} & \mathbf{0} & \mathbf{0} & \mathbf{0} \\ \mathbf{0} & \mathbf{0} & \mathbf{0} & \mathbf{0} & \mathbf{0} \\ \bar{B}'_{TS} & \bar{B}'_{TS} & -L'_T & -L'_T & \mathbf{0} \end{pmatrix} \chi(t - r(t)) + \begin{pmatrix} \mathbf{0} \\ \bar{F}_S(t) \\ \mathbf{0} \\ \bar{F}_T(t) \\ \mathbf{0} \end{pmatrix} + \begin{pmatrix} \mathbf{0} \\ \Phi_S(t) \\ \mathbf{0} \\ \Phi_T(t) \\ \mathbf{0} \end{pmatrix} \quad (4.19) \\
&= M_1 \chi(t) + M_2 \chi(t - r(t)) + \Lambda_2(t) + \Lambda_3(t)
\end{aligned}$$

Theorem 4.2.2. *Consider the multi-group MASs with dynamics (4.1),(4.2) and control protocol (4.5). Suppose that Assumption 4.1.1 and Assumption 4.1.2 hold, while LMI condition (4.14) is satisfied with $\epsilon > 0$, $0 < \rho < 1$, $\sigma < \frac{\ln(\rho^{-1})}{\omega + \frac{\beta}{\rho}}$,*

$$\begin{aligned}
\omega &= PM_1 + M_1^T P + 2(\bar{\alpha} + \bar{\gamma})P + \epsilon I_{6n-2m}, \\
\beta &= \frac{\|PM_2\|^2}{\epsilon} \lambda_{\max}(P^{-1}).
\end{aligned}$$

Then the asymptotic stabilization of distributed formation control is guaranteed, and the group-wise state mismatch among agents and virtual leaders converges to zero asymptotically. Moreover, suppose the maximal structure energy is bounded by $E \geq H(t) > 0$ and $\zeta_{ij} = \zeta_{ii^\beta} > \frac{2E}{r_s}$, then collision-motion can be achieved.

Proof. For $t \neq t_k$, consider the energy-like Lyapunov function $H(t)$ given by

$$H(t) = \frac{1}{2} \chi^T(t) P \chi(t) \quad (4.20)$$

Since $\chi^T(t) P \Lambda_3(t) \leq 0$ by the properties of braking and gyroscopic forces. Taking the

derivative of $H(t)$ based on Assumption 4.1.1 gives:

$$\begin{aligned}
\dot{H}(t) &\leq \frac{1}{2}\chi^T(t)(PM_1 + M_1^T P)\chi(t) + \frac{1}{2}\chi^T(t)PM_2\chi(t-r(t)) + \frac{1}{2}\chi^T(t-r(t))M_2^T P\chi(t) \\
&\quad + (\bar{\alpha} + \bar{\gamma})\chi^T(t)P\chi(t) + \chi^T(t)P\Lambda_3(t) \\
&\leq \frac{1}{2}\chi^T(t)[PM_1 + M_1^T P + 2(\bar{\alpha} + \bar{\gamma})P]P^{-1}P\chi(t) + \frac{\epsilon}{2}\chi^T(t)\chi(t) \\
&\quad + \frac{\|PM_2\|^2}{2\epsilon}\chi^T(t-r(t))\chi(t-r(t)) \\
&\leq \frac{1}{2}\chi^T(t)[PM_1 + M_1^T P + 2(\bar{\alpha} + \bar{\gamma})P + \epsilon I_{6n-2m}]P^{-1}P\chi(t) \\
&\quad + \frac{\|PM_2\|^2}{2\epsilon}\lambda_{\max}(P^{-1})\chi^T(t-r(t))P\chi(t-r(t)) \\
&\leq \omega H(t) + \beta \sup_{s \in [-r, 0]} H(t+s)
\end{aligned} \tag{4.21}$$

Then at each impulsive instant t_k , we obtain

$$\begin{aligned}
\Delta \bar{v}_S(t_k^-) &= -L_S \bar{x}_S(t_k^-) - L_S \bar{v}_S(t_k^-) + \bar{B}_{ST} \bar{x}_T(t_k^-) + \bar{B}_{ST} \bar{v}_T(t_k^-) - c \bar{x}_S(t_k^-) - d \bar{v}_S(t_k^-) \\
\Delta \bar{a}_T(t_k^-) &= -L_T \bar{x}_T(t_k^-) - L_T \bar{v}_T(t_k^-) + \bar{B}_{TS} \bar{x}_S(t_k^-) + \bar{B}_{TS} \bar{v}_S(t_k^-) \\
&\quad - c \bar{x}_T(t_k^-) - d \bar{v}_T(t_k^-) - d_a \bar{a}_T(t_k^-)
\end{aligned} \tag{4.22}$$

then once again we obtain

$$H(t_k) = \chi^T(t_k^-)(I_{6n-2m} + \Omega)^T P(I_{6n-2m} + \Omega)\chi(t_k^-) \leq \rho H(t_k^-) \tag{4.23}$$

Thus, according to Lemma 3.1.2, the asymptotic stabilization of distributed formation control is guaranteed as well. With the same argument in Theorem 3.2.1, collision/obstacle avoidance is guaranteed and the rest of the proof is omitted. \square

4.3 Numerical Simulations

In this section, we provide some numerical examples and computer simulations to verify the results in Theorem 4.2.1 and Theorem 4.2.2. The simulation time is set to be 60s. We consider $N=20$ agents along with three virtual leaders, and divide them into three groups

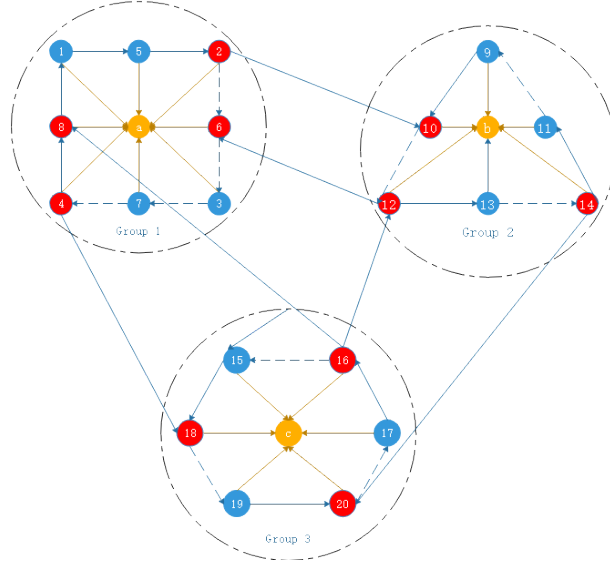
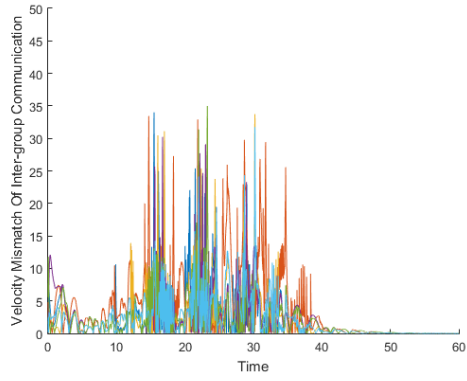


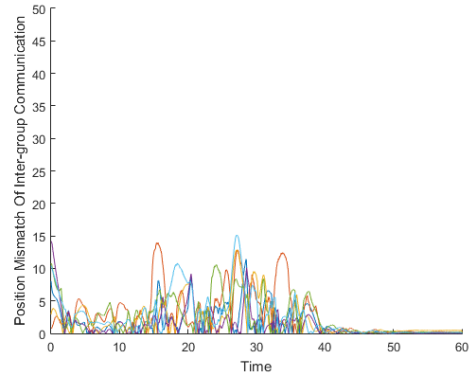
Figure 4.2: Connectivity of the overall topology for simulation

as shown in Figure 4.2. In each group, half of agents have second-order dynamics, while the other half have third-order dynamics. For the follower agents, the initial positions are randomly chosen from $[-30, 0]^2$, initial velocities are randomly chosen from $[-10, 10]^2$ and initial accelerations are randomly chosen from $[-5, 5]^2$. We set the nonlinear functions $f(v_i(t)) = 0.01\sqrt{v_i(t)^2 + 5}$, $f(v_s^0(t)) = 0.01\sqrt{v_s^0(t)^2 + 5}$ and the disturbances $\phi(v_i(t)) = 0.01\sin(v_i(t))$, $\phi(v_s^0(t)) = 0.01\sin(v_s^0(t))$. For the initial values of three virtual leaders, $x_1^0(0)$, $x_2^0(0)$ and $x_3^0(0)$ are randomly chosen from $[-30, 10]^2$, while $v_1^0(0) = v_2^0(0) = v_3^0(0) = [0.5, 0.5]$. Meanwhile, $\alpha_x = \alpha_v = 0$, $b_{ij} = 1.5$, $c = 0.5$, $d = 0.5$, and the impulsive effect occurs every 0.25s. Moreover, we construct a dense obstacle field, which contains eight dynamical obstacles initially centred at $[-30, 10]$, $[-20, 20]$, $[-10, 10]$, $[0, 20]$, $[10, 10]$, $[20, 20]$, $[30, 10]$ and $[40, 20]$. They all have a radius of 5 and are moving horizontally at a speed of 0.5.

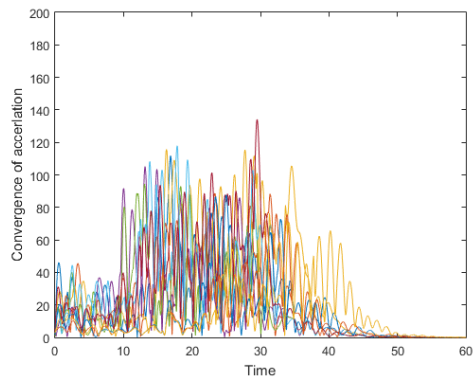
Example 1. Based on Figure 4.3(a)-(b), both velocity and position mismatch trajectories of inter-group communication are asymptotically convergent, which indicates the asymptotic stabilization of group-wise desired configuration can be guaranteed; while the asymptotic convergence of acceleration is shown in Figure 4.3(c). From the formation evolution indicated in Figure 4.4, all the agents pass through the dynamical obstacles successfully without any inter-agent/obstacle collision, and the desired configuration is maintained afterwards. Based on Figure 4.5, both velocity and position mismatch trajectories in each



(a)



(b)



(c)

Figure 4.3: Convergence of (a) velocity mismatch of inter-group communication (b) position mismatch of inter-group communication (c) acceleration

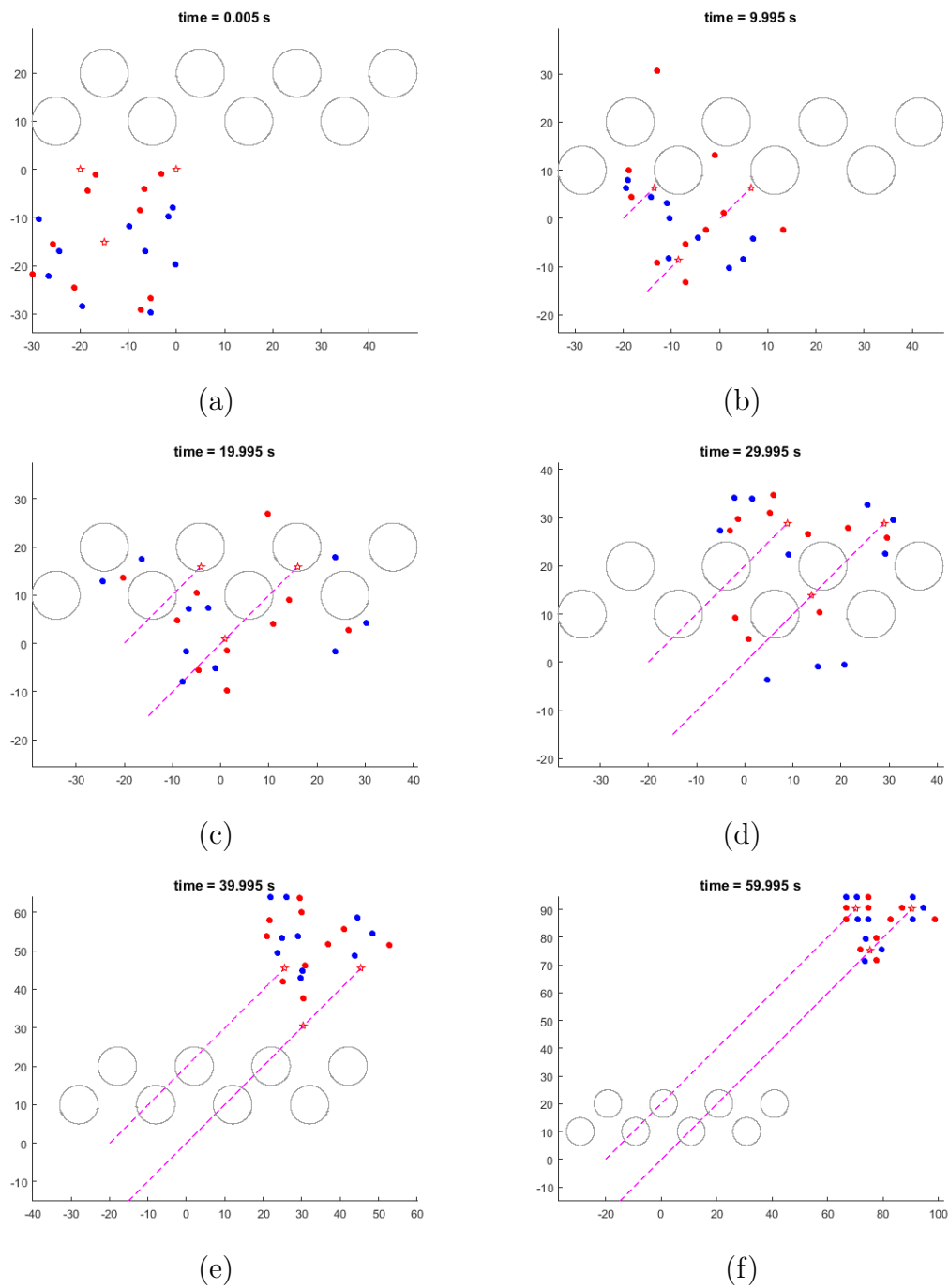
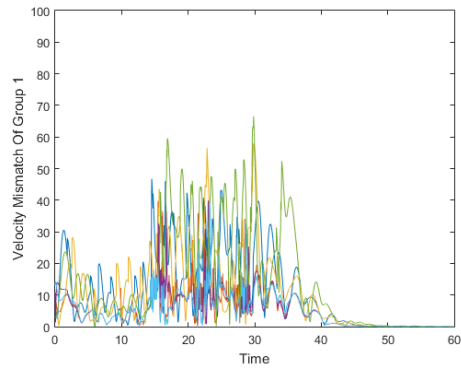
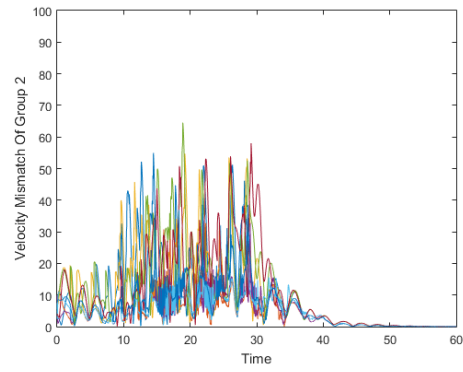


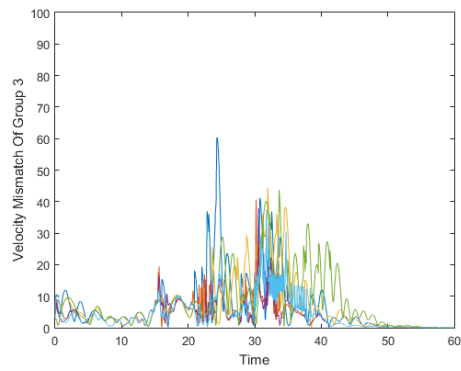
Figure 4.4: Formation evolution for $N=20$ agents without time delay (2nd-order dynamics in red scatter points, 3rd-order dynamics in blue scatter points, and virtual leaders in red pentagrams)



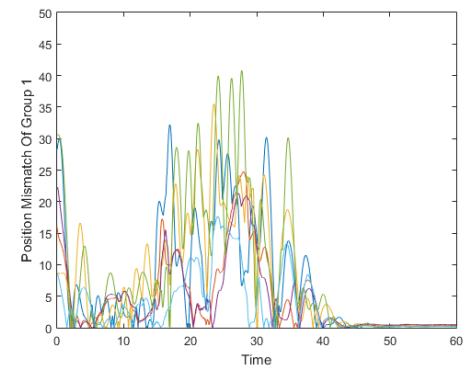
(a)



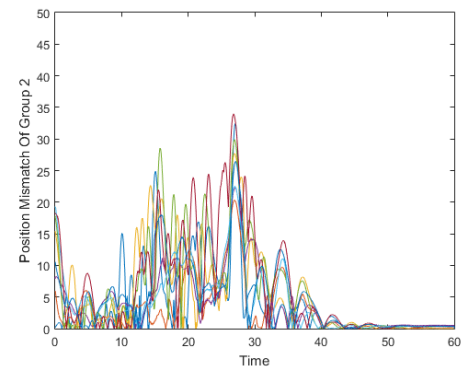
(b)



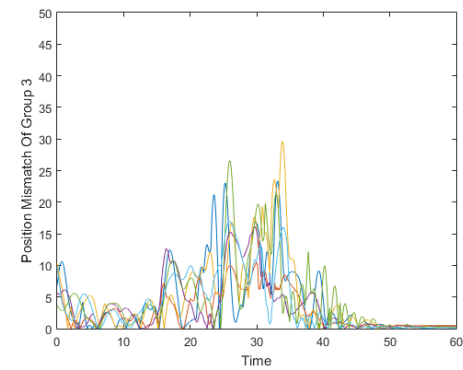
(c)



(d)



(e)



(f)

Figure 4.5: Convergence of (a) velocity mismatch of group 1 (b) velocity mismatch of group 2 (c) velocity mismatch of group 3 (d) position mismatch of group 1 (e) position mismatch of group 2 and (f) position mismatch of group 3

group converge to zero asymptotically as well. Consequently, the distributed hybrid impulsive formation control objectives are achieved for individual groups and group-wise, thus Theorem 4.2.1 is valid.

Example 2. In this example, we set the bounded system time-delay to be

$$0 \leq r(t) = \frac{1}{2}e^{-0.02t} \sin^2(t) \leq 0.5s$$

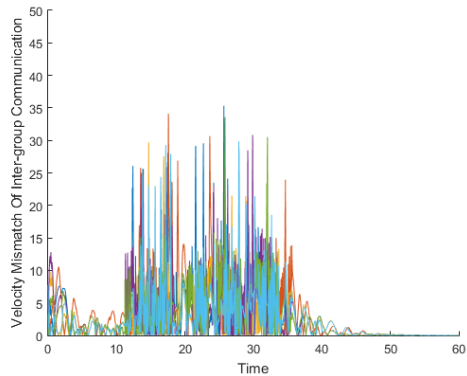
From Figure 4.6 to Figure 4.8, similar convergence behavior can be observed, where both intergroup communication errors and communication errors of individual groups are eliminated without any motion of collision. As a result, the time-varying delay can be implemented to achieve hybrid impulsive formation objectives and therefore the analytical results from Theorem 4.2.2 are also applicable.

Example 3. The purpose of this example is to demonstrate how different sizes of time delays in our hybrid impulsive schemes affect the speed of convergence in order to obtain the desired configuration. Without loss of generality, the real-time control component regarding collision avoidance is excluded since it has no significant impact on formation generation. Meanwhile, the initial states of agents and all the other parameters remain fixed. Under three feasible but different values of time delay, Figure 4.9(a)-(c) illustrates the asymptotic convergence of velocity mismatch, position mismatch and acceleration mismatch of agent 1 with third-order dynamics respectively. We observe a clear pattern that larger time delays lead to slower speed of convergence. Nevertheless, as the time delay exceeds the acceptable range for maintaining the current upper bound of the impulsive interval σ , the trajectory of the state mismatch blows up and fails to achieve asymptotic stability, as shown in Figure 4.9(d).

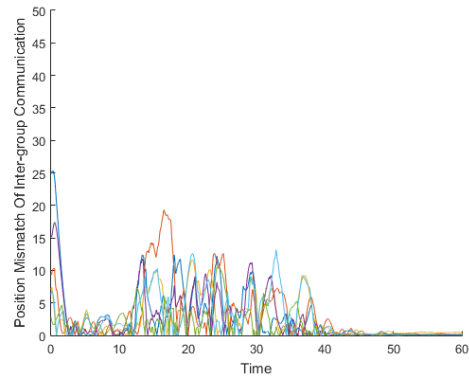
Example 4. We compare the proposed braking/gyroscopic strategy with a conventional artificial potential function approach discussed in [89]:

$$\begin{aligned} \psi_\alpha(\|x_i(t) - x_j(t)\|_\sigma) &= \int_{\|d\|_\sigma}^{\|x_i(t) - x_j(t)\|_\sigma} \varphi(s) ds \\ \varphi(s) &= \begin{cases} -\frac{25(s - \|d\|_\sigma)(s - \|r_s\|)}{s + 0.2}, & s \in [0, \|r_s\|_\sigma] \\ 0, & s \in [\|r_s\|_\sigma, +\infty) \end{cases} \end{aligned} \quad (4.24)$$

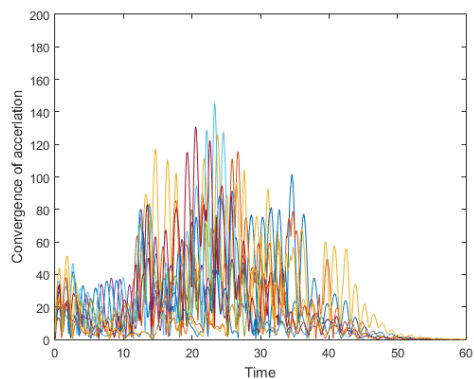
where $d = x_i^d - x_j^d$. Meanwhile, in order to assess the performance of the two strategies,



(a)



(b)



(c)

Figure 4.6: Convergence of (a) velocity mismatch of inter-group communication (b) position mismatch of inter-group communication (c) acceleration

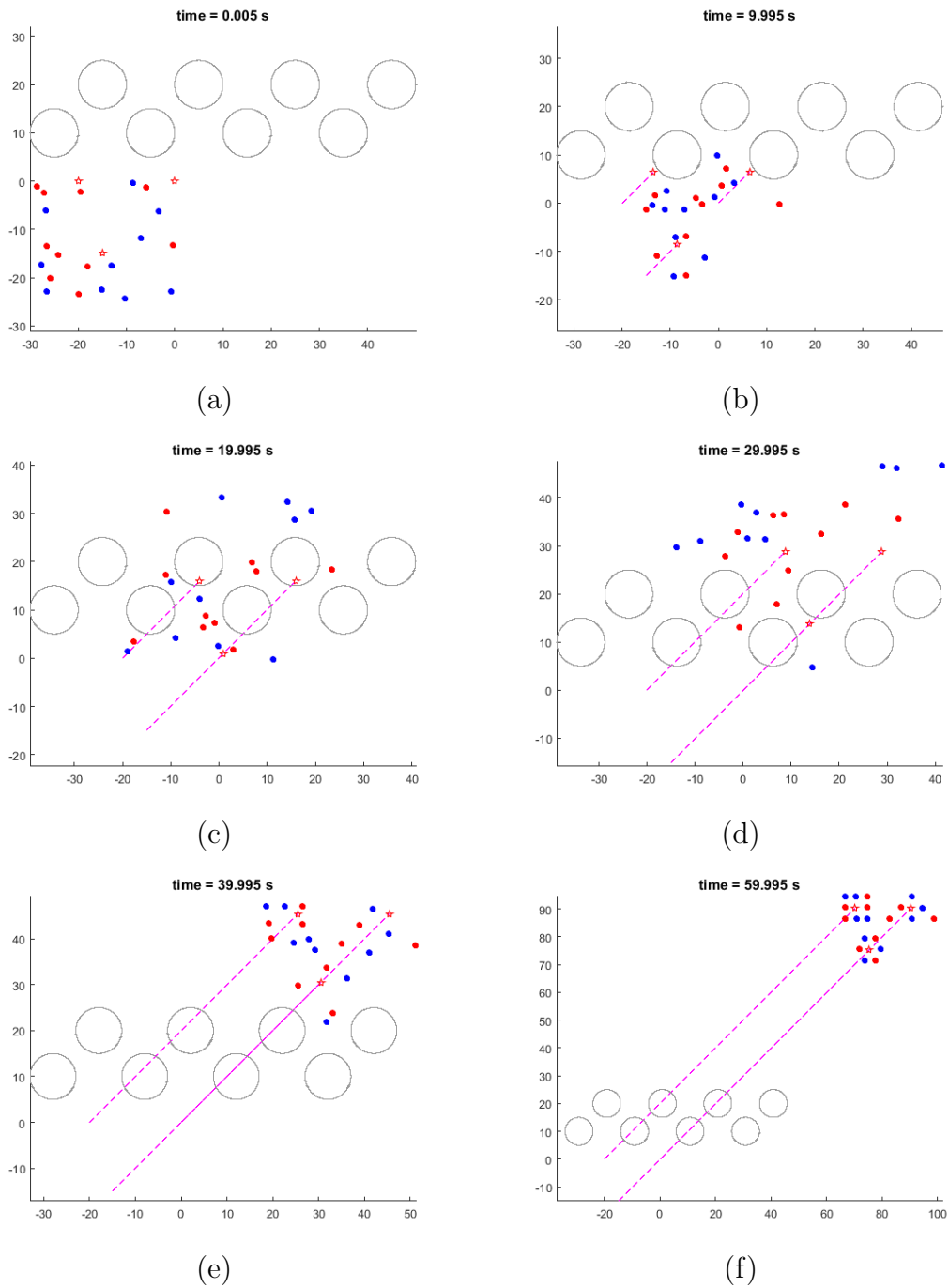
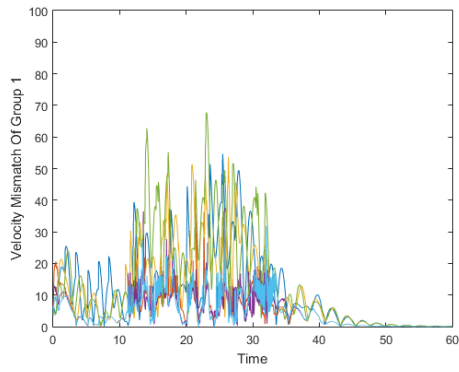
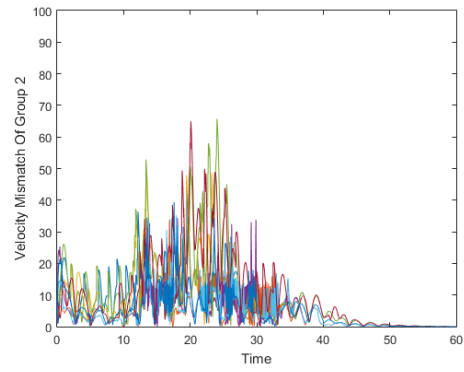


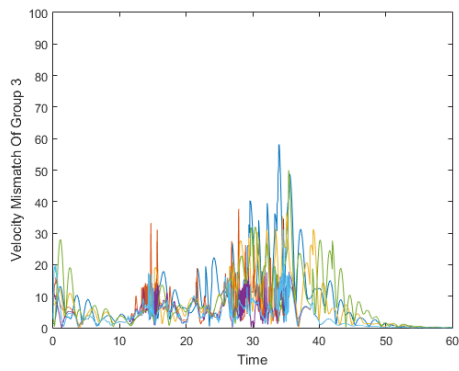
Figure 4.7: Formation evolution for $N=20$ agents with time delay (2nd-order dynamics in red scatter points, 3rd-order dynamics in blue scatter points, and virtual leaders in red pentagrams)



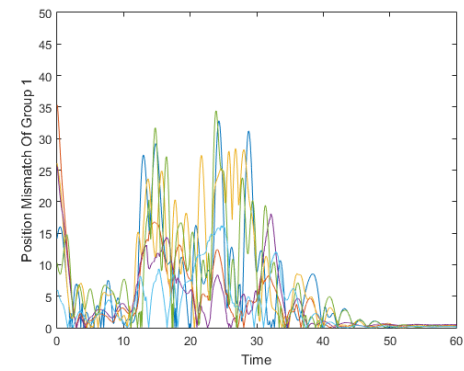
(a)



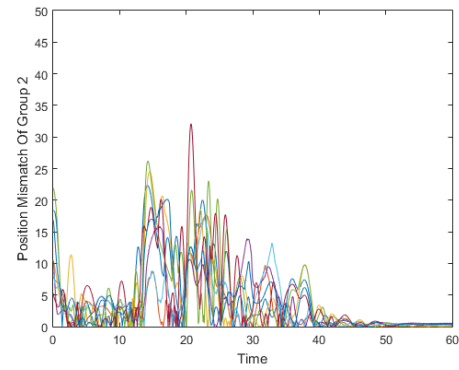
(b)



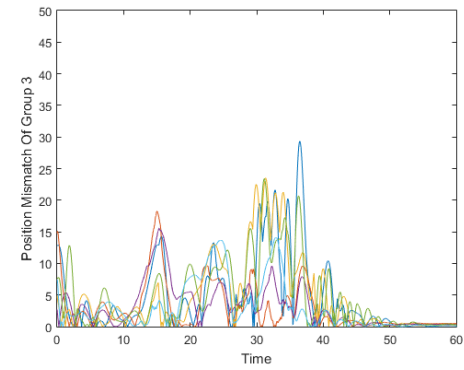
(c)



(d)

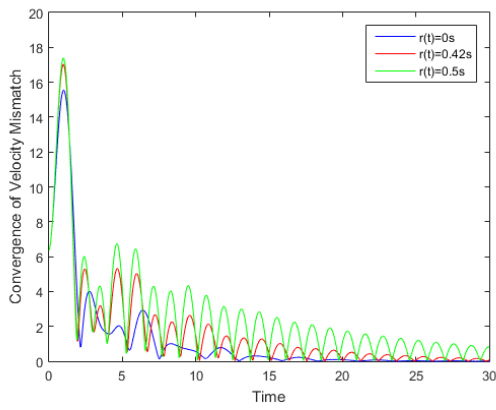


(e)

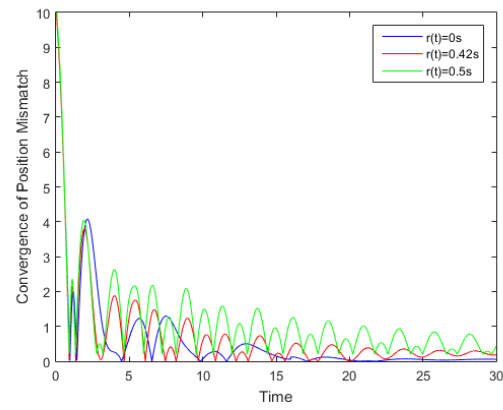


(f)

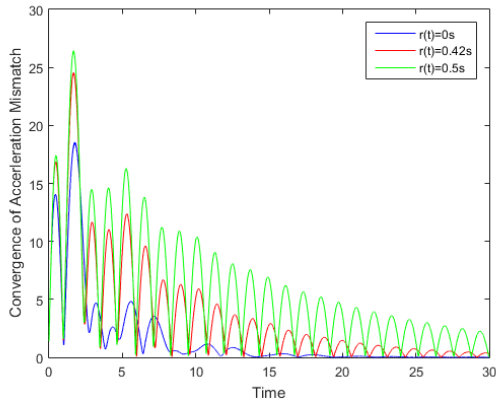
Figure 4.8: Convergence of (a) velocity mismatch of group 1 (b) velocity mismatch of group 2 (c) velocity mismatch of group 3 (d) position mismatch of group 1 (e) position mismatch of group 2 and (f) position mismatch of group 3



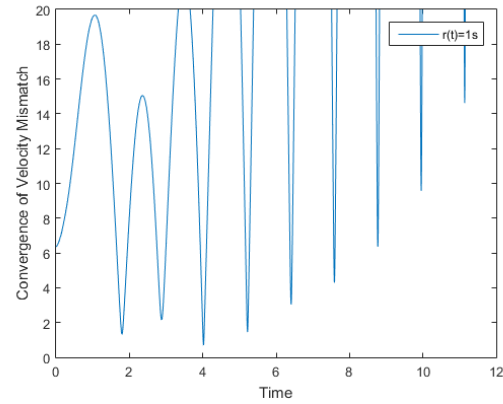
(a)



(b)



(c)



(d)

Figure 4.9: Convergence of (a) velocity mismatch (b) position mismatch (c) acceleration of agent 1 with $r(t)=0s$, $r(t)=0.42s$ and $r(t)=0.5s$ (d) velocity mismatch of agent 1 with $r(t)=1s$.

Distortion index	Mean	SD
Braking/gyroscopic forces	1.0679	1.4724
Artificial potential function	1.2054	2.3160

Table 4.1: Comparison of distortion index of agent 1

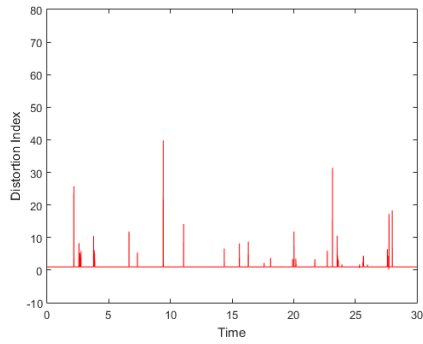
the distortion index function $\Omega_i(t)$ is defined as:

$$\Omega_i(t) = \frac{\|u_{di}(t) + P_G(\hat{v}_i(t))\|}{\|u_{di}(t)\|} \quad (4.25)$$

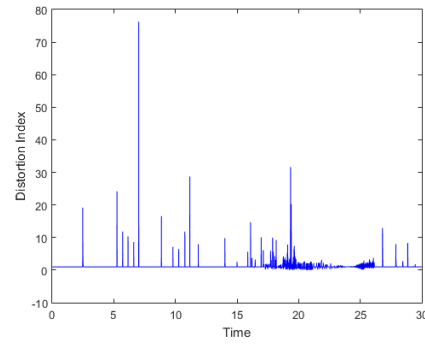
where $u_{di}(t)$ is the sum of control components in (4.6) excluding $P_G(\hat{v}_i(t))$, which are in charge of the desired formation configuration. More specifically, larger amplitudes of $\Omega_i(t)$ indicate that collision/obstacle avoidance mechanisms interfere more with the primary task of maintaining desired configurations. For a single simulation, Figure 4.10 illustrates the evolution of the distortion index function of agent 1 and agent 4 respectively. It appears that the distortion index function displays a lower amplitude due to braking/gyroscopic forces, and significantly fewer controls are activated. In addition, we have performed a total of 10 simulation runs. The mean value and standard deviation of the distortion index function of agent 1 over 30 seconds are reported in Table 4.1. Compared with the ideal case of no interference (i.e., $\Omega_i(t) = 1$), the braking/gyroscopic forces generated 13.84% less distortion and had lower standard deviation (SD) of 1.4724.

As a result, the braking/gyroscopic approach provides better overall performance than the standard artificial potential function approach.

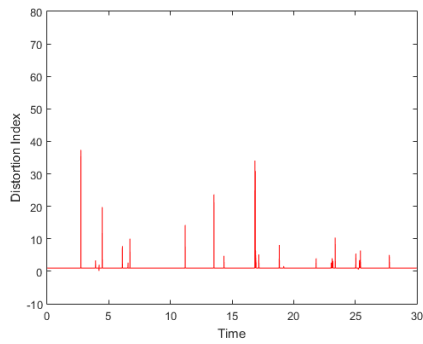
Remark 4.3.1. *In this chapter, we have studied the multi-group formation control problem for heterogeneous multi-agent systems using a hybrid impulsive framework. Particularly, the followers consist of second-order and third-order dynamics, and the coupling information exchange among them remains hybrid and directed. To achieve asymptotic formation stabilization, hybrid impulsive control protocols have been proposed with and without time-varying delays. For systems with destabilizing continuous dynamics and stabilizing discrete dynamics, some sufficient stability criteria have been derived with respect to Lipschitz constant, coupling strength, and length of impulsive interval. In the meantime, braking and gyroscopic forces have been used to avoid inter-agent collisions and dynamical obstacles. The effectiveness of this method has been demonstrated in the numerical examples, which prevents undesired local minima and generates less interference with the primary task of maintaining the desired configuration.*



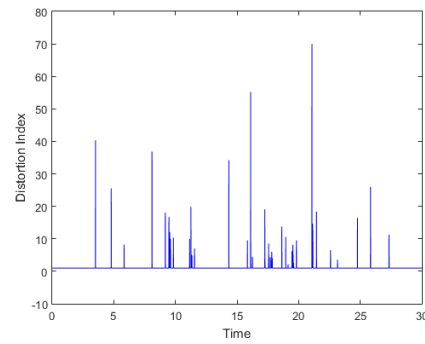
(a)



(b)



(c)



(d)

Figure 4.10: Distortion index of agent 1 via (a) braking/gyroscopic forces in this paper (b) artificial potential functions; Distortion index of agent 4 via (c) braking/gyroscopic forces in this paper (d) artificial potential functions.

Chapter 5

Hybrid Event-triggered Impulsive Control of MASs via Pinning Mechanism

In this chapter, we aim to design the distributed leader-following formation control protocols under the hybrid impulsive framework via event-triggered and pinning control mechanisms. In addition, extra features involving transmittal delays and strong nonlinearity of intrinsic dynamics are employed as well.

5.1 Event-triggered Mechanism

An event-triggered mechanism (ETM) is a control system technique used to reduce the communication and computational requirements of a control system. When the ETM takes place, control actions are only taken when a certain event or condition is met, such as a change in a system parameter or a threshold being reached is detected, rather than constantly updating and transmitting information in traditional time-triggered control. By using event-triggered mechanisms, the communication and computation requirements of the control system can be significantly reduced, leading to the more efficient and less resource-intensive MASs (i.e., reduce communication delays and increase the overall speed of the system). The precedent works such as [90, 91, 92] have extensively studied the design of event-triggered strategies for nonlinear impulsive multi-agent systems along with Zeno behaviour prevention. Meanwhile, Lyapunov Stability for impulsive systems via event-triggered impulsive control has been investigated in [93].

5.2 Pinning Mechanism

Pinning control is a control technique used to stabilize multi-agent systems by selectively controlling a subset of the MAS agents/nodes, called the "pinned agents/nodes". The pinned agents are then controlled in a way that influences the behavior of the other agents in the network, leading to stability of the entire network. Its corresponding control inputs can be designed based on various criteria associated with Lyapunov stability analysis, such as the degree of the agents, the eigenvalues of the topological Laplacian matrices. In practice, pinning mechanism becomes more efficient and less complex than fully controlling all the agents in the MASs. Meanwhile, it can be more robust to uncertainties and disturbances, as the control input is only applied to a subset of the agents. Furthermore, pinning mechanism has been widely studied in the field of control theory, and various approaches have been developed, including static and dynamic pinning control. Static pinning control applies a fixed control input to the pinned nodes, while dynamic pinning control adapts the control input based on the current state of the network. In [94, 95], the typical leader-following consensus of multi-agent systems via pinning control is introduced, while the synchronization of nonlinear complex dynamical networks via pinning impulsive strategy has been investigated in [96, 97, 98, 99]. Gao et al.[100] proposed a dynamic pinning control algorithm for flocking motion.

5.3 Problem Formulation

Consider a group of $n + 1$ networked unmanned aerial vehicles (UAV) equipped with sensors which detect the orientation information in terms of other neighbors as well as global coordinate frame. In light of fixed attitudes and dynamics alignment with the virtual leader, the i -th agent's dynamics can be described as:

$$\begin{cases} \dot{\eta}_i(t) = v_i(t) \\ \dot{v}_i(t) = \alpha_x \eta_i(t) + \alpha_v v_i(t) - \beta_v v_i(t) + f(v_i(t)) + \phi(v_i(t)) + \tau_i, \quad i = 1, 2, \dots, n \end{cases} \quad (5.1)$$

where $\eta_i \in \mathbb{R}^3$ and $v_i \in \mathbb{R}^3$ are bounded position and velocity states respectively; α_x and α_v are effective values for self-propulsion, while β_v is the constant gain for friction force. Meanwhile, $f(v_i(t))$, $\phi(v_i(t))$ and τ_i represent the nonlinear intrinsic dynamics, external disturbance and the control input respectively. Accordingly, the dynamics of virtual leader is constructed as:

$$\begin{cases} \dot{\eta}_0(t) = v_0(t) \\ \dot{v}_0(t) = \alpha_x \eta_0(t) + \alpha_v v_0(t) - \beta_v v_0(t) + f(v_0(t)) + \phi(v_0(t)) \end{cases} \quad (5.2)$$

where its signals are bounded. In addition, let $\hat{\eta}_i(t) = \eta_i(t) - \eta_0(t) - \eta_i^d \in \mathbb{R}^3$ where η_i^d is the prescribe desired displacement between agent i and the leader, $\hat{v}_i(t) = v_i(t) - v_0(t) \in \mathbb{R}^3$, $\hat{\xi}_i = [\hat{\eta}_i^T, \hat{v}_i^T]^T \in \mathbb{R}^6$, $\bar{\eta}(t) = [\hat{\eta}_1^T(t), \dots, \hat{\eta}_n^T(t)]^T$, $\bar{v}(t) = [\hat{v}_1^T(t), \dots, \hat{v}_n^T(t)]^T$ and $\bar{\xi}(t) = [\bar{\eta}^T(t), \bar{v}^T(t)]^T$.

Definition 5.3.1. *The leader-following multi-agent systems (5.1) and (5.2) are said to achieve local formation stabilization if there exists a nonempty open ball B_ν with radius ν such that $\bar{\xi}(\mathbf{0}_{4n}) \in B_\nu$ implies $\lim_{t \rightarrow \infty} \|\bar{\xi}(t)\| = 0$, and collision-free motion is guaranteed.*

Assumption 5.3.1. *Suppose that $\tilde{f}(x)$ is continuously differentiable and for any continuous function $y : \mathbb{R}^+ \rightarrow \mathbb{R}^{3n}$, there exists a continuous and nondecreasing function $s : \mathbb{R}^+ \rightarrow \mathbb{R}^+$ satisfying $s(0) = 0$ and*

$$\|\tilde{f}(y(t) + x) - \tilde{f}(y(t)) - \bar{F}(t)x\| = \|\bar{R}(t, x)\| \leq s(\delta)\|x\|$$

for any $x \in \bar{B}_\delta$ and $t \in \mathbb{R}$, where $\bar{F}(t)$ is the Jacobian of \tilde{f} evaluated at $y(t)$, $\bar{R}(t, x)$ is the nonlinear residual term satisfying $\|\bar{R}(t, x)\| = o(\|x\|)$. \tilde{f} is said to have strong (weak) nonlinearity if $\lim_{\delta \rightarrow \infty} s(\delta)$ is infinite (finite).

Remark 5.3.1. *In Figure 5.1, the interaction topology of the network is illustrated. Here, the virtual leader acts as the root node of the spanning tree at each impulsive instant, and it generates partial communication with followers due to the pinning control mechanism. In the mean time, the strongly connected and balanced topology will also be reformed from a hybrid topology within non-impulsive interval (i.e., links with dashed lines are recovered).*

5.4 Formation Stabilization

5.4.1 Delay-free Hybrid Event-triggered Pinning Impulsive control (HETPIC)

Denote the sequence $\{t_l, l \in \mathbb{N}^+\}$ as the set of event-triggered impulsive instants which will only be activated as the designed events occur and satisfies $0 = t_0 < t_1 < \dots < t_l < t_{l+1} < \dots$, $\lim_{l \rightarrow \infty} t_l = \infty$. The hybrid event-triggered impulsive formation control protocols via pinning mechanism are proposed in this part; while the corresponding stability criteria for maintaining formation control objectives are also derived. Firstly, the real-time

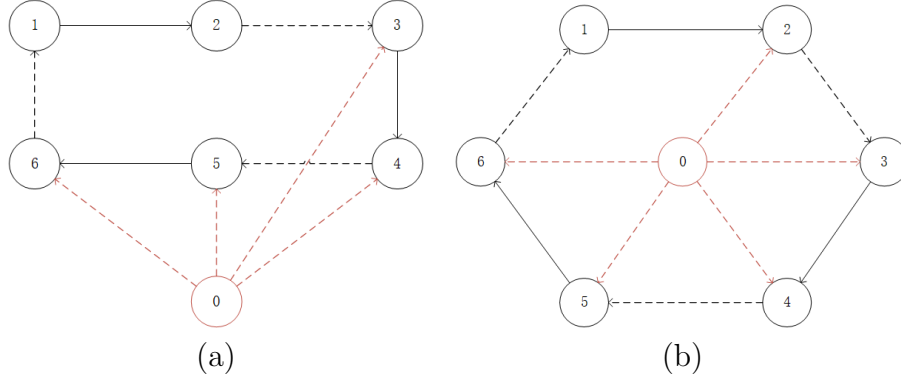


Figure 5.1: (a) Connectivity of the communication topology (a) before and (b) after switching

hybrid event-triggered impulsive control protocol for $t \in [t_l, t_{l+1})$ and $i = 1, 2, \dots, n$ can be constructed as follows:

$$\tau_i(t) = k_1 P_C(\hat{\eta}_i(t), \hat{v}_i(t)) + k_2 P_D(\hat{\eta}_i(t), \hat{v}_i(t)) + k_3 P_L(\hat{\eta}_i(t), \hat{v}_i(t)) - \alpha_x \eta_i^d + \hat{P}_{22}^{-1} P_G(\hat{v}_i(t)) \quad (5.3)$$

where k_1, k_2, k_3 are constant gains for adjustment, and $\hat{P}_{22} \in \mathbb{R}^{3 \times 3}$ is a positive definite gain matrix. $P_C(\hat{\eta}_i(t), \hat{v}_i(t)) = -\sum_{j \in N_i^1} b_{ij}(\hat{\eta}_i(t) - \hat{\eta}_j(t)) - \sum_{j \in N_i^1} b_{ij}(\hat{v}_i(t) - \hat{v}_j(t))$, $P_D(\hat{\eta}_i(t), \hat{v}_i(t)) = -\sum_{l=1}^{\infty} \sum_{j \in N_i} b_{ij}(\hat{\eta}_i(t) - \hat{\eta}_j(t))\delta(t - t_l) - \sum_{l=1}^{\infty} \sum_{j \in N_i} b_{ij}(\hat{v}_i(t) - \hat{v}_j(t))\delta(t - t_l)$, $P_G(\hat{v}_i(t)) = \Theta_i(\hat{v}_i(t)) + \Theta_i^{obs}(\hat{v}_i(t)) + G_i(\hat{v}_i(t)) + G_i^{obs}(\hat{v}_i(t))$, and

$$P_L(\hat{\eta}_i(t), \hat{v}_i(t)) = \begin{cases} -\sum_{l=1}^{\infty} [c\hat{\eta}_i(t) + d\hat{v}_i(t)]\delta(t - t_l), & i \in \mathcal{D}_k \\ \mathbf{0}_3, & i \notin \mathcal{D}_k \end{cases}$$

where $N_i^1 \subset N_i$ is the neighbor set of the hybrid topology when $t \neq t_l$. b_{ij} stands for variation of coupling strengths with respect to other follower agents; $c > 0, d > 0$ are the navigation feedback gains of position and velocity respectively. \mathcal{D}_k represents the index set with $k \in \mathbb{N}$ which is defined as follows: the vector states $\hat{\xi}_1(t_l), \dots, \hat{\xi}_n(t_l)$ are reordered so that $\|\hat{\xi}_{p_1}(t_l)\| \geq \|\hat{\xi}_{p_2}(t_l)\| \geq \dots \geq \|\hat{\xi}_{p_{s_k}}(t_l)\| \geq \|\hat{\xi}_{p_{s_k+1}}(t_l)\| \dots \geq \|\hat{\xi}_{p_n}(t_l)\|$, then $\mathcal{D}_k = \{p_1, \dots, p_{s_k}\}$ and s_k is the total number of elements in \mathcal{D}_k . Denote $f(\hat{v}_i(t)) = f(v_i(t)) - f(v_0(t))$, $\phi(\hat{v}_i(t)) = \phi(v_i(t)) - \phi(v_0(t))$, $\bar{f}(\bar{v}(t)) = [f(\hat{v}_1(t))^T, \dots, f(\hat{v}_n(t))^T]^T$ and $\bar{\phi}(\bar{v}(t)) = [\phi(\hat{v}_1(t))^T, \dots, \phi(\hat{v}_n(t))^T]^T$. Then the corresponding error dynamics of (5.1) and

(5.2) can be written as:

$$\left\{ \begin{array}{l} \dot{\hat{\xi}}_i(t) = \begin{pmatrix} \mathbf{0}_{3 \times 3} & I_3 \\ \alpha_x I_3 & (\alpha_v - \beta_v) I_3 \end{pmatrix} \hat{\xi}_i(t) \\ \quad + \begin{pmatrix} \mathbf{0}_3 \\ f(\hat{v}_i(t)) + \phi(\hat{v}_i(t)) + k_1 P_C(\hat{\eta}_i(t), \hat{v}_i(t)) \end{pmatrix}, \quad t \neq t_l \\ \Delta \hat{v}_i(t_l) = k_2 \left(-\sum_{j \in N_i} b_{ij} (\hat{\eta}_i(t_l) - \hat{\eta}_j(t_l)) - \sum_{j \in N_i} b_{ij} (\hat{v}_i(t_l) - \hat{v}_j(t_l)) \right) \\ \quad - k_3 (c\hat{\eta}_i(t_l) - d\hat{v}_i(t_l)), \quad t = t_l, \quad i \in \mathcal{D}_k \\ \Delta \hat{v}_i(t_l) = k_2 \left(-\sum_{j \in N_i} b_{ij} (\hat{\eta}_i(t_l) - \hat{\eta}_j(t_l)) - \sum_{j \in N_i} b_{ij} (\hat{v}_i(t_l) - \hat{v}_j(t_l)) \right), \quad t = t_l, \quad i \notin \mathcal{D}_k \end{array} \right. \quad (5.4)$$

where $\Delta \hat{v}_i(t_l) = \hat{v}_i(t_l^+) - \hat{v}_i(t_l^-)$ and for simplicity we take $\hat{v}_i(t_l) = \hat{v}_i(t_l^+)$. Additionally, in order to separate connectivity of pinned agents from the overall network, we define $\tilde{c} = \begin{pmatrix} cI_{3s_k} & \mathbf{0}_{3s_k \times 3(n-s_k)} \\ \mathbf{0}_{3(n-s_k) \times 3s_k} & \mathbf{0}_{3(n-s_k) \times 3(n-s_k)} \end{pmatrix} \in \mathbb{R}^{3n \times 3n}$ and $\tilde{d} = \begin{pmatrix} dI_{3s_k} & \mathbf{0}_{3s_k \times 3(n-s_k)} \\ \mathbf{0}_{3(n-s_k) \times 3s_k} & \mathbf{0}_{3(n-s_k) \times 3(n-s_k)} \end{pmatrix} \in \mathbb{R}^{3n \times 3n}$. Thus the error dynamics can be expressed as the following compact form:

$$\left\{ \begin{array}{l} \dot{\tilde{\xi}}(t) = \left[\begin{pmatrix} \mathbf{0}_{3n \times 3n} & I_{3n} \\ \alpha_x I_{3n} & (\alpha_v - \beta_v) I_{3n} \end{pmatrix} + \begin{pmatrix} \mathbf{0}_{3n \times 3n} & \mathbf{0}_{3n \times 3n} \\ -k_1 L' & -k_1 L' \end{pmatrix} \right] \tilde{\xi}(t) \\ \quad + \begin{pmatrix} \mathbf{0}_{2n} \\ \bar{f}(\bar{v}(t)) + \bar{\phi}(\bar{v}(t)) + [\hat{P}_{22}^{-1} \otimes I_n] P_G(\hat{v}_i(t)) \otimes \mathbf{1}_n \end{pmatrix}, \quad t \neq t_l \\ \Delta \bar{v}(t_l) = -(k_3 \tilde{c} + k_2 L) \bar{\eta}(t_l) - (k_3 \tilde{d} + k_2 L) \bar{v}(t_l), \quad t = t_l, \quad i \in \mathcal{D}_k \\ \Delta \bar{v}(t_l) = -k_2 L \bar{\eta}(t_l) - k_2 L \bar{v}(t_l), \quad t = t_l, \quad i \notin \mathcal{D}_k \end{array} \right. \quad (5.5)$$

where L' represents the Laplacian matrix in terms of b_{ij} within non-impulse interval, and $\bar{F}(t)$ is the Jacobian of $\tilde{f}(\bar{v}(t)) = \bar{f}(\bar{v}(t)) + \bar{\phi}(\bar{v}(t))$.

Theorem 5.4.1. *Consider the leader-following multi-agent systems with dynamics (5.1) and (5.2) followed by control protocol (5.3), while the Lyapunov-based event-triggered impulsive strategy with $\theta_l \in \mathbb{R}^+$ is chosen as*

$$\begin{aligned} t_l &= \min\{t_l^f, t_l^e\} \\ t_l^e &= \inf\{t > t_{l-1} : \frac{1}{2} \tilde{\xi}^T(t) P \tilde{\xi}(t) - \frac{e^{\theta_l}}{2} \tilde{\xi}^T(t_{l-1}^-) P \tilde{\xi}(t_{l-1}^-) \geq 0\}, \quad \sum_{l=1}^{\infty} \theta_l = \infty \end{aligned} \quad (5.6)$$

where $\{t_l^f\}_{l=1}^\infty$ is the forced impulse sequence. Suppose Assumption 5.3.1 and Assumption 3.1.1 hold, $P = \begin{pmatrix} P_{11} & \mathbf{0}_{3n \times 3n} \\ \mathbf{0}_{3n \times 3n} & P_{22} \end{pmatrix} = \begin{pmatrix} \hat{P}_{11} \otimes I_n & \mathbf{0}_{3n \times 3n} \\ \mathbf{0}_{3n \times 3n} & \hat{P}_{22} \otimes I_n \end{pmatrix} \in \mathbb{R}^{6n \times 6n}$ is a positive definite matrix, and the maximal structure energy is bounded by $E \geq H_1(t) > 0$, $\zeta_{ij} = \zeta_{ii}^\beta > \frac{2E}{r_s}$. If the following conditions are satisfied:

$$M \geq \theta_p + \sum_{l=1}^{p-1} \theta_l + (p-1) \ln \rho_{max} \xrightarrow{p \rightarrow \infty} -\infty, \quad p \in \mathbb{Z}^+, \quad p \geq 2 \quad (5.7)$$

$$0 < \rho = \lambda_{max}(\Omega_1^T P \Omega_1 P^{-1}) < 1 \quad (5.8)$$

$$0 < \lambda_{max}(\Omega_2^T P \Omega_2 P^{-1}) \leq 1 \quad (5.9)$$

with $c = \sup\{\mu > 0 | s(\mu) \leq \bar{s}\} < \infty$ for a given constant $\bar{s} > 0$,

$$\bar{F}_1(t) = \begin{pmatrix} \mathbf{0}_{3n \times 3n} & I_{3n} \\ \alpha_x I_{2n} - k_1 L' & (\alpha_v - \beta_v) I_{3n} - k_1 L' + \bar{F}(t) \end{pmatrix}$$

$$\Omega_1 = \begin{pmatrix} I_{3n} & \mathbf{0}_{3n \times 3n} \\ -(k_3 \tilde{c} + k_2 L) & I_{2n} - (k_3 \tilde{d} + k_2 L) \end{pmatrix}$$

$$\Omega_2 = \begin{pmatrix} I_{3n} & \mathbf{0}_{3n \times 3n} \\ -k_2 L & I_{2n} - k_2 L \end{pmatrix}$$

$\omega_1 = \lambda_{max}(\Delta_1)$, $\Delta_1 = QP^{-1} + 2\bar{s}I_{6n}$, $\rho_{max} = 1 - \frac{s_k}{n}(1 - \rho)$. Then the error dynamics (5.5) will be driven to zero asymptotically with $\|\bar{\xi}(0)\| \leq \nu = \sqrt{\frac{\lambda_{min}(P)c^2}{e^\theta \lambda_{max}(P)}}$, all the local formation control objectives will be achieved and Zeno effect is prevented.

Proof. Construct the following Lyapunov function for $t \in [t_l, t_{l+1})$ as:

$$H_1(t) = \frac{1}{2} \bar{\xi}^T(t) P \bar{\xi}(t) \quad (5.10)$$

By the properties of braking and gyroscopic forces, we obtain $\bar{v}^T(t) P_{22} P_{22}^{-1} [P_G(\hat{v}_i(t)) \otimes \mathbf{1}_n] \leq 0$. Since the state variables are bounded, then there exists a positive constant matrix Q

such that $P\bar{F}_1(t) + \bar{F}_1^T(t)P \leq Q$. Therefore, based on Assumption 5.3.1 and (5.5), we take the time derivative of $H_1(t)$ with $\|\bar{\xi}(t)\| \leq c < \infty$ which gives:

$$\begin{aligned}
\dot{H}_1(t) &= \frac{1}{2}[\bar{\xi}^T(t)P\dot{\bar{\xi}}(t) + \dot{\bar{\xi}}^T(t)P\bar{\xi}(t)] \\
&\leq \frac{1}{2}\bar{\xi}^T(t)[P\bar{F}_1(t) + \bar{F}_1^T(t)P]\bar{\xi}(t) + \frac{1}{2}(\bar{\xi}^T(t)P\bar{R}(t) + \bar{R}^T(t)P\bar{\xi}(t)) \\
&\quad + \bar{v}^T P_{22}P_{22}^{-1}P_G(\bar{v}(t)) \\
&\leq \frac{1}{2}\bar{\xi}^T(t)QP^{-1}P\bar{\xi}(t) + s(\delta)\bar{\xi}^T(t)P\bar{\xi}(t) \\
&\leq \frac{1}{2}\lambda_{max}(QP^{-1} + 2sI_{6n})\bar{\xi}^T(t)P\bar{\xi}(t) \\
&\leq \lambda_{max}(\Delta_1)H_1(t) = \omega_1 H_1(t)
\end{aligned} \tag{5.11}$$

Then at each event-triggered impulsive instant t_l , we have:

$$\begin{aligned}
\Delta \bar{v}(t_l^-) &= -(k_3\tilde{c} + k_2L)\bar{\eta}(t_l^-) - (k_3\tilde{d} + k_2L)\bar{v}(t_l^-), \quad i \in \mathcal{D}_k \\
\Delta \bar{v}(t_l^-) &= -k_2L\bar{\eta}(t_l^-) - k_2L\bar{v}(t_l^-), \quad i \notin \mathcal{D}_k
\end{aligned} \tag{5.12}$$

Meanwhile, according to definition of ρ_{max} , for any $i \notin \mathcal{D}_k$ we have

$$\begin{aligned}
\frac{1}{2}(1 - \rho_{max}) \sum_{i \notin \mathcal{D}_k} \hat{\xi}_i^T(t_l^-) \hat{P} \hat{\xi}_i(t_l^-) &\leq \frac{1}{2}(1 - \rho_{max})(n - s_k) \min_{i \in \mathcal{D}_k} \{\hat{\xi}_i^T(t_l^-) \hat{P} \hat{\xi}_i(t_l^-)\} \\
&= \frac{s_k}{2}(\rho_{max} - \rho) \min_{i \in \mathcal{D}_k} \{\hat{\xi}_i^T(t_l^-) \hat{P} \hat{\xi}_i(t_l^-)\} \\
&\leq \frac{1}{2}(\rho_{max} - \rho) \sum_{i \in \mathcal{D}_k} \hat{\xi}_i^T(t_l^-) \hat{P} \hat{\xi}_i(t_l^-)
\end{aligned} \tag{5.13}$$

Based on (5.9) we also have

$$\begin{aligned}
\sum_{i \notin \mathcal{D}_k} \hat{\xi}_i^T(t_l) \hat{P} \hat{\xi}_i(t_l) &\leq \lambda_{max}(\Omega_2^T P \Omega_2 P^{-1}) \sum_{i \notin \mathcal{D}_k} \hat{\xi}_i^T(t_l^-) \hat{P} \hat{\xi}_i(t_l^-) \\
&\leq \sum_{i \notin \mathcal{D}_k} \hat{\xi}_i^T(t_l^-) \hat{P} \hat{\xi}_i(t_l^-)
\end{aligned} \tag{5.14}$$

It follows from (5.8), (5.13) and (5.14) that:

$$\begin{aligned}
H_1(t_l) &= \frac{1}{2} \sum_{i \in \mathcal{D}_k} \hat{\xi}_i^T(t_l) \hat{P} \hat{\xi}_i(t_l) + \frac{1}{2} \sum_{i \notin \mathcal{D}_k} \hat{\xi}_i^T(t_l) \hat{P} \hat{\xi}_i(t_l) \\
&= \frac{1}{2} \sum_{i \in \mathcal{D}_k} \hat{\xi}_i^T(t_l) \hat{P} \hat{\xi}_i(t_l) + \frac{1}{2} (1 - \rho_{max}) \sum_{i \notin \mathcal{D}_k} \hat{\xi}_i^T(t_l) \hat{P} \hat{\xi}_i(t_l) + \frac{\rho_{max}}{2} \sum_{i \notin \mathcal{D}_k} \hat{\xi}_i^T(t_l) \hat{P} \hat{\xi}_i(t_l) \\
&\leq \frac{1}{2} \lambda_{max}(\Omega_1^T P \Omega_1 P^{-1}) \sum_{i \in \mathcal{D}_k} \hat{\xi}_i^T(t_l^-) \hat{P} \hat{\xi}_i(t_l^-) + \frac{1}{2} (\rho_{max} - \rho) \sum_{i \notin \mathcal{D}_k} \hat{\xi}_i^T(t_l^-) \hat{P} \hat{\xi}_i(t_l^-) \\
&\quad + \frac{\rho_{max}}{2} \sum_{i \notin \mathcal{D}_k} \hat{\xi}_i^T(t_l^-) \hat{P} \hat{\xi}_i(t_l^-) \\
&\leq \frac{1}{2} (\rho + (\rho_{max} - \rho)) \sum_{i \in \mathcal{D}_k} \hat{\xi}_i^T(t_l^-) \hat{P} \hat{\xi}_i(t_l^-) + \frac{\rho_{max}}{2} \sum_{i \notin \mathcal{D}_k} \hat{\xi}_i^T(t_l^-) \hat{P} \hat{\xi}_i(t_l^-) \\
&= \rho_{max} H_1(t_l^-) = e^{-(-\ln \rho_{max})} H_1(t_l^-)
\end{aligned} \tag{5.15}$$

Based on Lemma 3.1.2, we require $\sup_{l \in \mathbb{N}^+} \{t_l^f - t_{l-1}^f\} < \frac{\ln(\rho_{max}^{-1})}{\omega_1}$. Furthermore, according to (5.6) and (5.15), we have:

$$\begin{aligned}
H_1(t) &\leq e^{\theta_1} H_1(t_0^-) = e^{\theta_1} H_1(t_0), \quad \forall t \in [t_0, t_1) \\
H_1(t) &\leq e^{\theta_2} H_1(t_1^-) \leq e^{\theta_1 + \theta_2 - (-\ln \rho_{max})} H_1(t_0), \quad \forall t \in [t_1, t_2) \\
H_1(t) &\leq e^{\theta_3} H_1(t_2^-) \leq e^{\theta_1 + \theta_2 + \theta_3 - (-2 \ln \rho_{max})} H_1(t_0), \quad \forall t \in [t_2, t_3) \\
&\dots \\
H_1(t) &\leq e^{\theta_p} H_1(t_{p-1}^-) \leq e^{[\theta_p + \sum_{l=1}^{p-1} \theta_l + (p-1) \ln \rho_{max}]} H_1(t_0), \quad \forall t \in [t_{p-1}, t_p)
\end{aligned} \tag{5.16}$$

Hence, based on (5.7) and (5.16), the asymptotic convergence of the error dynamics is successfully achieved.

Additionally, we consider the following four cases to examine Zeno effect:

- (a) $\{t_l\}_{l=1}^\infty$ fully coincides with $\{t_l^e\}_{l=1}^\infty$. By taking the integral over the interval $[t_{l-1}, t_l)$ along with (5.11) we have:

$$e^{\theta_l} H_1(t_{l-1}) \leq e^{\theta_l} H_1(t_{l-1}^-) \leq H_1(t_l^-) \leq e^{\lambda_{max}(\Delta_1)(t_l - t_{l-1})} H_1(t_{l-1}) \tag{5.17}$$

which gives $t_l - t_{l-1} > \frac{\theta_l}{\lambda_{max}(\Delta_1)}$, and it recursively follows that $t_l \geq \frac{1}{\lambda_{max}(\Delta_1)} \sum_{l=1}^p \theta_l + t_0$. Combine with $\sum_{l=1}^\infty \theta_l = \infty$, it further implies $t_l \rightarrow \infty$ as $p \rightarrow \infty$.

- (b) $\{t_l\}_{l=1}^\infty$ fully coincides with $\{t_l^f\}_{l=1}^\infty$. It follows from $\inf\{t_l - t_{l-1}\} = \inf\{t_l^f - t_{l-1}^f\} > 0$.
- (c) $t_l = t_l^f$ and $t_{l-1} = t_{l-1}^e$. It follows from $\inf\{t_l - t_{l-1}\} = \inf\{t_l^f - t_{l-1}^e\} > \inf\{t_l^f - t_{l-1}^f\} > 0$.
- (d) $t_l = t_l^e$ and $t_{l-1} = t_{l-1}^f$. Similar to (5.17), one can derive $e^{\theta_l} H_1(t_{l-1}) \leq H_1(t_l^-) = H_1(t_l^{e-}) = e^{\theta_l} H_1(t_{l-1}^-) \leq e^{\lambda_{\max}(\Delta_1)(t_l - t_{l-1})} H_1(t_{l-1})$ so that $\inf\{t_l - t_{l-1}\} \geq \frac{\theta_l}{\lambda_{\max}(\Delta_1)}$.

Hence, the Zeno effect (i.e., there exists infinite impulses in a finite amount of time) does not occur. In addition, denote $\bar{\theta} = \max\{\theta_1, M\}$, it follows from (5.16) that

$$\|\bar{\xi}(t)\| \leq \sqrt{\frac{e^{\bar{\theta}} \lambda_{\max}(P) \nu^2}{\lambda_{\min}(P)}} = c, \quad t \geq t_0 \quad (5.18)$$

Thus, the initial attainable range $\nu = \sqrt{\frac{\lambda_{\min}(P) c^2}{e^{\bar{\theta}} \lambda_{\max}(P)}}$. The proof of collision-free motion with respect to $H_1(t)$ follows the same procedure as that of the Theorem 3.4.1, thus omitted. As a result, all the local formation control objectives are achieved with $\|\bar{\xi}(0)\| \leq \nu$. \square

Remark 5.4.1. Notice that if the forced impulse sequence $\{t_l^f\}_{l=1}^\infty$ is excluded, then the asymptotic convergence of the error dynamics fails to obtain in the case of zero or finite number of event-triggered instants generated. The proposed event-triggered strategy (5.6) together with condition (5.7) ensure that infinite event-triggering instants will be activated while achieving asymptotic stability. Furthermore, since the proposed event-triggered strategy is Lyapunov-based, this allows it to be adapted by a wide variety of Lyapunov functions.

Remark 5.4.2. Based on the sufficient conditions provided in Theorem 5.4.1, the LMI condition (5.8) and the size of the impulsive interval are dependent on coupling strength, impulsive strength, navigation feedback gain and also nonlinearity strength. Specifically, larger values of nonlinearity strength and smaller coupling strengths lead to stronger destabilizing effects on continuous dynamics. Hence, more frequent event-triggered impulses with stronger strength (i.e., ρ_{\max} is closer to 0) are required to maintain stability and faster convergence speed. This can be achieved by either increasing the magnitude of navigation feedback gains and total number of pinned agents s_k , or reducing the value of event-triggered threshold θ_l . In practice, due to the boundness of state variables, feasible choices of matrix P and ρ_{\max} can be calculated by solving the LMI condition (5.8) according to pre-determined system and control parameters, which then gives the maximum allowable value of θ_l and length of impulsive interval.

Algorithm 5.4.1 Formation Stabilization Algorithm via Control Law (5.3) and Strategy (5.6)

Require: Initialize $\eta_i, v_i, \eta_i^d, f(v_i)$ and $\phi(v_i)$ for $i \in \{0, \dots, n\}$.

Initialize system parameters α_x, α_v and β_v

Initialize control parameters, such as b_{ij}, c, d and so on.

Set up the communication topology.

Ensure: Definition 5.3.1 is satisfied

- 1: Compute feasible values of positive matrix P , impulsive strength ρ_{max} and maximal triggering threshold $\bar{\theta}$ by solving LMI (5.8) for a given pinning fraction s_k .
 - 2: set $l = 1$.
 - 3: **for** $t \in [t_0, t_{end}]$ **do**
 - 4: **if** $\frac{1}{2}\bar{\xi}^T(t)P\bar{\xi}(t) - \frac{e^{\theta_l}}{2}\bar{\xi}^T(t_{l-1}^-)P\bar{\xi}(t_{l-1}^-) \geq 0$ and $t \geq t_l^f$ **then**
 - 5: The event has occurred at $t = t_l^e$ and t_l is recorded as t_l^f .
 - 6: Update $\bar{\xi}(t)$ using the protocol (5.3) evaluated at t_l^f .
 - 7: Update last event-triggering instant t_{l-1} to t_l^f .
 - 8: **else if** $\frac{1}{2}\bar{\xi}^T(t)P\bar{\xi}(t) - \frac{e^{\theta_l}}{2}\bar{\xi}^T(t_{l-1}^-)P\bar{\xi}(t_{l-1}^-) \geq 0$ and $t < t_l^f$ **then**
 - 9: The event has occurred at $t = t_l^e$ and t_l is recorded as t_l^e .
 - 10: Update $\bar{\xi}(t)$ using the protocol (5.3) evaluated at t_l^e .
 - 11: Update last event-triggering instant t_{l-1} to t_l^e .
 - 12: **else if** $t = t_l^f$ **then**
 - 13: The forced impulse has occurred at $t = t_l^f$ and t_l is recorded as t_l^f .
 - 14: Update $\bar{\xi}(t)$ using the protocol (5.3) evaluated at t_l^f .
 - 15: Update last event-triggering instant t_{l-1} to t_l^f .
 - 16: **else**
 - 17: Update $\bar{\xi}(t)$ using the protocol (5.3) evaluated at t , which belongs to the interval $[t_{l-1}, t_l)$.
 - 18: **end if**
 - 19: $l = l + 1$
 - 20: **end for**
-

Remark 5.4.3. To facilitate solving practical problems, the algorithm framework for compact error dynamics (5.5) via protocol (5.3) and event-triggered strategy (5.6) in Theorem 5.4.1 is presented (see Algorithm 5.4.1) as follows:

Remark 5.4.4. Notice that the Lipschitz condition (i.e., $\|f(u) - f(v)\| \leq \kappa_1 \|u - v\|$ and $\|\phi(u) - \phi(v)\| \leq \kappa_2 \|u - v\|$ where $\kappa_1, \kappa_2 > 0$ for all $u, v \in \mathbb{R}^{3n}$) can be viewed as exhibiting weak nonlinearity in Assumption 5.3.1, where $\|\tilde{f}(y_i(t) + x) - \tilde{f}(y_i(t))\| \leq \kappa_1 \|x\|$ and $\delta = \sup\{r > 0 | s(r) \leq \bar{s}\} = \infty$ clearly holds true.

5.4.2 HETPIC with Transmittal Delays

In real applications, time-delay is inevitable in the sampling and transmission of impulsive information in dynamical systems. Therefore, we focus on the control problem involving delayed coupling feedback in this subsection, as the corresponding protocol is constructed as follows for $i = 1, 2, \dots, n$:

$$\begin{aligned} \tau_i &= k_1 P_C(\hat{\eta}_i(t - r(t)), \hat{v}_i(t - r(t))) + k_2 P_D(\hat{\eta}_i(t), \hat{v}_i(t)) + k_3 P_L(\hat{\eta}_i(t), \hat{v}_i(t)) \\ &\quad - \alpha_x \eta_i^d + \hat{P}_{22}^{-1} P_G(\hat{v}_i(t)) \end{aligned} \quad (5.19)$$

where $r(t)$ is the time-varying continuous delay satisfying $r(t) \leq h$ for some constant $h > 0$. Similar to (5.5), the overall compact form of error dynamics can be obtained as follows:

$$\left\{ \begin{aligned} \dot{\bar{\xi}}(t) &= \begin{pmatrix} \mathbf{0}_{3n \times 3n} & I_{3n} \\ \alpha_x I_{3n} & (\alpha_v - \beta_v) I_{3n} \end{pmatrix} \bar{\xi}(t) + \begin{pmatrix} \mathbf{0}_{3n \times 3n} & \mathbf{0}_{3n \times 3n} \\ -k_1 L' & -k_1 L' \end{pmatrix} \bar{\xi}(t - r(t)) \\ &\quad + \begin{pmatrix} \mathbf{0}_{3n} \\ \bar{f}(\bar{v}(t)) + \bar{\phi}(\bar{v}(t)) + [\hat{P}_{22}^{-1} \otimes I_n] P_G(\hat{v}_i(t)) \otimes \mathbf{1}_n \end{pmatrix}, \quad t \neq t_l \\ \Delta \bar{v}(t_l) &= -k_2 L \bar{\eta}(t_l) - k_2 L \bar{v}(t_l) - k_3 \tilde{c} \bar{\eta}(t_l) - k_3 \tilde{d} \bar{v}(t_l), \quad t = t_l, \quad i \in \mathcal{D}_k \\ \Delta \bar{v}(t_l) &= -k_2 L \bar{\eta}(t_l) - k_2 L \bar{v}(t_l), \quad t = t_l, \quad i \notin \mathcal{D}_k \end{aligned} \right. \quad (5.20)$$

Theorem 5.4.2. Consider the leader-following multi-agent systems with dynamics (5.1) and (5.2) followed by control protocol (5.19), while the Lyapunov-based event-triggered impulsive strategy with $\theta_l \in \mathbb{R}^+$ is chosen as

$$t_l = \inf\{t > t_{l-1} : \frac{1}{2} \bar{\xi}^T(t) P \bar{\xi}(t) - e^{\theta_l - \delta t} \max\{\frac{1}{2} e^{\delta t_{l-1}} \bar{\xi}^T(t_{l-1}) P \bar{\xi}(t_{l-1}), \frac{1}{2} e^{\delta t_0} \bar{\xi}^T(t_0) P \bar{\xi}(t_0)\} \geq 0\} \quad (5.21)$$

where $\sum_{l=1}^{\infty} \theta_l = \infty$, $\delta > 0$ is a given constant. Suppose Assumptions 5.3.1 and 3.1.1 hold, $P = \begin{pmatrix} P_{11} & \mathbf{0}_{3n \times 3n} \\ \mathbf{0}_{3n \times 3n} & P_{22} \end{pmatrix} = \begin{pmatrix} \hat{P}_{11} \otimes I_n & \mathbf{0}_{3n \times 3n} \\ \mathbf{0}_{3n \times 3n} & \hat{P}_{22} \otimes I_n \end{pmatrix}$ is a positive definite matrix with appropriate dimension, M is a positive constant so that $\theta_l \in (0, M]$, and the maximal structure energy is bounded by $E \geq H_2(t) > 0$, $\zeta_{ij} = \zeta_{ii^\beta} > \frac{2E}{r_s}$. If there exists $\varepsilon_1 > 0$ and the following conditions are satisfied:

$$\theta_l + \sum_{p=1}^{l-1} (\theta_{l-p} + \ln \rho_{max}) \leq M, \quad \forall l \geq 2 \quad (5.22)$$

$$0 < \rho = \lambda_{max}(\Omega_1^T P \Omega_1 P^{-1}) < 1 \quad (5.23)$$

$$0 < \lambda_{max}(\Omega_2^T P \Omega_2 P^{-1}) \leq 1 \quad (5.24)$$

with $c = \sup\{\mu > 0 | s(\mu) \leq \bar{s}\} < \infty$ for a given constant $\bar{s} > 0$, $\rho_{max} = 1 - \frac{s_k}{n}(1 - \rho)$,

$$\bar{F}_2(t) = \begin{pmatrix} \mathbf{0}_{3n \times 3n} & I_{3n} \\ \alpha_x I_{3n} & (\alpha_v - \beta_v) I_{3n} + \bar{F}(t) \end{pmatrix}$$

$$\Omega_1 = \begin{pmatrix} I_{3n} & \mathbf{0}_{3n \times 3n} \\ -(k_3 \tilde{c} + k_2 L) & (I_{2n} - (k_3 \tilde{d} + k_2 L)) \end{pmatrix}$$

$$\Omega_2 = \begin{pmatrix} I_{3n} & \mathbf{0}_{3n \times 3n} \\ -k_2 L & I_{2n} - k_2 L \end{pmatrix}$$

$\omega_2 = \lambda_{max}(\Delta_2)$, $\omega_3 = \frac{\Delta_3 \lambda_{max}(P^{-1})}{\varepsilon_1}$, $\Delta_2 = QP^{-1} + \varepsilon_1 P^{-1} + 2\bar{s}I_{6n}$, $\Delta_3 = \|P\Delta_4\|^2$ and $\Delta_4 = \begin{pmatrix} \mathbf{0}_{3n \times 3n} & \mathbf{0}_{3n \times 3n} \\ -k_1 L' & -k_1 L' \end{pmatrix}$. Then the error dynamics (5.20) will be driven to zero asymptotically with $\|\bar{\xi}(0)\| \leq \nu = \sqrt{\frac{\lambda_{min}(P)c^2}{e^M \lambda_{max}(P)}}$, all the local formation control objectives will be achieved and Zeno effect is prevented.

Proof. Similar to Theorem 5.4.1, take the energy-like Lyapunov function $H_2(t) = \frac{1}{2} \bar{\xi}^T(t) P \bar{\xi}(t)$ for $t \in [t_l, t_{l+1})$. Again, we are able to obtain $P\bar{F}_2(t) + \bar{F}_2^T(t)P \leq Q$ for some $Q > 0$, then the time derivative of H_2 with $\|\bar{\xi}(t)\| \leq c < \infty$ can be derived as:

$$\begin{aligned} \dot{H}_2(t) &= \frac{1}{2} \bar{\xi}^T(t) [P\bar{F}_2(t) + \bar{F}_2^T(t)P] \bar{\xi}(t) \\ &+ \frac{1}{2} \bar{\xi}^T(t) P \Delta_4 \bar{\xi}(t - r(t)) + \bar{\xi}^T(t - r(t)) \Delta_4^T P \bar{\xi}(t) \\ &+ \frac{1}{2} (\bar{\xi}^T(t) P \bar{R}(t) + \bar{R}^T(t) P \bar{\xi}(t)) + \bar{v}^T P_{22} P_{22}^{-1} P_G(\bar{v}(t)) \end{aligned} \quad (5.25)$$

and it further derives that

$$\begin{aligned}
\dot{H}_2(t) &\leq \frac{1}{2}\bar{\xi}^T(t)Q\bar{\xi}(t) + \frac{\varepsilon_1}{2}\bar{\xi}^T(t)\bar{\xi}(t) + \frac{\Delta_3}{2\varepsilon_1}\bar{\xi}^T(t-r(t))\bar{\xi}(t-r(t)) + s(\mu)\bar{\xi}^T(t)P\bar{\xi}(t) \\
&\leq \frac{1}{2}\bar{\xi}^T(t)QP^{-1}P\bar{\xi}(t) + \frac{\varepsilon_1}{2}\bar{\xi}^T(t)P^{-1}P\bar{\xi}(t) + \frac{\Delta_3}{2\varepsilon_1}\bar{\xi}^T(t-r(t))P^{-1}P\bar{\xi}(t-r(t)) + \bar{s}\bar{\xi}^T(t)P\bar{\xi}(t) \\
&\leq \frac{1}{2}\lambda_{max}(QP^{-1} + \varepsilon_1P^{-1} + 2\bar{s}I_{6n})\bar{\xi}^T(t)P\bar{\xi}(t) + \frac{\Delta_3\lambda_{max}(P^{-1})}{2\varepsilon_1}\bar{\xi}^T(t-r(t))P\bar{\xi}(t-r(t)) \\
&= \frac{1}{2}\lambda_{max}(\Delta_2)\bar{\xi}^T(t)P\bar{\xi}(t) + \frac{\Delta_3\lambda_{max}(P^{-1})}{2\varepsilon_1}\bar{\xi}^T(t-r(t))P\bar{\xi}(t-r(t)) \\
&= \lambda_{max}(\Delta_2)H_2(t) + \frac{\Delta_3\lambda_{max}(P^{-1})}{2\varepsilon_1}H_2(t-r(t)) \leq \omega_2H_2(t) + \omega_3 \sup_{s \in [-h,0]} H_2(t+s)
\end{aligned} \tag{5.26}$$

Accordingly, at each impulsive instant t_l , we still obtain the same results as derived in (5.12)-(5.15) so that

$$H_2(t_l) \leq \rho_{max}H_2(t_l^-) = e^{\ln \rho_{max}} H_2(t_l^-) \tag{5.27}$$

Furthermore, we demonstrate the error dynamics does not exhibit Zeno behaviour with t_{l-1} as the last event-triggering instant by introducing

$$U(t) = \begin{cases} e^{\delta(t-t_0)}H_2(t), & t \in [t_0, \infty) \\ H_{20}, & t \in [t_0 - h, t_0) \end{cases} \tag{5.28}$$

where $H_{20} = \sup_{s \in [-h,0]} H_2(t_0 + s)$. Since $U(t_1^-) = e^{\theta_1} \max\{U(t_0), H_{20}\} = e^{\theta_1} H_{20} > H_{20}$, then there exists a $t_1 = \sup\{t \in [t_0, t_1) | U(t) \leq H_{20}\}$ so that $U(t_1) = H_{20}$. Then we obtain:

$$\begin{aligned}
H_{20} &\leq U(t) \leq U(t_1^-), \quad t \in [\tilde{t}_1, t_1) \\
U(t+s) &\leq \begin{cases} U(t_1^-), & t+s \in [t_0, t_1) \\ H_{20}, & t+s \in [t_0-h, t_0) \end{cases} \\
&\leq \begin{cases} e^{\theta_1}U(t), & t+s \in [t_0, t_1) \\ U(t), & t+s \in [t_0-h, t_0) \end{cases} \\
&\leq e^M U(t) \quad \forall t \in [\tilde{t}_1, t_1), \quad \forall s \in [-h, 0]
\end{aligned} \tag{5.29}$$

By repeating the above procedure and set $\tilde{t}_l = \sup\{t \in [t_{l-1}, t_l) | U(t) \leq \max\{U(t_{l-1}), H_{20}\}\}$

so that $U(\tilde{t}_l) = \max\{U(t_{l-1}), H_{20}\}$, thus followed by (5.21) and (5.22) we further have:

$$\begin{aligned}
H_{20} &\leq \max\{U(t_{l-1}), H_{20}\} \leq U(t) \leq U(t_l^-), \quad t \in [\tilde{t}_l, t_l) \\
U(t+s) &\leq \begin{cases} U(t_l^-), & t+s \in [t_{l-1}, t_l) \\ U(t_{l-1}^-), & t+s \in [t_{l-2}, t_{l-1}) \\ \dots \\ U(t_1^-), & t+s \in [t_0, t_1) \\ H_{20}, & t+s \in [t_0-h, t_0), \quad \forall t \in [\tilde{t}_l, t_l), \quad \forall s \in [-h, 0] \end{cases} \quad (5.30)
\end{aligned}$$

Finally, according to (5.28)-(5.30), define $\pi_l = \theta_1$ for $l = 1$ and $\pi_l = \max_{k=1, \dots, l-1} \{\theta_l + \sum_{p=1}^k (\theta_{l-p} + \ln \rho_{max})\}$ for $l \geq 2$, it yields:

$$\begin{aligned}
U(t+s) &\leq \begin{cases} e^{\theta_l} U(t), & t+s \in [t_{l-1}, t_l) \\ (e^{\theta_{l-1}} \vee e^{\pi_{l-1}}) U(t), & t+s \in [t_{l-2}, t_{l-1}) \\ \dots \\ e^{\theta_1} U(t), & t+s \in [t_0, t_1) \\ U(t), & t+s \in [t_0-h, t_0) \end{cases} \quad (5.31) \\
&\leq e^M U(t), \quad \forall t \in [\tilde{t}_l, t_l), \quad \forall s \in [-h, 0]
\end{aligned}$$

which is equivalent to:

$$e^{\delta(t+s-t_0)} H_2(t+s) \leq e^{M+\delta(t-t_0)} H_2(t), \quad \forall t \in [\tilde{t}_l, t_l), \quad \forall s \in [-h, 0] \quad (5.32)$$

Combine (5.26) and (5.32), we have:

$$\begin{aligned}
\dot{U}(t) &\leq \delta e^{\delta(t-t_0)} H_2(t) + \omega_2 e^{\delta(t-t_0)} H_2(t) + \omega_3 e^{\delta(t-t_0)} \sup_{s \in [-h, 0]} H_2(t+s) \\
&\leq e^{\delta(t-t_0)} (\delta + \omega_2 + \omega_3 e^{M-\delta s}) H_2(t) \\
&= (\delta + \omega_2 + \omega_3 e^{M-\delta s}) U(t), \quad \forall t \in [\tilde{t}_l, t_l), \quad \forall s \in [-h, 0]
\end{aligned} \quad (5.33)$$

then

$$e^{(\delta+\omega_2+\omega_3 e^{M-\delta s})(t_l-\tilde{t}_l)} U(\tilde{t}_l) \geq U(t_l^-) \geq e^{\theta_l} \max\{U(t_{l-1}), H_{20}\} = e^{\theta_l} U(\tilde{t}_l) \quad (5.34)$$

holds by taking the integral of (5.33) within $[\tilde{t}_l, t_l)$. As a result, based on (5.21), the Zeno behaviour does not occur since $t_l - t_{l-1} \geq t_l - \tilde{t}_l \geq \frac{\theta_l}{(\delta+\omega_2+\omega_3 e^{M+\delta h})}$ and $t_l \xrightarrow{l \rightarrow \infty} \infty$. Meanwhile, it can be recursively deduced that $U(t) < e^{\theta_l} \max\{U(t_{l-1}), H_{20}\} \leq \max\{e^{\theta_l}, e^{\pi_l}\} H_{20}$ for

$t \in [t_{l-1}, t_l)$ and $l \in \mathbb{N}^+$, then we have $U(t) = e^{\delta(t-t_0)}H_2(t) \leq e^M H_{20}, \forall t \geq t_0$, which implies $H_2(t) \leq e^M H_{20} e^{-\delta(t-t_0)}, \forall t \geq t_0$. Therefore, the error dynamics converges to zero asymptotically without Zeno effect. Furthermore, according to (5.31), one can obtain

$$\|\bar{\xi}(t)\| \leq \sqrt{\frac{e^M \lambda_{\max}(P) \nu^2}{\lambda_{\min}(P)}} = c, \quad t \geq t_0 \quad (5.35)$$

Thus, the initial attainable range $\nu = \sqrt{\frac{\lambda_{\min}(P)c^2}{e^M \lambda_{\max}(P)}}$. The proof of collision-free motion with respect to $H_2(t)$ follows the same procedure as that of the Theorem 3.2.1 and thus is omitted. Consequently, all the local formation control objectives are achieved with $\|\bar{\xi}(0)\| \leq \nu$. \square

Remark 5.4.5. Accordingly, the algorithm framework for compact error dynamics (5.20) via protocol (5.19) and event-triggered strategy (5.21) in Theorem 5.4.2 is presented (see Algorithm 5.4.2) as follows:

Remark 5.4.6. As opposed to (5.6), the forced impulse sequence has been removed as indicated in the improved event-triggered strategy (5.21), while the formation control objectives can still be guaranteed in terms of continuous time-varying delay as illustrated in Theorem 5.4.2. Meanwhile,

$$\frac{1}{2} \bar{\xi}^T(t) P \bar{\xi}(t) = e^{\theta_l - \delta t} \max\left\{\frac{1}{2} e^{\delta t_{l-1}} \bar{\xi}^T(t_{l-1}) P \bar{\xi}(t_{l-1}), \frac{1}{2} e^{\delta t_0} \bar{\xi}^T(t_0) P \bar{\xi}(t_0)\right\}$$

can be viewed as an event-triggered impulse surface, where the triggering instant is allocated upon hitting the surface. The magnitude of θ_l here also exhibits negative correlation with respect to the convergence rate and the amount of impulsive instants generated; while the strategy is also applicable for different choices of $H_2(t)$. Moreover, in both theorems, the pinning mechanism assigned to the fraction of agents further minimises the transmission complexity between followers and the leader.

Remark 5.4.7. There are many existing literatures regarding event-triggered control of impulsive systems, for instance, event-triggered impulsive control for real-time dynamics [93] and for nonlinear dynamics with constant continuous delay [90] have been investigated respectively in order to maintain Lyapunov stability. Nevertheless, very few formation stabilization results has been addressed for multi-agent systems with continuous time-varying delay effects. Meanwhile, due to frequent exposure to malicious attacks and transmission latency in reality, it has become increasingly critical for agents to exchange information via stabilizing event-triggered impulses on top of delayed continuous communication. In this way, the reliability and confidentiality of the data can be enhanced. Therefore, Theorem 5.4.2 provides more generalized criteria of maintaining asymptotic stabilization.

Algorithm 5.4.2 Formation Stabilization Algorithm via Control Law (5.19) and Strategy (5.21)

Require: Initialize $\eta_i, v_i, \eta_i^d, f(v_i)$ and $\phi(v_i)$ for $i \in \{0, \dots, n\}$.

Initialize system parameters α_x, α_v and β_v

Initialize control parameters, such as b_{ij}, c, d and so on.

Initialize time-varying delay $r(t)$ and impulse delay τ_l .

Set up the communication topology.

Ensure: Definition 5.3.1 is satisfied

- 1: Compute feasible values of positive matrix P , impulsive strength ρ_1, ρ_2 and maximal triggering threshold M by solving LMI (5.23) for a given pinning fraction s_k and positive constant δ .
 - 2: When $t - r(t) < 0$, $P_C(\hat{\eta}_i(t - r(t)), \hat{v}_i(t - r(t)))$ is computed as $P_C(\hat{\eta}_i(0), \hat{v}_i(0))$ in the protocol (5.19).
 - 3: set $l = 1$.
 - 4: **for** $t \in [t_0, t_{end}]$ **do**
 - 5: **if** $\frac{1}{2}e^{\delta t_{l-1}} \bar{\xi}^T(t_{l-1}) P \bar{\xi}(t_{l-1}) \geq \frac{1}{2}e^{\delta t_0} \bar{\xi}^T(t_0) P \bar{\xi}(t_0)$ **then**
 - 6: **if** $\frac{1}{2} \bar{\xi}^T(t) P \bar{\xi}(t) - e^{\theta_l - \delta t} \frac{1}{2} e^{\delta t_{l-1}} \bar{\xi}^T(t_{l-1}) P \bar{\xi}(t_{l-1}) \geq 0$ **then**
 - 7: The event has occurred and event instant is recorded as t_l .
 - 8: Update $\bar{\xi}(t)$ using the protocol (5.19) evaluated at t_l .
 - 9: Update last event-triggering instant t_{l-1} to t_l .
 - 10: **else**
 - 11: Update $\bar{\xi}(t)$ using the protocol (5.19) evaluated at t , which belongs to the interval $[t_{l-1}, t_l)$.
 - 12: **end if**
 - 13: **else**
 - 14: **if** $\frac{1}{2} \bar{\xi}^T(t) P \bar{\xi}(t) - e^{\theta_l - \delta t} \frac{1}{2} e^{\delta t_0} \bar{\xi}^T(t_0) P \bar{\xi}(t_0) \geq 0$ **then**
 - 15: The event has occurred and event instant is recorded as t_l .
 - 16: Update $\bar{\xi}(t)$ using the protocol (5.19) evaluated at t_l .
 - 17: Update last event-triggering instant t_{l-1} to t_l .
 - 18: **else**
 - 19: Update $\bar{\xi}(t)$ using the protocol (5.19) evaluated at t , which belongs to the interval $[t_{l-1}, t_l)$.
 - 20: **end if**
 - 21: **end if**
 - 22: $l = l + 1$
 - 23: **end for**
-

5.5 Numerical simulations

In this section, numerical simulations based on the multi-quadrotor system are given to illustrate the correctness of the theoretical results. A quadrotor is a typical type of UAV equipped with coaxial rotors and sensing device, which has increased practicality in reality due to its unique abilities of high maneuverability (i.e., vertical take off and landing (VTOL)) and small size with low inertia. For instance, search-and-rescue, emergency response, military surveillance and atmospheric sampling can be considered as its potential applications [101]. The dynamics of a quadrotor can be classified into trajectory dynamics with respect to outer-loop control and the attitude dynamics with respect to inner-loop control [102, 103] (see Figure 5.2). Meanwhile, a detailed description of a common hardware structure of the quadrotor platform can be found in [102, 104] (see Figure 5.3).

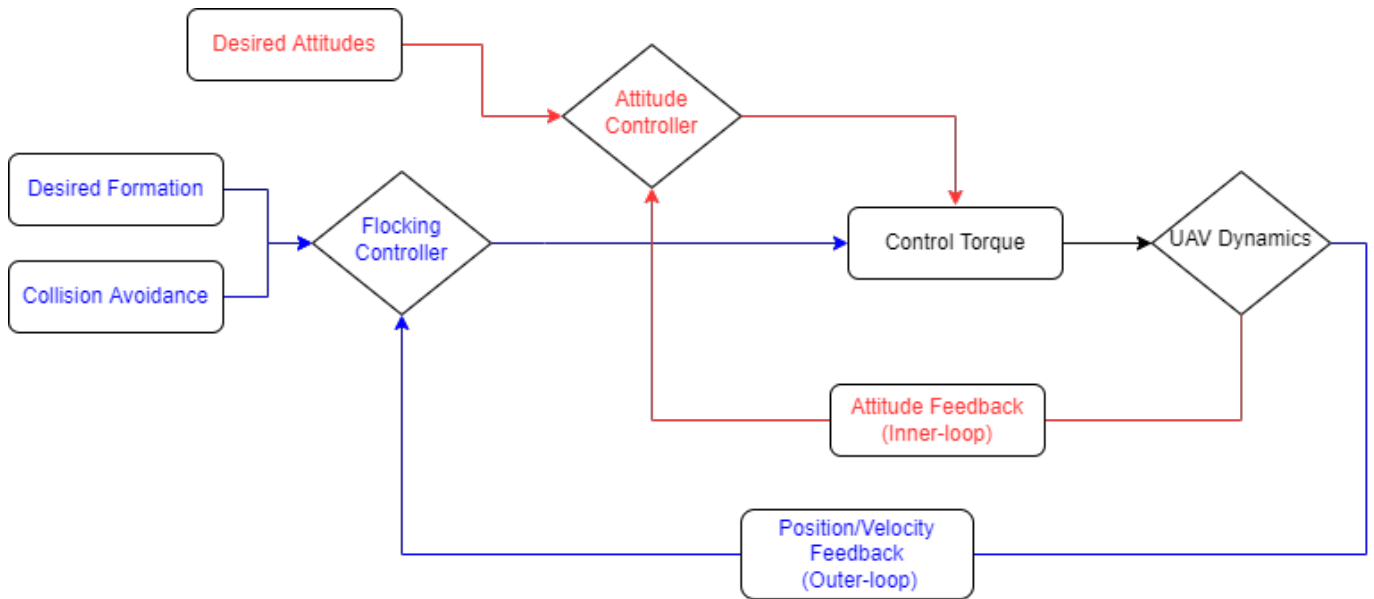


Figure 5.2: Two-loop feedback control scheme for the multi-quadrotor system

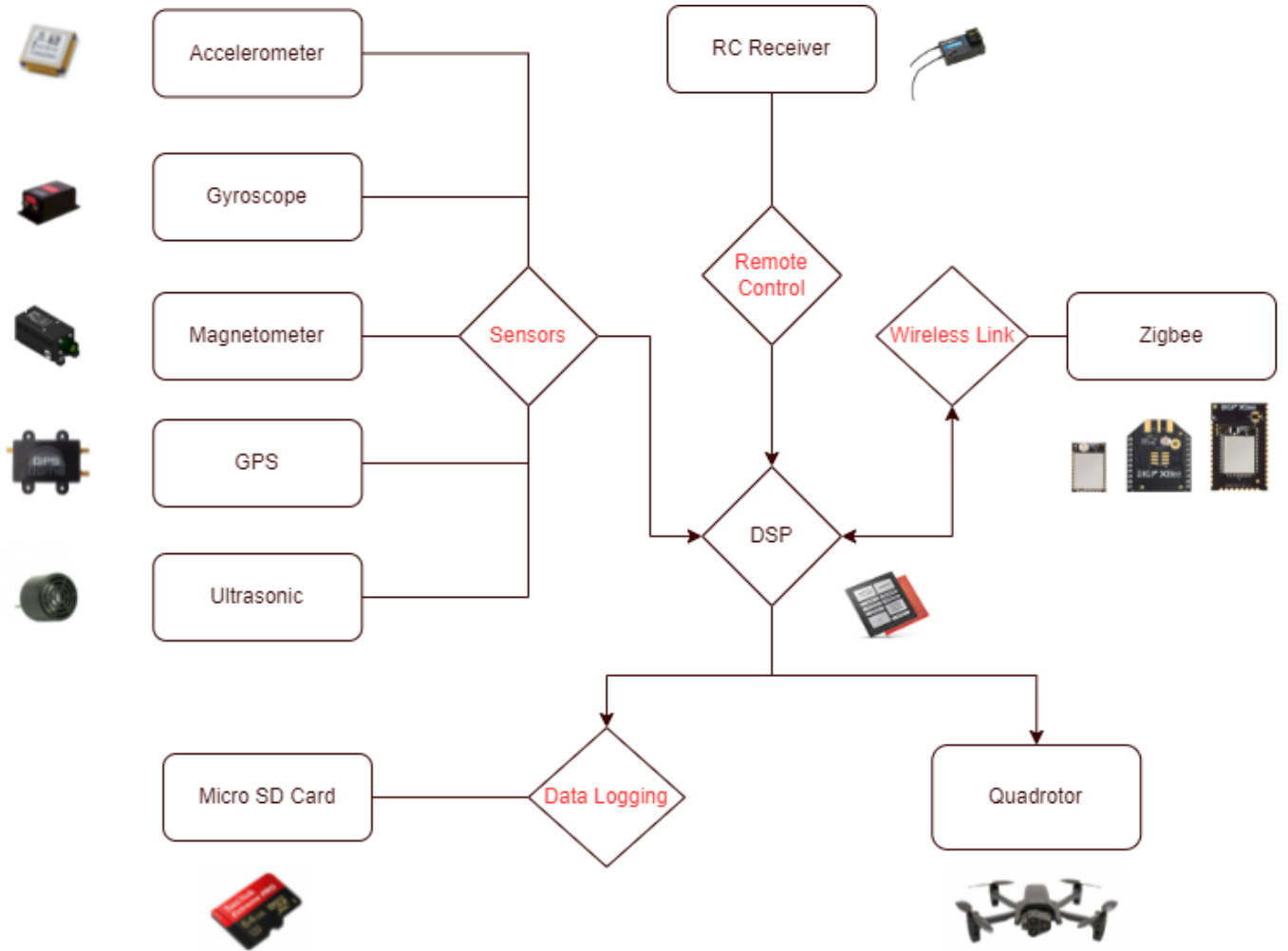


Figure 5.3: Hardware structure of the quadrotor platform

Since the formation control is mainly concerned with positions and velocities, we consider the following error trajectory dynamics by utilizing the specific parameter settings:

$$\begin{cases} \dot{\hat{\eta}}_i(t) = \hat{v}_i(t) \\ \dot{\hat{v}}_i(t) = -0.25\hat{\eta}_i(t) + 15\hat{v}_i(t) + 0.025(\hat{v}_i(t))^2 + 0.05 \tanh(\hat{v}_i(t)), \quad i = 1, 2, \dots, n \end{cases}$$

Here, we have $\alpha_x = -0.25$, $\alpha_v = 20$, and $\beta_v = 5$. Meanwhile, the sum of $f(\hat{v}_i(t)) + \phi(\hat{v}_i(t)) = 0.025(\hat{v}_i(t))^2 + 0.05 \tanh(\hat{v}_i(t))$ satisfies Assumption 5.3.1 with strong nonlinearity. The de-

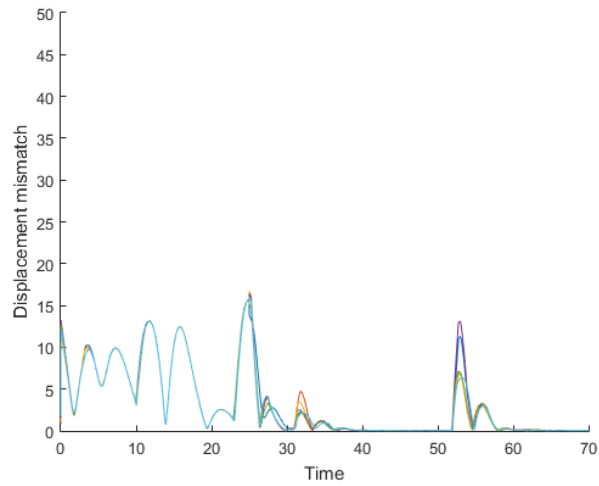
sired formation configuration is established based on Figure 5.1 with $n=6$, where both communication topologies prior to and after switching remain strongly connected as assumed in Assumption 3.1.1. The detection range of each agent is set to be 6m and the maximum velocity for each agent is 20m/s. The total simulation time is set to be $t_{end} = 70s$, and the topology switching occurs at $t = 25s$.

For the follower agents, the initial positions and velocities are randomly chosen from admissible range $[3, 8]^2 \times [0.5, 1]$ and $[-1, 1]^3$ respectively. For the initial value of the virtual leader, we set $\eta_0(0) = [0, -5, 0.5]^T$ and $v_0(0) = [0.5, 0.5, 0]^T$. For the pinning mechanism, we pinned $s_k = 4$ agents at impulsive instant with even index and $s_k = 5$ at instant with odd index, respectively. Moreover, initialize $b_{ij} = 1.5$, $c = d = 2$, $k_1 = 0.2$, $k_2 = 0.04$, $k_3 = 0.015$, $\delta = 0.04$ and the forced impulsive effect occurs every 1s. In addition, two horizontally moving cylindrical obstacles with radius of 1 and speed of $0.45m/s$ are constructed.

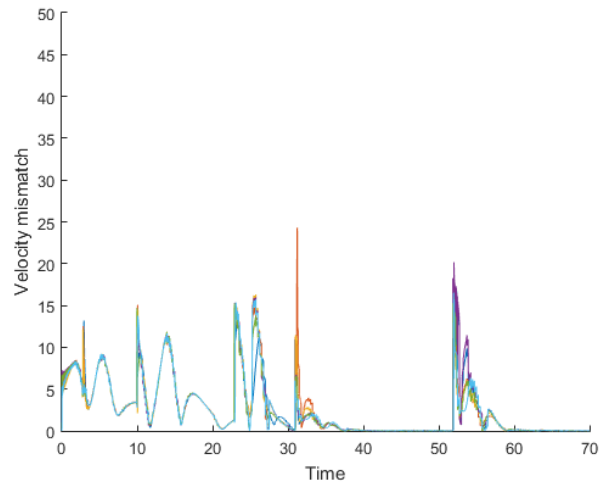
Case I: Formation stabilization via protocol (5.3) and strategy (5.6). By solving condition (5.8) using LMI Toolkit of MATLAB, we obtain feasible values of $\omega_1 = 6.431$, $\rho = 0.314$, $\rho_{max} = 0.543$ and $\bar{\theta} = 0.61$. The formation stabilization evolution, error convergence and distribution of triggered instants with distinct threshold are given in Figure 5.4 and Figure 5.5.

Case II: Formation stabilization via protocol (5.19) and strategy (5.21). Here we set the continuous time delay $r(t) = 10e^{-0.02t}$. By solving LMI condition (5.23), we obtain feasible values of $\omega_2 = 4.163$, $\omega_3 = 2.585$, $\rho = 0.357$, $\rho_{max} = 0.571$, and $M = 0.95$. Similarly, the corresponding simulations are given in Figure 5.6 and Figure 5.7.

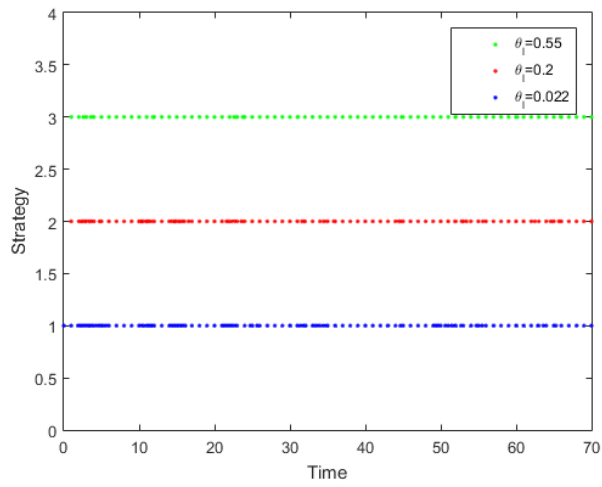
In the above simulation cases, the formation evolution trajectories demonstrate the successful generation of desired configuration while maintaining collision-free motion with environmental obstacles involved (see Figure 5.4-5.7, 5.8). Meanwhile, the displacement and velocity mismatch are all converging to zero asymptotically. Moreover, the total number of triggered instants decreases as θ_l increases (i.e, 247 instants with $\theta_l = 0.022$, 116 instants with $\theta_l = 0.2$ and 84 instants with $\theta_l = 0.55$ in Figure 5.5(c)). Hence, both of our designed algorithms are valid for formation stabilization and collision/obstacle avoidance.



(a)

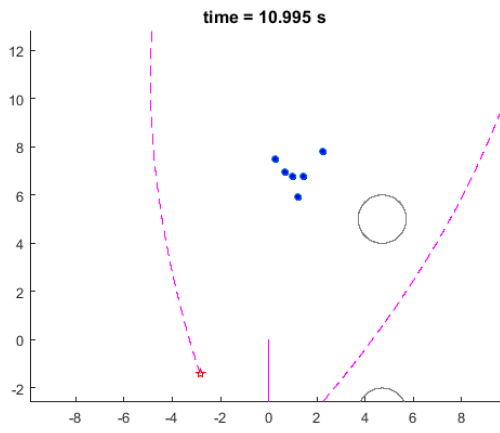


(b)

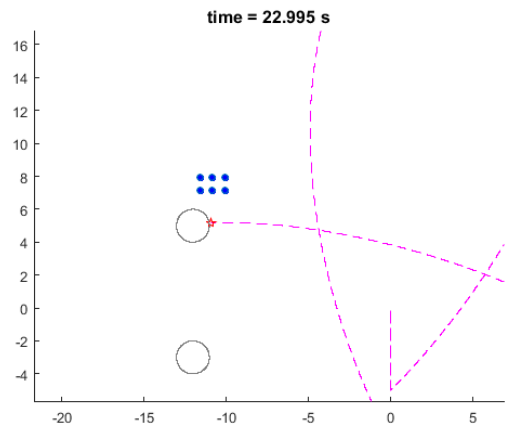


(c)

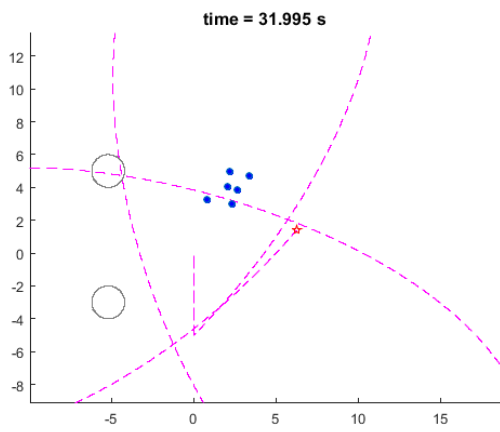
Figure 5.4: (a) Displacement mismatch (b) Velocity mismatch (c) Triggered instants of strategy (5.6) with $\theta_l=0.022, 0.2, 0.55$.



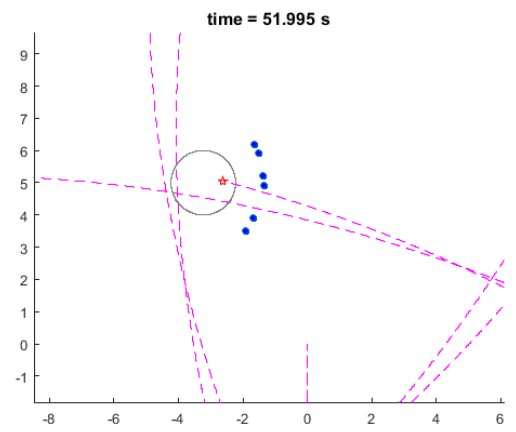
(a)



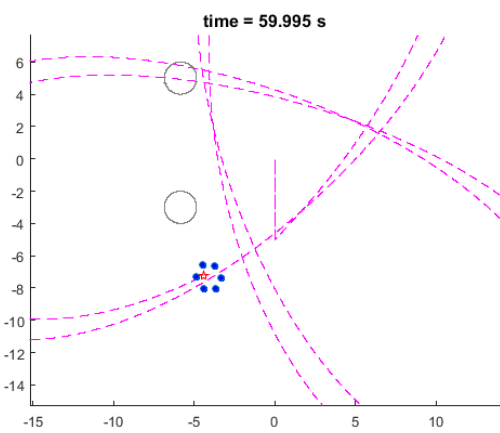
(b)



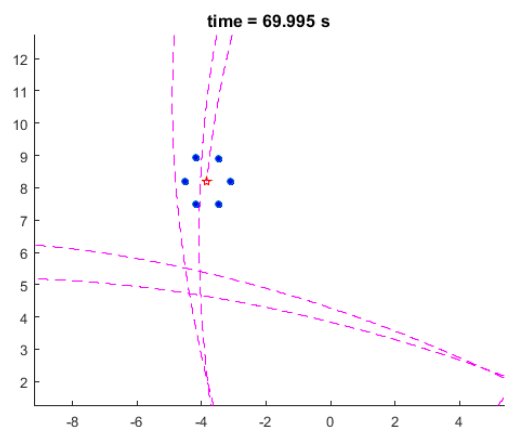
(c)



(d)

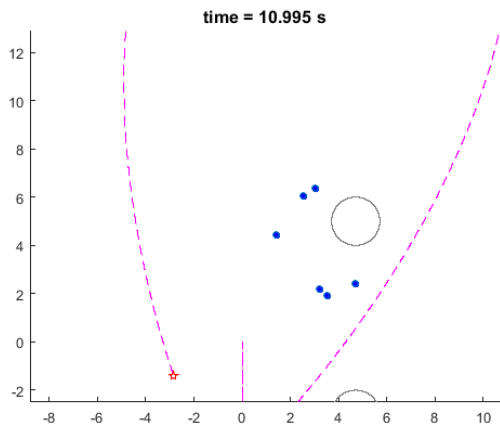


(e)

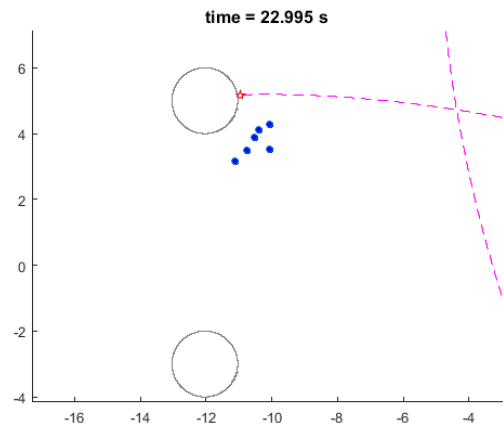


(f)

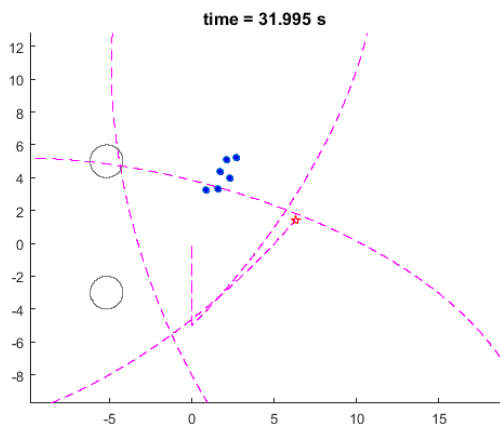
Figure 5.5: 2D formation evolution for $n=6$ agents with real-time inputs



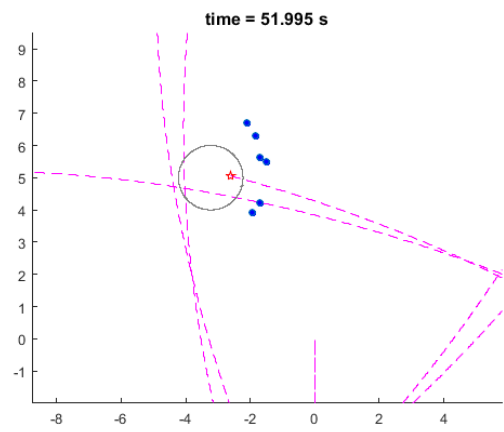
(a)



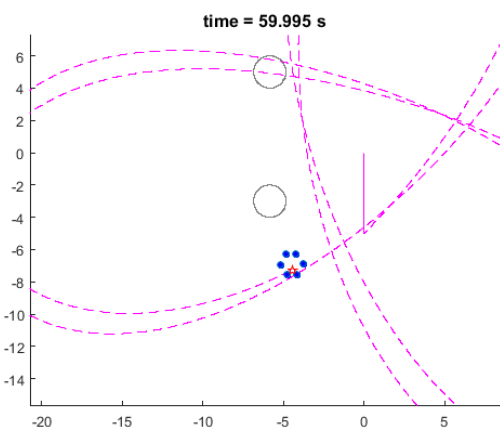
(b)



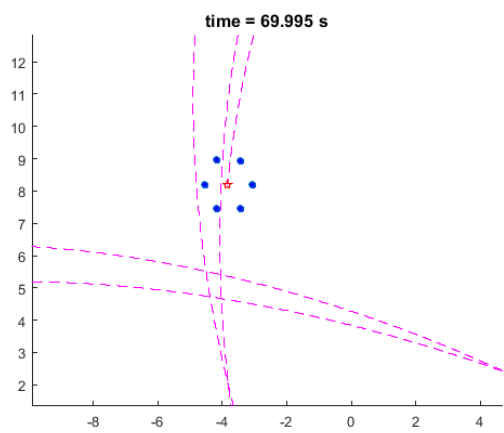
(c)



(d)



(e)



(f)

Figure 5.6: 2D formation evolution for $n=6$ agents with delayed inputs

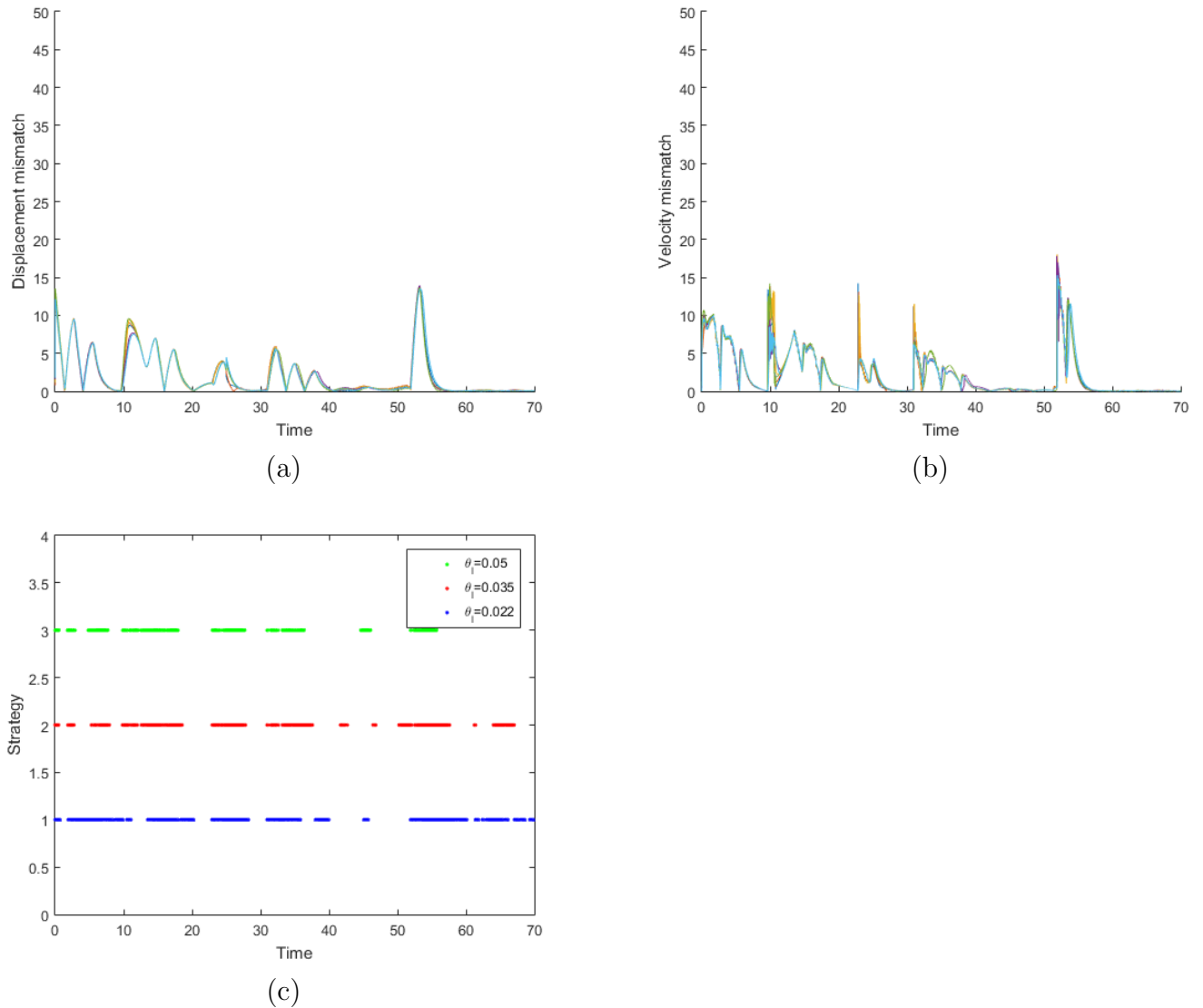


Figure 5.7: (a) Displacement mismatch (b) Velocity mismatch (c) Triggered instants of strategy (5.21) with $\theta_l=0.022, 0.035, 0.05$.

Next, we give some discussions for the control efficiency comparisons among our proposed hybrid impulsive protocols and the fully continuous protocol provided in [105]. We fix the initial states, set $\theta_l = 0.022$ and the simulation step to be 0.005s for control of

variables. Denote the control inputs $\bar{\tau}(t) = [\tau_1^T(t), \dots, \tau_n^T(t)]^T$ for $n = 6$. In particular, we rely on the following three aspects to assess the performances in more details:

1. **Number of control:** We denote $N_u(t)$ as the total number of control of $\bar{\tau}$ during simulation interval $(t_0, t]$.
2. **Cost of control:** For $Q_1 = 0.01I_{4n}$ and $Q_2 = 0.01I_{2n}$, we define the cost of control during $(t_0, t]$ as:

$$C_u(t) = \int_{t_0}^t (\bar{\xi}^T(s)Q_1\bar{\xi}(s) + \bar{\tau}^T(s)Q_2\bar{\tau}(s))ds$$

3. **Time efficiency (TE):** We calculate the time spent for reaching desired configuration after switching. Less time spent implies a higher time efficiency.

Control Method	$N_u(70)$	$C_u(70)$	TE
Continuous [105]	84000	86.03	4.22s
Case I	42471	68.59	4.64s
Case II	51060	72.61	4.47s

Table 5.1: Comparison among different types of control protocols.

Based on Table 5.1, one can see that both our schemes have a significantly lower $N_u(70)$ in comparison with the continuous scheme proposed by [105]. This also indicates a 50.88% and 60.79% usage rate respectively, which improves the efficiency and confidentiality of data transmission. Despite that our schemes experienced reasonably longer convergence time due to current settings of time delays and θ_l , the continuous scheme has the highest cost of control. Meanwhile, following the removal of the forced impulse sequence, we examine the sensitivity of varying the magnitude of θ_l or time delays on the performance of the strategy (5.21). As indicated in Table 2, increasing θ_l will results in a decrease of $N_u(t)$ and $C_u(t)$, but lower time efficiency; while reducing the size of delays lead to a value decrease of all three aspects. Therefore, our proposed schemes provide better performances.

Furthermore, we exam how different sizes of time delays in our second scheme affect the speed of convergence in order to obtain the desired configuration. Under three different sizes of time-varying delay $r(t)$, Figure 5.9 illustrates the convergence behaviours of velocity and position mismatch of agent 1 respectively. There is a clear pattern that larger $r(t)$

Strategy (5.21)	$N_u(70)$	$C_u(70)$	TE
Delay-free inputs & $\theta_l = 0.022$	48612	64.46	4.16s
Delay-free inputs & $\theta_l = 0.018$	53604	66.15	3.91s
Delayed inputs & $\theta_l = 0.022$	51060	72.61	4.47s

Table 5.2: Comparison among different parameter settings of strategy (5.21).

results in an increased volatility of trajectory and a slower convergence rate. Therefore, the size of delays affects the rate of convergence in a negative manner.

Finally, under strategy (5.21), we investigate the efficiency improvements by comparing the use of braking and gyroscopic forces with a standard artificial potential field approach illustrated in [89]. Here, in order to assess the performance of the two strategies, we utilize the distortion index function $\Omega_i(t)$ defined as follows:

$$\Omega_i(t) = \frac{\|\tau_{di}(t) + \hat{P}_{22}P_G(\hat{v}_i(t))\|}{\|\tau_{di}(t)\|} \quad (5.36)$$

where $\tau_{di}(t)$ is the sum of control components in (5.19) excluding $\hat{P}_{22}P_G(\hat{v}_i(t))$, which are in charge of the desired configuration generation. Specifically, larger values of $\Omega_i(t)$ indicate that collision/obstacle avoidance mechanisms interfere more with the primary task of maintaining the desired configuration, and $\Omega_i(t) = 1$ implies no interference. We have performed a total of 10 simulation runs, the mean value and standard deviation of $\Omega_1(t)$ and $\Omega_4(t)$ over 70 seconds are reported in Table 5.3 and Table 5.4. Contrary to the artificial potential field approach, braking and gyroscopic forces yield 10.83% and 14.16% less distortion, and they also show lower standard deviations (Std) of 2.3747 and 1.7083, respectively. As a result, the braking and gyroscopic forces are more efficient.

Distortion index	Mean	Std
Braking/gyroscopic forces	1.1763	2.3747
Artificial potential field	1.2846	2.9382

Table 5.3: Comparison of distortion index of agent 1

Distortion index	Mean	Std
Braking/gyroscopic forces	1.1309	1.7083
Artificial potential field	1.2725	2.6948

Table 5.4: Comparison of distortion index of agent 4

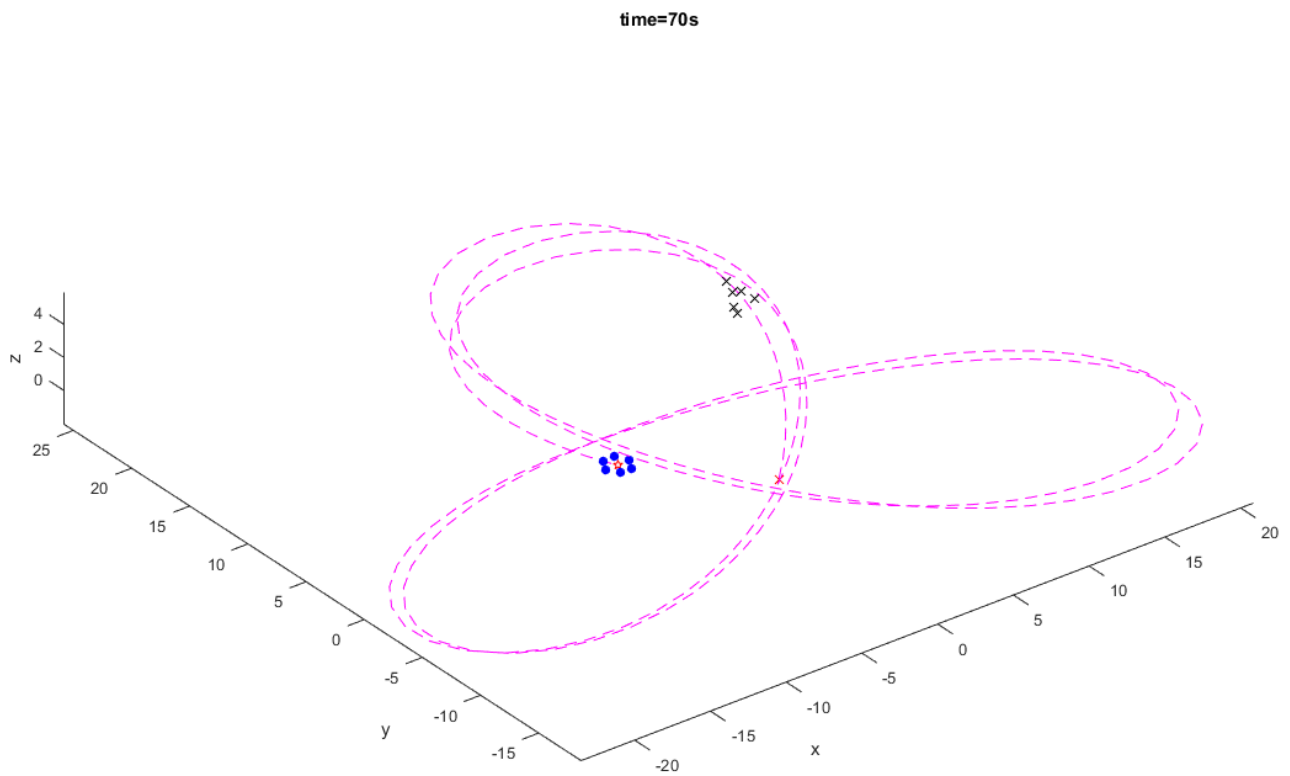
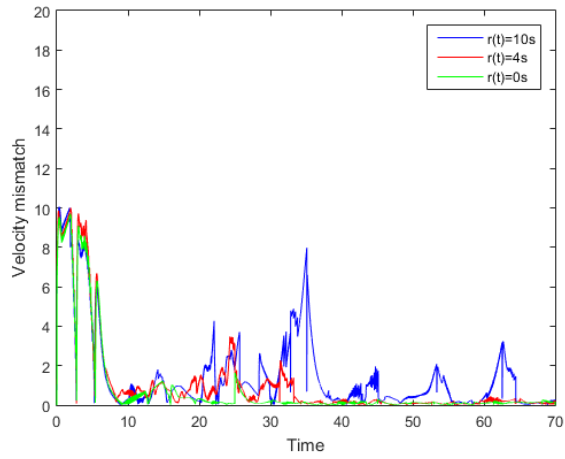
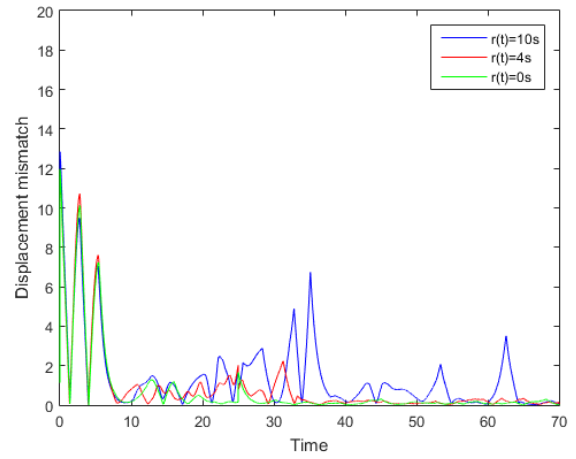


Figure 5.8: 3D formation tracking trajectories



(a)



(b)

Figure 5.9: Convergence of (a) velocity mismatch (b) displacement mismatch of agent 1 with $r(t)=0s$, $r(t)=4s$ and $r(t)=10s$.

Chapter 6

Finite-time Hybrid Impulsive Control of MASs via Intermittent Communication

This chapter focuses on developing a finite-time leader-following formation control for nonlinear MASs under the hybrid impulsive framework by utilizing aperiodic intermittent communication and delayed impulses.

6.1 Finite-time Stability

Finite-time stability (FTS) refers to a property of a dynamical system where the system's state converges to a fixed point or a bounded region within a finite time period. In other words, the system settles down to a stable state within a finite time period, rather than asymptotically over an infinite time horizon. FTS is a desirable property for controlling multi-agent systems and can be particularly important in real-time control applications, where a rapid response is often required. In the study of finite-time stability, significant progress has been made to date. By implementing aperiodically intermittent control, finite-time synchronization of delayed dynamical networks associated with strong Lyapunov condition for continuous dynamics was discussed in [106, 107, 108]; while fixed-time synchronization via generalized adaptive and quantized intermittent control was studied in [109]. In [110], fixed-time global cluster synchronization for complex dynamical networks through aperiodically intermittent control was investigated in terms of weak Lyapunov inequality

condition for continuous dynamics, namely, $\dot{V}(t) \leq -qV^r(t) + pV(t)$ with $0 < r < 1$ and tunable gains $p, q > 0$.

6.2 Intermittent Communication

During intermittent communication, the control signal is switched on and off, with periods of no control interspersed with periods of active control. Intermittent control is capable of reducing energy consumption and increasing the lifespan of the actuator or control device, as the control input is not applied continuously. Moreover, it can help to avoid saturation or instability in the system, which can occur if the control input is applied continuously at high levels. However, intermittent control can be more difficult to analyze than continuous control, as the system dynamics can be more complex and the intermittent nature of the control signal can introduce additional sources of nonlinearity. The concept of intermittent control has received considerable attention in recent years. In [111], the synchronization problem of delayed multi-agent systems through periodic intermittent impulsive control has been proposed; while [112] further studied the synchronization of delayed multi-agent systems in finite-time using periodic intermittent control with multiple switching periods. The aperiodically intermittent nonlinear stabilization of delayed stochastic complex-valued networks was investigated in [113]; while the aperiodically intermittent adaptive synchronization of delayed stochastic complex-valued networks was discussed in [114]. Moreover, the synchronization and stabilization problem of continuous dynamical systems was addressed via time-triggered and event-triggered aperiodic intermittent control respectively in [115].

6.3 Problem Formulation

Consider a class of second-order dynamical systems with total of n agents and the dynamics of each agent is modelled as follows:

$$\dot{\xi}_i(t) = A\xi_i(t) + Bf(\xi_i(t)) + u_i, \quad i = 1, 2, \dots, n \quad (6.1)$$

while the dynamics of (virtual) leader is described as:

$$\dot{\xi}_0(t) = A\xi_0(t) + Bf(\xi_0(t)) \quad (6.2)$$

where $\xi_i(t) = [p_i^T(t), v_i^T(t)]^T \in \mathbb{R}^4$, $\xi_0(t) = [p_0^T(t), v_0^T(t)] \in \mathbb{R}^4$; while $p_i, v_i, p_0, v_0 \in \mathbb{R}^2$ are bounded position/velocity states of i -th follower and leader accordingly, $p_{di} \in \mathbb{R}^2$

represents the constant desired displacement vector of agent i with respect to the virtual leader. $A = \begin{pmatrix} \mathbf{0}_{2 \times 2} & A_{12} \\ A_{21} & A_{22} \end{pmatrix}$, $B = \begin{pmatrix} B_{11} & \mathbf{0}_{2 \times 2} \\ \mathbf{0}_{2 \times 2} & B_{22} \end{pmatrix} \in \mathbb{R}^4$ are known constant gain matrices, $u_i = [u_{pi}^T, u_{vi}^T] \in \mathbb{R}^4$ is the hybrid impulsive coupled control input to be designed hereafter, $f(\xi_i(t)) : \mathbb{R}^4 \rightarrow \mathbb{R}^4$ is the nonlinear function of intrinsic dynamics. For consistency, the right continuity with $\xi_i(t) = \xi_i(t^+)$ and $\Delta \xi_i(t) = \xi_i(t^+) - \xi_i(t^-)$ are considered.

Additionally, for the sake of establishing the compact tracking error between system (6.1) and (6.2), let the tracking error $\hat{\xi}_i(t) = [\hat{p}_i^T(t), \hat{v}_i^T(t)]^T$, $\hat{p}_i(t) = p_i(t) - p_0(t) - p_{di}$, and $\hat{v}_i(t) = v_i(t) - v_0(t)$. Also, denote the compact tracking error $\bar{\xi}(t) = [\bar{p}^T(t), \bar{v}^T(t)]^T$, $\bar{p}(t) = [\hat{p}_1^T(t), \dots, \hat{p}_n^T(t)]^T$, $\bar{v}(t) = [\hat{v}_1^T(t), \dots, \hat{v}_n^T(t)]^T$, $\bar{f}(\bar{\xi}(t)) = [f^T(\bar{p}(t)), f^T(\bar{v}(t))]^T$, $\bar{u}_p = [u_{p1}^T, \dots, u_{pn}^T]^T$, $\bar{u}_v = [u_{v1}^T, \dots, u_{vn}^T]^T$ and $\bar{u} = [\bar{u}_p^T, \bar{u}_v^T]^T$. Hence, the compact error dynamics can be described directly as follows:

$$\dot{\bar{\xi}}(t) = \bar{A}\bar{\xi}(t) + \bar{B}\bar{f}(\bar{\xi}(t)) + \bar{u} \quad (6.3)$$

with $\bar{A} = \begin{pmatrix} \mathbf{0}_{2n \times 2n} & A_{12} \otimes I_n \\ A_{21} \otimes I_n & A_{22} \otimes I_n \end{pmatrix}$ and $\bar{B} = \begin{pmatrix} B_{11} \otimes I_n & \mathbf{0}_{2n \times 2n} \\ \mathbf{0}_{2n \times 2n} & B_{22} \otimes I_n \end{pmatrix}$.

Definition 6.3.1. *Local finite-time formation tracking of MASs (6.1) and (6.2) is attained if a nonempty open ball B_ν of radius ν and a constant $T > 0$ exist such that $\bar{\xi}(\mathbf{0}_{4n}) \in B_\nu$ implies $\lim_{t \rightarrow T} \|\bar{\xi}(t)\| = 0$ and $\|\bar{\xi}(t)\| = 0$ for all $t > T$.*

Definition 6.3.2. *In general, an aperiodic intermittent control $(u(t), \{t_m, s_m\})$ has the form as follows*

$$\begin{cases} 0, & t \in [s_m, t_{m+1}) \\ u(t), & t \in [t_m, s_m) \end{cases} \quad (6.4)$$

where $m \geq 0$, $u(t)$ represents the control input to be devised, t_m, s_m describe the non-overlapping starting and final time of m -th aperiodic intermittent control interval respectively, t_{m+1} is the final time of m -th control-free interval, and $s_m - t_m$ represents the m -th control width. In particular, denote

$$\begin{aligned} s_m - t_m &= \zeta_m, & \inf_m (s_m - t_m) &= \underline{\zeta}, & \sup_m (s_m - t_m) &= \bar{\zeta} \\ t_{m+1} - t_m &= \omega_m, & \inf_m (t_{m+1} - t_m) &= \underline{\omega}, & \sup_m (t_{m+1} - t_m) &= \bar{\omega}, \quad m = 0, 1, 2, \dots \end{aligned} \quad (6.5)$$

where $0 < \underline{\zeta} \leq \zeta_m \leq \bar{\zeta}$ and $0 < \underline{\omega} \leq \omega_m \leq \bar{\omega}$.

Lemma 6.3.1. [107] *For $x_1, x_2, \dots, x_N \in \mathbb{R}^n$ and $0 < q < 2$, the following inequality holds:*

$$\|x_1\|^q + \|x_2\|^q + \dots + \|x_N\|^q \geq (\|x_1\|^2 + \|x_2\|^2 + \dots + \|x_N\|^2)^{\frac{q}{2}} \quad (6.6)$$

6.4 Formation Stabilization

This section illustrates the formation stabilization via our finite-time hybrid impulsive intermittent control scheme (FTHIIC) for leader-following MASs (6.1) and (6.2). Without loss of generality, consider total of $\bar{m} \in \mathbb{N}^+$ aperiodic intermittent intervals, set $\{t_l^m, l = 1, 2, \dots, \gamma_m\}$ as the impulse sequence in the m -th intermittent control interval $[t_m, s_m)$ for $m = 0, 1, 2, \dots, \bar{m} - 1$ and $[t_m, \infty)$ for $m = \bar{m}$, which satisfies $t_m < t_1^m < t_2^m < \dots < t_{\gamma_m}^m < s_m$ and $1 \leq \gamma_L \leq \gamma_m \leq \gamma_M < \infty$. Meanwhile, we set the impulse delay $\bar{\tau}$ with $\bar{\tau} < h_1 = \inf\{t_{l+1}^m - t_l^m\}$ for $l = 0, \dots, \gamma_m - 1$.

6.4.1 FTHIIC with Stabilizing Impulses

Firstly, we analyze finite-time stability through aperiodic intermittent transmission in terms of general nonlinear impulsive systems, where the continuous part of the dynamics derives from the weak Lyapunov inequality with time-varying gains.

Theorem 6.4.1. *Suppose function $V(t) \in \nu_0$, $\phi = \bar{\xi}(s) \in \mathcal{PC}$, functions $\alpha_1, \alpha_2 \in \mathcal{K}_\infty$, $P_1(t), P_2(t) : \mathbb{R}^+ \rightarrow \mathbb{R}$, $H(t) : \mathbb{R}^+ \rightarrow \mathbb{R}$, $Q_1(t) : \mathbb{R}^+ \rightarrow \mathbb{R}^+$. If there exists some constants $\rho_1 > 0, \rho_2 \geq 0, r \in (0, 1), \mu_1, \mu_2, \mu_3 > 0, \theta \geq 0, \lambda \geq \eta > 0, \beta \in (0, 1]$, and $\rho_1 + \rho_2 < \beta$ so that the following criteria are obtained for $m = 0, 1, 2, \dots, \bar{m}, \bar{m} < \infty$ and $t \geq t_0 \geq 0$:*

$$\alpha_1(\|\bar{\xi}\|) \leq V(t, \bar{\xi}) \leq \alpha_2(\|\bar{\xi}\|) \quad (6.7)$$

$$\begin{cases} \dot{V}(t) \leq -Q_1(t)V^r(t) + P_1(t)V(t), & t \geq t_{\bar{m}}, \quad t \neq t_l^{\bar{m}} \\ V(t) \leq \rho_1^{\frac{1}{1-r}}V(t^-) + \rho_2^{\frac{1}{1-r}}V(t^- - \bar{\tau}), & t = t_l^{\bar{m}} \\ \dot{V}(t) \leq H(t)V(t), & s_m \leq t < t_{m+1}, \quad m = 0, 1, \dots, \bar{m} - 1 \\ \dot{V}(t) \leq P_2(t)V(t), & t_m \leq t < s_m, \quad t \neq t_l^m \\ V(t) \leq \rho_1^{\frac{1}{1-r}}V(t^-) + \rho_2^{\frac{1}{1-r}}V(t^- - \bar{\tau}), & t = t_l^m, \quad m = 0, 1, \dots, \bar{m} - 1 \end{cases} \quad (6.8)$$

$$\int_{t_0}^t |P_2(s)|ds \leq \mu_1(t - t_0), \quad \int_{t_0}^t |H(s)|ds \leq \mu_2(t - t_0), \quad t < t_{\bar{m}} \quad (6.9)$$

$$\int_{t_{\bar{m}}}^{\infty} |P_1(s)|ds \leq \mu_3 \quad (6.10)$$

$$\eta(t - t_0) \leq \int_{t_{\bar{m}}}^t Q_1(s)ds \leq \lambda(t - t_0) + \theta \quad (6.11)$$

$$\beta((1 - \rho_1 e^{-\mu_3(1-r)})\lambda - e^{-\mu_3(1-r)}\rho_2\eta) \geq \eta(\beta - \rho_1 - \rho_2) \quad (6.12)$$

$$t_{\gamma_{\bar{m}}}^{\bar{m}} \leq t_{\bar{m}} + \frac{\beta\gamma_{\bar{m}}^{-1}(\beta - \rho_1 - \rho_2)V^{1-r}(t_{\bar{m}})}{((1 - \rho_1 e^{-\mu_3(1-r)})\lambda - e^{-\mu_3(1-r)}\rho_2\eta)(1-r)} - \frac{(1 - \rho_1 e^{-\mu_3(1-r)})\theta + e^{-\mu_3(1-r)}\rho_2\eta\bar{\tau}}{(1 - \rho_1 e^{-\mu_3(1-r)})\lambda - e^{-\mu_3(1-r)}\rho_2\eta} \quad (6.13)$$

Then the convergence of $V(t)$ in finite time to zero solution is guaranteed for aperiodic intermittent impulse sequence $\{t_l^m, l = 1, \dots, \gamma_m\}$; while the settling time T_N is given by

$$T_N = \frac{\beta^{(\bar{m}+1)\gamma_L} e^{(\mu_3 + \mu_1 \bar{\zeta} \bar{m} + \bar{m} \mu_2 (\bar{\omega} - \bar{\zeta}))(1-r)} V^{1-r}(t_0)}{\eta(1-r)} + \bar{m}(\bar{\omega} + \bar{\zeta}) \quad (6.14)$$

Proof. Multiplying $V^{-r}(t)$ to both sides of (6.8) yields,

$$\begin{cases} \left\{ \begin{array}{l} V^{-r}(t)\dot{V}(t) \leq P_1(t)V^{1-r}(t) - Q_1(t), \quad t \geq t_{\bar{m}}, \quad t \neq t_l^{\bar{m}} \\ V^{1-r}(t) \leq (\rho_1^{\frac{1}{1-r}}V(t^-) + \rho_2^{\frac{1}{1-r}}V(t^- - \bar{\tau}))^{1-r} \leq \rho_1 V^{1-r}(t^-) + \rho_2 V^{1-r}(t^- - \bar{\tau}), \quad t = t_l^{\bar{m}} \end{array} \right. \\ V^{-r}(t)\dot{V}(t) \leq H(t)V^{1-r}(t), \quad t \in [s_m, t_{m+1}), \quad m = 0, 1, \dots, \bar{m} - 1 \\ \left\{ \begin{array}{l} V^{-r}(t)\dot{V}(t) \leq P_2(t)V^{1-r}(t), \quad t \in [t_m, s_m), \quad t \neq t_l^m, \quad m = 0, 1, \dots, \bar{m} - 1 \\ V^{1-r}(t) \leq (\rho_1^{\frac{1}{1-r}}V(t^-) + \rho_2^{\frac{1}{1-r}}V(t^- - \bar{\tau}))^{1-r} \leq \rho_1 V^{1-r}(t^-) + \rho_2 V^{1-r}(t^- - \bar{\tau}), \quad t = t_l^m \end{array} \right. \end{cases} \quad (6.15)$$

Let $M(t) = V^{1-r}(t)$, then (6.15) can be rewritten as:

$$\begin{cases} \left\{ \begin{array}{l} \dot{M}(t) \leq (1-r)|P_1(t)|M(t) + (r-1)Q_1(t), \quad t \geq t_{\bar{m}}, \quad t \neq t_l^{\bar{m}} \\ M(t) \leq \rho_1 M(t^-) + \rho_2 M(t^- - \bar{\tau}), \quad t = t_l^{\bar{m}} \end{array} \right. \\ \dot{M}(t) \leq (1-r)|H(t)|M(t), \quad t \in [s_m, t_{m+1}), \quad m = 0, 1, \dots, \bar{m} - 1 \\ \left\{ \begin{array}{l} \dot{M}(t) \leq (1-r)|P_2(t)|M(t), \quad t \in [t_m, s_m), \quad t \neq t_l^m \\ M(t) \leq \rho_1 M(t^-) + \rho_2 M(t^- - \bar{\tau}), \quad t = t_l^m, \quad m = 0, 1, \dots, \bar{m} - 1 \end{array} \right. \end{cases} \quad (6.16)$$

Then based on (6.10), (6.11), and (6.16) that, for $t \geq t_{\bar{m}}$ it yields

$$M(t) \leq e^{(1-r)\int_{t_{\bar{m}}}^t |P_1(s)| ds} M(t_{\bar{m}}) - (1-r) \int_{t_{\bar{m}}}^t Q_1(s) e^{(1-r)\int_s^t |P_1(z)| dz} ds, \quad t \in [t_{\bar{m}}, t_1^{\bar{m}}) \quad (6.17)$$

Since $\rho_1 + \rho_2 \in (0, 1)$ and $h_1 > \bar{\tau} > 0$, based on (6.13) one has

$$\begin{aligned}
M(t) &\leq e^{(1-r) \int_{t_1^{\bar{m}}}^t |P_1(s)| ds} M(t_1^{\bar{m}}) - (1-r) \int_{t_1^{\bar{m}}}^t Q_1(s) e^{\int_s^t |P_1(z)| dz} e^{(1-r)s} ds \\
&\leq \rho_1 e^{(1-r) \int_{t_1^{\bar{m}}}^t |P_1(s)| ds} M(t_1^{\bar{m}-}) + \rho_2 e^{(1-r) \int_{t_1^{\bar{m}}}^t |P_1(s)| ds} M(t_1^{\bar{m}-} - \bar{\tau}) \\
&\quad + (r-1) \int_{t_1^{\bar{m}}}^{t_{\bar{m}}} Q_1(s) e^{(1-r) \int_s^t |P_1(z)| dz} ds + (r-1) \int_{t_{\bar{m}}}^t Q_1(s) e^{(1-r) \int_s^t |P_1(z)| dz} ds \\
&\leq \rho_1 e^{(1-r) \int_{t_{\bar{m}}}^t |P_1(s)| ds} M(t_{\bar{m}}) + \rho_2 e^{(1-r) (\int_{t_{\bar{m}}}^{t_1^{\bar{m}-\bar{\tau}}} |P_1(s)| ds + \int_{t_1^{\bar{m}}}^t |P_1(s)| ds)} M(t_{\bar{m}}) \\
&\quad + (r-1) \int_{t_1^{\bar{m}}}^{t_{\bar{m}}} Q_1(s) e^{(1-r) \int_s^t |P_1(z)| dz} ds \\
&\quad - \rho_1 (r-1) e^{(1-r) \int_{t_1^{\bar{m}}}^t |P_1(s)| ds} \int_{t_1^{\bar{m}}}^{t_{\bar{m}}} Q_1(s) e^{(1-r) \int_s^{t_1^{\bar{m}}} |P_1(z)| dz} ds \\
&\quad - \rho_2 (r-1) e^{(1-r) \int_{t_1^{\bar{m}}}^t |P_1(s)| ds} \int_{t_1^{\bar{m}-\bar{\tau}}}^{t_{\bar{m}}} Q_1(s) e^{(1-r) \int_s^{t_1^{\bar{m}-\bar{\tau}}} |P_1(z)| dz} ds \\
&\quad + (r-1) \int_{t_{\bar{m}}}^t Q_1(s) e^{(1-r) \int_s^t |P_1(z)| dz} ds \\
&\leq (\rho_1 + \rho_2) e^{(1-r) \int_{t_{\bar{m}}}^t |P_1(s)| ds} M(t_{\bar{m}}) + (r-1) (1 - \rho_1 e^{-\mu_3(1-r)}) e^{(1-r) \int_{t_{\bar{m}}}^t |P_1(s)| ds} \int_{t_1^{\bar{m}}}^{t_{\bar{m}}} Q_1(s) ds \\
&\quad - \rho_2 (r-1) e^{(1-r) \int_{t_1^{\bar{m}}}^t |P_1(s)| ds} \int_{t_1^{\bar{m}-\bar{\tau}}}^{t_{\bar{m}}} Q_1(s) ds + (r-1) \int_{t_{\bar{m}}}^t Q_1(s) e^{(1-r) \int_s^t |P_1(z)| dz} ds \\
&\leq e^{(1-r) \int_{t_{\bar{m}}}^t |P_1(s)| ds} ((\rho_1 + \rho_2) M(t_{\bar{m}}) + (1-r) (1 - \rho_1 e^{-\mu_3(1-r)}) (\lambda(t_1^{\bar{m}} - t_{\bar{m}}) + \theta) \\
&\quad - e^{-\mu_3(1-r)} \rho_2 (1-r) \eta (t_1^{\bar{m}} - t_{\bar{m}}) + e^{-\mu_3(1-r)} \rho_2 \eta \bar{\tau} (1-r)) \\
&\quad + (r-1) \int_{t_{\bar{m}}}^t Q_1(s) e^{(1-r) \int_s^t |P_1(z)| dz} ds \\
&= e^{(1-r) \int_{t_{\bar{m}}}^t |P_1(s)| ds} ((\rho_1 + \rho_2) M(t_{\bar{m}}) + (1-r) [(1 - \rho_1 e^{-\mu_3(1-r)}) \lambda - e^{-\mu_3(1-r)} \rho_2 \eta] (t_1^{\bar{m}} - t_{\bar{m}}) \\
&\quad + ((1 - \rho_1 e^{-\mu_3(1-r)}) \theta + e^{-\mu_3(1-r)} \rho_2 \eta \bar{\tau})) - (1-r) \int_{t_{\bar{m}}}^t Q_1(s) e^{(1-r) \int_s^t |P_1(z)| dz} ds \\
&\leq \beta e^{(1-r) \int_{t_{\bar{m}}}^t |P_1(s)| ds} M(t_{\bar{m}}) - (1-r) \int_{t_{\bar{m}}}^t Q_1(s) e^{(1-r) \int_s^t |P_1(z)| dz} ds, \quad t \in [t_1^{\bar{m}}, t_2^{\bar{m}})
\end{aligned} \tag{6.18}$$

and

$$M(t) \leq \beta^2 e^{(1-r) \int_{t_{\bar{m}}}^t |P_1(s)| ds} M(t_{\bar{m}}) + (r-1) \int_{t_{\bar{m}}}^t Q_1(s) e^{(1-r) \int_s^t |P_1(z)| dz} ds, \quad t \in [t_{\bar{m}}, t_3^{\bar{m}}) \quad (6.19)$$

Followed by mathematical induction recursively and $\gamma_L \leq \gamma_{\bar{m}}$ we can deduce that

$$\begin{aligned} M(t) &\leq \beta^{\gamma_L} e^{(1-r) \int_{t_{\bar{m}}}^t |P_1(s)| ds} M(t_{\bar{m}}) + (r-1) \int_{t_{\bar{m}}}^t Q_1(s) e^{(1-r) \int_s^t |P_1(z)| dz} ds \\ &\leq \beta^{\gamma_L} e^{\mu_3(1-r)} M(t_{\bar{m}}) + \eta(r-1)(t - t_{\bar{m}}), \quad t \in [t_{\gamma_{\bar{m}}}, \infty) \end{aligned} \quad (6.20)$$

While for $t \in [s_{m-1}, t_m)$ for all $m = 1, 2, \dots, \bar{m}$, it directly yields:

$$M(t) \leq e^{(1-r) \int_{s_{m-1}}^t |H(s)| ds} M(s_{m-1}) \leq e^{\mu_2(\omega_{m-1} - \zeta_{m-1})(1-r)} M(s_{m-1}) \quad (6.21)$$

Then for $t \in [t_{m-1}, s_{m-1})$ for all $m = 1, 2, \dots, \bar{m}$, similar to (6.18), we have

$$\begin{aligned} M(t) &\leq e^{(1-r) \int_{t_1^{m-1}}^t |P_2(s)| ds} M(t_1^{m-1}) \\ &\leq \rho_1 e^{(1-r) \int_{t_1^{m-1}}^t |P_2(s)| ds} M(t_1^{(m-1)-}) + \rho_2 e^{(1-r) \int_{t_1^m}^t |P_2(s)| ds} M(t_1^{(m-1)-} - \bar{\tau}) \\ &\leq \rho_1 e^{(1-r) \int_{t_{m-1}}^t |P_2(s)| ds} M(t_{m-1}) + \rho_2 e^{(1-r)(\int_{t_{m-1}}^{t_1^{m-1}} |P_2(s)| ds + \int_{t_1^{m-1}}^t |P_2(s)| ds)} M(t_{m-1}) \\ &\leq (\rho_1 + \rho_2) e^{(1-r) \int_{t_{m-1}}^t |P_2(s)| ds} M(t_{m-1}) \\ &\leq \beta e^{(1-r) \int_{t_{m-1}}^t |P_2(s)| ds} M(t_{m-1}), \quad t \in [t_1^{m-1}, t_2^{m-1}) \end{aligned} \quad (6.22)$$

and again by mathematical induction it gives:

$$\begin{aligned} M(t) &\leq \beta^{\gamma_L} e^{(1-r) \int_{t_{m-1}}^t |P_2(s)| ds} M(t_{m-1}) \\ &\leq \beta^{\gamma_L} e^{\mu_1 \zeta_m (1-r)} M(t_{m-1}), \quad t \in [t_{\gamma_{m-1}}^{m-1}, s_{m-1}) \end{aligned} \quad (6.23)$$

Combine (6.20), (6.21) and (6.23), since $\mu_1, \mu_2, \eta > 0$ and $r \in (0, 1)$, then we have

$$\begin{aligned} M(t) &\leq \beta^{(\bar{m}+1)\gamma_L} e^{(\mu_3 + \sum_{q=0}^{\bar{m}-1} \mu_1 \zeta_q + \sum_{q=0}^{\bar{m}-1} \mu_2(\omega_q - \zeta_q))(1-r)} M(t_0) - \eta(1-r)(t - t_{\bar{m}}) \\ &= \beta^{(\bar{m}+1)\gamma_L} e^{(\mu_3 + \sum_{q=0}^{\bar{m}-1} \mu_1 \zeta_q + \sum_{q=0}^{\bar{m}-1} \mu_2(\omega_q - \zeta_q))(1-r)} M(t_0) \\ &\quad - \eta(1-r)[(t - t_{\bar{m}}) + (t_{\bar{m}} - t_{\bar{m}-1}) + \dots + (t_1 - t_0)] \\ &\quad + \eta(1-r)[(t_{\bar{m}} - t_{\bar{m}-1}) + \dots + (t_1 - t_0)] \\ &\leq \beta^{(\bar{m}+1)\gamma_L} e^{(\mu_3 + \sum_{q=0}^{\bar{m}-1} \mu_1 \zeta_q + \sum_{q=0}^{\bar{m}-1} \mu_2(\omega_q - \zeta_q))(1-r)} M(t_0) \\ &\quad - \eta(1-r)[(t - t_{\bar{m}}) + (t_{\bar{m}} - t_{\bar{m}-1}) + \dots + (t_1 - t_0)] + \eta \bar{m}(\bar{\omega} + \bar{\zeta})(1-r) \\ &\leq \beta^{(\bar{m}+1)\gamma_L} e^{(\mu_3 + \mu_1 \bar{\zeta} \bar{m} + \bar{m} \mu_2(\bar{\omega} - \bar{\zeta}))(1-r)} M(t_0) - \eta(1-r)(t - t_0) + \eta \bar{m}(\bar{\omega} + \bar{\zeta})(1-r), \quad t \geq t_{\gamma_{\bar{m}}}^{\bar{m}} \end{aligned} \quad (6.24)$$

According to last inequality of (6.24), a finite T_N exists so that $M(t) = 0$ holds; while

$$M(t) \leq e^{(\mu_3 + \mu_1 \bar{\zeta} \bar{m} + \bar{m} \mu_2 (\bar{\omega} - \bar{\zeta})) (1-r)} M(t_0), \quad t \geq t_{\gamma \bar{m}} \quad (6.25)$$

and (6.7) yields

$$\alpha_1^{1-r} (\|\bar{\xi}(t)\|) \leq e^{(\mu_3 + \mu_1 \bar{\zeta} \bar{m} + \bar{m} \mu_2 (\bar{\omega} - \bar{\zeta})) (1-r)} (\alpha_2 (\|\bar{\xi}(0)\|))^{1-r} \quad (6.26)$$

Thus, we have $M(t) = 0$ holds for all $t \geq t_0 + T_N$ (i.e., $V(t)$ is convergent to zero in finite time), where the corresponding settling time T_N is calculated as:

$$T_N = \frac{\beta^{(\bar{m}+1)\gamma_L} e^{(\mu_3 + \mu_1 \bar{\zeta} \bar{m} + \bar{m} \mu_2 (\bar{\omega} - \bar{\zeta})) (1-r)} V^{1-r}(t_0)}{\eta(1-r)} + \bar{m}(\bar{\omega} + \bar{\zeta}) \quad (6.27)$$

while $T_N \geq t_{\gamma \bar{m}}^{\bar{m}}$ holds since it follows from (6.12) and (6.13) that

$$\begin{aligned} t_{\gamma \bar{m}}^{\bar{m}} &\leq t_{\bar{m}} + \frac{\beta^{\gamma_L - 1} (\beta - \rho_1 - \rho_2) V^{1-r}(t_{\bar{m}})}{((1 - \rho_1 e^{-\mu_3(1-r)})\lambda - e^{-\mu_3(1-r)}\rho_2\eta)(1-r)} - \frac{(1 - \rho_1 e^{-\mu_3(1-r)})\theta + e^{-\mu_3(1-r)}\rho_2\eta\bar{\tau}}{(1 - \rho_1 e^{-\mu_3(1-r)})\lambda - e^{-\mu_3(1-r)}\rho_2\eta} \\ &\leq t_{\bar{m}} + \frac{\beta^{\gamma_L} e^{\mu_3(1-r)} V^{1-r}(t_{\bar{m}})}{\eta(1-r)} \leq T_N \end{aligned} \quad (6.28)$$

Therefore, the settling time T_N always occurs on the interval $[t_{\gamma \bar{m}}^{\bar{m}}, \infty)$. □

Next, we investigate whether the finite-time stability results presented in Theorem 6.4.1 can be adapted into our formation tracking stabilization. In particular, we construct the formation tracking control components via aperiodic intermittent transmission for $i = 1, 2, \dots, n$ as follows:

$$\begin{aligned} u_{pi}(t) &= \begin{cases} -k_3 g(t) \hat{p}_i(t), & t \geq t_{\bar{m}} \\ \mathbf{0}_2, & t \in [s_m, t_{m+1}) \\ \mathbf{0}_2, & t \in [t_m, s_m), \quad m = 0, 1, \dots, \bar{m} - 1 \end{cases} \\ u_{vi}(t) &= \begin{cases} -A_{21} p_{di}^T + k_1 P_C(\hat{p}_i(t), \hat{v}_i(t)) + k_2 P_D(\hat{p}_i(t), \hat{v}_i(t)) + k_2 P_E(\hat{p}_i(t), \hat{v}_i(t)) - k_3 g(t) \hat{v}_i(t) \\ t \geq t_{\bar{m}} \\ \mathbf{0}_2, & t \in [s_m, t_{m+1}) \\ -A_{21} p_{di}^T + k_1 P_C(\hat{p}_i(t), \hat{v}_i(t)) + k_2 P_D(\hat{p}_i(t - \bar{\tau}), \hat{v}_i(t - \bar{\tau})) + k_2 P_E(\hat{p}_i(t), \hat{v}_i(t)), \\ t \in [t_m, s_m), \quad m = 0, 1, \dots, \bar{m} - 1 \end{cases} \end{aligned} \quad (6.29)$$

then our compact controller for finite-time stabilization is designed as

$$\bar{u}(t) = [u_{p_i}^T(t), u_{v_i}^T(t)]^T \otimes \mathbf{1}_n + k_3 \bar{u}_F(t) \quad (6.30)$$

where

$$\begin{aligned} P_C(\hat{p}_i(t), \hat{v}_i(t)) &= - \sum_{j \in N_i^1} b_{ij}(\hat{p}_i(t) - \hat{p}_j(t)) - \sum_{j \in N_i^1} b_{ij}(\hat{v}_i(t) - \hat{v}_j(t)) \\ P_D(\hat{p}_i(t), \hat{v}_i(t)) &= - \sum_{l=1}^{\infty} \sum_{j \in N_i} b_{ij}(\hat{p}_i(t) - \hat{p}_j(t)) \delta(t - t_l^m) \\ &\quad - \sum_{l=1}^{\infty} \sum_{j \in N_i} b_{ij}(\hat{v}_i(t) - \hat{v}_j(t)) \delta(t - t_l^m) \\ P_E(\hat{p}_i(t), \hat{v}_i(t)) &= - \sum_{l=1}^{\infty} c \hat{p}_i(t) \delta(t - t_l^m) - \sum_{l=1}^{\infty} c \hat{v}_i(t) \delta(t - t_l^m) \\ \bar{u}_F(t) &= \begin{cases} -\bar{d}(t) \frac{[\lambda_{max}(P)]^{q_2}}{\lambda_{min}(P)} |\bar{\xi}(t)|^{q_1} \text{sign}(\bar{\xi}(t)), & t \geq t_{\bar{m}} \\ \mathbf{0}_{4n}, & t < t_{\bar{m}} \end{cases} \end{aligned} \quad (6.31)$$

where k_1, k_2, k_3 are positive gains, $0 \leq q_1 < 1$, $q_2 = \frac{1+q_1}{2}$, P is a positive definite matrix, $\delta(\cdot)$ represents the Dirac function, $N_i^1 \subset N_i$ describes the neighbor set with respect to hybrid topology within non-impulse interval. b_{ij} acts as coupling strength, $c > 0$ represents impulsive tracking gain, $\bar{d}(t), g(t) > 0$ is the continuous time-varying tunable gains, $\text{sign}(\cdot)$ denotes the signum function and $|x|^\mu = \sum_{i=1}^n |x_i(t)|^\mu$.

Remark 6.4.1. *Based on Assumption 3.1.1, Figure 6.1 illustrates the overall topology of transmission via our hybrid impulsive control protocol (6.29) for $t \geq t_{\bar{m}}$. Notice that the information transmission (i.e., red solid lines) topology contains a spanning tree with respect to control component $u_{p_i}(t)$, where leader agent 0 acts as a root node. Meanwhile, the topological structure (i.e., blue solid lines) during non-impulse intervals with respect to control component $u_{v_i}(t)$ also contains a spanning tree, and the strongly connected and balanced transmission topology (i.e., blue dashes) will be restored at each impulsive instant.*

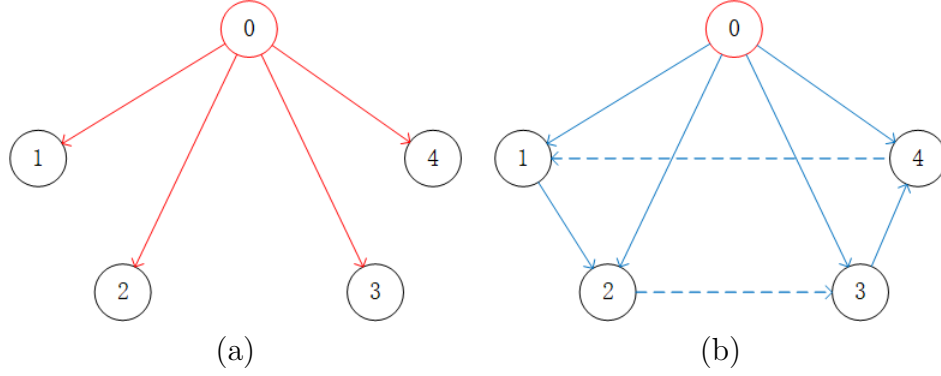


Figure 6.1: (a) Communication topology structure with respect to $u_{pi}(t)$ (b) Communication topology structure with respect to $u_{vi}(t)$

Then rewriting the compact error dynamics of (6.1) and (6.2) with aperiodic intermittent communications as:

$$\dot{\bar{\xi}}(t) = \bar{A}\bar{\xi}(t) + \bar{B}\bar{f}(\bar{\xi}(t)), \quad t \in [s_m, t_{m+1}) \quad (6.32)$$

and

$$\begin{cases} \dot{\bar{\xi}}(t) = \bar{A}\bar{\xi}(t) + \bar{B}\bar{f}(\bar{\xi}(t)) + \bar{E}_1\bar{\xi}(t), & t \neq t_l^m, \quad t < t_{\bar{m}}, \quad t \in [t_m, s_m) \\ \dot{\bar{\xi}}(t) = \bar{A}\bar{\xi}(t) + \bar{B}\bar{f}(\bar{\xi}(t)) + \bar{E}_1\bar{\xi}(t) - g(t)\bar{\xi}(t) - k_3\bar{d}(t)\frac{(\lambda_{\max}(P))^{q_2}}{\lambda_{\min}(P)}|\bar{\xi}(t)|^{q_1}\text{sign}(\bar{\xi}(t)) \\ \quad t \neq t_l^m, \quad t \geq t_{\bar{m}} \\ \Delta\bar{v}(t) = -k_2L\bar{p}(t - \bar{\tau}) - k_2L\bar{v}(t - \bar{\tau}) - k_2c\bar{p}(t) - k_2c\bar{v}(t), & t = t_l^m, \quad t < t_{\bar{m}}, \quad t \in [t_m, s_m) \\ \Delta\bar{v}(t) = -k_2L\bar{p}(t) - k_2L\bar{v}(t) - k_2c\bar{p}(t) - k_2c\bar{v}(t), & t = t_l^m, \quad t \geq t_{\bar{m}} \end{cases} \quad (6.33)$$

where $\bar{E}_1 = \begin{pmatrix} \mathbf{0}_{2n \times 2n} & \mathbf{0}_{2n \times 2n} \\ -k_1L' & -k_1L' \end{pmatrix}$, and denote L' as the Laplacian matrix during impulse-free interval. In addition, denote $\bar{E}_2 = \begin{pmatrix} I_{2n} & \mathbf{0}_{2n \times 2n} \\ -k_2(L + cI_{2n}) & I_{2n} - k_2(L + cI_{2n}) \end{pmatrix}$, $\bar{E}_3 = \begin{pmatrix} I_{2n} & \mathbf{0}_{2n \times 2n} \\ -k_2cI_{2n} & I_{2n} - k_2cI_{2n} \end{pmatrix}$ and $\bar{E}_4 = \begin{pmatrix} \mathbf{0}_{2n \times 2n} & \mathbf{0}_{2n \times 2n} \\ -k_2L & -k_2L \end{pmatrix}$ for the following use.

Theorem 6.4.2. Consider the leader-follower MASs (6.1)-(6.2) that are equipped with hybrid impulsive control protocol (6.29) via aperiodic intermittent communication. Suppose Assumption 3.1.1, Assumption 5.3.1 and all the hypotheses in Theorem 6.4.1 hold with $\rho_1 = \pi_3^{1-q_2}$, $\rho_2 = \pi_4^{1-q_2}$, $\mu_1 = \eta_2$, $\mu_2 = \eta_1$, $0 \leq q_1 < 1$, $q_2 = \frac{1+q_1}{2}$, $P_1(t) = \eta_3(t)$, $P_2(t) = \eta_1$, $H(t) = \eta_2$ and $Q_1(t) = 2^{q_2} k_3 \bar{d}(t)$; while $P \in \mathbb{R}^{4n \times 4n}$ is positive definite, $\bar{F}(t)$ is bounded with $\|\bar{F}(t)\| \leq f_{max}$, and $\bar{R}(t) = \bar{R}(t, \bar{\xi})$. If there exists constants $\varepsilon_1, \varepsilon_2 > 0$, and $Q \in \mathbb{R}^{4n \times 4n} > 0$ so that the following criteria are satisfied:

$$P\bar{B}\bar{F}(t) + \bar{F}^T(t)\bar{B}^T P \leq Q \quad (6.34)$$

$$\ln(\pi_3 + \pi_4) < 0 \quad (6.35)$$

with $\eta_1 = \lambda_{max}(P)^{-1} \|P\bar{A} + \bar{A}^T P + Q\| + 2\bar{s}\lambda_{max}(P\bar{B}P^{-1})$, $\eta_2 = \lambda_{max}((P\bar{A} + \bar{A}^T P + Q + 2\bar{s}I_{4n}P\bar{B} + P\bar{E}_1 + \bar{E}_1^T P)P^{-1})$, $\eta_3(t) \geq \eta_2 - 2g(t)$, $\pi_0 = \lambda_{max}(\bar{E}_2^T P\bar{E}_2 P^{-1})$, $\pi_1 = \lambda_{max}((\bar{E}_3 + \bar{E}_4)^T P(\bar{E}_3 + \bar{E}_4)P^{-1})$, $\pi_2 = 2\lambda_{max}(P)\bar{r}^2 \|\bar{E}_4\|^2 \kappa \lambda_{max}(P^{-1})$, $\pi_3 = \max\{\pi_0, \pi_1(1 + \varepsilon_2) + \pi_2(1 + \varepsilon_2^{-1})\}$, $\pi_4 = 0$, $\kappa = (1 + \varepsilon_1)\|\bar{A} + \bar{E}_1\|^2 + (1 + \varepsilon_1^{-1})\|\bar{B}\|^2(f_{max} + \bar{s})^2$ and $\delta = \sup\{r > 0 : s(r) \leq \bar{s}\} < \infty$ for a given constant $\bar{s} > 0$. Then the local formation tracking is achieved with $\|\bar{\xi}(0)\| \leq \nu$ in finite time T_N given by

$$T_N = \frac{\beta^{(\bar{m}+1)\gamma_L} e^{(\mu_3 + \eta_2 \bar{\zeta} \bar{m} + \bar{m} \eta_1 (\bar{\omega} - \bar{\zeta})) (1 - q_2)} H_1^{1 - q_2}(0)}{\eta(1 - q_2)} + \bar{m}(\bar{\omega} + \bar{\zeta}) \quad (6.36)$$

Proof. To begin with, our Lyapunov function is chosen as follows:

$$H_1(t) = \frac{1}{2} \bar{\xi}^T(t) P \bar{\xi}(t) \quad (6.37)$$

where (6.7) is obtained with $\alpha_1(\|\bar{\xi}\|) = \frac{1}{2} \lambda_{min}(P) \|\bar{\xi}\|^2$, $\alpha_2(\|\bar{\xi}\|) = \frac{1}{2} \lambda_{max}(P) \|\bar{\xi}\|^2$. Then based on Assumption 5.3.1, (6.32), (6.33) and (6.8), we can take the time derivative of H_1 with $\|\bar{\xi}(t)\| \leq \delta$. As $t \in [s_m, t_{m+1})$, one has

$$\begin{aligned} \dot{H}_1(t) &\leq \frac{1}{2} \bar{\xi}^T(t) (P\bar{A} + \bar{A}^T P) \bar{\xi}(t) + \frac{1}{2} \bar{\xi}^T(t) (P\bar{B}\bar{F}(t) + \bar{F}^T(t)\bar{B}^T P) \bar{\xi}(t) \\ &\quad + \frac{1}{2} (\bar{\xi}^T(t) P\bar{B}\bar{R}(t) + \bar{R}^T(t)\bar{B}^T P \bar{\xi}(t)) \\ &\leq \frac{1}{2} \bar{\xi}^T(t) (P\bar{A} + \bar{A}^T P + Q) \bar{\xi}(t) + s(r) \lambda_{max}(P\bar{B}P^{-1}) \bar{\xi}^T(t) P \bar{\xi}(t) \\ &\leq \frac{1}{2} \|P\bar{A} + \bar{A}^T P + Q\| \lambda_{max}(P^{-1}) \bar{\xi}^T(t) P \bar{\xi}(t) + s(r) \lambda_{max}(P\bar{B}P^{-1}) \bar{\xi}^T(t) P \bar{\xi}(t) \\ &\leq \left[\frac{1}{2} \|P\bar{A} + \bar{A}^T P + Q\| \lambda_{max}(P^{-1}) + \bar{s} \lambda_{max}(P\bar{B}P^{-1}) \right] \bar{\xi}^T(t) P \bar{\xi}(t) \\ &\leq \eta_1 H_1(t) \end{aligned} \quad (6.38)$$

Meanwhile, Lemma 6.3.1 implies

$$\begin{aligned} [\lambda_{max}(P)]^{q_2} \bar{\xi}^T(t) |\bar{\xi}(t)|^{q_1} \text{sign}(\bar{\xi}(t)) &\geq [\lambda_{max}(P)]^{q_2} (\bar{\xi}^T(t) \bar{\xi}(t))^{\frac{1+q_1}{2}} \\ &= [\lambda_{max}(P)]^{q_2} (\bar{\xi}^T(t) \bar{\xi}(t))^{q_2} \geq (\bar{\xi}^T(t) P \bar{\xi}(t))^{q_2} \end{aligned} \quad (6.39)$$

Hence, when $t \geq t_{\bar{m}}$ and $t \neq t_l^{\bar{m}}$, we have

$$\begin{aligned} \dot{H}_1(t) &\leq \frac{1}{2} \bar{\xi}^T(t) (P\bar{A} + \bar{A}^T P) \bar{\xi}(t) + \frac{1}{2} \bar{\xi}^T(t) (P\bar{B}\bar{F}(t) + \bar{F}^T(t) \bar{B}^T P) \bar{\xi}(t) + \frac{1}{2} \bar{\xi}^T(t) (P\bar{E}_1 + \bar{E}_1^T P) \bar{\xi}(t) \\ &\quad - \bar{\xi}^T(t) g(t) I_{4n} P \bar{\xi}(t) - k_3 \bar{d}(t) (\bar{\xi}^T(t) P \bar{\xi}(t))^{q_2} + \frac{1}{2} (\bar{\xi}^T(t) P \bar{B} \bar{R}(t) + \bar{R}^T(t) \bar{B}^T P \bar{\xi}(t)) \\ &\leq \frac{1}{2} \bar{\xi}^T(t) (P\bar{A} + \bar{A}^T P + Q) \bar{\xi}(t) + s(r) \bar{\xi}^T(t) P \bar{B} \bar{\xi}(t) + \frac{1}{2} \bar{\xi}^T(t) (P\bar{E}_1 + \bar{E}_1^T P) \bar{\xi}(t) \\ &\quad - \bar{\xi}^T(t) g(t) I_{4n} P \bar{\xi}(t) - k_3 \bar{d}(t) (\bar{\xi}^T(t) P \bar{\xi}(t))^{q_2} \\ &\leq \frac{1}{2} \bar{\xi}^T(t) [P\bar{A} + \bar{A}^T P + Q + 2\bar{s} I_{4n} P \bar{B} + P\bar{E}_1 + \bar{E}_1^T P - 2g(t) I_{4n} P] \bar{\xi}(t) \\ &\quad - k_3 \bar{d}(t) (\bar{\xi}^T(t) P \bar{\xi}(t))^{q_2} \\ &\leq \eta_3(t) H_1(t) - 2^{q_2} k_3 \bar{d}(t) [\frac{1}{2} \bar{\xi}^T(t) P \bar{\xi}(t)]^{q_2} \leq \eta_3(t) H_1(t) - 2^{q_2} k_3 \bar{d}(t) H_1^{q_2}(t) \end{aligned} \quad (6.40)$$

and when $t \in [t_m, s_m)$ for $m = 0, 1, \dots, \bar{m} - 1$ we directly have

$$\begin{aligned} \dot{H}_1(t) &\leq \frac{1}{2} \bar{\xi}^T(t) [P\bar{A} + \bar{A}^T P + Q + 2\bar{s} I_{4n} P \bar{B} + P\bar{E}_1 + \bar{E}_1^T P] \bar{\xi}(t) \\ &\leq \eta_2 H_1(t) \end{aligned} \quad (6.41)$$

Moreover, when $t = t_l^{\bar{m}}$, one can obtain

$$\begin{aligned} \frac{1}{2} \bar{\xi}^T(t_l^m) P \bar{\xi}(t_l^m) &= \frac{1}{2} \bar{\xi}^T(t_l^{m-}) \bar{E}_2^T P \bar{E}_2 \bar{\xi}(t_l^{m-}) \\ &\leq \frac{1}{2} \lambda_{max}(\bar{E}_2^T P \bar{E}_2 P^{-1}) \bar{\xi}^T(t_l^{m-}) P \bar{\xi}(t_l^{m-}) \\ &= \pi_0 H_1(t_l^{m-}) \end{aligned} \quad (6.42)$$

When $t = t_l^m$ for $m = 0, 1, \dots, \bar{m} - 1$, we have

$$\bar{\xi}(t_l^{m-}) - \bar{\xi}(t_l^m - \bar{\tau}) = \int_{t_l^{m-\bar{\tau}}}^{t_l^m} ((\bar{A} + \bar{E}_1) \bar{\xi}(s) + \bar{B} \bar{f}(s)) ds \quad (6.43)$$

and

$$\bar{\xi}(t_l^m) = (\bar{E}_3 + \bar{E}_4)\bar{\xi}(t_l^{m-}) - \bar{E}_4 \int_{t_l^{m-\bar{\tau}}}^{t_l^m} ((\bar{A} + \bar{E}_1)\bar{\xi}(s) + \bar{B}\bar{f}(s))ds = \Gamma_1 + \Gamma_2 \quad (6.44)$$

where $\Gamma_1 = (\bar{E}_3 + \bar{E}_4)\bar{\xi}(t_l^{m-})$ and $\Gamma_2 = -\bar{E}_4 \int_{t_l^{m-\bar{\tau}}}^{t_l^m} ((\bar{A} + \bar{E}_1)\bar{\xi}(s) + \bar{B}\bar{f}(s))ds$. By applying Schwartz's inequality and Lemma 3.2.1 we have:

$$\begin{aligned} \Gamma_1^T P \Gamma_1 &= \bar{\xi}(t_l^{m-})^T (\bar{E}_3 + \bar{E}_4)^T P (\bar{E}_3 + \bar{E}_4) \bar{\xi}(t_l^{m-}) \\ &\leq \frac{1}{2} \lambda_{max} ((\bar{E}_3 + \bar{E}_4)^T P (\bar{E}_3 + \bar{E}_4) P^{-1}) H_1(t_l^{m-}) = \pi_1 H_1(t_l^{m-}) \end{aligned} \quad (6.45)$$

$$\begin{aligned} \Gamma_2^T P \Gamma_2 &\leq \lambda_{max}(P) \|\bar{E}_4\|^2 \left[\int_{t_l^{m-\bar{\tau}}}^{t_l^m} ((\bar{A} + \bar{E}_1)\bar{\xi}(s) + \bar{B}\bar{f}(s))ds \right]^T \left[\int_{t_l^{m-\bar{\tau}}}^{t_l^m} ((\bar{A} + \bar{E}_1)\bar{\xi}(s) + \bar{B}\bar{f}(s))ds \right] \\ &\leq \lambda_{max}(P) \bar{\tau} \|\bar{E}_4\|^2 \int_{t_l^{m-\bar{\tau}}}^{t_l^m} ((\bar{A} + \bar{E}_1)\bar{\xi}(s) + \bar{B}\bar{f}(s))^T ((\bar{A} + \bar{E}_1)\bar{\xi}(s) + \bar{B}\bar{f}(s))ds \\ &\leq \lambda_{max}(P) \bar{\tau} \|\bar{E}_4\|^2 \int_{t_l^{m-\bar{\tau}}}^{t_l^m} (1 + \varepsilon_1) \|\bar{A} + \bar{E}_1\|^2 \bar{\xi}^T(s) \bar{\xi}(s) + (1 + \varepsilon_1^{-1}) \|\bar{B}\|^2 (f_{max} + \bar{s})^2 \bar{\xi}^T(s) \bar{\xi}(s) \\ &\leq \lambda_{max}(P) \bar{\tau} \|\bar{E}_4\|^2 \int_{t_l^{m-\bar{\tau}}}^{t_l^m} \kappa \bar{\xi}^T(s) \bar{\xi}(s) ds \\ &\leq 2\lambda_{max}(P) \bar{\tau}^2 \|\bar{E}_4\|^2 \kappa \lambda_{max}(P^{-1}) \sup_{s \in [-\bar{\tau}, 0]} H_1(t_l^{m-} + s) \\ &= \pi_2 \sup_{s \in [-\bar{\tau}, 0]} H_1(t_l^{m-} + s) = \pi_2 H_1(t_l^{m-}) \end{aligned} \quad (6.46)$$

Based on (6.45) and (6.46), it gives:

$$\begin{aligned} 2H_1(t_l^m) &= (\Gamma_1 + \Gamma_2)^T P (\Gamma_1 + \Gamma_2) \\ &\leq (1 + \varepsilon_2) \Gamma_1^T P \Gamma_1 + (1 + \varepsilon_2^{-1}) \Gamma_2^T P \Gamma_2 \\ &\leq [\pi_1(1 + \varepsilon_2) + \pi_2(1 + \varepsilon_2^{-1})] H_1(t_l^{m-}) \end{aligned} \quad (6.47)$$

Thus,

$$H_1(t_l^m) \leq \pi_3 H_1(t_l^{m-}) + \pi_4 H_1(t_l^{m-} - \bar{\tau}) \quad (6.48)$$

Therefore, by combining (6.38), (6.40), (6.41), (6.48), and using Theorem 6.4.1, $H_1(t)$ is convergent to zero solution in T_N given by

$$T_N = \frac{\beta^{(\bar{m}+1)\gamma_L} e^{(1-q_2)(\mu_3 + \bar{m}\eta_2\bar{\zeta} + \bar{m}\eta_1(\bar{\omega} - \bar{\zeta}))} H_1^{1-q_2}(0)}{\eta(1 - q_2)} + \bar{m}(\bar{\omega} + \bar{\zeta}) \quad (6.49)$$

In addition, since $\sup_{s \in [-\bar{\tau}, 0]} \|\bar{\xi}(s)\| = \|\bar{\xi}(0)\| = \nu$, it follows from (6.26) that

$$\left(\frac{1}{2}\lambda_{\min}(P)\|\bar{\xi}(t)\|^2\right)^{1-q_2} \leq e^{(\mu_3 + \bar{m}\eta_2\bar{\zeta} + \bar{m}\eta_1(\bar{\omega} - \underline{\zeta}))} \left(\frac{1}{2}\lambda_{\max}(P)\nu^2\right)^{1-q_2} \quad (6.50)$$

and

$$\|\bar{\xi}(t)\| \leq \frac{2[e^{(\mu_3 + \bar{m}\eta_2\bar{\zeta} + \bar{m}\eta_1(\bar{\omega} - \underline{\zeta}))} (\frac{1}{2}\lambda_{\max}(P)\nu^2)^{1-q_2}]^{\frac{1}{1-q_2}}}{\lambda_{\min}(P)} = \delta, \quad \forall t \geq t_0 \quad (6.51)$$

Therefore, the local finite-time formation tracking is guaranteed for the leader-following MASs when initial states $\|\bar{\xi}(0)\| \leq \nu$. \square

Remark 6.4.2. According to both theorems derived above, the finite-time formation tracking of MASs can be successfully realized via aperiodic intermittent communication. Condition (6.49) and $0 < \beta < 1$ indicate that the lowest number of impulsive instants in each intermittent interval, the total number of intermittent control intervals, the intermittent communication rate (i.e., $\frac{s_m - t_m}{t_{m+1} - t_m}$) and the bound of time-varying gains can all influence the size of the settling time T_N . Specifically, by fixing the other parameters involved, a larger value of η , γ_L and smaller value of β will lead to the reduction of formation tracking settling time. Meanwhile, in contrast to many existing literature such as [106, 107, 108, 109] regarding fully continuous dynamics, we have explicitly taken into account delayed impulses and demonstrated the novelty of our results for nonlinear impulsive systems.

6.4.2 FTHIIC with Impulsive Disturbances

Notice that the stabilizing impulses are solely considered in Theorem 6.4.1, yet the control channel is frequently experiencing external disturbances in reality. Thus, we modify the impulsive part of system (6.33) for $t \in [t_m, s_m)$ as

$$\begin{cases} \Delta \bar{v}(t) = -k_2 L \bar{p}(t) - k_2 L \bar{v}(t) - k_2 c \bar{p}(t) - k_2 c \bar{v}(t) + k_4 (\bar{p}(t) + \bar{v}(t)), & t = t_i^m, \quad t < t_{\bar{m}} \\ \Delta \bar{v}(t) = -k_2 L \bar{p}(t - \bar{\tau}) - k_2 L \bar{v}(t - \bar{\tau}) - k_2 c \bar{p}(t) - k_2 c \bar{v}(t) + k_4 (\bar{p}(t) + \bar{v}(t)), & t = t_i^m, \quad t \geq t_{\bar{m}} \end{cases} \quad (6.52)$$

where $k_4(\bar{p}(t) + \bar{v}(t))$ represents external impulsive disturbances with strength $k_4 > 0$.

We also reset $\bar{E}_2 = \begin{pmatrix} I_{2n} & \mathbf{0}_{2n \times 2n} \\ -k_2(L + cI_{2n}) + k_4 I_{2n} & I_{2n} - k_2(L + cI_{2n}) + k_4 I_{2n} \end{pmatrix}$ and $\bar{E}_4 = \begin{pmatrix} I_{2n} & \mathbf{0}_{2n \times 2n} \\ -k_2 c I_{2n} + k_4 I_{2n} & I_{2n} - k_2 c I_{2n} + k_4 I_{2n} \end{pmatrix}$. Then in comparison to Theorem 6.4.1 and Theorem 6.4.2 respectively, we obtain the following finite-time formation tracking results.

They indicate that our proposed control protocol (6.29) is also capable to compensate for impulsive disturbances that are relatively large.

Theorem 6.4.3. *Suppose there exists some constants $\rho_1 > 1, \rho_2 \geq 0, \vartheta \in [1, \rho_1 + \rho_2]$. If all the hypotheses in Theorem 6.4.1 are true apart from that (6.12) and (6.13) are replaced by:*

$$t_{\bar{m}} + \frac{\vartheta^{\gamma_{\bar{m}}-1}(\rho_1 + \rho_2 - \vartheta)V^{1-r}(t_{\bar{m}})}{(1-r)(e^{-\mu_3(1-r)}(\rho_1 + \rho_2) - 1)\eta} + \frac{e^{-\mu_3(1-r)}\rho_2\eta\bar{\tau}}{(e^{-\mu_3(1-r)}(\rho_1 + \rho_2) - 1)\eta} \leq t_{\gamma_{\bar{m}}}^{\bar{m}} \leq t_{\bar{m}} + \frac{\vartheta^{\gamma_M}e^{\mu_3(1-r)}V^{1-r}(t_{\bar{m}})}{\eta(1-r)} \quad (6.53)$$

with $\rho_1 e^{-\mu_3(1-r)} > 1$. Then the convergence of $V(t)$ in finite time to zero solution is guaranteed for aperiodic intermittent impulse sequence $\{t_l^m, l = 1, \dots, \gamma_m\}$; while the settling time T_N is given by

$$T_N = \frac{\vartheta^{(\bar{m}+1)\gamma_M}e^{(\mu_3+\mu_1\bar{\zeta}\bar{m}+\bar{m}\mu_2(\bar{\omega}-\bar{\zeta}))(1-r)}V^{1-r}(t_0)}{\eta(1-r)} + \bar{m}(\bar{\omega} + \bar{\zeta}) \quad (6.54)$$

Proof. Followed from (6.15)-(6.18), in this case, since $\rho_1 \geq 1, \rho_2 > 0$ and (6.53) holds, it gives for $t \geq t_{\bar{m}}$ that

$$\begin{aligned} M(t) &\leq e^{(1-r)\int_{t_1^{\bar{m}}}^t |P_1(s)|ds} M(t_1^{\bar{m}}) + (r-1) \int_{t_1^{\bar{m}}}^t Q_1(s) e^{(1-r)\int_s^t |P_1(z)|dz} ds \\ &\leq \rho_1 e^{(1-r)\int_{t_1^{\bar{m}}}^t |P_1(s)|ds} M(t_1^{\bar{m}-}) + \rho_2 e^{(1-r)\int_{t_1^{\bar{m}}}^t |P_1(s)|ds} M(t_1^{\bar{m}-} - \bar{\tau}) \\ &\quad + (r-1) \int_{t_1^{\bar{m}}}^{t_{\bar{m}}} Q_1(s) e^{(1-r)\int_s^t |P_1(z)|dz} ds + (r-1) \int_{t_{\bar{m}}}^t Q_1(s) e^{(1-r)\int_s^t |P_1(z)|dz} ds \\ &\leq \rho_1 e^{(1-r)\int_{t_{\bar{m}}}^t |P_1(s)|ds} M(t_{\bar{m}}) + \rho_2 e^{(1-r)(\int_{t_{\bar{m}}}^{t_1^{\bar{m}-\bar{\tau}}} |P_1(s)|ds + \int_{t_1^{\bar{m}}}^t |P_1(s)|ds)} M(t_{\bar{m}}) \\ &\quad + (r-1) \int_{t_1^{\bar{m}}}^{t_{\bar{m}}} Q_1(s) e^{(1-r)\int_s^t |P_1(z)|dz} ds + \rho_1(1-r) e^{(1-r)\int_{t_1^{\bar{m}}}^t |P_1(s)|ds} \int_{t_1^{\bar{m}}}^{t_{\bar{m}}} Q_1(s) e^{(1-r)\int_s^t |P_1(z)|dz} ds \\ &\quad + \rho_2(1-r) e^{(1-r)\int_{t_1^{\bar{m}}}^t |P_1(s)|ds} \int_{t_1^{\bar{m}-\bar{\tau}}}^{t_{\bar{m}}} Q_1(s) e^{(1-r)\int_s^t |P_1(z)|dz} ds + (r-1) \int_{t_{\bar{m}}}^t Q_1(s) e^{(1-r)\int_s^t |P_1(z)|dz} ds \\ &\leq (\rho_1 + \rho_2) e^{(1-r)\int_{t_{\bar{m}}}^t |P_1(s)|ds} M(t_{\bar{m}}) - (1-r)(1 - \rho_1 e^{-\mu_3(1-r)}) e^{(1-r)\int_{t_{\bar{m}}}^t |P_1(s)|ds} \int_{t_1^{\bar{m}}}^{t_{\bar{m}}} Q_1(s) ds \\ &\quad + \rho_2(1-r) e^{(1-r)\int_{t_1^{\bar{m}}}^t |P_1(s)|ds} \int_{t_1^{\bar{m}-\bar{\tau}}}^{t_{\bar{m}}} Q_1(s) ds + (r-1) \int_{t_{\bar{m}}}^t Q_1(s) e^{(1-r)\int_s^t |P_1(z)|dz} ds \end{aligned} \quad (6.55)$$

thus

$$\begin{aligned}
M(t) &\leq e^{(1-r)\int_{t_{\bar{m}}}^t |P_1(s)|ds} ((\rho_1 + \rho_2)M(t_{\bar{m}}) - (1-r)(\rho_1 e^{-\mu_3(1-r)} - 1)\eta(t_1^{\bar{m}} - t_{\bar{m}}) \\
&\quad - e^{-\mu_3(1-r)}\rho_2(1-r)\eta(t_1^{\bar{m}} - t_{\bar{m}}) + e^{-\mu_3(1-r)}\rho_2\eta\bar{\tau}(1-r)) + (r-1) \int_{t_{\bar{m}}}^t Q_1(s)e^{(1-r)\int_s^t |P_1(z)|dz} ds \\
&= e^{(1-r)\int_{t_{\bar{m}}}^t |P_1(s)|ds} ((\rho_1 + \rho_2)M(t_{\bar{m}}) - (1-r)[(\rho_1 e^{-\mu_3(1-r)} - 1 + e^{-\mu_3(1-r)}\rho_2)\eta(t_1^{\bar{m}} - t_{\bar{m}}) \\
&\quad - e^{-\mu_3(1-r)}\rho_2\eta\bar{\tau}]) + (r-1) \int_{t_{\bar{m}}}^t Q_1(s)e^{(1-r)\int_s^t |P(z)|dz} ds \\
&\leq \vartheta e^{(1-r)\int_{t_{\bar{m}}}^t |P_1(s)|ds} M(t_{\bar{m}}) + (r-1) \int_{t_{\bar{m}}}^t Q_1(s)e^{(1-r)\int_s^t |P_1(z)|dz} ds, \quad t \in [t_1^{\bar{m}}, t_2^{\bar{m}}]
\end{aligned} \tag{6.56}$$

Similar to (6.18)-(6.24), we obtain

$$\begin{aligned}
M(t) &\leq \vartheta^{\gamma_M} e^{\mu_3(1-r)} M(t_{\bar{m}}) - \eta(1-r)(t - t_{\bar{m}}), \quad t \geq t_{\gamma_{\bar{m}}}^{\bar{m}} \\
M(t) &\leq e^{\mu_2(\omega_{m-1} - \zeta_{m-1})(1-r)} M(s_{m-1}), \quad t \in [s_{m-1}, t_m] \\
M(t) &\leq \vartheta^{\gamma_M} e^{\mu_1 \zeta_{m-1}(1-r)} M(t_{m-1}), \quad t \in [t_{m-1}, s_{m-1}), \quad m = 1, \dots, \bar{m}
\end{aligned} \tag{6.57}$$

Since $\mu_1, \mu_2, \mu_3, \eta > 0$ and $r \in (0, 1)$, for $t \in [t_{\gamma_{\bar{m}}}^{\bar{m}}, \infty)$, we can deduce from (6.57) that

$$\begin{aligned}
M(t) &\leq \vartheta^{(\bar{m}+1)\gamma_M} e^{(\mu_3 + \mu_1 \bar{\zeta}_{\bar{m}} + \bar{m}\mu_2(\bar{\omega} - \bar{\zeta})) (1-r)} M(t_0) \\
&\leq \vartheta^{(\bar{m}+1)\gamma_M} e^{(\mu_3 + \mu_1 \bar{\zeta}_{\bar{m}} + \bar{m}\mu_2(\bar{\omega} - \bar{\zeta})) (1-r)} M(t_0) - \eta(1-r)(t - t_0) + \eta \bar{m}(\bar{\omega} + \bar{\zeta})(1-r),
\end{aligned} \tag{6.58}$$

Accordingly, the settling time T_N is given by

$$T_N = \frac{\vartheta^{(\bar{m}+1)\gamma_M} e^{(\mu_3 + \mu_1 \bar{\zeta}_{\bar{m}} + \bar{m}\mu_2(\bar{\omega} - \bar{\zeta})) (1-r)} V^{1-r}(t_0)}{\eta(1-r)} + \bar{m}(\bar{\omega} + \bar{\zeta}) \tag{6.59}$$

while (6.58) leads to

$$\alpha_1^{1-r} (\|\bar{\xi}(t)\|) \leq \vartheta^{(\bar{m}+1)\gamma_M} e^{(\mu_3 + \mu_1 \bar{\zeta}_{\bar{m}} + \bar{m}\mu_2(\bar{\omega} - \bar{\zeta})) (1-r)} (\alpha_2(\|\bar{\xi}(0)\|))^{1-r} \tag{6.60}$$

In addition, similar to (6.28), $T_N \geq t_{\gamma_{\bar{m}}}^{\bar{m}}$ holds based on (6.53), where

$$\begin{aligned}
t_{\gamma_{\bar{m}}}^{\bar{m}} &\leq t_{\bar{m}} + \frac{\vartheta^{\gamma_M - 1} (\rho_1 + \rho_2 - \vartheta) V^{1-r}(t_{\bar{m}}) + (1-r)e^{-\mu_3(1-r)} \rho_2 \bar{\tau}}{(1-r)(e^{-\mu_3(1-r)} (\rho_1 + \rho_2) - 1)\eta} \\
&\leq t_{\bar{m}} + \frac{\vartheta^{\gamma_M} e^{\mu_3(1-r)} V^{1-r}(t_{\bar{m}})}{\eta(1-r)} \leq T_N
\end{aligned} \tag{6.61}$$

The proof is completed. \square

Theorem 6.4.4. *Suppose all the hypotheses in Theorem 6.4.2 excluding (6.35) are guaranteed with \bar{E}_2, \bar{E}_3 defined based on (6.52). Then the local formation tracking is achieved with $\|\bar{\xi}(0)\| \leq \nu$ in finite time T_N given by*

$$T_N = \frac{\vartheta^{(\bar{m}+1)\gamma_M} e^{(1-q_2)(\mu_3 + \eta_2 \bar{\zeta} \bar{m} + \bar{m} \eta_1 (\bar{\omega} - \bar{\zeta}))} H_1^{1-q_2}(0)}{\eta(1-q_2)} + \bar{m}(\bar{\omega} + \bar{\zeta}) \quad (6.62)$$

Proof. Followed from (6.40), (6.40) and (6.48), for $t \in [t_m, s_m)$ we also have

$$\begin{aligned} \dot{H}_1(t) &\leq \eta_2 H_1(t), \quad t \in [t_{m-1}, s_{m-1}), \quad m = 1, \dots, \bar{m} \\ \dot{H}_1(t) &\leq \eta_3(t) H_1(t) - 2^{q_2} k_3 \bar{d}(t) H_1^{q_2}(t), \quad t \geq t_{\bar{m}} \\ H_1(t_l^m) &\leq \pi_3 H_1(t_l^{m-}) + \pi_4 H_1(t_l^{m-} - \bar{\tau}), \quad t = t_l^m, \quad m = 0, \dots, \bar{m} \end{aligned} \quad (6.63)$$

Then the settling time T_N in (6.62) is maintained according to Theorem 6.4.3. Based on (6.58) and $\vartheta > 1$, we obtain

$$\|\bar{\xi}(t)\| \leq \frac{2[\vartheta^{(\bar{m}+1)\gamma_M} e^{(\mu_3 + \bar{m}\eta_2 \bar{\zeta} + \bar{m}\eta_1 (\bar{\omega} - \bar{\zeta}))} (\frac{1}{2} \lambda_{\max}(P) \nu^2)^{1-q_2}]^{\frac{1}{1-q_2}}}{\lambda_{\min}(P)} = \delta, \quad \forall t \geq t_0 \quad (6.64)$$

□

Remark 6.4.3. *Theorem 6.4.3 and Theorem 6.4.4 have proven that locally finite-time formation tracking control under impulsive disturbances can also be achieved. Nevertheless, as $\vartheta > 1$, a significantly longer settling time T_N is required in order to compensate for the negative impulsive effect caused by external impulsive disturbances.*

6.4.3 FTS via Average Impulsive Interval

In view of Theorem 6.4.1, the number of impulsive instants γ_m during each aperiodic intermittent control interval remains uniformly bounded; yet it can be unknown and indefinite in practice. In general, it can be assumed that the impulsive instants occur on all intermittent control intervals together as an impulsive sequence that satisfies the average impulsive interval condition as described in Definition 3.5.3. Then, we obtain the following results compared to Theorem 6.4.1.

Corollary 6.4.1. *Consider the case where all the hypotheses in Theorem 6.4.1 are true, then the convergence of $V(t)$ in finite time to zero solution is guaranteed for impulse sequence $\{t_l^m, l = 1, \dots, \gamma_m, m < \bar{m}\}$ associated with average impulsive interval T_α ; while the*

corresponding settling time T_N is given by

$$T_N = \begin{cases} \frac{\beta^{\bar{m}(\frac{\bar{\zeta}}{T_\alpha} - \varrho) + \gamma_L} e^{(\mu_3 + \mu_1 \bar{\zeta} \bar{m} + \bar{m} \mu_2 (\bar{\omega} - \bar{\zeta})) (1-r)} V^{1-r}(t_0)}{\eta(1-r)} + \bar{m}(\bar{\omega} + \bar{\zeta}), & \beta^{\frac{1}{T_\alpha}} e^{\mu_1(1-r)} > 1 \\ \frac{\beta^{\bar{m}(\frac{\bar{\zeta}}{T_\alpha} - \varrho) + \gamma_L} e^{(\mu_3 + \mu_1 \bar{\zeta} \bar{m} + \bar{m} \mu_2 (\bar{\omega} - \bar{\zeta})) (1-r)} V^{1-r}(t_0)}{\eta(1-r)} + \bar{m}(\bar{\omega} + \bar{\zeta}), & 0 < \beta^{\frac{1}{T_\alpha}} e^{\mu_1(1-r)} < 1 \\ \frac{\beta^{-\varrho \bar{m} + \gamma_L} e^{\mu_3 + \mu_2 \bar{m} (\bar{\omega} - \bar{\zeta}) (1-r)} V^{1-r}(t_0)}{\eta(1-r)} + \bar{m}(\bar{\omega} + \bar{\zeta}), & \beta^{\frac{1}{T_\alpha}} e^{\mu_1(1-r)} = 1 \end{cases} \quad (6.65)$$

Proof. By repeating the same process (6.15)-(6.24) in Theorem 6.4.1, for $t \in [t_{\bar{m}}^m, \infty)$, it follows from $0 < \beta < 1$ and Definition 3.5.3 that

$$\begin{aligned} M(t) &\leq \beta^{\gamma_L} e^{(1-r) \int_{t_{\bar{m}}}^t |P(s)| ds} M(t_{\bar{m}}) - (1-r) \int_{t_{\bar{m}}}^t Q(s) e^{(1-r) \int_s^t |P(z)| dz} ds \\ &\leq \beta^{\gamma_L} e^{\mu_3(1-r)} M(t_{\bar{m}}) - \eta(1-r)(t - t_{\bar{m}}) \end{aligned} \quad (6.66)$$

Then, use mathematical induction yields,

$$M(t) \leq \begin{cases} \beta^{\gamma_L} e^{\mu_3(1-r)} \beta^{-\bar{m} \varrho} (\beta^{\frac{1}{T_\alpha}} e^{\mu_1(1-r)})^{\bar{\zeta} \bar{m}} e^{\mu_2 \bar{m} (\bar{\omega} - \bar{\zeta}) (1-r)} M(t_0) - \eta(1-r)(t - t_0) \\ + \eta \bar{m} (\bar{\omega} + \bar{\zeta}) (1-r), & \beta^{\frac{1}{T_\alpha}} e^{\mu_1(1-r)} > 1 \\ \beta^{\gamma_L} e^{\mu_3(1-r)} \beta^{-\bar{m} \varrho} (\beta^{\frac{1}{T_\alpha}} e^{\mu_1(1-r)})^{\bar{\zeta} \bar{m}} e^{\mu_2 \bar{m} (\bar{\omega} - \bar{\zeta}) (1-r)} M(t_0) - \eta(1-r)(t - t_0) \\ + \eta \bar{m} (\bar{\omega} + \bar{\zeta}) (1-r), & 0 < \beta^{\frac{1}{T_\alpha}} e^{\mu_1(1-r)} < 1 \\ \beta^{\gamma_L} e^{\mu_3(1-r)} \beta^{-\bar{m} \varrho} e^{\mu_2 \bar{m} (\bar{\omega} - \bar{\zeta}) (1-r)} M(t_0) \\ - \eta(1-r)(t - t_0) + \eta \bar{m} (\bar{\omega} + \bar{\zeta}) (1-r), & \beta^{\frac{1}{T_\alpha}} e^{-\mu_1(r-1)} = 1 \end{cases} \quad (6.67)$$

Therefore, the settling time T_N is obtained as follows:

$$T_N = \begin{cases} \frac{\beta^{\gamma_L} e^{\mu_3(1-r)} \beta^{\bar{m}(\frac{\bar{\zeta}}{T_\alpha} - \varrho)} e^{(\mu_1 \bar{\zeta} \bar{m} + \bar{m} \mu_2 (\bar{\omega} - \bar{\zeta})) (1-r)} V^{1-r}(t_0)}{\eta(1-r)} + \bar{m}(\bar{\omega} + \bar{\zeta}), & \beta^{\frac{1}{T_\alpha}} e^{\mu_1(1-r)} > 1 \\ \frac{\beta^{\gamma_L} e^{\mu_3(1-r)} \beta^{\bar{m}(\frac{\bar{\zeta}}{T_\alpha} - \varrho)} e^{(\mu_1 \bar{\zeta} \bar{m} + \bar{m} \mu_2 (\bar{\omega} - \bar{\zeta})) (1-r)} V^{1-r}(t_0)}{\eta(1-r)} + \bar{m}(\bar{\omega} + \bar{\zeta}), & 0 < \beta^{\frac{1}{T_\alpha}} e^{\mu_1(1-r)} < 1 \\ \frac{\beta^{\gamma_L} e^{\mu_3(1-r)} \beta^{-\varrho \bar{m}} e^{\mu_2 \bar{m} (\bar{\omega} - \bar{\zeta}) (1-r)} V^{1-r}(t_0)}{\eta(1-r)} + \bar{m}(\bar{\omega} + \bar{\zeta}), & \beta^{\frac{1}{T_\alpha}} e^{\mu_1(1-r)} = 1 \end{cases} \quad (6.68)$$

We omit the rest of proof, as it follows directly from Theorem 6.4.1. \square

Remark 6.4.4. Based on Corollary 6.4.1, other than the total number of intermittent control intervals and intermittent communication rate, the size of average impulsive interval T_α also affects both the convergence of zero solution of system (6.3) as well as the magnitude of settling time. Specifically, $T_\alpha = \frac{\ln \beta}{\mu_1(r-1)}$ can be viewed as the critical value separating the different behaviours of finite time error convergence.

6.4.4 FTS with State-dependent Control Width

Besides the implementation of average impulsive interval, further generalization in practice is applicable by replacing state-independent control width ζ_m with state-dependent ones:

$$\zeta_m = \begin{cases} 0, & m = 0 \\ \min\{\Gamma > 0 : V^{1-r}(t_m + \Gamma) \leq \kappa V^{1-r}(t_{m-1} + \zeta_{m-1})\}, & m = 1, 2, \dots, \bar{m} - 1 \end{cases} \quad (6.69)$$

where threshold value $0 < \kappa < 1$. Let $\chi > 0$ to be the uniform control-free width when each ζ_m is detected for $m = 1, 2, \dots, \bar{m} - 1$, and $\zeta_{max} = \max_{m=0,1,\dots,\bar{m}-1}\{\zeta_m\}$. Then, the manual setting of upper and lower bound of ζ_m (i.e., $\bar{\zeta}$ and $\underline{\zeta}$) can be avoided for aperiodic intermittent control intervals. For simplicity, we consider the case when $T_\alpha = \frac{\ln \beta}{\mu_1(r-1)}$, while the other cases can be derived analogously. Therefore, we obtain the following results regarding the relationship among settling time, control-free width, state-dependent threshold and total number of aperiodic intermittent communication interval.

Corollary 6.4.2. *Consider the case where all the hypotheses in Corollary 6.4.1 are true with $\chi > 0$, $T_\alpha = \frac{\ln \beta}{\mu_1(r-1)}$ and state-dependent control width ζ_m in (6.69), then the convergence of $V(t)$ in finite time to zero solution is guaranteed for aperiodic intermittent impulse sequence $\{t_l^m, l = 1, \dots, \gamma_m, m < \bar{m}\}$ associated with average impulsive interval T_α ; while the corresponding settling time T_N is given by*

$$T_N = \frac{\kappa^{\bar{m}-1} \beta^{\gamma_L} e^{(\mu_3 + \mu_2 \chi)(1-r)} V^{1-r}(t_0)}{\eta(1-r)} + \bar{m}(\zeta_{max} + \chi) \quad (6.70)$$

Proof. Based on (6.69) and continuity of $V(t)$ on $[t_m, s_m]$ for $m = 1, \dots, \bar{m} - 1$, it yields

$$M(t_m + \zeta_{\bar{m}}) = \kappa M(t_{m-1} + \zeta_{m-1}) \quad (6.71)$$

Thus, since $0 < \kappa < 1$, it follows from (6.66) and (6.71) that

$$\begin{aligned} M(t) &\leq \beta^{\gamma_L} e^{\mu_3(1-r)} M(t_{\bar{m}}) - \eta(1-r)(t - t_{\bar{m}}) \\ &\leq \beta^{\gamma_L} e^{\mu_3(1-r)} e^{\mu_2 \chi(1-r)} M(t_{\bar{m}-1} + \zeta_{\bar{m}-1}) - \eta(1-r)(t - t_{\bar{m}}) \\ &\leq \kappa \beta^{\gamma_L} e^{\mu_3(1-r)} e^{\mu_2 \chi(1-r)} M(t_{\bar{m}-2} + \zeta_{\bar{m}-2}) - \eta(1-r)(t - t_{\bar{m}}) \\ &\leq \kappa^{\bar{m}-1} \beta^{\gamma_L} e^{\mu_3(1-r)} e^{\mu_2 \chi(1-r)} M(t_0) - \eta(1-r)(t - t_0) \\ &\quad + \eta(1-r) \bar{m}(\zeta_{max} + \chi), \quad t \in [t_{\gamma_{\bar{m}}}, \infty) \end{aligned} \quad (6.72)$$

Therefore, T_N can be expressed as

$$\begin{aligned}
T_N &= \frac{\kappa^{\bar{m}-1} \beta^{\gamma_L} e^{\mu_3(1-r)} e^{\mu_2 \chi(1-r)} V^{1-r}(t_0) + \eta(1-r) \bar{m}(\zeta_{max} + \chi)}{\eta(1-r)} \\
&= \frac{\kappa^{\bar{m}-1} \beta^{\gamma_L} e^{\mu_3(1-r)} e^{\mu_2 \chi(1-r)} V^{1-r}(t_0)}{\eta(1-r)} + \bar{m}(\zeta_{max} + \chi)
\end{aligned} \tag{6.73}$$

□

6.5 Numerical Simulations

Two representative simulation examples are demonstrated in order to show how theoretical results in Theorem 6.4.2 and Theorem 6.4.4 can be used to achieve formation tracking in finite time. The corresponding topology connectivity of leader-follower MASs (6.3) is indicated in Figure 6.1. The initial position $p_i(0)$ and velocity $v_i(0)$ are arbitrarily generated within the admissible area range of $[-15, -10]^2$ and $[5, 10]^2$ accordingly; while initial states of the leader are chosen to be $p_0(0) = [0, -5]^T$ and $v_0(0) = [0.1, 0.1]^T$. We set the nonlinear intrinsic dynamics with $f(\hat{p}_i(t)) = 0.3(p_i^T(t)p_i(t) - p_0^T(t)p_0(t))$ and $f(\hat{v}_i(t)) = 0.1(v_i(t) - v_0(t))^T(v_i(t) - v_0(t))$. For the system and control parameter settings, we take $b_{ij} = 1.5$, $c = 5$, $k_1 = 0.15$, $k_2 = 0.015$, $k_3 = 7.5$, $k_4 = 2.5$, $q_1 = 0$, $q_2 = \frac{1}{2}$, $A = \begin{pmatrix} 0 & 1 \\ -0.2 & 0.5 \end{pmatrix} \otimes I_2$ and $B = \begin{pmatrix} 0.1 & 0 \\ 0 & 0.5 \end{pmatrix} \otimes I_2$. Furthermore, the intermittent communication is established as $t_m - t_{m-1} = 1s$ with $\zeta_m = 0.95s$ when m is even, and $t_m - t_{m-1} = 1.5s$ with $\zeta_m = 1.4s$ when m is odd. Hence, we obtain $\bar{\zeta} = 1.4s$, $\underline{\zeta} = 0.95s$, $\bar{\omega} = 1.5s$, $\underline{\omega} = 1s$.

Example 1. (Stabilizing Impulses) We set the time-varying tunable gain $d(t) = 2^{\frac{1}{3}} \cos^2(4t)$ so that $\eta = 4$, $\lambda = 8$ and $\theta = 0.1$ are feasible. The impulsive time delay is chosen as $\bar{\tau} = 0.01s$; while by using LMI toolbox, we obtain $\pi_3 = 0.525$, $\eta_1 = 2.44$, $\eta_2 = 5.12$ and set $g(t) = \frac{5.2}{1+e^{-0.02t}}$, $\eta_3(t) = \frac{0.1}{1+2e^{0.05t}}$ so that $\mu_3 = 0.69$. Hence, condition (6.12) and (6.13) are satisfied by choosing $\bar{m} = 3$ and $\beta = 0.975$; while the settling time $T_N = 4.914s$ is obtained. The impulses are generated every $0.05s$ in the last intermittent control interval, whereas $0.15s$ for the rest of intermittent control interval. Thus, $\gamma_L = 6$ and $\gamma_M = 28$. The formation trajectories in Figure 6.2(a)-(b) illustrate the effectiveness of finite-time formation tracking mechanism while maintaining desired formation. According to Figure 6.2(c)-(d), both velocity mismatch and displacement mismatch with respect to virtual

leader are converging to zero solution in settling time T_N with the presence of intermittent control mechanism. As a result, our formation tracking control of leader-following MASs with intermittent communication and delayed stabilizing impulses in finite time is guaranteed; hence Theorem 6.4.1 and Theorem 6.4.2 provide valid theoretical results.

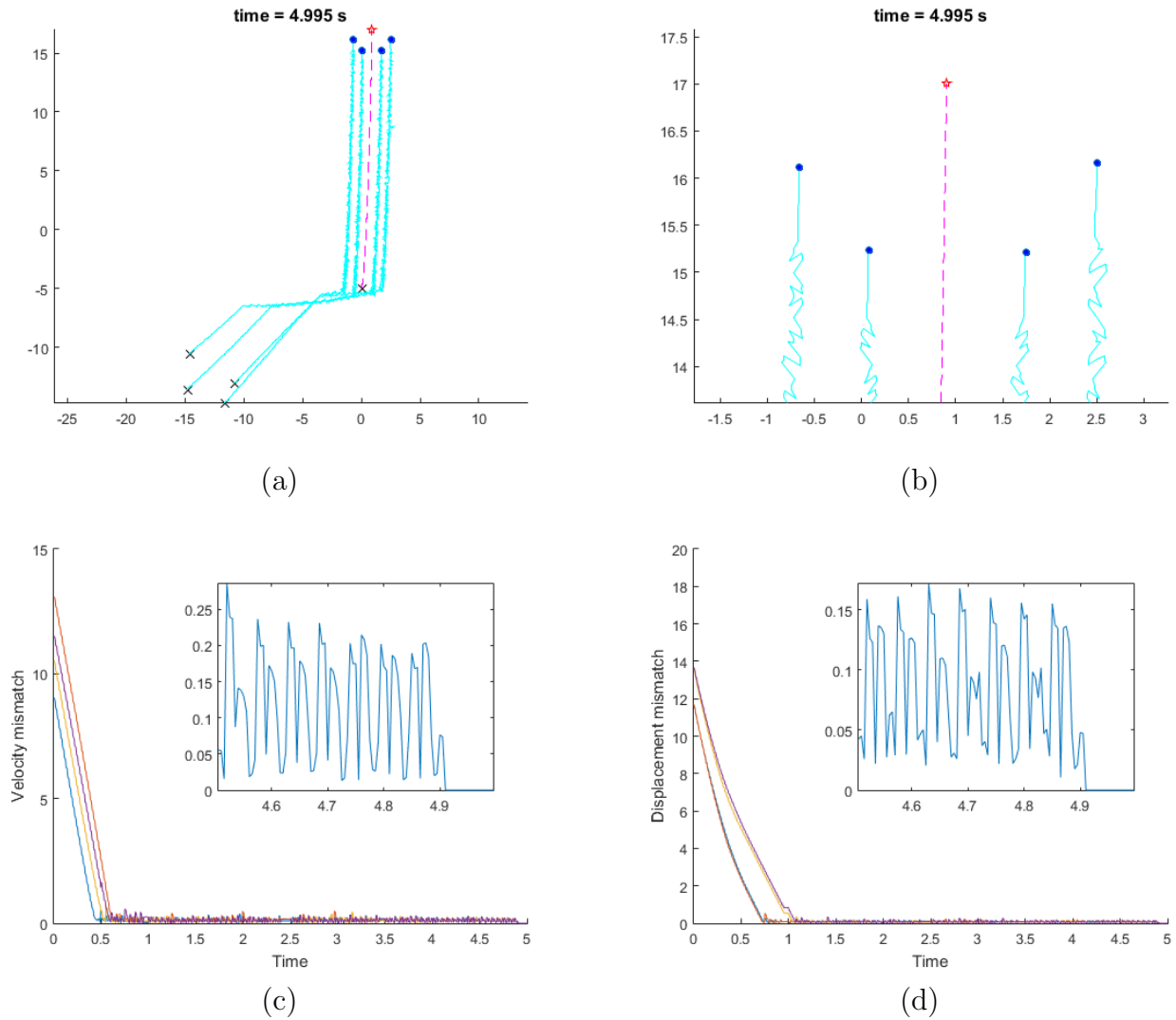


Figure 6.2: (a)&(b) Trajectory evolution of MASs (6.3) over stabilizing impulses (c) Velocity mismatch of error dynamics (d) Displacement mismatch of error dynamics

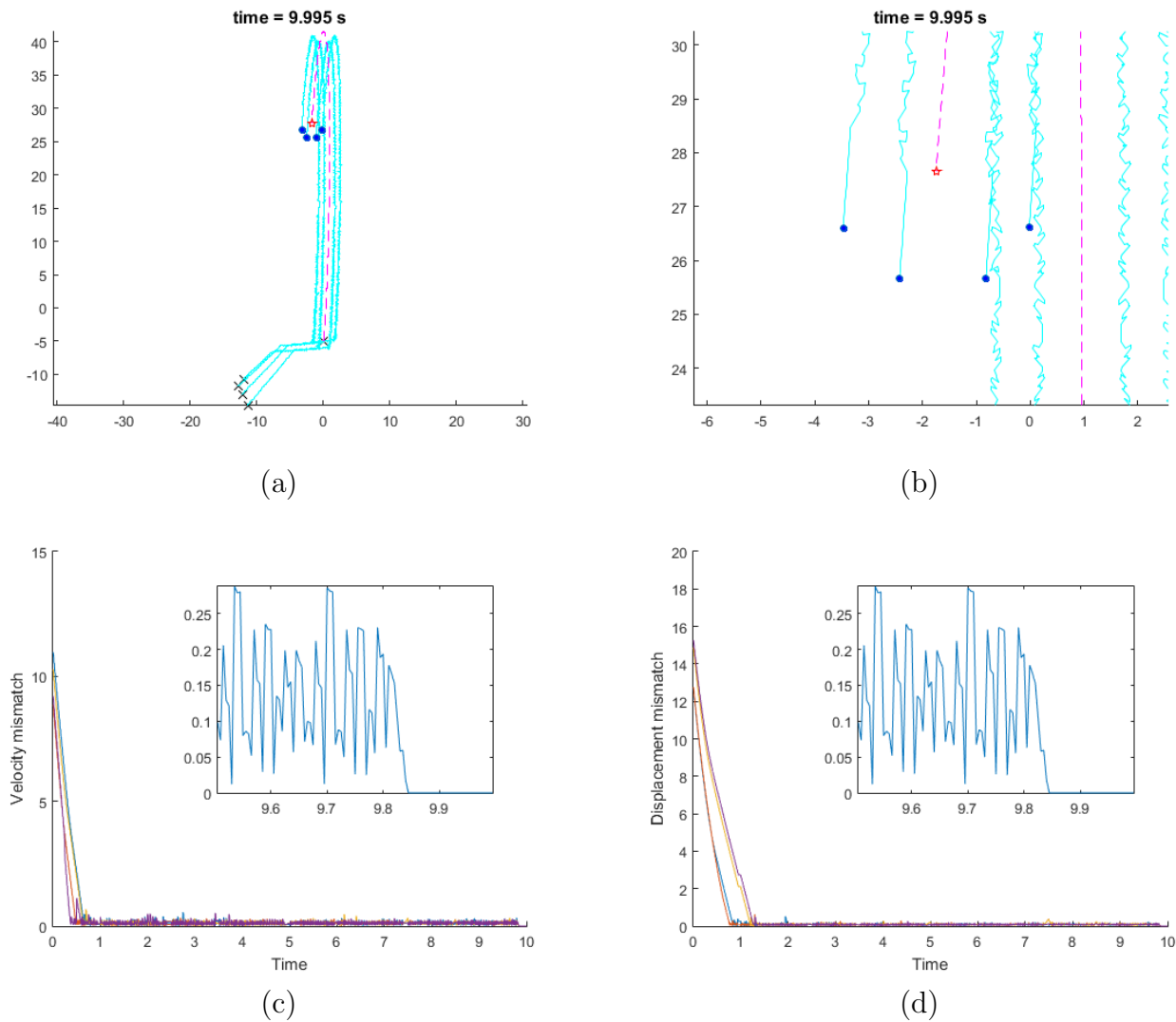


Figure 6.3: (a)&(b) Trajectory evolution of MASs (6.3) over stabilizing impulses and impulsive disturbances (c) Velocity mismatch of error dynamics (d) Displacement mismatch of error dynamics

Example 2. (Stabilizing Impulses & Impulsive Disturbance) We use a different time-varying tunable gain $d(t) = 2^{\frac{4}{3}} \cos^2(4t)$ so that $\eta = 15$, $\lambda = 25$ and $\theta = 0.1$ are feasible, and keep the same impulse generation setting as previous example. With LMI toolbox,

we obtain $\pi_3 = 2.047$, $\eta_1 = 2.06$, $\eta_2 = 4.94$. Similarly, by considering $\vartheta = 1.045$, while $g(t) = \frac{5.2}{1+e^{-0.02t}}$ and $\eta_3(t) = \frac{0.1}{1+2e^{0.05t}}$ remains with $\mu_3 = 0.56$, then condition (6.53) is satisfied by choosing $\bar{m} = 7$; while the settling time $T_N = 9.844s$ is obtained, which is significantly longer than the previous example with stabilizing impulses. Accordingly, the effectiveness of finite-time formation tracking mechanism while maintaining desired formation are shown in Figure 6.3(a)-(b). Meanwhile, based on Figure 6.3(c)-(d), the convergence of velocity and displacement mismatch in finite time can still be maintained via intermittent control while experiencing impulsive disturbance. Therefore, the hybrid impulsive intermittent formation tracking control of MASs with finite-time stability are accomplished as well according to the theoretical analysis illustrated in Theorem 6.4.3 and Theorem 6.4.4.

Chapter 7

Application to Self-driving Vehicle Platoons

Self-driving, also known as autonomous driving, refers to the ability of a vehicle to operate and navigate without human input or intervention. This is achieved through the use of advanced technologies, such as sensors, cameras, and artificial intelligence (AI) algorithms, which allow the vehicle to perceive and understand its environment and make decisions based on that information. There are different levels of autonomy for self-driving vehicles, including that

- the driver is fully in control of the vehicle,
- the vehicle can assist the driver in certain driving tasks but still requires the driver to be ready to take control of the vehicle if necessary,
- the vehicle is completely self-driving and requires no human input or intervention.

Self-driving vehicles have great potential to revolutionize the transportation industry, as they can improve safety, reduce traffic congestion, and increase mobility for people who cannot drive, such as the elderly or disabled. Overall, self-driving technology is rapidly advancing in the future of transportation.

Meanwhile, vehicle platoon control is a technique used to manage groups of vehicles traveling closely together, typically in a convoy or a platoon formation. Similar to self-driving, the goal of platoon control serves the purpose to improve traffic flow, reduce fuel consumption, and increase safety on the road as well. The platoon is usually led by a lead

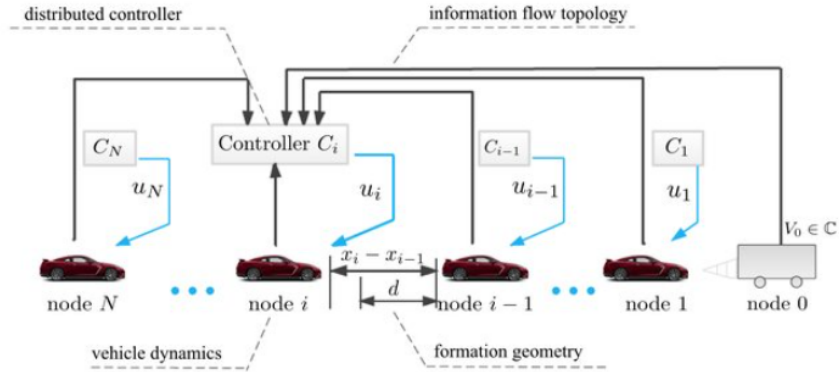


Figure 7.1: Structure of a vehicle platoon

vehicle, which is equipped with advanced communication and sensing technologies that allow it to coordinate with the other vehicles in the platoon. The following vehicles are equipped with sensors that allow them to detect the movements of the lead vehicle and adjust their speed and direction accordingly. Platoon control systems can be classified into two types:

- **Centralized platoon control systems** rely on a central controller that manages the speed and direction of all the vehicles in the platoon,
- **Decentralized platoon control systems** rely on each vehicle in the platoon to communicate with the other vehicles and adjust its speed and direction based on the actions of the lead vehicle. (See Figure 7.1 [116])

Indeed, vehicle platoon control is also likely to play an increasingly important role in the future of autonomous vehicles and smart transportation systems.

Nevertheless, there are also challenges and concerns associated with self-driving vehicles platoon in terms of the control reliability, such as compensating communication malfunction, dealing with unexpected road conditions, and ensuring platoon stability.

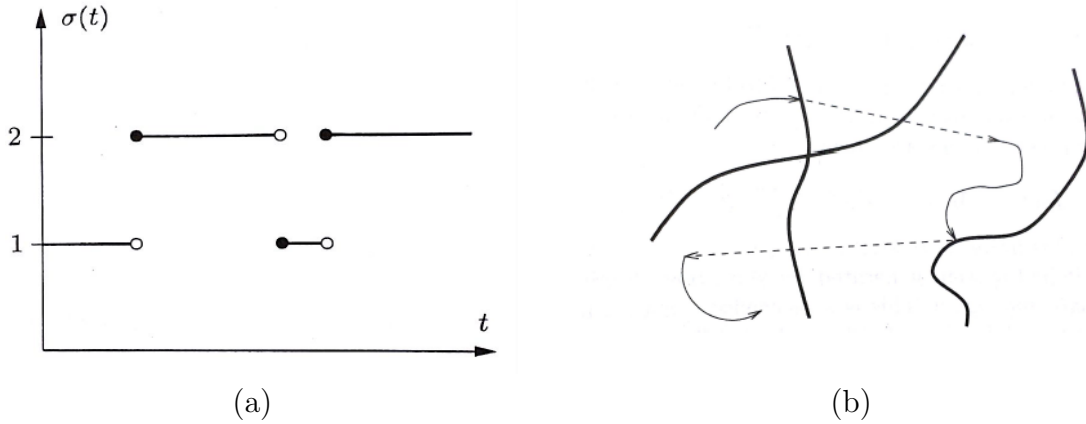


Figure 7.2: Switching via (a) time-dependent and (b) state-dependent signals

7.1 Switched System

A switched system is a type of dynamical system that consists of a collection of subsystems, each of which is active for only a limited period of time. The switching between subsystems is typically determined by a control mechanism or a set of rules that govern the behavior of the system. Thus, in the following context, we focus on how switching control is used to stabilize a nonlinear continuous MASs. (i.e.,

$$\dot{x}(t) = f(t, x(t)) + u_{\sigma(t, x(t))}(t, x(t))$$

where $\sigma(t, x(t)) : \mathbb{R}^+ \times \mathbb{R}^+ \rightarrow \Sigma_0$ is the switching signal function taking a finite index set $\Sigma_0 = 1, 2, \dots, q$ with total of q mode.) Then, based on the expression of $\sigma(t, x(t))$, there are two specific types of switching signal (See Figure 7.2 in [117]):

1. **Time-dependent switching:** the switching between subsystems is determined by time-varying conditions (i.e., $\sigma(t)$).
2. **State-dependent switching:** the switching between subsystems is determined by the system's current states (i.e., $\sigma(t, x(t))$). In particular, the solution trajectory is jumping across the switching surfaces.

Meanwhile, it is inevitable to consider that information flows among different nodes of dynamical systems are not always fixed and stable in many practical applications, such

as robotics, power systems, and communications networks. Instead, mode (subsystem) adjustments are required to deal with the establishment of new communication links and potential transmission failures. Hence, under certain governing switching rules and switching signals, the class of switched systems plays a crucial role in achieving stability among different connection topologies. Considerable research attention has been paid to preserve stability of switched systems with stable and unstable modes. A survey of results on stabilization of switched nonlinear systems with unstable modes has been conducted in [118, 119], while stability of a class of multi-agent tracking systems with unstable subsystems is introduced in [120]. By utilizing mode-dependent average dwell time approach on the switching signals, generalized exponential stability of switched systems can be found in [121, 122], and later the approach has been extended to synchronization of delayed coupled switched neural networks in [123]. Moreover, in contrast to time-dependent switching signals, the state-dependent switching control delayed switched systems with stable and unstable modes can be found in [124, 125]. In this way, the sequence of switching instants is no longer required to be pre-determined. Therefore, we aim to derive sufficient stability criteria of vehicle platoon by using time-dependent and state-dependent switching control, respectively.

7.2 Problem Formulation

Consider a platoon consisting of n vehicles and one virtual leader, where the dynamics of each vehicle can be modelled as follows:

$$\begin{cases} \dot{p}_i(t) = v_i(t) \\ \dot{v}_i(t) = a_i(t) + u_i^{obs} \\ \dot{a}_i(t) = f(v_i(t), a_i(t)) + b_i + u_i, \quad i = 1, 2, \dots, n \end{cases} \quad (7.1)$$

and a virtual leader is planted to regulate the overall vehicle platoon by

$$\begin{cases} \dot{p}_0(t) = v_0(t) \\ \dot{v}_0(t) = a_0(t) \\ \dot{a}_0(t) = -\frac{1}{\kappa}a_0(t) \end{cases} \quad (7.2)$$

Based on [126], the above dynamics encompasses the engine dynamics, brake system and aerodynamics drag. Specifically, $p_i, v_i, a_i \in \mathbb{R}^2$ are bounded position, velocity and acceleration states of the i -th follower vehicle, while $p_0, v_0, a_0 \in \mathbb{R}^2$ are states for virtual leader,

$\xi_i = [p_i^T, v_i^T, a_i^T]^T$. Meanwhile, $u_i^{obs} \in \mathbb{R}^2$ is the control input in charge of collision avoidance, while $u_i \in \mathbb{R}^2$ is the hybrid impulsive control input to be designed hereafter. The nonlinear intrinsic dynamics $f(v_i(t), a_i(t))$ is specified as:

$$f(v_i(t), a_i(t)) = -\frac{1}{\kappa}(a_i(t) + \frac{\zeta\phi c_d}{2m}v_i^T(t)v_i(t) + \frac{d_m}{m}) - \frac{\zeta\phi c_d}{m}v_i^T(t)a_i(t), \quad i = 1, \dots, n \quad (7.3)$$

and we set the nonlinear engine control input b_i as

$$b_i = \frac{1}{2\kappa m}\zeta\phi c_d v_i^T(t)v_i(t) + \frac{d_m}{\kappa m} + \frac{\kappa\zeta\phi c_d}{\kappa m}v_i^T(t)a_i(t), \quad i = 1, \dots, n \quad (7.4)$$

where ζ denotes the specific mass of the air, ϕ is the cross sectional area, c_d describes the drag coefficient, m denotes the mass of vehicle, d_m represents the mechanical drag, κ is the inertial time-lag and the term $\frac{\zeta\phi c_d}{2m}$ models the air resistance. To avoid Zeno phenomenon, denote $l_{\sigma(t_s)}$ as the number of impulsive instants between switching instants t_s and t_{s+1} , then we consider the sequence $\{t_{s,l_{\sigma(t_s)}}, s \in \mathbb{N}, l \in \mathbb{N}^+\}$ as the set of impulsive instants which satisfies $t_s < t_{s,1_{\sigma(t_s)}} < \dots < t_{s,l_{\sigma(t_s)}-1} < t_{s,l_{\sigma(t_s)}} < t_{s+1}$, $\lim_{s \rightarrow \infty} t_{s,l} = \infty$, $l_{\sigma(t_s)} \leq \bar{m} < \infty$ for all $\sigma(t_s) \in \Sigma_0$ and $0 < h_1 = \inf\{t_{s,l_{\sigma(t_s)}} - t_{s,l_{\sigma(t_s)}-1}\} \leq \sup\{t_{s,l_{\sigma(t_s)}} - t_{s,l_{\sigma(t_s)}-1}\} = h_2 < \infty$. For consistency, the right continuity with $p_i(t) = p_i(t^+)$ and $\Delta p_i(t) = p_i(t^+) - p_i(t^-)$ are considered.

Next, consider $\hat{p}_i(t) = p_i(t) - p_0(t) - p_{di}$ where $p_{di} \in \mathbb{R}^2$ prescribe the desired displacement between the i -th follower and the leader vehicle, $\hat{v}_i(t) = v_i(t) - v_0(t)$ and $\hat{a}_i(t) = a_i(t) - a_0(t)$. Then we denote $\bar{p} = [\hat{p}_1^T, \dots, \hat{p}_n^T]^T$, $\bar{v} = [\hat{v}_1^T, \dots, \hat{v}_n^T]^T$, $\bar{a} = [\hat{a}_1^T, \dots, \hat{a}_n^T]^T$, $\bar{u} = [u_1^T, \dots, u_n^T]^T$, $\hat{\xi}_i = [\hat{p}_i^T, \hat{v}_i^T, \hat{a}_i^T]^T$ and $\bar{\xi} = [\bar{p}^T, \bar{v}^T, \bar{a}^T]^T$. By substituting (7.3) and (7.4) into (7.1), thus the i -th error dynamics can be described as follows:

$$\begin{cases} \dot{\hat{\xi}}_i(t) &= A\hat{\xi}_i(t) + \begin{pmatrix} \mathbf{0}_2 \\ u_i^{obs} \\ u_i \end{pmatrix}, \quad i = 1, \dots, n \\ \hat{\xi}_{it_0} &= \varphi_i \end{cases} \quad (7.5)$$

where $A = \begin{pmatrix} \mathbf{0}_{2 \times 2} & I_2 & \mathbf{0}_{2 \times 2} \\ \mathbf{0}_{2 \times 2} & \mathbf{0}_{2 \times 2} & I_2 \\ \mathbf{0}_{2 \times 2} & \mathbf{0}_{2 \times 2} & -(\frac{1}{\kappa})I_2 \end{pmatrix}$, $\hat{\xi}_{it_0}$ is defined as $\hat{\xi}_{it} = \hat{\xi}_i(t + s)$ for $s \in [-\tau_{max}, 0]$ $\varphi_i \in \mathcal{PC}([-\tau_{max}, 0], \mathbb{R}^6)$ for $\tau_{max} > 0$.

Here, additional preliminaries are provided for later use.

Assumption 7.2.1. Assume there exists a linear convex combination $U = \sum_{\bar{s}=1}^q \alpha_{\bar{s}} Q_{\bar{s}}$ for $\bar{s} = 1, 2, \dots, q$, where $Q_{\bar{s}} = \theta_{\bar{s}} I_{6n} \in \mathbb{R}^{6n \times 6n}$ is the matrix to be defined hereafter, and $\alpha_{\bar{s}} \in (0, 1)$ with $\sum_{\bar{s}=1}^q \alpha_{\bar{s}} = 1$. Then there exists $\eta_1 > 1$ and matrix $Q > 0$ so that $U \leq \eta_1 Q$.

Lemma 7.2.1. For given matrix $\bar{Q} > 0$ and constant $\eta_1 > 1$, define the switching region

$$\Omega_{\bar{s}} = \{x \in \mathbb{R}^n : x^T Q_{\bar{s}} x \leq \eta_1 x^T \bar{Q} x\}, \quad \bar{s} = 1, 2, \dots, q \quad (7.6)$$

then $\mathbb{R}^n = \cup_{\bar{s}=1}^q \Omega_{\bar{s}}$.

Proof. Suppose there exists a non-empty region $S \subset \mathbb{R}^n$ such that $S = \mathbb{R}^n \setminus \cup_{\bar{s}=1}^q \Omega_{\bar{s}}$. Then for all $x \in S$, $x \neq 0$, we have

$$x^T Q_{\bar{s}} x > \eta_1 x^T \bar{Q} x \quad (7.7)$$

Based on the definition of $\alpha_{\bar{s}}$ and U in Assumption 7.2.1, we can further deduce that

$$\sum_{\bar{s}=1}^q \alpha_{\bar{s}} x^T Q_{\bar{s}} x = x^T U x \leq \eta_1 x^T \bar{Q} x \quad (7.8)$$

which leads to the contradiction that S is non-empty since $\eta_1 \geq 1$, and thus complete the proof. \square

Definition 7.2.1. The desired cooperative control objectives of the vehicle platoon are achieved if for any given bounded initial states such that

$$\begin{aligned} \lim_{t \rightarrow \infty} \|\hat{p}_i(t) - \hat{p}_j(t)\| &= p_{di} - p_{dj} \\ \lim_{t \rightarrow \infty} \|\hat{v}_i(t)\| &= 0 \\ \lim_{t \rightarrow \infty} \|\hat{a}_i(t)\| &= 0 \end{aligned} \quad (7.9)$$

and the collision-free motion is guaranteed.

Definition 7.2.2. (State-dependent Switching Rule) At each switching, we determine the next mode according to the minimum rule:

$$p(x) = \min_{\bar{s} \in \{1, \dots, q\}} \{x^T Q_{\bar{s}} x\} \quad (7.10)$$

To derive globally exponential stability of the given delayed switched system, we

1. switch only when x hits the boundary of the current switching region $\Omega_{\bar{s}}$.
2. Choose each mode (including the first mode) by applying the minimum rule (7.10).

Remark 7.2.1. *During the entire control switching process, the vehicle platoon dynamics may switch from a stable subsystem to another stable subsystem or an unstable subsystem, and vice versa. Therefore, we additionally set $T_S(t_0, t)$ and $T_U(t_0, t)$ as the total time length of stable and unstable subsystem respectively from t_0 to t . Moreover, the definition of mode-dependent average dwell time can be utilized.*

Definition 7.2.3. [122] *For a switching signal $\sigma(t)$ and any $0 \leq t \leq T$, $\forall \bar{s} = \sigma(t) \in \Sigma_0 = \{1, 2, \dots, q\}$, let $N_{\sigma(t)}(t, T)$ be the number of the switching instants activated subject to the subsystem with switch mode \bar{s} over the interval $[t, T)$, and let $T_{\bar{s}}(t, T)$ denote the total running time of the subsystem with switch mode \bar{s} over the interval $[t, T)$. Thus, the corresponding mode-dependent average dwell time (MDADT) is equal to $\tau_{\bar{s}} > 0$ if there exists a positive integer $\varrho_{\bar{s}}$ so that:*

$$N_{\sigma(t)}(t, T) \leq \frac{T_{\bar{s}}(t, T)}{\tau_{\bar{s}}} + \varrho_{\bar{s}} \quad (7.11)$$

where ϱ_s is the mode-dependent chatter bounds.

Remark 7.2.2. *Figure 7.3 demonstrates the overall communication topology of the vehicle platoon via hybrid impulsive control protocol. Specifically, the topology structure in Figure 7.3(a) is also called the predecessor-following. The root node (i.e., agent 0) represents the remote control centre. Meanwhile, to avoid repetition of analysis regarding collision avoidance illustrated in Chapter 3-5, the following platoon stabilization results are conducted without collision avoidance component.*

7.3 Vehicle Platoon Control via Time-dependent Switching

In order to adapt more practical situation and increase control efficiency in reality, it is worth considering the mode switching of the control inputs, which results in the combination of stable and unstable subsystems. First, the cooperative control protocol via state-independent switching is designed as follows:

$$u_i = k_1 P_C(\cdot, \cdot, \cdot) + k_2 P_D(\cdot, \cdot, \cdot) + k_3 P_L(\cdot, \cdot, \cdot), \quad u_i^{obs} = \hat{P}_{22}^{-1}(\sigma(t)) P_G(\hat{v}_i(t)) \quad (7.12)$$

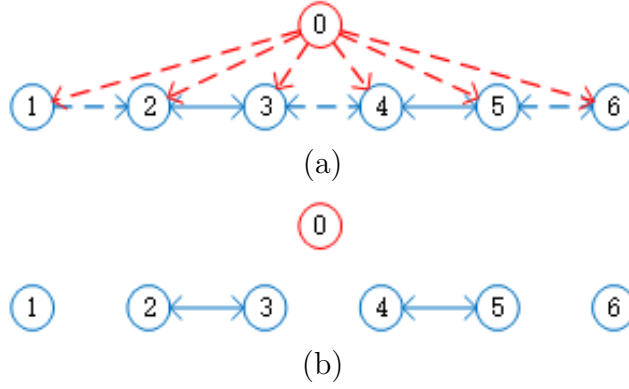


Figure 7.3: (a) Topology structure of leader-following vehicle platoon at $t \neq t_{s,l}$ (b) Topology structure of leader-following vehicle platoon at $t = t_{s,l}$

with

$$\begin{aligned}
P_C(\cdot, \cdot, \cdot) &= - \sum_{j \in N_i^1} b_{ij}(\sigma(t))(\hat{p}_i(t - r(t)) - \hat{p}_j(t - r(t))) - \sum_{j \in N_i^1} b_{ij}(\sigma(t))(\hat{v}_i(t - r(t)) - \hat{v}_j(t - r(t))) \\
&\quad - \sum_{j \in N_i^1} b_{ij}(\sigma(t))(\hat{a}_i(t - r(t)) - \hat{a}_j(t - r(t))) \\
P_D(\cdot, \cdot, \cdot) &= - \sum_{l=1}^{\infty} \sum_{j \in N_i} b_{ij}(\sigma(t))(\hat{p}_i(t - \bar{\tau}) - \hat{p}_j(t - \bar{\tau}))\delta(t - t_l) \\
&\quad - \sum_{l=1}^{\infty} \sum_{j \in N_i} b_{ij}(\sigma(t))(\hat{v}_i(t - \bar{\tau}) - \hat{v}_j(t - \bar{\tau}))\delta(t - t_l) \\
&\quad - \sum_{l=1}^{\infty} \sum_{j \in N_i} b_{ij}(\sigma(t))(\hat{a}_i(t - \bar{\tau}) - \hat{a}_j(t - \bar{\tau}))\delta(t - t_l) \\
P_L(\cdot, \cdot, \cdot) &= - \sum_{l=1}^{\infty} c_i(\sigma(t))\hat{p}_i(t)\delta(t - t_l) - \sum_{l=1}^{\infty} c_i(\sigma(t))\hat{v}_i(t)\delta(t - t_l) - \sum_{l=1}^{\infty} c_i(\sigma(t))\hat{a}_i(t)\delta(t - t_l) \\
P_G(\hat{v}_i(t)) &= \Theta_i(\hat{v}_i(t)) + \Theta_i^{obs}(\hat{v}_i(t)) + G(\hat{v}_i(t)) + G^{obs}(\hat{v}_i(t))
\end{aligned} \tag{7.13}$$

where k_1, k_2, k_3 are positive gains, $\hat{P}_{22}(\sigma(t)) \in \mathbb{R}^{2 \times 2}$ is a positive definite matrix, $\delta(\cdot)$ is the Dirac function, $N_i = \{j = 1, \dots, n \mid \|p_i(t) - p_j(t)\| \leq r_s\}$, where r_s represents the sensing

radius, $N_i^1 \subset N_i$ is the neighbor set associated with the hybrid topology within non-impulse interval, $b_{ij}(\sigma(t))$ is the coupling strength, and $c_i(\sigma(t))$ represents the impulsive tracking gain. $r(t)$ is the continuous time-varying delay satisfying $0 < r(t) \leq h < \infty$ and $\dot{r}(t) < 1$, $\bar{\tau}$ is the constant impulse delay satisfying $0 < \bar{\tau} < h_1 < \infty$.

Remark 7.3.1. Figure 7.4 illustrates some other potential interaction topology of vehicle platoon under different control mode. The structure in Figure 7.4(a) is called two-predecessor following, which enhances the communication among vehicles and stability in comparison to predecessor following topology. Figure 7.4(b) describes the case when control inputs are fully deactivated (i.e., $u_i = 0$), thus each vehicle performs independently and leads to an unstable subsystem.

Remark 7.3.2. Throughout the rest of theoretical analysis, we assume $q = 4$ and there are $q_s = 3$ stable subsystems with $\bar{s} = \sigma(t) \in \Sigma_S = \{1, 2, 4\}$ while $q - q_s = 1$ unstable subsystems with $\bar{s} = \sigma(t) \in \Sigma_U = \{3\}$. In particular, $\sigma(t) = 1$, $\sigma(t) = 2$, $\sigma(t) = 3$ and $\sigma(t) = 4$ correspond to the vehicle platoon structure of predecessor-following single string, two-predecessor-following, full control deactivation and predecessor-following parallel string respectively.

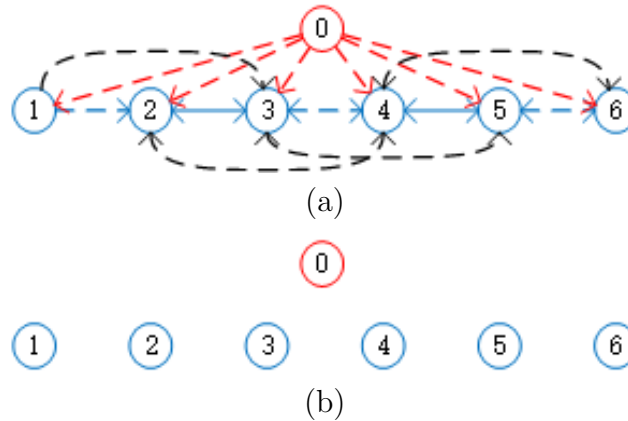


Figure 7.4: (a) Two-predecessor following (b) Full control deactivation

Then the compact error dynamics of (7.5) can be rewritten as:

$$\begin{cases} \dot{\bar{\xi}}(t) &= \bar{A}\bar{\xi}(t) + \bar{E}_{1\sigma(t)}\bar{\xi}(t - r(t)) + \begin{pmatrix} \mathbf{0}_{2n} \\ P_{22}^{-1}(\sigma(t))(P_G(\bar{v}(t)) \otimes \mathbf{1}_n) \\ \mathbf{0}_{2n} \end{pmatrix}, \quad t \neq t_{s,l} \\ \Delta\bar{a}(t) &= -k_3 C_{\sigma(t)}\bar{p}(t) - k_3 C_{\sigma(t)}\bar{v}(t) - k_3 C_{\sigma(t)}\bar{a}(t) \\ &\quad - k_2 L_{\sigma(t)}\bar{p}(t - \bar{\tau}) - k_2 L_{\sigma(t)}\bar{v}(t - \bar{\tau}) - k_2 L_{\sigma(t)}\bar{a}(t - \bar{\tau}), \quad t = t_{s,l} \\ \bar{\xi}_{t_0} &= \bar{\varphi} \end{cases} \quad (7.14)$$

where $\bar{\varphi} = \varphi_i \otimes \mathbf{1}_n$, $\bar{A} = A \otimes I_n$, $P_{22}(\sigma(t)) = \hat{P}_{22}(\sigma(t)) \otimes I_n$, $\bar{E}_{1\sigma(t)} = \begin{pmatrix} \mathbf{0}_{2n \times 2n} & \mathbf{0}_{2n \times 2n} & \mathbf{0}_{2n \times 2n} \\ \mathbf{0}_{2n \times 2n} & \mathbf{0}_{2n \times 2n} & \mathbf{0}_{2n \times 2n} \\ k_1 L'_{\sigma(t)} & k_1 L'_{\sigma(t)} & k_1 L'_{\sigma(t)} \end{pmatrix}$, $C_{\sigma(t)} = \text{diag}\{c_1(\sigma(t)), \dots, c_n(\sigma(t))\}$ and L' represents the Laplacian matrix in terms of $b_{ij}(\sigma(t))$ within non-impulse interval. In addition, denote $\bar{E}_{2\sigma(t)} = \begin{pmatrix} \mathbf{0}_{2n \times 2n} & \mathbf{0}_{2n \times 2n} & \mathbf{0}_{2n \times 2n} \\ \mathbf{0}_{2n \times 2n} & \mathbf{0}_{2n \times 2n} & \mathbf{0}_{2n \times 2n} \\ -k_2 L_{\sigma(t)} & -k_2 L_{\sigma(t)} & -k_2 L_{\sigma(t)} \end{pmatrix}$ and $\bar{E}_{3\sigma(t)} = \begin{pmatrix} I_{2n} & \mathbf{0}_{2n \times 2n} & \mathbf{0}_{2n \times 2n} \\ \mathbf{0}_{2n \times 2n} & I_{2n} & \mathbf{0}_{2n \times 2n} \\ -k_3 C_{\sigma(t)} I_{2n} & -k_3 C_{\sigma(t)} I_{2n} & I_{2n} - k_3 C_{\sigma(t)} I_{2n} \end{pmatrix}$ for later use.

Theorem 7.3.1. *Consider the leader-following vehicle platoon with dynamics (7.1) and (7.2) followed by control protocol (7.12). Suppose Assumption 3.1.1 holds,*

$$P_{\bar{s}} = \begin{pmatrix} \hat{P}_{11}(\bar{s}) \otimes I_n & \hat{P}_{12}(\bar{s}) \otimes I_n & \hat{P}_{31}(\bar{s}) \otimes I_n \\ \hat{P}_{21}(\bar{s}) \otimes I_n & \hat{P}_{22}(\bar{s}) \otimes I_n & \hat{P}_{23}(\bar{s}) \otimes I_n \\ \hat{P}_{31}(\bar{s}) \otimes I_n & \hat{P}_{32}(\bar{s}) \otimes I_n & \hat{P}_{33}(\bar{s}) \otimes I_n \end{pmatrix} \in \mathbb{R}^{6n \times 6n}$$

is a positive definite matrix, $\tau_{max} = h + \bar{\tau}$, $\beta_{\bar{s}} \geq 1$, $\gamma^* \in (0, -\gamma_1)$, $\varepsilon_0, \varepsilon_1, \varepsilon_2 > 0$, $\bar{s}, \hat{s} \in \{1, 2, 3, 4\}$ are distinct switching modes, and the maximal structure energy is bounded by $E_{max} \geq H_{\bar{s}}(t) > 0$, $\zeta_{ij} = \zeta_{ii^\beta} > \frac{2E_{max}}{r_s}$. If the following conditions are satisfied:

$$\begin{pmatrix} P_{\bar{s}}\bar{A} + \bar{A}^T P_{\bar{s}} + (1 - \eta_2)P_{\bar{s}} + \varepsilon_0 I_{6n} & \mathbf{0}_{6n \times 6n} \\ \mathbf{0}_{6n \times 6n} & \frac{q_{\bar{s}} \lambda_{max}(P_{\bar{s}}^{-1})}{2\varepsilon_0} I_{6n} - (1 - \dot{r}(t))P_{\bar{s}} \end{pmatrix} < 0, \quad \forall \bar{s} \in \Sigma_S \quad (7.15)$$

$$P_{\bar{s}} \leq \beta_{\bar{s}} P_{\hat{s}}, \quad \bar{s} \neq \hat{s} \quad (7.16)$$

$$\ln(\rho_{1\bar{s}} + \rho_{2\bar{s}} + W_{\bar{s}}) < -\eta_2 h_2, \quad \forall \bar{s} \in \Sigma_S \quad (7.17)$$

$$\begin{cases} \sum_{\bar{s}=1}^{q_s} (\frac{\ln \beta_{\bar{s}}}{\tau_{\bar{s}}} - \alpha_1^{min}) < 0 \\ \sum_{\bar{s}=q_s+1}^q (\frac{\ln \beta_{\bar{s}}}{\tau_{\bar{s}}} + \eta_2) > 0 \end{cases} \quad (7.18)$$

$$\frac{T_S(t_0, t)}{T_U(t_0, t)} \geq \frac{-\gamma_2 - \gamma^*}{\gamma_1 + \gamma^*} \quad (7.19)$$

with $\eta_2 \geq \lambda_{max}((P_{\bar{s}}\bar{A} + \bar{A}^T P_{\bar{s}} + P_{\bar{s}})P^{-1})$, $W_{\bar{s}} = \frac{\tau_{max} \lambda_{max}(P_{\bar{s}})}{\lambda_{min}(P_{\bar{s}})}$, $\gamma_1 = \sum_{\bar{s}=1}^{q_s} (\frac{\ln \beta_{\bar{s}}}{\tau_{\bar{s}}} - \alpha_1^{min})$, $\gamma_2 = \sum_{\bar{s}=1}^{q_s} (\frac{\ln \beta_{\bar{s}}}{\tau_{\bar{s}}} + \eta_2)$, $\pi_{1\bar{s}} = \lambda_{max}((\bar{E}_{3\bar{s}} + \bar{E}_{2\bar{s}})^T P_{\bar{s}} (\bar{E}_{3\bar{s}} + \bar{E}_{2\bar{s}}) P_{\bar{s}}^{-1})$, $\pi_{2\bar{s}} = 2\lambda_{max}(P_{\bar{s}}) \bar{r}^2 \|\bar{E}_{2\bar{s}}\|^2 \kappa \lambda_{max}(P_{\bar{s}}^{-1})$, $\kappa_{\bar{s}} = (1 + \varepsilon_1) \|\bar{A}\|^2 + (1 + \varepsilon_1^{-1}) \|\bar{E}_{1\bar{s}}\|^2$, $\rho_{1\bar{s}} = \pi_{1\bar{s}}(1 + \varepsilon_2)$, $\rho_{2\bar{s}} = \pi_{2\bar{s}}(1 + \varepsilon_2^{-1})$, $\theta_{\bar{s}} = \|P_{\bar{s}} \bar{E}_{1\bar{s}}\|^2$. Then the collision-free cooperative control of vehicle platoon is achieved with exponential stability.

Proof. Denote $V_{1\bar{s}}(t) = V_{1\bar{s}}(t, \bar{\xi}(t))$ and $V_{2\bar{s}}(t) = V_{2\bar{s}}(t, \bar{\xi}_t)$, then we construct the following Lyapunov-Krasovskii functional for $t \in [t_s, t_{s+1})$:

$$H_{\bar{s}}(t) = V_{1\bar{s}}(t) + V_{2\bar{s}}(t) = \frac{1}{2} \bar{\xi}^T(t) P_{\bar{s}} \bar{\xi}(t) + \frac{1}{2} \int_{t-r(t)}^t \bar{\xi}^T(s) P_{\bar{s}} \bar{\xi}(s) ds \quad (7.20)$$

Once collision avoidance mechanism remains off, based on (7.15), we can take the time derivative of $H_{\bar{s}}$ with $\bar{s} \in \{1, 2, 4\}$ for $t \neq t_{s, l_{\bar{s}}}$ which gives:

$$\begin{aligned} \dot{H}_{\bar{s}}(t) &= \frac{1}{2} \bar{\xi}^T(t) (P_{\bar{s}} \bar{A} + \bar{A}^T P_{\bar{s}}) \bar{\xi}(t) + \frac{1}{2} \bar{\xi}^T(t) P_{\bar{s}} \bar{E}_{1\bar{s}} \bar{\xi}(t-r(t)) + \frac{1}{2} \bar{\xi}^T(t-r(t)) \bar{E}_{1\bar{s}}^T P_{\bar{s}} \bar{\xi}(t) \\ &\quad + \frac{1}{2} \bar{\xi}^T(t) P_{\bar{s}} \bar{\xi}(t) - \frac{1}{2} (1 - \dot{r}(t)) \bar{\xi}^T(t-r(t)) P_{\bar{s}} \bar{\xi}(t-r(t)) \\ &\leq \frac{1}{2} \bar{\xi}^T(t) (P_{\bar{s}} \bar{A} + \bar{A}^T P_{\bar{s}}) \bar{\xi}(t) + \frac{\varepsilon_0}{2} \bar{\xi}^T(t) \bar{\xi}(t) + \frac{\theta_{\bar{s}}}{2\varepsilon_0} \bar{\xi}^T(t-r(t)) \bar{\xi}(t-r(t)) + \eta_2 H_{\bar{s}}(t) \\ &\quad - \frac{\eta_2}{2} \bar{\xi}^T(t) P_{\bar{s}} \bar{\xi}(t) + \frac{1}{2} \bar{\xi}^T(t) P_{\bar{s}} \bar{\xi}(t) - \frac{1}{2} (1 - \dot{r}(t)) \bar{\xi}^T(t-r(t)) P_{\bar{s}} \bar{\xi}(t-r(t)) \\ &= \frac{1}{2} \bar{\xi}^T(t) (P_{\bar{s}} \bar{A} + \bar{A}^T P_{\bar{s}} + (1 - \eta_2) P_{\bar{s}} + \varepsilon_0 I_{6n}) \bar{\xi}(t) + \eta_2 H_{\bar{s}}(t) \\ &\quad + \frac{\theta_{\bar{s}}}{2\varepsilon_0} \bar{\xi}^T(t-r(t)) \bar{\xi}(t-r(t)) - \frac{1}{2} (1 - \dot{r}(t)) \bar{\xi}^T(t-r(t)) P_{\bar{s}} \bar{\xi}(t-r(t)) \\ &\leq \eta_2 H_{\bar{s}}(t) \end{aligned} \quad (7.21)$$

and with $\bar{s} \in \{3\}$ so that

$$\begin{aligned}
\dot{H}_{\bar{s}}(t) &= \frac{1}{2}\bar{\xi}^T(t)(P_{\bar{s}}\bar{A} + \bar{A}^T P_{\bar{s}})\bar{\xi}(t) + \frac{1}{2}\bar{\xi}^T(t)P_{\bar{s}}\bar{\xi}(t) - \frac{1}{2}(1 - \dot{r}(t))\bar{\xi}^T(t - r(t))P_{\bar{s}}\bar{\xi}(t - r(t)) \\
&= \frac{1}{2}\bar{\xi}^T(t)(P_{\bar{s}}\bar{A} + \bar{A}^T P_{\bar{s}} + P_{\bar{s}})\bar{\xi}(t) - \frac{1}{2}(1 - \dot{r}(t))\bar{\xi}^T(t - r(t))P_{\bar{s}}\bar{\xi}(t - r(t)) \\
&\leq \eta_2 H_{\bar{s}}(t)
\end{aligned} \tag{7.22}$$

Meanwhile, one can obtain for $t = t_{s,l_{\bar{s}}}$ and $\bar{s} \in \{1, 2, 4\}$ that:

$$\bar{\xi}(t_{s,l_{\bar{s}}}^-) - \bar{\xi}(t_{s,l_{\bar{s}}} - \bar{\tau}) = \int_{t_{s,l_{\bar{s}}} - \bar{\tau}}^{t_{s,l_{\bar{s}}}} \bar{A}\bar{\xi}(s) + \bar{E}_{1\bar{s}}\bar{\xi}(s - r(s))ds \tag{7.23}$$

and

$$\bar{\xi}(t_{s,l_{\bar{s}}}) = (\bar{E}_{3\bar{s}} + \bar{E}_{2\bar{s}})\bar{\xi}(t_{s,l_{\bar{s}}}^-) - \bar{E}_{2\bar{s}} \int_{t_{s,l_{\bar{s}}} - \bar{\tau}}^{t_{s,l_{\bar{s}}}} \bar{A}\bar{\xi}(z) + \bar{E}_{1\bar{s}}\bar{\xi}(z - r(z))dz = \Gamma_1 + \Gamma_2 \tag{7.24}$$

where $\Gamma_{1\bar{s}} = (\bar{E}_{3\bar{s}} + \bar{E}_{2\bar{s}})\bar{\xi}(t_{s,l_{\bar{s}}}^-)$ and $\Gamma_{2\bar{s}} = -\bar{E}_{2\bar{s}} \int_{t_{s,l_{\bar{s}}} - \bar{\tau}}^{t_{s,l_{\bar{s}}}} \bar{A}\bar{\xi}(z) + \bar{E}_{1\bar{s}}\bar{\xi}(z - r(z))dz$. By applying Schwartz's inequality and Lemma 3.2.1 we have:

$$\begin{aligned}
\Gamma_{1\bar{s}}^T P_{\bar{s}} \Gamma_{1\bar{s}} &= \bar{\xi}(t_{s,l_{\bar{s}}}^-)^T (\bar{E}_{3\bar{s}} + \bar{E}_{2\bar{s}})^T P_{\bar{s}} (\bar{E}_{3\bar{s}} + \bar{E}_{2\bar{s}}) \bar{\xi}(t_{s,l_{\bar{s}}}^-) \\
&\leq \frac{1}{2} \lambda_{max}((\bar{E}_{3\bar{s}} + \bar{E}_{2\bar{s}})^T P_{\bar{s}} (\bar{E}_{3\bar{s}} + \bar{E}_{2\bar{s}}) P_{\bar{s}}^{-1}) V_{1\bar{s}}(t_{s,l_{\bar{s}}}^-) = \pi_{1\bar{s}} V_{1\bar{s}}(t_{s,l_{\bar{s}}}^-)
\end{aligned} \tag{7.25}$$

$$\begin{aligned}
\Gamma_{2\bar{s}}^T P_{\bar{s}} \Gamma_{2\bar{s}} &\leq \lambda_{max}(P_{\bar{s}}) \|\bar{E}_{2\bar{s}}\|^2 \left[\int_{t_{s,l_{\bar{s}}} - \bar{\tau}}^{t_{s,l_{\bar{s}}}} \bar{A}\bar{\xi}(z) + \bar{E}_{1\bar{s}}\bar{\xi}(z - r(z))dz \right]^T \left[\int_{t_{s,l_{\bar{s}}} - \bar{\tau}}^{t_{s,l_{\bar{s}}}} \bar{A}\bar{\xi}(z) + \bar{E}_{1\bar{s}}\bar{\xi}(z - r(z))dz \right] \\
&\leq \lambda_{max}(P_{\bar{s}}) \bar{\tau} \|\bar{E}_{2\bar{s}}\|^2 \int_{t_{s,l_{\bar{s}}} - \bar{\tau}}^{t_{s,l_{\bar{s}}}} (\bar{A}\bar{\xi}(z) + \bar{E}_{1\bar{s}}\bar{\xi}(z - r(z)))^T (\bar{A}\bar{\xi}(z) + \bar{E}_{1\bar{s}}\bar{\xi}(z - r(z))) dz \\
&\leq \lambda_{max}(P_{\bar{s}}) \bar{\tau} \|\bar{E}_{2\bar{s}}\|^2 \int_{t_{s,l_{\bar{s}}} - \bar{\tau}}^{t_{s,l_{\bar{s}}}} [(1 + \varepsilon_1) \|\bar{A}\|^2 \bar{\xi}^T(z) \bar{\xi}(z) \\
&\quad + (1 + \varepsilon_1^{-1}) \|\bar{E}_{1\bar{s}}\|^2 \bar{\xi}^T(z - r(z)) \bar{\xi}(z - r(z))] dz \\
&\leq \lambda_{max}(P_{\bar{s}}) \bar{\tau} \|\bar{E}_{2\bar{s}}\|^2 \int_{t_{s,l_{\bar{s}}} - \bar{\tau}}^{t_{s,l_{\bar{s}}}} \kappa_{\bar{s}} \sup_{r(z) \in [0, h]} \bar{\xi}^T(z - r(z)) \bar{\xi}(z - r(z)) dz \\
&\leq 2\lambda_{max}(P_{\bar{s}}) \bar{\tau}^2 \|\bar{E}_{2\bar{s}}\|^2 \kappa_{\bar{s}} \lambda_{max}(P_{\bar{s}}^{-1}) \sup_{z \in [-h - \bar{\tau}, 0]} V_{1\bar{s}}(t_{s,l_{\bar{s}}}^- + z) \\
&\leq \pi_{2\bar{s}} \sup_{z \in [-\tau_{max}, 0]} V_{1\bar{s}}(t_{s,l_{\bar{s}}}^- + z)
\end{aligned} \tag{7.26}$$

Based on (7.25) and (7.26), it gives:

$$\begin{aligned}
2V_{1\bar{s}}(t_s, l_{\bar{s}}) &= (\Gamma_{1\bar{s}} + \Gamma_{2\bar{s}})^T P_{\bar{s}} (\Gamma_{1\bar{s}} + \Gamma_{2\bar{s}}) \\
&\leq (1 + \varepsilon_2) \Gamma_{1\bar{s}}^T P_{\bar{s}} \Gamma_{1\bar{s}} + (1 + \varepsilon_2^{-1}) \Gamma_{2\bar{s}}^T P_{\bar{s}} \Gamma_{2\bar{s}} \\
&\leq \pi_{1\bar{s}} (1 + \varepsilon_2) V_{1\bar{s}}(t_{s, l_{\bar{s}}}^-) + \pi_{2\bar{s}} (1 + \varepsilon_2^{-1}) \sup_{z \in [-\tau_{max}, 0]} V(t_{s, l_{\bar{s}}}^- + z)
\end{aligned} \tag{7.27}$$

Thus, (7.27) yields,

$$V_{1\bar{s}}(t_s, l_{\bar{s}}) \leq \rho_{1\bar{s}} V_{1\bar{s}}(t_{s, l_{\bar{s}}}^-) + \rho_{2\bar{s}} \sup_{z \in [-\tau_{max}, 0]} \{V_{1\bar{s}}(t_{s, l_{\bar{s}}}^- + z)\} \tag{7.28}$$

From condition (7.17), (7.21) and (7.27), Lemma 3.1.3 is now applicable. Hence, there exists a constant $\alpha_{1\bar{s}} > 0$ such that

$$H_{\bar{s}}(t) \leq H_{\bar{s}}(t_s) e^{(\alpha_1^{\max} + \eta_2) i_{S\bar{s}} h_2} e^{-\alpha_1^{\min}(t-t_s)}, \quad \bar{s} \in \Sigma_S, \quad t \in [t_s, t_{s+1}) \tag{7.29}$$

where $0 < \alpha_1^{\min} \leq \alpha_{1\bar{s}} \leq \alpha_1^{\max}$ for all $\bar{s} \in \Sigma_S$, $i_{S\bar{s}} \in \mathbb{N}$ is the first index of impulsive instant such that $t_{s, i_{S\bar{s}}} - \tau_{max} \geq t_s$ for all $\bar{s} \in \Sigma_S$. Next, we aim to establish the relation similar to (7.29) among unstable subsystems. Similarly, there exist $i_{U\bar{s}} \in \mathbb{N}$ and another constant $\alpha_{2\bar{s}} > 0$ for all $\bar{s} \in \Sigma_U$ such that

$$\ln\left(1 + \frac{\tau_{max} \lambda_{max}(P_{\bar{s}})}{\lambda_{min}(P_{\bar{s}})}\right) = \alpha_{2\bar{s}} h_1, \quad \bar{s} \in \Sigma_U, \quad t \in [t_s, t_{s+1}) \tag{7.30}$$

where $\alpha_2^{\min} \leq \alpha_{2\bar{s}} \leq \alpha_2^{\max}$ for all $\bar{s} \in \Sigma_U$. Also, for $t \in [t_s, t_{s, i_{U\bar{s}}})$ we have

$$H_{\bar{s}}(t) = H_{\bar{s}}(t) e^{-\alpha_{2\bar{s}}(t-t_s)} e^{\alpha_{2\bar{s}}(t-t_s)} \leq F_{\bar{s}} e^{\alpha_{2\bar{s}}(t-t_s)} \tag{7.31}$$

where $F_{\bar{s}} = \sup_{t \in [t_s, t_{s, i_{U\bar{s}}})} \{H_{\bar{s}}(t)\}$. Then we prove that

$$H_{\bar{s}}(t) \leq F_{\bar{s}} e^{\alpha_{2\bar{s}}(t_s, l_{\bar{s}} + 1 - t_s)} e^{\eta_2(t-t_s)}, \quad t \in [t_s, l_{\bar{s}}, t_s, l_{\bar{s}} + 1), \quad l_{\bar{s}} \geq i_{U\bar{s}} \tag{7.32}$$

When $l_{\bar{s}} = i_{U\bar{s}}$, in the absence of control impulses, we can get that

$$V_{1\bar{s}}(t_s, i_{U\bar{s}}) \leq H_{\bar{s}}(t_{s, i_{U\bar{s}}}^-) \leq F_{\bar{s}} e^{\alpha_{2\bar{s}}(t_s, i_{U\bar{s}} - t_s)} \tag{7.33}$$

By (7.31) and the continuity of $V_{2\bar{s}}$, it gives

$$\begin{aligned}
V_{2\bar{s}}(t_s, i_{U\bar{s}}) &\leq V_{2\bar{s}}(t_{s, i_{U\bar{s}}}^-) \\
&\leq \frac{\tau_{max} \lambda_{max}(P_{\bar{s}})}{2} \sup_{z \in [-\tau_{max}, 0]} \|\bar{\xi}(t_s, i_{U\bar{s}} + z)\|^2 \\
&\leq W_{\bar{s}} F_{\bar{s}} e^{\alpha_{2\bar{s}}(t_s, i_{U\bar{s}} - \tau_{max} - t_s)} \\
&\leq W_{\bar{s}} F_{\bar{s}} e^{\alpha_{2\bar{s}}(t_s, i_{U\bar{s}} - t_s)}
\end{aligned} \tag{7.34}$$

Then, (7.33) and (7.34) imply that

$$\begin{aligned}
H_{\bar{s}}(t_{s,i_{U_{\bar{s}}}}) &= V_{1\bar{s}}(t_{s,i_{U_{\bar{s}}}}) + V_{2\bar{s}}(t_{s,i_{U_{\bar{s}}}}) \\
&\leq (1 + W_{\bar{s}})F_{\bar{s}}e^{\alpha_{2\bar{s}}(t_{s,i_{U_{\bar{s}}}-t_s)} \\
&= e^{\alpha_{2\bar{s}}h_1}F_{\bar{s}}e^{\alpha_{2\bar{s}}(t_{s,i_{U_{\bar{s}}}-t_s)} \\
&\leq e^{\alpha_{2\bar{s}}(t_{s,i_{U_{\bar{s}}+1}-t_{s,i_{U_{\bar{s}}})}F_{\bar{s}}e^{(\alpha_{2\bar{s}}+\eta_2)(t_{s,i_{U_{\bar{s}}}-t_s)} \\
&= e^{\alpha_{2\bar{s}}(t_{s,i_{U_{\bar{s}}+1}-t_s)}F_{\bar{s}}e^{\eta_2(t_{s,i_{U_{\bar{s}}}-t_s)}
\end{aligned} \tag{7.35}$$

Thus, (7.32) holds true for $t = t_{s,i_{\bar{s}}}$, and

$$H_{\bar{s}}(t) \leq H_{\bar{s}}(t_{s,i_{U_{\bar{s}}}})e^{\eta_2(t-t_{s,i_{U_{\bar{s}}})} \leq F_{\bar{s}}e^{\alpha_{2\bar{s}}(t_{s,i_{U_{\bar{s}}+1}-t_s)}e^{\eta_2(t-t_s)}, \quad t \in (t_{s,i_{U_{\bar{s}}}}, t_{s,i_{U_{\bar{s}}+1}}) \tag{7.36}$$

implies (7.32) holds true for $t \in (t_{s,i_{U_{\bar{s}}}}, t_{s,i_{U_{\bar{s}}+1}})$. Therefore, (7.32) is obtained for $l_{\bar{s}} = i_{U_{\bar{s}}}$. Moreover, suppose (7.32) holds true for $l_{\bar{s}} \leq j_{\bar{s}}$ with $j_{\bar{s}} > i_{U_{\bar{s}}}$. Then when $t = t_{s,j_{\bar{s}}}$, from (7.31) and (7.32) we have

$$\begin{aligned}
H_{\bar{s}}(t_{s,j_{\bar{s}}+1} + z) &\leq F_{\bar{s}}e^{\alpha_{2\bar{s}}(t_{s,j_{\bar{s}}+1}+z-t_s)} \\
&\leq F_{\bar{s}}e^{\alpha_{2\bar{s}}(t_{s,j_{\bar{s}}+1}-t_s)}e^{\eta_2(t_{s,j_{\bar{s}}+1}-t_s)}, \quad z \in [-\tau_{max}, 0], \quad t_{s,j_{\bar{s}}+1} + z < t_{s,i_{U_{\bar{s}}}}
\end{aligned} \tag{7.37}$$

and

$$\begin{aligned}
H_{\bar{s}}(t_{s,j_{\bar{s}}+1} + z) &\leq F_{\bar{s}}e^{\alpha_{2\bar{s}}(t_{s,j_{\bar{s}}+1}+z-t_s)}e^{\eta_2(t_{s,j_{\bar{s}}+1}+z-t_s)} \\
&\leq F_{\bar{s}}e^{\alpha_{2\bar{s}}(t_{s,j_{\bar{s}}+1}-t_s)}e^{\eta_2(t_{s,j_{\bar{s}}+1}-t_s)}, \quad z \in [-\tau_{max}, 0], \quad t_{s,j_{\bar{s}}+1} + z \geq t_{s,i_{U_{\bar{s}}}}
\end{aligned} \tag{7.38}$$

For all $z \in [-\tau_{max}, 0]$, combining (7.37) and (7.38) gives

$$H_{\bar{s}}(t_{s,j_{\bar{s}}+1} + z) \leq F_{\bar{s}}e^{\alpha_{2\bar{s}}(t_{s,j_{\bar{s}}+1}-t_s)}e^{\eta_2(t_{s,j_{\bar{s}}+1}-t_s)} \tag{7.39}$$

Furthermore, similar to (7.33) and (7.34), (7.39) implies that

$$\begin{aligned}
V_{1\bar{s}}(t_{s,j_{\bar{s}}+1}) &\leq F_{\bar{s}}e^{\alpha_{2\bar{s}}(t_{s,j_{\bar{s}}+1}-t_s)}e^{\eta_2(t_{s,j_{\bar{s}}+1}-t_s)} \\
V_{2\bar{s}}(t_{s,j_{\bar{s}}+1}) &\leq W_{\bar{s}}F_{\bar{s}}e^{\alpha_{2\bar{s}}(t_{s,j_{\bar{s}}+1}-t_s)}e^{\eta_2(t_{s,j_{\bar{s}}+1}-t_s)}
\end{aligned} \tag{7.40}$$

Then, (7.40) leads to

$$\begin{aligned}
H_{\bar{s}}(t_{s,j_{\bar{s}}+1}) &\leq (1 + W_{\bar{s}})F_{\bar{s}}e^{\alpha_{2\bar{s}}(t_{s,j_{\bar{s}}+1}-t_s)}e^{\eta_2(t_{s,j_{\bar{s}}+1}-t_s)} \\
&\leq e^{\alpha_{2\bar{s}}(t_{s,j_{\bar{s}}+2}-t_{s,j_{\bar{s}}+1})}F_{\bar{s}}e^{\alpha_{2\bar{s}}(t_{s,j_{\bar{s}}+1}-t_s)}e^{\eta_2(t_{s,j_{\bar{s}}+1}-t_s)} \\
&= F_{\bar{s}}e^{\alpha_{2\bar{s}}(t_{s,j_{\bar{s}}+2}-t_s)}e^{\eta_2(t_{s,j_{\bar{s}}+1}-t_s)}
\end{aligned} \tag{7.41}$$

which satisfies (7.32) for $t = t_{s,j_{\bar{s}}+1}$, and

$$H_{\bar{s}}(t) \leq H_{\bar{s}}(t_{s,j_{\bar{s}}+1})e^{\eta_2(t-t_{s,j_{\bar{s}}+1})} \leq F_{\bar{s}}e^{\alpha_2 i_{U_{\bar{s}}}(t_{s,j_{\bar{s}}+2}-t_{s,j_{\bar{s}}+1})} e^{\eta_2(t-t_{s,j_{\bar{s}}+1})}, \quad t \in (t_{s,j_{\bar{s}}+1}, t_{s,j_{\bar{s}}+2}) \quad (7.42)$$

implies (7.32) holds true for $t \in (t_{s,j_{\bar{s}}+1}, t_{s,j_{\bar{s}}+2})$. Therefore, (7.32) is obtained for $l_{\bar{s}} = j_{\bar{s}} + 1$. Consequently, (7.32) holds true for all $l_{\bar{s}} \geq i_{U_{\bar{s}}}$ by using mathematical induction, which gives

$$H_{\bar{s}}(t) \leq H_{\bar{s}}(t_s)e^{\eta_2 i_{U_{\bar{s}}} h_2} e^{\alpha_2^{\max} \bar{m} h_2} e^{\eta_2(t-t_s)}, \quad \bar{s} \in \Sigma_U, \quad t \in [t_s, t_{s+1}) \quad (7.43)$$

By combining (7.16), (7.29) and (7.43), for any $t \geq t_0$, we have

$$\begin{aligned} H_{\bar{s}}(t) &\leq H_{\sigma(t_0)}(t_0) [\beta_{\sigma(t_s)} \beta_{\sigma(t_{s-1})} \dots \beta_{\sigma(t_1)}] e^{((\alpha_1^{\max} + \eta_2) i_{S_{\bar{s}}} + \eta_2 i_{U_{\bar{s}}}) h_2} e^{\alpha_2^{\max} \bar{m} h_2} e^{-\alpha_1^{\min} T_S(t_0, t) + \eta_2 T_U(t_0, t)} \\ &\leq \zeta H_{\sigma(t_0)}(t_0) \left(\prod_{\bar{s}=1}^q \beta_{\bar{s}}^{N_{\bar{s}}(t_0, t)} \right) e^{-\alpha_1^{\min} T_S(t_0, t) + \eta_2 T_U(t_0, t)} \\ &\leq \zeta H_{\sigma(t_0)}(t_0) \exp \left\{ \sum_{\bar{s}=1}^q \ln \beta_{\bar{s}} \left(\varrho_{\bar{s}} + \frac{T_{\bar{s}}(t_0, t)}{\tau_{\bar{s}}} \right) \right\} e^{-\alpha_1^{\min} T_S(t_0, t) + \eta_2 T_U(t_0, t)} \\ &\leq \bar{\zeta} H_{\sigma(t_0)}(t_0) \exp \left\{ \sum_{\bar{s}=1}^{q_s} \left(\frac{\ln \beta_{\bar{s}}}{\tau_{\bar{s}}} - \alpha_1^{\min} \right) T_S(t_0, t) + \sum_{\bar{s}=q_s+1}^q \left(\frac{\ln \beta_{\bar{s}}}{\tau_{\bar{s}}} + \eta_2 \right) T_U(t_0, t) \right\} \\ &\leq \bar{\zeta} H_{\sigma(t_0)}(t_0) \exp \{ \gamma_1 T_S(t_0, t) + \gamma_2 T_U(t_0, t) \} \end{aligned} \quad (7.44)$$

where $\zeta = e^{\alpha_2^{\max} \bar{m} h_2} \max_{\bar{s} \in \Sigma_S} \{ e^{(\alpha_1^{\max} + \eta_2) i_{S_{\bar{s}}} h_2} \} \max_{\bar{s} \in \Sigma_U} \{ e^{\eta_2 i_{U_{\bar{s}}} h_2} \}$, $\bar{\zeta} = \zeta \prod_{\bar{s}=1}^q \beta_{\bar{s}}^{\varrho_{\bar{s}}}$. From condition (7.18) and (7.19), we can get

$$(\gamma_1 + \gamma^*) T_S(t_0, t) + (\gamma_2 + \gamma^*) T_U(t_0, t) = \gamma_1 T_S(t_0, t) + \gamma_2 T_U(t_0, t) + \gamma^* (T_S(t_0, t) + T_U(t_0, t)) \leq 0 \quad (7.45)$$

and it gives

$$\gamma_1 T_S(t_0, t) + \gamma_2 T_U(t_0, t) \leq -\gamma^* (t - t_0) \quad (7.46)$$

Combine (7.44) and (7.46), it gives directly that

$$H_{\bar{s}}(t) \leq \bar{\zeta} H_{\sigma(t_0)}(t_0) e^{-\gamma^* (t - t_0)} \quad (7.47)$$

In addition, since

$$H_{\sigma(t_0)}(t_0) \leq \frac{\max\{1, \tau_{max}\} \max_{\bar{s}=1, \dots, q} \{\lambda_{max}(P_{\bar{s}})\}}{2} \|\bar{\varphi}\|_{\tau_{max}}^2 \quad (7.48)$$

we end up with

$$\begin{aligned}\|\bar{\xi}(t)\|^2 &\leq \frac{\bar{\zeta}\mu_{max}}{\mu_{min}} e^{-\gamma^*(t-t_0)} \|\bar{\varphi}\|_{\tau_{max}}^2 \\ \|\bar{\xi}(t)\| &\leq \sqrt{\frac{\bar{\zeta}\mu_{max}}{\mu_{min}}} e^{-\frac{\gamma^*}{2}(t-t_0)} \|\bar{\varphi}\|_{\tau_{max}}\end{aligned}\tag{7.49}$$

where $\mu_{max} = \frac{\max\{1, \tau_{max}\} \max_{\bar{s}=1, \dots, q} \{\lambda_{max}(P_{\bar{s}})\}}{2}$ and $\mu_{min} = \frac{\min_{\bar{s}=1, \dots, q} \{\lambda_{min}(P_{\bar{s}})\}}{2}$. Thus, the exponential stability of the vehicle platoon is achieved under the proposed hybrid impulsive control protocol (7.12). Meanwhile, same collision avoidance proof as shown in Theorem 3.4.1 can be applied to the vehicle platoon system, thus the absence of inter-collision and collision with environmental obstacles (i.e., vehicles outside the platoon, road blocks, median strip) under switching are guaranteed. \square

Remark 7.3.3. *Over the past years, most of the existing cooperative control results have focused on the switching process regarding continuous dynamics such as [125, 127, 128]. In [124], stability and stabilization of impulsive switched systems have been considered, yet the sequences of switching and impulsive instants are coincided. Meanwhile, [123] investigated the impulsive switched neural network under stable continuous dynamics with time-varying delay, where the real-time impulses only play the role of accelerating stability convergence or creating disturbances. Therefore, Theorem 7.3.1 has provided more general and sufficient results for achieving exponential stabilization under destabilizing continuous dynamics while taking both time-varying delay and delayed impulses into the design of hybrid impulsive control protocol. Specifically, condition (7.17) and (7.18) indicate that the stability of vehicle platoon is highly sensitive to impulsive strengths $\rho_{1\bar{s}}, \rho_{2\bar{s}}$, mode-dependent average dwell time $\tau_{\bar{s}}$ and switching parameter $\beta_{\bar{s}}$; whereas condition (7.19) establish the feasible ratio to the total time length that allowed for stable and unstable subsystems. In addition, $\beta_{\bar{s}} > 1$ indicates the slow switching scheme, while fast switching is adopted when $0 < \beta_{\bar{s}} < 1$ and switching signals satisfy the reverse MDADT condition instead (i.e., $N_{\sigma(t)}(t, T) \geq \frac{T_{\bar{s}}(t, T)}{\tau_{\bar{s}}} - \varrho_{\bar{s}}$).*

Remark 7.3.4. *The setup of control-free interval in Theorem 7.3.1 aims to describe the situation with respect to temporal malfunction or necessary energy management of controller. It helps to increase the fault tolerance efficiently during stabilization process. Meanwhile, it gives $\rho_{1\bar{s}} = 1, \rho_{2\bar{s}}, i_{U\bar{s}}, \bar{m} = 0$ in the absence of control impulses. Otherwise, with impulsive disturbances (i.e., $\rho_{1\bar{s}} + \rho_{2\bar{s}} > 1$), we can modify (7.30) by*

$$\ln(\rho_{1\bar{s}} + \rho_{2\bar{s}} + \frac{\tau_{max}\lambda_{max}(P_{\bar{s}})}{\lambda_{min}(P_{\bar{s}})}) = \alpha_{2\bar{s}}h_1, \quad \bar{s} \in \Sigma_U, \quad t \in [t_s, t_{s+1})$$

and the rest of results can be obtained accordingly.

7.4 Vehicle Platoon Control via State-dependent Switching

Notice that the switching process in Theorem 7.3.1 is time-dependent, this means that the overall stability of dynamics relies on the total time length of stable and unstable subsystems, which needs to be pre-determined. Therefore, in order to further minimize manual interference and increase automation capabilities in practice, we apply our control protocols via state-dependent switching in the following section. Compared to Theorem 7.3.1, we consider switching modes with stabilizing control impulses (i.e., $\bar{s} \in \Sigma_S$) in terms of the switching rule presented in Definition 7.2.2.

Theorem 7.4.1. *Consider the leader-following vehicle platoon with dynamics (7.1) and (7.2) followed by control protocol (7.12). Suppose Assumption 3.1.1 and Assumption 7.2.1 hold,*

$$P = \begin{pmatrix} \hat{P}_{11} \otimes I_n & \hat{P}_{12} \otimes I_n & \hat{P}_{31} \otimes I_n \\ \hat{P}_{21} \otimes I_n & \hat{P}_{22} \otimes I_n & \hat{P}_{23} \otimes I_n \\ \hat{P}_{31} \otimes I_n & \hat{P}_{32} \otimes I_n & \hat{P}_{33} \otimes I_n \end{pmatrix} \in \mathbb{R}^{6n \times 6n}$$

is a positive definite matrix, $\bar{Q} > 0$, $\eta_1 > 1$, $\tau_{max} = h + \bar{\tau}$, $\alpha_{\bar{s}} \in (0, 1)$, $\varepsilon_0, \varepsilon_1, \varepsilon_2, \varepsilon_4, \varepsilon_5 > 0$, and the maximal structure energy is bounded by $E_{max} \geq H(t) > 0$, $\zeta_{ij} = \zeta_{ii^\beta} > \frac{2E_{max}}{r_s}$. If the following conditions are satisfied for $\bar{s} \in \{1, 2, 4\}$:

$$\frac{1}{\rho_3 + \rho_4} > e^{(\eta_3 + \frac{\eta_4}{\rho_3 + \rho_4})h_2} > 1 \quad (7.50)$$

with $\pi_{1\bar{s}} = \lambda_{max}((\bar{E}_{3\bar{s}} + \bar{E}_{2\bar{s}})^T P (\bar{E}_{3\bar{s}} + \bar{E}_{2\bar{s}}) P^{-1})$, $\pi_{2\bar{s}} = 2\lambda_{max}(P) \bar{\tau}^2 \|\bar{E}_{2\bar{s}}\|^2 \kappa \lambda_{max}(P^{-1})$, $\kappa_{\bar{s}} = (1 + \varepsilon_1) \|\bar{A}\|^2 + (1 + \varepsilon_1^{-1}) \|\bar{E}_{1\bar{s}}\|^2$, $\theta_{\bar{s}} = \|P \bar{E}_{1\bar{s}}\|^2$,

$$\begin{aligned} \rho_3 &= \max_{\bar{s}=1, \dots, q} \{\pi_{1\bar{s}}(1 + \varepsilon_2)\} \\ \rho_4 &= \max_{\bar{s}=1, \dots, q} \{\pi_{2\bar{s}}(1 + \varepsilon_2^{-1})\} \\ \eta_3 &= \lambda_{max}((P \bar{A} + \bar{A}^T P + \varepsilon_0 I_{6n}) P^{-1}) \\ \eta_4 &= \frac{\eta_1 \lambda_{max}(\bar{Q}) \lambda_{max}(P^{-1})}{\varepsilon_0} \end{aligned}$$

Then the collision-free cooperative control of vehicle platoon is achieved with exponential stability.

Proof. Based on Assumption 7.2.1, we construct the following common Lyapunov function for $t \in [t_s, t_{s+1})$:

$$H(t) = \frac{1}{2} \bar{\xi}^T(t) P \bar{\xi}(t) \quad (7.51)$$

which gives that

$$\frac{\lambda_{\min}(P)}{2} \|\bar{\xi}^T(t)\|^2 \leq H(t) \leq \frac{\lambda_{\max}(P)}{2} \|\bar{\xi}^T(t)\|^2 \quad (7.52)$$

and $H(t)$ is now continuous everywhere except at each impulsive instants. Then we can take the time derivative of $H(t)$ when $t \neq t_{s, l_{\sigma}(t_s)}$ by applying Lemma 7.2.1:

$$\begin{aligned} \dot{H}(t) &= \frac{1}{2} \bar{\xi}^T(t) (P\bar{A} + \bar{A}^T P) \bar{\xi}(t) + \frac{1}{2} \bar{\xi}^T(t) P \bar{E}_{1\bar{s}} \bar{\xi}(t-r(t)) + \frac{1}{2} \bar{\xi}^T(t-r(t)) \bar{E}_{1\bar{s}}^T P \bar{\xi}(t) \\ &\leq \frac{1}{2} \bar{\xi}^T(t) (P\bar{A} + \bar{A}^T P) \bar{\xi}(t) + \frac{\varepsilon_0}{2} \bar{\xi}^T(t) \bar{\xi}(t) + \frac{\theta_{\bar{s}}}{2\varepsilon_0} \bar{\xi}^T(t-r(t)) \bar{\xi}(t-r(t)) \\ &= \frac{1}{2} \bar{\xi}^T(t) (P\bar{A} + \bar{A}^T P + \varepsilon_0 I_{6n}) \bar{\xi}(t) + \frac{\theta_{\bar{s}}}{2\varepsilon_0} \bar{\xi}^T(t-r(t)) \bar{\xi}(t-r(t)) \\ &\leq \frac{1}{2} \bar{\xi}^T(t) (P\bar{A} + \bar{A}^T P + \varepsilon_0 I_{6n}) \bar{\xi}(t) + \frac{\eta_1 \lambda_{\max}(\bar{Q}) \lambda_{\max}(P^{-1})}{2\varepsilon_0} \bar{\xi}^T(t-r(t)) P \bar{\xi}(t-r(t)) \\ &= \eta_3 H(t) + \eta_4 H(t-r(t)) \\ &\leq \eta_3 H(t) + \eta_4 \sup_{s \in [-\tau_{\max}, 0]} H(t+s) \end{aligned} \quad (7.53)$$

Meanwhile, similar to (7.23)-(7.27), one can obtain when $t = t_{s, l_{\bar{s}}}$ that:

$$\begin{aligned} \Gamma_{1\bar{s}}^T P \Gamma_{1\bar{s}} &= \bar{\xi}(t_{s, l_{\bar{s}}}^-)^T (\bar{E}_{3\bar{s}} + \bar{E}_{2\bar{s}})^T P (\bar{E}_{3\bar{s}} + \bar{E}_{2\bar{s}}) \bar{\xi}(t_{s, l_{\bar{s}}}^-) \\ &\leq \frac{1}{2} \lambda_{\max}((\bar{E}_{3\bar{s}} + \bar{E}_{2\bar{s}})^T P (\bar{E}_{3\bar{s}} + \bar{E}_{2\bar{s}}) P^{-1}) H(t_{s, l_{\bar{s}}}^-) = \pi_{1\bar{s}} H(t_{s, l_{\bar{s}}}^-) \end{aligned} \quad (7.54)$$

$$\Gamma_{2\bar{s}}^T P \Gamma_{2\bar{s}} \leq 2\lambda_{\max}(P) \bar{\tau}^2 \|\bar{E}_{2\bar{s}}\|^2 \kappa_{\bar{s}} \lambda_{\max}(P) \sup_{z \in [-h-\bar{\tau}, 0]} H(t_{s, l_{\bar{s}}}^- + z) \leq \pi_{2\bar{s}} \sup_{z \in [-\tau_{\max}, 0]} H(t_{s, l_{\bar{s}}}^- + z) \quad (7.55)$$

and

$$\begin{aligned} 2H(t_{s, l_{\bar{s}}}) &= (\Gamma_{1\bar{s}} + \Gamma_{2\bar{s}})^T P (\Gamma_{1\bar{s}} + \Gamma_{2\bar{s}}) \\ &\leq (1 + \varepsilon_2) \Gamma_{1\bar{s}}^T P \Gamma_{1\bar{s}} + (1 + \varepsilon_2^{-1}) \Gamma_{2\bar{s}}^T P \Gamma_{2\bar{s}} \\ &\leq \pi_{1\bar{s}} (1 + \varepsilon_2) H(t_{s, l_{\bar{s}}}^-) + \pi_{2\bar{s}} (1 + \varepsilon_2^{-1}) \sup_{z \in [-\tau_{\max}, 0]} H(t_{s, l_{\bar{s}}}^- + z) \end{aligned} \quad (7.56)$$

Thus,

$$H(t_{s,l_{\bar{s}}}) \leq \rho_3 H(t_{s,l_{\bar{s}}}^-) + \rho_4 \sup_{z \in [-\tau_{max}, 0]} \{H(t_{s,l_{\bar{s}}}^- + z)\} \quad (7.57)$$

Since $\eta_3, \eta_4, \rho_3, \rho_4, P$ are all independent of the choice of the switching mode; thus based on (7.50), we obtain $\lim_{t \rightarrow \infty} H(t) \rightarrow 0$ from Lemma 3.1.2. In addition, we denote the sequence $\{\hat{t}_l, l \in \mathbb{N}^+\}$ as the set of impulsive instants occurred on the entire time interval regardless of the switching mode. Hence, in order to further obtain the globally exponential stability, similar to Theorem 3.1 in [67], from (3.10) there exists a constant q and one can choose a small enough constant $\lambda > 0$ such that

$$q > \frac{e^{\lambda \tau_{max}}}{\rho_3 + \rho_4 e^{\lambda \tau_{max}}} > \frac{1}{\rho_3 + \rho_4 e^{\lambda \tau_{max}}} > e^{(\eta_3 + q\eta_4 + \lambda)h_2} \quad (7.58)$$

if $H(t+z) \leq qH(t)$ for all $z \in [-\tau_{max}, 0]$ and $\bar{q} = qe^{-\lambda \tau_{max}} > 1$. Then, choose $M > \frac{\bar{q} \lambda_{max}(P)}{2} > 0$, let $F(t) = e^{\lambda(t-t_0)} H(t)$ for $t \geq t_0 - \tau_{max}$ and $\bar{\xi} \in \mathcal{PC}([-\tau_{max}, 0], \mathbb{R}^{6n})$ be the initial states of $\bar{\xi}(t)$, it gives

$$F(t) \leq \frac{\lambda_{max}(P)}{2} \|\bar{\xi}\|_{\tau_{max}}^2 < \frac{M}{\bar{q}} \|\bar{\xi}\|_{\tau_{max}}^2 < M \|\bar{\xi}\|_{\tau_{max}}^2, \quad t \in [t_0 - \tau_{max}, t_0] \quad (7.59)$$

and hence we shall show

$$F(t) \leq M \|\bar{\xi}\|_{\tau_{max}}^2, \quad t \geq t_0 \quad (7.60)$$

By applying mathematical induction, we first prove

$$F(t) < M \|\bar{\xi}\|_{\tau_{max}}^2, \quad t \in [t_0 - \tau_{max}, \hat{t}_1) \quad (7.61)$$

by contradiction. Suppose there exists some $t \in (t_0, \hat{t}_1)$ such that $F(t) > M \|\bar{\xi}\|_{\tau_{max}}^2$ and let $t^* = \inf\{t \in [t_0, \hat{t}_1) : F(t) \geq M \|\bar{\xi}\|_{\tau_{max}}^2\}$, it can be deduced by the continuity of $F(t)$ on $t \in [t_0, \hat{t}_1)$ that

$$\begin{aligned} F(t^*) &= M \|\bar{\xi}\|_{\tau_{max}}^2, \quad t^* \in (t_0, \hat{t}_1) \\ F(t) &< M \|\bar{\xi}\|_{\tau_{max}}^2, \quad t \in [t_0 - \tau_{max}, t^*) \end{aligned} \quad (7.62)$$

Then we define $t^{**} = \sup\{t \in [t_0, t^*] : F(t) \leq \frac{M}{\bar{q}} \|\bar{\xi}\|_{\tau_{max}}^2\}$, it yields that

$$\begin{aligned} F(t^{**}) &= \frac{M}{\bar{q}} \|\bar{\xi}\|_{\tau_{max}}^2, \quad t^{**} \in (t_0, t^*) \\ F(t) &> \frac{M}{\bar{q}} \|\bar{\xi}\|_{\tau_{max}}^2, \quad t \in (t^{**}, t^*) \end{aligned} \quad (7.63)$$

Based on (7.62) and (7.63), one can get

$$F(t+z) \leq M\|\bar{\xi}\|_{\tau_{max}}^2 \leq \bar{q}F(t), \quad t \in [t^{**}, t^*], \quad z \in [-\tau_{max}, 0] \quad (7.64)$$

and implies that

$$H(t+z) = e^{-\lambda(t+z-t_0)}F(t+z) \leq \bar{q}e^{-\lambda(t+z-t_0)}F(t) \leq \bar{q}e^{\lambda\tau_{max}}H(t) = qH(t), \quad z \in [-\tau_{max}, 0] \quad (7.65)$$

and

$$F(t^*) \leq F(t^{**})e^{(\eta_3+q\eta_4+\lambda)h_2} \leq \frac{M}{\bar{q}}\|\bar{\xi}\|_{\tau_{max}}^2 e^{(\eta_3+q\eta_4+\lambda)h_2} < M\|\bar{\xi}\|_{\tau_{max}}^2 \quad (7.66)$$

which contradicts (7.62), thus (7.61) holds. Next, suppose that for some $l \in \mathbb{N}$, $l \geq 1$

$$F(t) < M\|\bar{\xi}\|_{\tau_{max}}^2, \quad t \in [t_0 - \tau_{max}, \hat{t}_l] \quad (7.67)$$

and we aim to prove

$$F(t) < M\|\bar{\xi}\|_{\tau_{max}}^2, \quad t \in [\hat{t}_l, \hat{t}_{l+1}] \quad (7.68)$$

Again, suppose not, we can set $t^* = \inf\{t \in [\hat{t}_l, \hat{t}_{l+1}) : F(t) \geq M\|\bar{\xi}\|_{\tau_{max}}^2\}$ and since

$$F(\hat{t}_l) \leq \rho_3 F(\hat{t}_l^-) + \rho_4 e^{\lambda\tau_{max}} \sup_{z \in [-\tau_{max}, 0]} \{F(\hat{t}_l^- + z)\} \leq (\rho_3 + \rho_4 e^{\lambda\tau_{max}})M\|\bar{\xi}\|_{\tau_{max}}^2 < M\|\bar{\xi}\|_{\tau_{max}}^2 \quad (7.69)$$

we have

$$\begin{aligned} F(t^*) &= M\|\bar{\xi}\|_{\tau_{max}}^2, \quad t^* \in (\hat{t}_l, \hat{t}_{l+1}) \\ F(t) &< M\|\bar{\xi}\|_{\tau_{max}}^2, \quad t \in [\hat{t}_l, t^*) \end{aligned} \quad (7.70)$$

Then we define $t^{**} = \sup\{t \in [\hat{t}_l, t^*) : F(t) \leq (\rho_3 + \rho_4 e^{\lambda\tau_{max}})M\|\bar{\xi}\|_{\tau_{max}}^2\}$, it gives that

$$\begin{aligned} F(t^{**}) &= (\rho_3 + \rho_4 e^{\lambda\tau_{max}})M\|\bar{\xi}\|_{\tau_{max}}^2, \quad t^{**} \in (\hat{t}_l, t^*) \\ F(t) &> (\rho_3 + \rho_4 e^{\lambda\tau_{max}})M\|\bar{\xi}\|_{\tau_{max}}^2, \quad t \in (t^{**}, t^*) \end{aligned} \quad (7.71)$$

Based on (7.58), (7.70) and (7.71), we have

$$F(t+z) \leq M\|\bar{\xi}\|_{\tau_{max}}^2 \leq \frac{1}{\rho_3 + \rho_4 e^{\lambda\tau_{max}}}F(t) < \bar{q}F(t), \quad t \in [t^{**}, t^*], \quad z \in [-\tau_{max}, 0] \quad (7.72)$$

and

$$F(t^*) \leq F(t^{**})e^{(\eta_3+q\eta_4+\lambda)h_2} \leq e^{(\eta_3+q\eta_4+\lambda)h_2}(\rho_3 + \rho_4 e^{\lambda\tau_{max}})M\|\bar{\xi}\|_{\tau_{max}}^2 < M\|\bar{\xi}\|_{\tau_{max}}^2 \quad (7.73)$$

which leads to a contradiction, thus (7.68) holds as well. In addition, above process is consistent with the construction of $\Omega_{\bar{s}}$ in Lemma 7.2.1. Consequently, (7.60) holds true and from (7.52) we obtain the globally exponential stability as

$$\|\bar{\xi}(t)\| \leq \sqrt{\frac{2M}{\lambda_{\min}(P)}} \|\bar{\xi}\|_{\tau_{max}} e^{-\frac{\lambda}{2}(t-t_0)}, \quad t \geq t_0 \quad (7.74)$$

Finally, the proof of collision-free motion with respect to $H(t)$ follows the same procedure as that of the Theorem 3.4.1 and thus is omitted. \square

Remark 7.4.1. *Theorem 7.4.1 illustrates the exponential stabilization of vehicle platoon with state-dependent switching via stabilizing control impulses, which does not require to set up the switching sequence before the control process. Specifically, the state-dependent switching consists of the construction of convex switching region as indicated in Lemma 7.2.1 and the design of corresponding switching rule in Definition 7.2.2. Meanwhile, sufficient stability criteria are derived in terms of impulsive strengths and uniform upper bound of the convex switching region.*

7.5 Numerical Simulations

In this section, we provide two numerical examples to verify the theoretical results presented in Theorem 7.3.1 and Theorem 7.4.1. The simulation time is set to be 50s. We consider $N=6$ agents to simulate a horizontally moving vehicle platoon with desired configuration and switching as indicated in Figure 7.3 and Figure 7.4. The initial positions, velocities and accelerations of follower vehicles are randomly chosen from feasible range of $[-5, 20] \times [-3, 3]$, $[0, 3]^2$ and $[-5, 5]^2$ respectively, while the virtual leader starts with $p_0 = [15, 0]^T$, $v_0 = [2.5, 0]^T$ and $a_0 = [1, 1]^T$. The time delays are chosen to be $r(t) = \frac{1}{250}e^{-0.02t}$ and $\bar{\tau} = 0.02s$. Meanwhile, $b_{ij}(\sigma(t)) = 1.5$, $c_i(\sigma(t)) = 0.8$, $\kappa = 2$, $k_1 = 0.15$, $k_2 = 0.015$, $k_3 = 0.005$ and control impulses occur every 0.025s (i.e., $h_1 = h_2 = 0.025$). Moreover, a horizontal path of width 8m with two lanes and six additional moving agents (in black) are constructed,

Example 1. The time-dependent switching signals are designed in Figure 7.5(d) where $\bar{s} = \sigma(t) \in \{1, 2, 3, 4\}$. Specifically, $\sigma(t) = 1$, $\sigma(t) = 2$, $\sigma(t) = 3$ and $\sigma(t) = 4$ correspond to the vehicle platoon structure of predecessor-following, two-predecessor-following, full control deactivation and predecessor-following with parallel string respectively. By using LMI

toolbox, we obtain $\eta_2 = 3.65$, $\rho_{11} = 0.278$, $\rho_{21} = 0.623$, $\rho_{12} = 0.235$, $\rho_{22} = 0.598$, $\rho_{13} = 1$, $\rho_{23} = 0$, $\rho_{14} = 0.256$, $\rho_{24} = 0.614$, $\gamma^* = 1.52$ and $\beta_{\bar{s}} = 0.75$ so that conditions (7.17)-(7.19) are satisfied. From the trajectory evolution indicated in Figure 7.6, we observe that six vehicles (leader vehicle in red) are able to pass through other moving vehicles successfully without any inter-vehicle/obstacle collision or hitting crash barrier, and the desired vehicle platoon configuration has been switched from single string to parallel string structure afterwards. Based on Figure 7.5, the trajectories of position, velocity and acceleration mismatch are all convergent, which implies the exponential stabilization of desired vehicle platoon configuration can be guaranteed. Consequently, the cooperative control of vehicle platoon are achieved via the proposed distributed hybrid impulsive control protocol with time-dependent switching, thus Theorem 7.3.1 is valid.

Example 2. According to state-dependent switching rule (7.2.2), we consider implementing signal $\bar{s} = \sigma(t) \in \{1, 2, 4\}$, where $\sigma(t) = 3$ (i.e., full control deactivation) is excluded as the exponential stability fails to hold. By using LMI toolbox, we obtain $\eta_3 = 3.23$, $\eta_4 = 0.53$, $\mu = 1$, $q = 1.43$, $\rho_3 = 0.294$ and $\rho_4 = 0.611$ so that condition (7.50) is satisfied. Similar to previous example, based on the trajectory evolution indicated in Figure 7.7, the vehicle platoon is experiencing collision-free motion, and its target configuration is achieved eventually. Based on Figure 7.8(a)-(c), the trajectories of position, velocity and acceleration mismatch are all convergent as well, which implies the exponential stabilization of desired vehicle platoon configuration can also be guaranteed. Moreover, different from pre-determined switching signals in Example 1, Figure 7.8(d) provides the scatter plot of overall state-dependent switching signals which are automatically adjusted by switching rule (7.2.2). Furthermore, when the states of vehicles are arbitrarily generated at the beginning, we observe a consistent change of switching signals subject to predecessor-following and two-predecessor-following as shown in Figure 7.8(e). Later on, as desired vehicle platoon structure gradually forms, $\sigma(t) = 2$ remains since two-predecessor-following structure generates a larger speed of exponential convergence. Consequently, the cooperative control of vehicle platoon are achieved via the proposed distributed hybrid impulsive control protocol with state-dependent switching, thus Theorem 7.4.1 is valid.

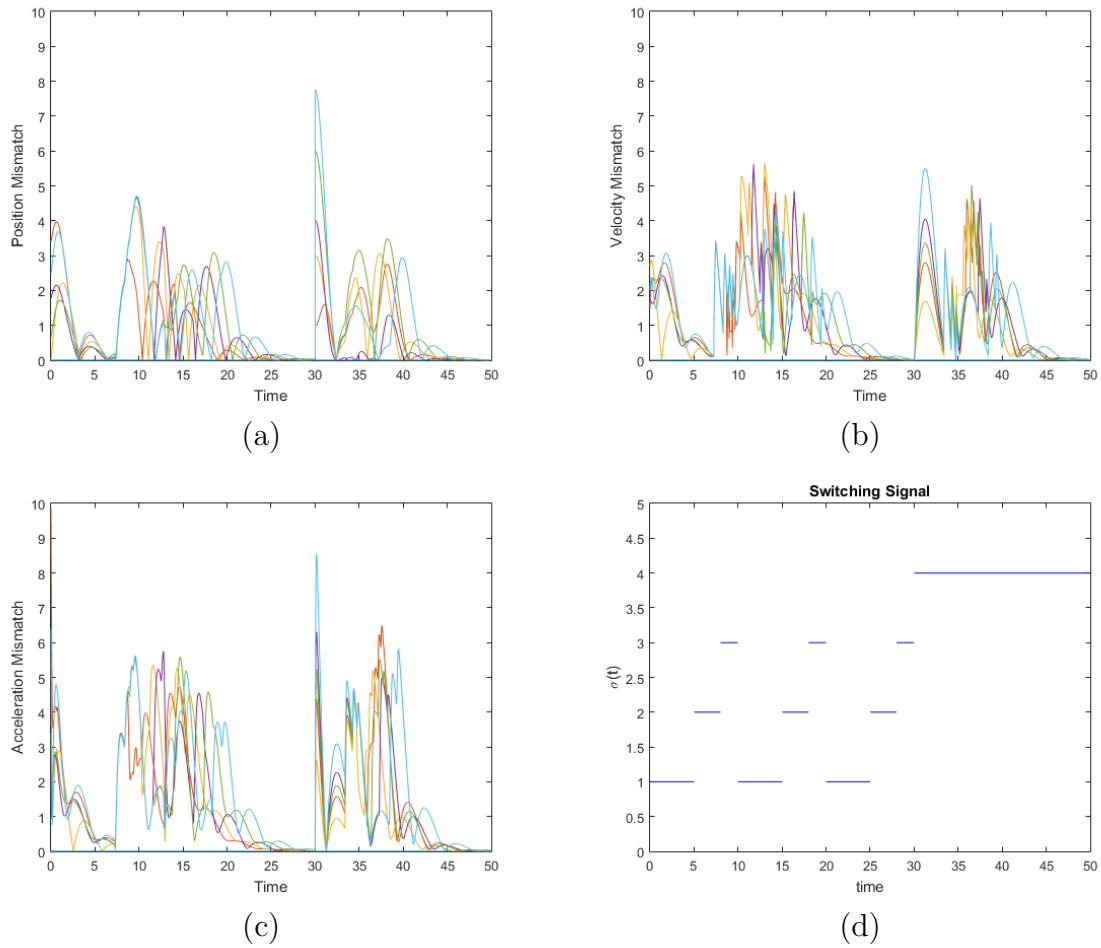


Figure 7.5: Convergence of (a) position (b) velocity (c) acceleration mismatch of vehicle platoon with time-dependent switching (d) Time-dependent switching signals

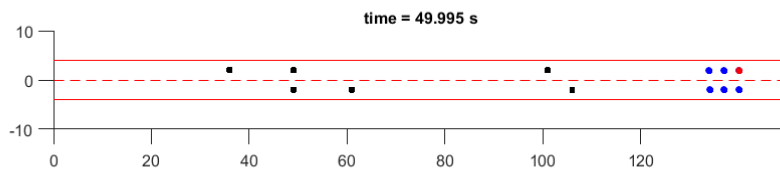
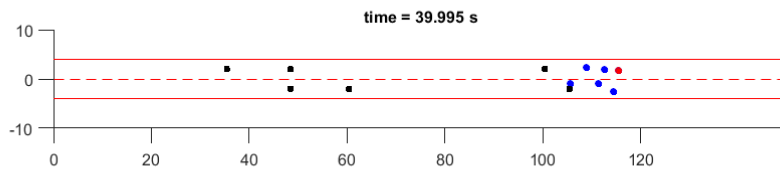
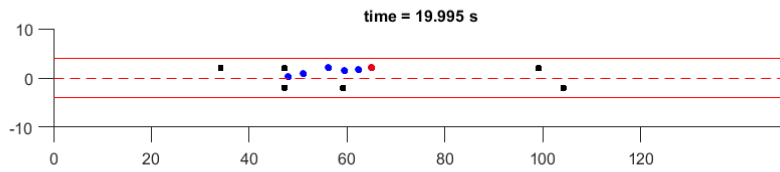
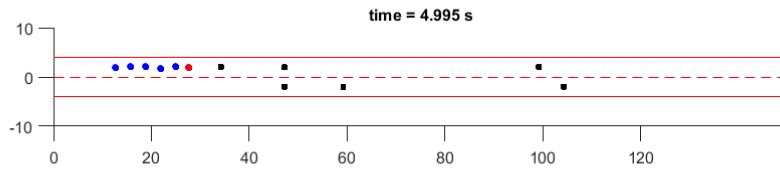


Figure 7.6: Evolution of vehicle platoon with time-dependent switching

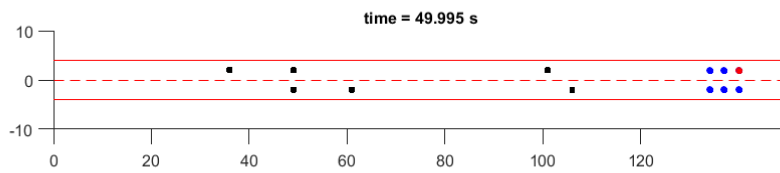
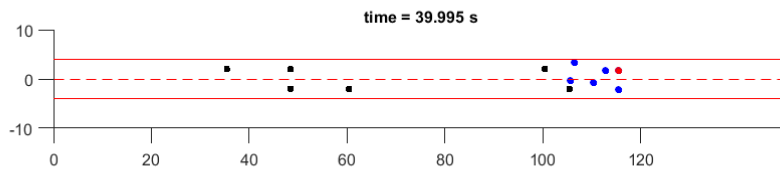
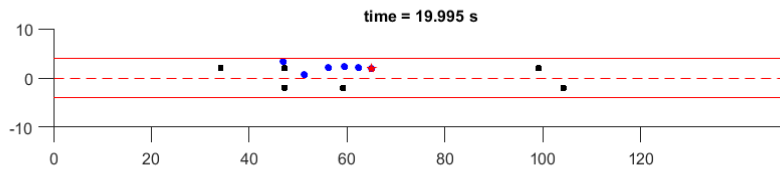
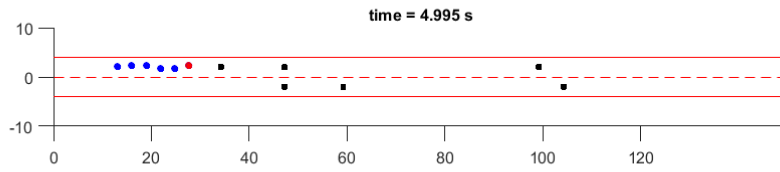


Figure 7.7: Evolution of vehicle platoon with state-dependent switching

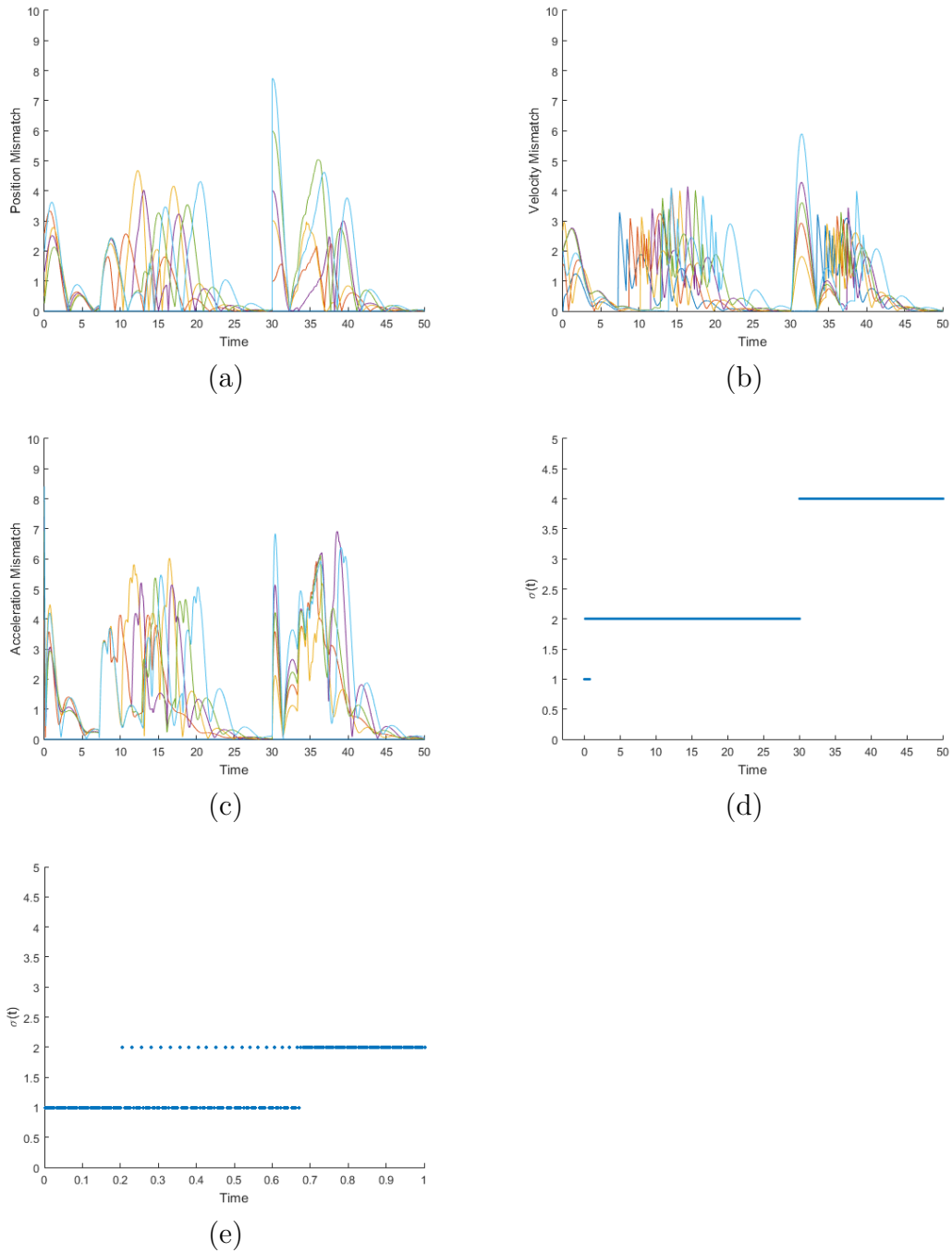


Figure 7.8: Convergence of (a) position (b) velocity (c) acceleration mismatch of vehicle platoon with state-dependent switching (d)-(e) State-dependent switching signals

Remark 7.5.1. *Under the concept of automated highway systems, in contrast to other applications in formation stabilization (i.e., satellite surveillance, drone display) with sufficiently less spacing restrictions and higher maneuverability, traffic management is the key and distinctive feature which allows driverless vehicles to perform efficiently within constrained environments (i.e., space/speed limits) so that traffic congestion relief can be achieved by reducing unnecessary vehicle headway while maintaining a designated platoon configuration. We have simulated highway lane conditions via numerical examples above. These examples suggest that our proposed collision avoidance mechanism can generate safe platoon passage as long as there is enough space ahead. Specifically, the braking force aims to prevent any types of road traffic collisions such as head-on and run-off-road collisions by reducing the vehicle's velocity to a safe level in a short distance, while the gyroscopic force is attached to guide the direction of avoidance motions (i.e., either clockwise or counterclockwise). In the meantime, based on our hybrid impulsive formation tracking and switching control protocols, the vehicle platoon can move in coordination with the desired configuration by eliminating tracking mismatches. This can then be consistently adjusted for different traffic conditions in terms of lane occupation. In general, our automated control results in this chapter can contribute to improving traffic management.*

Chapter 8

Conclusions and Future Research

In this chapter, we summarize the results throughout the thesis and also discuss some potential aspects of future research direction.

An investigation of the formation stabilization problems of multi-agent systems has been conducted in the present thesis, subject to the application of various control techniques under hybrid impulsive control framework. In addition, the improved collision avoidance mechanism is implemented to make this topic more practical.

In chapter 3, the formation stabilization of multi-agent systems via hybrid impulsive control along with the implementation of collision avoidance mechanisms has been studied. In section 3.2, a hybrid impulsive formation tracking control with continuous time-varying delay and delay-dependent impulses is discussed with the help of the Lyapunov function via the Razumikhin technique. Specifically, some sufficient stabilization criteria are derived in terms of small/large size discrete impulse delay, and distributed impulse delay respectively. These criteria indicate how the strength of impulse, the tolerance of instability with respect to continuous dynamics, and the size of time delays will affect the convergence of tracking error dynamics. In Section 3.3, the general setup of the collision avoidance mechanism is introduced. Meanwhile, in contrast to the conventional distributed artificial potential field (APF) approach proposed in [15], the implementation of braking and gyroscopic forces suggested by [30, 32] has the capability to overcome the major drawback of generating undesired local minima in APF approach and produce better performance by reducing additional work done. In Section 3.4, we have shown that the collision avoidance mechanism has a negative impact on formation stabilization when delay-dependent impulses occur. Due to this issue, we instead investigated input-to-state formation stabilization in terms of the arbitrary size of impulse delay in Section 3.5 by treating control inputs of collision

avoidance as external inputs. This is reasonable in practice since the mechanism will be deactivated once reaching out of sensing range, and the formation stabilization can still be achieved afterwards. By using the method of Lyapunov Krasovskii functional and impulsive comparison system, sufficient conditions benefiting from delayed control impulses have been derived to maintain input-to-state/integral input-to-state formation stabilization over impulse sequence classes with either a uniform upper bound $\mathcal{F}(h_2)$ or average impulsive interval $\mathcal{F}[T_\alpha, \varrho]$.

Chapter 4 has adapted the proposed hybrid impulsive control framework into multi-group formation stabilization for heterogeneous multi-agent systems, where agents consist of both second-order and third-order dynamics. In this multi-group setting, each subgroup with a different tracking leader is able to pursue its own control tasks. Nevertheless, with the construction of directed communication links among subgroups, the multi-group formation stabilization can also be converted into the stabilization problem of a single large group by combining the topological structure of each subgroup altogether, and this will not affect the respective formation tracking objectives of each subgroup. Moreover, extra feedback control on additional states is needed to compensate for the order difference of MASs. For systems with destabilizing continuous control and stabilizing delayed impulses, analytical and simulation results subject to hybrid impulsive protocols presented in Chapter 4 have illustrated the effectiveness of multi-group formation stabilization with collision-free motions and heterogeneous dynamics.

The hybrid event-triggered impulsive formation stabilization for multi-UAV systems with external disturbances has been investigated in Chapter 5. In Section 5.4, theoretical analysis of two event-triggered strategies has been carried out by incorporating additional features, including pinning mechanisms and delayed control inputs. We have derived some novel results regarding maintaining local asymptotic stability using the Lyapunov-Razumikhin technique, graph theory, and the concept of nonlinearity strength. Even though both strategies are advantageous for abrupt transmission, it is worth noting that strategy (5.6) has limitations in information exchange due to preset time-triggered instants (i.e., forced impulsive sequence), which may result in unnecessary resource consumption. On the contrary, the control instants of strategy (5.21) are automatically determined by the occurrence of a state-related event condition, thus making it more flexible in practice. In order to verify the applicability and efficiency of our proposed protocols, the numerical simulation is conducted in terms of a multi-quadrotor system with specific parameter settings. According to the trajectories of formation evolution and error convergence, successful stabilization and obstacle avoidance have been achieved. By making comparison with the continuous protocol presented in [105], our schemes demonstrate the reduction of usage rate and cost of control up to 49.12% and 33.46% respectively. In the meantime,

control performance can be further enhanced by reducing the delay size or increasing the triggering threshold within a feasible range. Moreover, braking and gyroscopic forces generate 12.50% less distortion on average than the artificial potential field presented in [89]. Consequently, our control results demonstrate better formation stabilization performance, which supports the discussion in Section 3.3.

Chapter 6 has investigated the finite-time formation tracking control of multi-agents via aperiodic intermittent communication and delayed impulses under the hybrid impulsive control framework. In Section 6.4, first of all, we have addressed finite-time stability in terms of a modified weak Lyapunov inequality condition for continuous dynamics with time-varying gains. The corresponding stability criteria suggest that the settling time is dependent on the total length of the aperiodic intermittent control interval and the strength of delayed control impulses. With or without the presence of external impulsive disturbances, we then derive finite-time formation stabilization results respectively using our proposed control protocols involving stabilizing delayed impulses. In addition to that, the number of impulsive instants during each aperiodic intermittent interval can be unknown and indefinite, so the average impulsive interval is used in order to obtain the finite-time stabilization. Lastly, on the basis of the average impulsive interval, we further modify the intermittent control width to be state-dependent. According to our numerical simulations in Chapter 6, we have validated that finite-time formation stabilization can be achieved by properly designing aperiodic intermittent control width and impulsive sequences.

The application of self-driving vehicle platoons has become a trending research area subject to formation control of multi-agent systems. Therefore, in Chapter 7, we have designed the hybrid impulsive cooperative control protocol of a vehicle platoon with time-dependent and state-dependent switching. The implementation of switching process enhances the robustness, adaptability and fault-tolerance of platoon in responding to dynamic changes of environment and failures in the control system. In Section 7.3, by employing the Lyapunov Krasovskii functional method with mode-dependent average dwell time, the time-dependent switching between stable and unstable control inputs has been studied so that exponential platoon stabilization can be achieved. Meanwhile, in Section 7.4, by using the Lyapunov Razumikhin technique with a common Lyapunov function, some sufficient conditions have been derived so that exponential stabilization can still be guaranteed with state-dependent switching. Furthermore, with the proper construction of a convex switching region and switching rule, the undesirable chattering effect can be avoided.

On top of the hybrid impulsive control framework, numerous types of control features including delayed impulses, heterogeneous dynamics, event-triggered pinning mechanism, aperiodic intermittent control, switching control; and stability characteristics such as input-to-state stability and finite-time stability are integrated for formation stabilization of multi-

agent systems. In addition, an improved version of braking and gyroscopic forces is utilized for collision avoidance against convex environmental obstacles. However, for our future research regarding MAS formation stabilization, the potential aspects include but are not limited to:

- The system's intrinsic dynamics or external interference are often unknown or difficult to detect in practice. Apart from observer-based output regulation, neural network-based adaptive control mechanism is worth investigating, along with system heterogeneity and partial control measurements.
- There are many real-world systems, such as electrical circuits, chemical reactors, and gene regulation networks, whose output depends not only on the current state but also on the past state. These systems are typically described as neutral systems since they have memory that extends both backward and forward in time. Therefore, investigating the stabilization problem of an impulsive neutral system presents unique challenges and opportunities.
- The design of collision avoidance mechanisms for non-convex obstacles still remains a challenging task, primarily due to their irregular shapes being difficult to accurately represent and the generation of multiple local minima. Therefore, a potential approach would be to develop information-driven guidance algorithms that prevent agents from becoming trapped in motion. Furthermore, the design of escape strategies from more complex non-convex obstacles and various obstacle constellations inside higher dimensional spaces can also be demanding.

References

- [1] B. L. Partridge. *The chorus-line hypothesis of maneuver in avian flocks*. Nature, 309(6):344–345, 1984.
- [2] C. W. Reynolds. *Flocks, herds, and schools: a distributed behavioral model*. Computer Graphics, 21(4):25-34, 1987.
- [3] T. Vicsek, A. Czirók, E. B. Jacob, I. Cohen, and O. Shochet. *Novel Type of Phase Transition in a System of Self-Driven Particles*. Physical review letters, 75(6):1226-1229, 1995.
- [4] N. Shimoyama, K. Sugawara, T. Mizuguchi, Y. Hayakawa, and M. Sano. *Collective Motion in a System of Motile Elements*. Physical review letters, 76(20):3870-3873, 1996.
- [5] J. Toner and Y. Tu. *Flocks, Herds, and Schools: A Quantitative Theory of Flocking*. Physical review. E, Statistical physics, plasmas, fluids, and related interdisciplinary topics, 58(4):4828-4858, 1998.
- [6] H. Levine, W. J. Rappel, and Cohen I. *Self-Organization in Systems of Self-Propelled Particles*. Physical review. E, Statistical physics, plasmas, fluids, and related interdisciplinary topics, 63(1):1-4, 2001.
- [7] D. Scharf, F. Hadaegh, and S. Ploen. *A Survey of Spacecraft Formation Flying Guidance and Control (Part II): Control*. In Proceedings of the American Control Conference, 4:2976-2985, 2004.
- [8] T. Balch and R. C. Arkin. *Behavior-Based Formation Control for Multirobot Teams*. IEEE transactions on robotics and automation, 14(6): 926-939, 1998.
- [9] I. F. Akyildiz, W. Su, Y. Sankarasubramaniam, and E. Cayirci. *A survey on sensor networks*. IEEE Communications Magazine, 40(8): 102-114, 2002.

- [10] T. Vicsek, I. Farkas, and D. Helbing. *Simulating Dynamical Features of Escape Panic*. Nature (London), 407(6803):487-490, 2000.
- [11] I. Suzuki and Yamashita M. *Distributed Anonymous Mobile Robots: Formation of Geometric Patterns*. SIAM journal on computing, 28(4):1347-1363, 1999.
- [12] A. Jadbabaie A, J. Lin, and A. S. Morse. *Coordination of groups of mobile autonomous agents using nearest neighbor rules*. IEEE Trans Automat Contr, 48(6):988–1001, 2003.
- [13] R. Olfati-Saber and R. M. Murray. *Consensus problems in networks of agents with switching topology and time-delays*. IEEE Trans Automat Contr, 49(9):1520–1533, 2004.
- [14] W. Ren W and R. W. Beard. *Consensus seeking in multiagent systems under dynamically changing interaction topologies*. IEEE Trans Automat Contr, 50(5):655–661, 2005.
- [15] R. Olfati-Saber. *Flocking for multi-agent dynamics systems: algorithms and theory*. IEEE Trans Automat Contr, 51:401-420, 2006.
- [16] R. Olfati-Saber and R. M. Murray. *Consensus problems in networks of agents with switching topology and time-delays*. IEEE Trans Automat Contr, 49(9):1520–1533, 2004.
- [17] Z. Hou, L. Cheng, and M. Tan. *Decentralized robust adaptive control for the multiagent system consensus problem using neural networks*. IEEE Trans. Syst. Man Cybern. Part B, 39(3):636–647, 2009.
- [18] G. Dong, H. Li, H. Ma, and R. Lu. *Distributed consensus of non-linear fractional-order multi-agent systems with directed topologies*. IEEE Trans Neural Netw Learn Syst, 32(2):653–662, 2020.
- [19] Z. Hou, L. Cheng, and M. Tan. *Finite-time consensus tracking neural network FTC of multi-agent systems*. IEEE Trans. Syst. Man Cybern. Part B, 39(3):636–647, 2009.
- [20] N. Nigam, S. Bieniawski, I. Kroo, and J. Vian. *Control of Multiple UAVs for Persistent Surveillance: Algorithm and Flight Test Results*. IEEE transactions on control systems technology, 20(5):1236-1251, 2012.

- [21] J. Han and Y. Chen. *Multiple UAV Formations for Cooperative Source Seeking and Contour Mapping of a Radiative Signal Field*. Journal of intelligent & robotic systems, 74:323-332, 2013.
- [22] R. W. Beard, J. Lawton, and F. Y Hadaegh. *A Coordination Architecture for Spacecraft Formation Control*. IEEE transactions on control systems technology, 9(6):777-790, 2001.
- [23] X. Li, D. Peng, and J. Cao. *Event-Triggered Impulsive Control for Nonlinear Delay Systems*. Automatica, 117:108981-, 2020.
- [24] S. Yu and X. Long. *Finite-time consensus for second-order multi-agent systems with disturbances by integral sliding mode*. Automatica, 54:158-165, 2015.
- [25] H. Rezaee and F. Abdollahi. *Robust Attitude Alignment in Multispacecraft Systems with Stochastic Links Failure*. Automatica, 118:109033-, 2020.
- [26] A. Izadipour, J. Ghaisari, and J. Askari. *Distributed robust adaptive flocking for uncertain nonlinear multi-agent systems with time-varying communication delay*. International journal of systems science, 51(1):72-86, 2020.
- [27] H. Su, X. Wang, and Z. Lin. *Flocking of Multi-Agents With a Virtual Leader*. IEEE Transactions on Automatic Control, 54(2):293-307, 2009.
- [28] P. Zhao, H. Erzberger, and Y. Liu. *Multiple-Aircraft-Conflict Resolution Under Uncertainties*. Journal of guidance, control, and dynamics, 44(11):2031-2049, 2021.
- [29] R. Olfati-Saber and R. M. Murray. *Distributed cooperative control of multiple vehicle formations using structural potential functions*. IFAC Proceedings, 35(1):495-500, 2002.
- [30] D. E. Chang, S. C. Shadden, J. E. Marsden, and R. Olfati-Saber. *Collision avoidance for multiple agent systems*. 42nd IEEE International Conference on Decision and Control, 1(1):539-543, 2003.
- [31] D. E. Chang and J. E. Marsden. *Gyroscopic forces and collision avoidance with convex obstacles*. New trends in nonlinear dynamics and control and their applications, Springer, 145-159, 2003.
- [32] L. Sabattini, C. Secchi, and C. Fantuzzi. *Collision avoidance for multiple Lagrangian dynamical systems with gyroscopic forces*. International journal of advanced robotic systems, 14(1):1-15, 2017.

- [33] V. Lakshmikantham, D. Bainov, and P. Simeonov. *Theory of Impulsive Differential Equations*. World Scientific, Singapore, 1989.
- [34] X. Liu and K. Zhang. *Impulsive systems on hybrid time domains*. Springer, 2019.
- [35] Q. Zhang, Y. Hao, Z. Yang, and Z. Chen. *Adaptive flocking of heterogeneous multi-agents systems with nonlinear dynamics*. *Neurocomputing*, 216: 72-77, 2016.
- [36] M. Wang, H. Su, M. Zhao, M. Z. Chen, and H. Wang. *Flocking of multiple autonomous agents with preserved network connectivity and heterogeneous nonlinear dynamics*. *Neurocomputing*, 115: 169-177, 2013.
- [37] J. Yu and L. Wang. *Group consensus of multi-agent systems with directed information exchange*. *International journal of systems science*, 43(2): 334-348, 2013.
- [38] Q. Xi, Z. Liang, and X. Li. *Uniform Finite-Time Stability of Nonlinear Impulsive Time-Varying Systems*. *Applied Mathematical Modelling*, 91: 913-922, 2021.
- [39] X. Lou and B. Cui. *Stochastic exponential stability for Markovian jumping BAM neural networks with time-varying delays*. *IEEE Transactions on Systems, Man, and Cybernetics, Part B*, 37(3): 713-719, 2007.
- [40] H. Ye, A. N. Michel, and K. Wang. *Qualitative analysis of Cohen-Grossberg neural networks with multiple delays*. *Physical Review E*, 51(3): 2611-2618, 1995.
- [41] P. Van Den Driessche and X. Zou. *Global attractivity in delayed Hopfield neural network models*. *SIAM Journal on Applied Mathematics*, 58(6): 1878-1890, 1998.
- [42] L. O. Chua and L. Yang. *Cellular Neural Networks: Theory*. *IEEE Transactions on Circuits and Systems*, 35(10): 1257-1272, 1988.
- [43] X. Liu and K. Zhang. *Synchronization of linear dynamical networks on time scales: Pinning control via delayed impulses*. *Automatica*, 72: 147-152, 2016.
- [44] W. Ren and E. Atkins. *Distributed multi-vehicle coordinated control via local information exchange*. *Int J Robust Nonlinear Control IFAC-Affiliated J*, 17(10-11): 1002-1033, 2007.
- [45] W. Ren, R. W. Beard, and E. Atkins. *Information consensus in multivehicle cooperative control*. *IEEE Control Syst Mag*, 27(2): 71-82, 2007a.

- [46] J. Zhu J, Y. Tian, and J. Kuang. *On the general consensus protocol of multi-agent systems with double-integrator dynamics*. Linear Algebra Appl, 431(5–7): 701–715, 2009.
- [47] A. Suratgar A. Adibzadeh, M. Menhaj, and M. Zamani. *Constrained optimal consensus in multi-agent systems with single-and double-integrator dynamics*. Int J Control, 93(3): 575–587, 2020.
- [48] W. He and J. Cao. *Consensus control for high-order multi-agent systems*. IET Control Theory Appl, 5(1): 231–238, 2011.
- [49] J. Fax and R. M. Murray. *Information Flow and Cooperative Control of Vehicle Formations*. IEEE transactions on automatic control, 49(9): 1465-1476, 2004.
- [50] K. Oh, M. Park, and H. Ahn. *A survey of multi-agent formation control*. Automatica, 53: 424–440, 2015.
- [51] Z. Liang and X. Liu. *Multi-group Hybrid Impulsive Flocking Control of Heterogeneous Multi-agent Systems*. Journal of the Franklin Institute, 359(18): 10455–10482, 2022.
- [52] Z. Liang and X. Liu. *Hybrid Event-triggered Impulsive Flocking Control for Multi-agent Systems via Pinning Mechanism*. Applied Mathematical Modelling, 114: 23-43, 2023.
- [53] W. Ren and Y. Cao. *Distributed Coordination of Multi-Agent Networks Emergent Problems, Models, and Issues*. Springer, 2010.
- [54] W. Ren and R. W. Beard. *Formation feedback control for multiple spacecraft via virtual structures*. IET Control Theory and Applications, 151(3): 357-368, 2004.
- [55] M. Ji, G. Ferrari-Trecate, M. Egerstedt, and A. Buffa. *Containment Control in Mobile Networks*. IEEE transactions on automatic control, 53(8): 1972-1975, 2008.
- [56] Y. Cao, D. Stuart, W. Ren, and Z. Meng. *Distributed Containment Control for Multiple Autonomous Vehicles With Double-Integrator Dynamics: Algorithms and Experiments*. IEEE transactions on control systems technology, 19(4): 929-938, 2011.
- [57] M. Basiri, A. N. Bishop, and P. Jensfelt. *Distributed Control of Triangular Formations with Angle-Only Constraints*. Systems & control letters, 59(2): 147-154, 2010.

- [58] M. Basiri, A. N. Bishop, and P. Jensfelt. *Formations of Vehicles in Cyclic Pursuit*. IEEE transactions on automatic control, 49(11): 1963-1974, 2004.
- [59] G. Ballinger and X. Liu. *Existence and uniqueness results for impulsive delay differential equations*. Dynamics of Continuous, Discrete and Impulsive Systems, Series A: Mathematical Analysis, 5 (1-4): 579-591, 1999.
- [60] J. Liu, Liu X, and W. Xie. *Existence and Uniqueness Results for Impulsive Hybrid Stochastic Delay Systems*. Appl Nonlinear Anal, 17: 37–53, 2010.
- [61] X. Liu and Q. Wang. *The method of Lyapunov functionals and exponential stability of impulsive systems with time delay*. Nonlinear Analysis, 66(7):1465-1484, 2007.
- [62] X. Liu, K. Zhang, and W-. C. Xie. *Stabilization of time-delay neural networks via delayed pinning impulses*. Chaos, Solitons Fractals, 93:223-234, 2016.
- [63] J. Li and J. Shen. *New comparison results for impulsive functional differential equations*. Applied Mathematics Letters, 23(4): 487-493, 2010.
- [64] X. Wu, Y. Tang, and W. Zhang. *Input-to-State Stability of Impulsive Stochastic Delayed Systems Under Linear Assumptions*. Automatica, 66: 195-204, 2016.
- [65] Y. Zheng, J. Ma, and L. Wang. *Consensus of Hybrid Multi-Agent Systems*. IEEE transaction on neural networks and learning systems, 29(4): 1359-1365, 2018.
- [66] Y. Zheng and L.Wang. *Consensus of switched multiagent systems*. IEEE transactions on circuits and systems, 63(3): 314-318, 2016.
- [67] P. Cheng, F. Deng, and F. Yao. *Exponential stability analysis of impulsive functional differential equations with delayed impulses*. Communications in Nonlinear Science and Numerical Simulation, 19 (6): 2104–2114, 2014.
- [68] E. Rimon and D. E. Koditschek. *Exact Robot Navigation Using Artificial Potential Functions*. IEEE transactions on robotics and automation, 8(5): 501-518, 1992.
- [69] H. G. Tanner, A. Jadbabaie, and G. J. Pappas. *Stable Flocking of Mobile Agents Part II: Dynamic Topology*. In Proceedings of the IEEE Conference on Decision and Control, 2: 2016-2021, 2003.
- [70] E. D. Sontag. *Comments on Integral Variants of ISS*. Systems & control letters, 34(1): 93-100, 1998.

- [71] J. P. Hespanha, D. Liberzon, and A. R. Teel. *Lyapunov Conditions for Input-to-State Stability of Impulsive Systems*. Automatica, 44(11): 2735-2744, 2008.
- [72] S. Dashkovskiy and A. Mironchenko. *Input-to-State Stability of Nonlinear Impulsive Systems*. SIAM journal on control and optimization, 51(3): 1962-1987, 2013.
- [73] J. Liu, X. Liu, and W. C. Xie. *Class \mathcal{KL} Estimates and Input-to-State Stability Analysis of Impulsive Switched Systems*. Systems & control letters, 61(6): 738-746, 2012.
- [74] X. Li, T. Zhang, and J. Wu. *Input-to-State Stability of Impulsive Systems via Event-Triggered Impulsive Control*. IEEE transactions on cybernetics, 52(7): 7187-7195, 2022.
- [75] X. Wu, Y. Tang, and W. Zhang. *Input-to-State Stability of Impulsive Stochastic Delayed Systems Under Linear Assumptions*. Automatica, 66: 195-204, 2016.
- [76] X. Fu, Q. Zhu, and Y. Guo. *Stabilization of Stochastic Functional Differential Systems with Delayed Impulses*. Applied mathematics and computation, 346: 776-789, 2019.
- [77] X. Li, X. Zhang, and S. Song. *Effect of Delayed Impulses on Input-to-State Stability of Nonlinear Systems*. Automatica, 76: 378-382, 2017.
- [78] X. Liu and K. Zhang. *Input-to-State Stability of Time-Delay Systems With Delay-Dependent Impulses*. IEEE transactions on automatic control, 65(4): 1676-1682, 2020.
- [79] J. Lu, D. W. C. Ho, and J. Cao. *A Unified Synchronization Criterion for Impulsive Dynamical Networks*. Automatica, 46(7): 1215-1221, 2010.
- [80] Y. Zheng, Y. Zhu, and L. Wang. *Consensus of heterogeneous multi-agent systems*. IET control theory & applications, 5(16): 1881-1888, 2011.
- [81] X. Li, C. Li, Y. Yang, and L. Mo. *Consensus for heterogeneous multi-agent systems with nonconvex input constraints and nonuniform time delays*. Journal of the Franklin Institute, 357(6): 3622-3635, 2020.
- [82] Y. Wang, X. Liu, J. Xiao, and Y. Shen. *Output Formation-Containment of Interacted Heterogeneous Linear Systems by Distributed Hybrid Active Control*. Automatica, 93: 26-32, 2018.

- [83] X. Jin, Z. Wang, Y. Feng, Y. Lu, C. Huang, and C. Zheng. *Impulsive Quasi-Containment Control in Heterogeneous Multiplex Networks*. Neurocomputing, 419: 37-46, 2021.
- [84] Q. Zhang, Y. Hao, Z. Yang, and Z. Chen. *Adaptive flocking of heterogeneous multi-agents systems with nonlinear dynamics*. Neurocomputing, 216: 72-77, 2016.
- [85] M. Wang, H. Su, M. Zhao, M. Z. Chen, and H. Wang. *Flocking of multiple autonomous agents with preserved network connectivity and heterogeneous nonlinear dynamics*. Neurocomputing, 115: 169-177, 2013.
- [86] J. Yu and L. Wang. *Group consensus of multi-agent systems with directed information exchange*. International journal of systems science, 43(2): 334-348, 2012.
- [87] T. Han, Z. H. Guan, M. Chi, B. Hu, T. Li, and X. H. Zhang. *Multi-formation control of nonlinear leader-following multi-agent systems*. ISA transactions, 69: 140-147, 2017.
- [88] J. Liu, J. Fang, Z. Li, and G. He. *Formation control with multiple leaders via event-triggering transmission strategy*. International journal of control, automation, and systems, 17 (6): 1494-1506, 2019.
- [89] G. Wen, Z. Duan, Z. Li, and G. Chen. *Flocking of Multi-Agent Dynamical Systems with Intermittent Nonlinear Velocity Measurements*. International journal of robust and nonlinear control, 22 (16): 1790-1805, 2012.
- [90] X. Li, D. Peng, and J. Cao. *Event-Triggered Impulsive Control for Nonlinear Delay Systems*. Automatica, 117: 108981-, 2020.
- [91] J. Han, H. Zhang, X. Liang, and Rui Wang. *Distributed Impulsive Control for Heterogeneous Multi-Agent Systems Based on Event-Triggered Scheme*. Journal of the Franklin Institute, 356 (16): 9972-9991, 2019.
- [92] T. Chen, S. Peng, and Z. Zhang. *Finite-time Consensus of Leader-following Nonlinear Multi-agent Systems via Event-triggered Impulsive Control*. IET Control Theory and Applications, 15 (7): 926-936, 2021.
- [93] X. Li, D. Peng, and J. Cao. *Lyapunov Stability for Impulsive Systems via Event-Triggered Impulsive Control*. IEEE Transactions on Automatic Control, 65 (11): 4908-4913, 2020.

- [94] Q. Song, J. Cao, and W. Yu. *Second-Order Leader-Following Consensus of Nonlinear Multi-Agent Systems via Pinning Control*. *Systems and Control Letters*, 59 (9): 553-562, 2010.
- [95] H. Hu, Q. Xuan, W. Yu, C. Zhang, and G. Xie. *Second-Order Consensus for Heterogeneous Multi-Agent Systems in the Cooperation-competition Network: A Hybrid Adaptive and Pinning Control Approach*. *Nonlinear Analysis. Hybrid Systems*, 20: 21-36, 2016.
- [96] W. He, F. Qian, and J. Cao. *Pinning-Controlled Synchronization of Delayed Neural Networks with Distributed-Delay Coupling via Impulsive Control*. *Neural Networks*, 85: 1-9, 2017.
- [97] Y. Li, J. Lou, Z. Wang, and F. E. Alsaadi. *Synchronization of Dynamical Networks with Nonlinearly Coupling Function Under Hybrid Pinning Impulsive Controllers*. *Journal of the Franklin Institute* 355, 355 (14): 6520-6530, 2018.
- [98] J. Lu, J. Kurths, J. Cao, N. Mahdavi, and C. Huang. *Synchronization Control for Nonlinear Stochastic Dynamical Networks: Pinning Impulsive Strategy*. *IEEE Transaction on Neural Networks and Learning Systems*, 23 (2): 285-292, 2012.
- [99] X. Liu and K. Zhang. *Synchronization of Linear Dynamical Networks on Time Scales: Pinning Control via Delayed Impulses*. *Automatica*, 72: 147-152, 2016.
- [100] J. Gao, X. Xu, N. Ding, and E. Li. *Flocking Motion of Multi-Agent System by Dynamic Pinning Control*. *IET Control Theory and Applications*, 11 (5): 714-722, 2017.
- [101] H. Shakhathreh, A. Al-Fuqaha A. H. Sawalmeh, and et al. *Unmanned aerial vehicles (UAVs): a survey on civil applications and key research challenges*. *IEEE Access*, 7: 48572-48634, 2019.
- [102] X. Dong, B. Yu, Z. Shi, and Y. Zhong. *Time-Varying Formation Control for Unmanned Aerial Vehicles: Theories and Applications*. *IEEE Transactions on Control Systems Technology*, 23 (1): 340-348, 2015.
- [103] I. Bayezit and B. Fidan. *Distributed cohesive motion control of flight vehicle formations*. *IEEE Trans. Ind. Electron*, 60 (12): 5763-5772, 2013.

- [104] X. Dong, Zhou Y, Z. Ren, and Y. Zhong. *Time-Varying Formation Tracking for Second-Order Multi-Agent Systems Subjected to Switching Topologies With Application to Quadrotor Formation Flying*. IEEE transactions on industrial electronics, 64 (6): 5014-5024, 2017.
- [105] X. Dong, Q. Li, R. Wang, and Z. Ren. *Time-Varying Formation Control for Second-Order Swarm Systems with Switching Directed Topologies*. Information Sciences, 369: 1-13, 2016.
- [106] J. Mei, M. Jiang, W. Xu, and B. Wang. *Finite-Time Synchronization Control of Complex Dynamical Networks with Time Delay*. Communications in nonlinear science & numerical simulation, 18 (9): 2462-2478, 2013.
- [107] T. Jing, D. Zhang, J. Mei, and Y. Fan. *Finite-Time Synchronization of Delayed Complex Dynamic Networks via Aperiodically Intermittent Control*. Journal of the Franklin Institute, 356 (10): 5464-5484, 2019.
- [108] T. Jing, D. Zhang, and T. Jing. *Finite-Time Synchronization of Hybrid-Coupled Delayed Dynamic Networks via Aperiodically Intermittent Control*. Neural processing letters, 52 (1): 291-311, 2020.
- [109] Y. Wu, C. Wang, and W. Li. *Generalized Quantized Intermittent Control with Adaptive Strategy on Finite-Time Synchronization of Delayed Coupled Systems and Applications*. Nonlinear dynamics, 95 (2): 1361-1377, 2018.
- [110] Q. Yang, H. Wu, and J. Cao. *Global Cluster Synchronization in Finite Time for Complex Dynamical Networks with Hybrid Couplings via Aperiodically Intermittent Control*. Optimal control applications & methods, 41 (4): 1097-1117, 2020.
- [111] X. Liu, X. Shen, and H. Zhang. *Intermittent Impulsive Synchronization of Chaotic Delayed Neural Networks*. Differential equations and dynamical systems, 19 (1-2): 149-169, 2011.
- [112] L. Li, Z. Tu, J. Mei, and et al. *Finite-time synchronization of complex delayed networks via intermittent control with multiple switched periods*. Nonlinear Dynamics, 85: 375-388, 2016.
- [113] P. Wang, B. Zhang, and H. Su. *Stabilization of Stochastic Uncertain Complex-Valued Delayed Networks via Aperiodically Intermittent Nonlinear Control*. IEEE transactions on systems, man, and cybernetics: systems, 49 (3): 649-662, 2019.

- [114] P. Wang, W. Jin, and H. Su. *Synchronization of Coupled Stochastic Complex-Valued Dynamical Networks with Time-Varying Delays via Aperiodically Intermittent Adaptive Control*. *Chaos*, 28 (4): 043114-043114 2018.
- [115] B. Liu, M. Yang, B. Xu, and G. Zhang. *Exponential Stabilization of Continuous-Time Dynamical Systems via Time and Event Triggered Aperiodic Intermittent Control*. *Applied mathematics and computation*, 398: 125713-, 2021.
- [116] Y. Wu, S. E. Li, Y. Zheng, and J. K. Hedrick. *Distributed sliding mode control for multi-vehicle systems with positive definite topologies*. 2016 IEEE 55th Conference on Decision and Control (CDC), 5213-5219, 2016.
- [117] D. Liberzon. *Switching in systems and control*. Boston: Birkhauser, 2003.
- [118] H. Yang, B. Jiang, and V. Cocquempot. *A Survey of Results and Perspectives on Stabilization of Switched Nonlinear Systems with Unstable Modes*. *Nonlinear analysis*, 13: 45-60, 2014.
- [119] H. Yang, B. Jiang, V. Cocquempot, and H. Zhang. *Stabilization of Switched Nonlinear Systems With All Unstable Modes: Application to Multi-Agent Systems*. *IEEE transactions on automatic control*, 56 (9): 2230-2235, 2011.
- [120] L. Dong, S. Chai, B. Zhang, S. K. Nguang, and A. Savvaris. *Stability of a Class of Multiagent Tracking Systems With Unstable Subsystems*. *IEEE transactions on cybernetics*, 47 (8): 2193-2202, 2017.
- [121] D. Xie, H. Zhang, H. Zhang, and B. Wang. *Exponential Stability of Switched Systems with Unstable Subsystems: A Mode-Dependent Average Dwell Time Approach*. *Circuits, systems, and signal processing*, 32 (6): 3093-3105, 2013.
- [122] X. Zhao, L. Zhang, P. Shi, and M. Liu. *Stability and Stabilization of Switched Linear Systems With Mode-Dependent Average Dwell Time*. *IEEE transactions on automatic control*, 57 (7): 1809-1815, 2012.
- [123] X. Xie, X Liu, and H Xu. *Synchronization of Delayed Coupled Switched Neural Networks: Mode-Dependent Average Impulsive Interval*. *Neurocomputing*, 365: 261-272, 2019.
- [124] Q. Wang and X. Liu. *Stability Criteria of a Class of Nonlinear Impulsive Switching Systems with Time-Varying Delays*. *Journal of the Franklin Institute*, 349 (3): 1030-1047, 2012.

- [125] D. Yang, X. Li, J. Shen, and Z. Zhou. *State-dependent Switching Control of Delayed Switched Systems with Stable and Unstable Modes*. *Mathematical methods in the applied sciences*, 41 (16): 6968-6983, 2018.
- [126] A. Ghasemi, R. Kazemi, and S. Azadi. *Stable Decentralized Control of a Platoon of Vehicles With Heterogeneous Information Feedback*. *IEEE transactions on vehicular technology*, 62 (9): 4299-4308, 2013.
- [127] D. Scharf, F. Hadaegh, and S. Ploen. *A Survey of Spacecraft Formation Flying Guidance and Control (Part II): Control*. In *Proceedings of the American Control Conference*, 4: 2976-2985, 2004.
- [128] T. Balch and R. C. Arkin. *Behavior-Based Formation Control for Multirobot Teams*. *IEEE transactions on robotics and automation*, 14 (6): 926-939, 1998.
- [129] A. Ghasemi, R. Kazemi, and S. Azadi. *Stable Decentralized Control of a Platoon of Vehicles With Heterogeneous Information Feedback*. *IEEE transactions on vehicular technology*, 62 (9): 4299-4308, 2013.